UNIVERSITY OF ILLINOIS
URBANA

AERONOMY REPORT NO. 38

D-REGION ION CHEMISTRY

by

S. M. Radicella

D. W. Stowe

July 15, 1970

Supported by
National Aeronautics and Space Administration
Grant ~~NGR-013~~ NGR-14-005-013

Aeronomy Laboratory
Department of Electrical Engineering
University of Illinois
Urbana, Illinois

CITATION POLICY

The material contained in this report is preliminary information circulated rapidly in the interest of prompt interchange of scientific information and may be later revised on publication in accepted aeronomic journals. It would therefore be appreciated if persons wishing to cite work contained herein would first contact the authors to ascertain if the relevant material is part of a paper published or in process.

A E R O N O M Y R E P O R T

N O. 3 8

D-REGION ION CHEMISTRY

by

S. M. Radicella

D. W. Stowe

July 15, 1970

Supported by
National Aeronautics and Space Administration
Grant ~~NGR-013~~ NAR-14-005-013

Aeronomy Laboratory
Department of Electrical Engineering
University of Illinois
Urbana, Illinois
UILU-ENG-70-261

ABSTRACT

The neutral composition of the mesosphere is reviewed with emphasis on nitrogen oxides and oxygen allotropes. Then ionization sources in the D region are studied including the effects of recent experimental results. Finally, the negative ion chemistry is discussed including the calculation of an "effective attachment factor, β_{eff}." On the basis of the experimental β_{eff}, a new fast binary attachment process is considered.

In the appendix, relevant experimental data is tabulated, and the diurnal variation of atomic oxygen and ozone concentrations is presented, based on recent values for the relevant rate coefficients.

TABLE OF CONTENTS

LIST OF FIGURES

LIST OF TABLES

1. D-REGION NEGATIVE-ION CHEMISTRY

1.1 Introduction

Electron-density distribution is, at this time, the best known parameter in the D region. From recent work, a general picture of this parameter can be deduced (Mechtly and Smith 1968a,b; Mechtly and Shirke 1968). Unlike the upper ionized regions, D-region structure is characterized by the attachment of electrons to neutral molecules to form, through complex chemistry, a large number of negative ions of variable distribution and mass. Electron density is therefore strongly controlled by the negative-ion chemistry. This, in turn, is determined by the rates of reactions that produce or eliminate different species of negative ions. Reaction rates depend upon the rate coefficients now quite well established by laboratory measurements (Fehsenfeld et al, 1967; Fehsenfeld and Ferguson, 1968) and upon the concentration of neutral species such as O, O_3 and NO. The experimental knowledge about the odd allotropes of oxygen is very limited, and theoretical computations depend upon several factors still doubtful. Recent direct estimates of NO concentration (Barth 1966; Pearce 1968) show much larger values than those obtained with indirect ionospheric methods based upon electron-density data and ion-reaction schemes widely accepted at this time. To accept the experimental data for the NO concentration will force a re-evaluation of the negative-ion chemistry, in a search for missing reactions, in order to reconciliate those data and direct measurements of electron density.

The first chapter of this report will review the neutral composition of the mesosphere, where D-region ionized species are very minor constituents. Nitrogen oxides and oxygen allotropes distributions will be discussed in more detail.

The second chapter will be devoted to a review of the sources of ionization in the undisturbed D region for both daytime and nighttime. The impact of high values of NO concentrations (Pearce, 1968) in relation to the ionization of nitric oxide by Lyman-alpha radiation will be described. The importance of precipitation of electrons, as a source of ionization during nighttime will be considered.

In the third chapter, the negative-ion chemistry will be discussed. An "effective attachment factor" β_{eff} is defined, this being the only term in the continuity equation for electrons and ions that depends upon the negative-ion schemes. Assuming steady state conditions, β_{eff} is computed from experimental electron-density profiles, calculated rate of ionization and laboratory deionization data. The problem introduced by different values of NO concentration will become evident during the discussion. It will be shown that in order to obtain theoretically the experimental β_{eff} a new fast binary attachment process should be postulated when NO concentration measurements are used.

2. NEUTRAL COMPOSITION OF THE MESOSPHERE

2.1 Introduction

The atmospheric region between roughly 50 and 90 km, called the mesosphere, is chemically very active. Photodissociation produces atomic species that, in a relatively dense medium, can react rapidly with other constituents forming a large number of more or less stable minor species. The absorption of solar ultraviolet radiation by ozone at wavelengths of 2100-3000 Å is a strong source of heating. The effect of this is the large temperature observed around 50 km. A decrease in temperature is observed above that height up to 80-90 km. This altitude gradient of temperature is important to the chemistry of the mesosphere because many reaction rate coefficients are strongly temperature dependent.

In the region of 50 to 90 km there are a number of three-body reactions among both neutral and ionic species. The passive third body is represented in most cases by the general atmospheric molecule, i.e., the concentration of the third body involved is the atmospheric number density itself.

Both the COSPAR International Reference Atmosphere (1965) and the U.S. Standard Atmosphere Supplement (1966) give experimental models of the neutral gas densities, temperature, and other parameters as a function of height, season and latitude. Below approximately 80 km a constant mean molecular mass or, what is equivalent, a constant mixing ratio can be assumed for the major constituents. The neutral atmospheric region between 80 and 120 km is the least known experimentally, and constituent distribution is still uncertain. Variations of O_2 distribution are very important because dissociation of molecular oxygen controls the chemistry of the odd allotropes of oxygen and

also some aspects of the ion chemistry. Figure 1 shows the concentration of O_2 from winter and summer at 45° latitude and low solar activity from the U.S. Standard Atmosphere Supplement (1966).

As a product of the chemical activity of the mesosphere, numerous neutral species are present in that region. Most of them have concentrations smaller by several orders of magnitude of O_2 or N_2. Such species are called minor constituents. Photodissociation of O_2, N_2, H_2O and CH_4 is the first step in the formation of: O, O_3, NO, NO_2, N_2O, H, OH, HO_2, H_2O, etc. Other minor constituents in the mesosphere could be clusters of neutral molecules like $(H_2O)\cdot NO$ could be produced in the region of low temperature around 80 km. Also chemically important is CO_2.

At this time, all the species mentioned above, the odd allotropes of oxygen and the oxides of nitrogen are considered the most important ones to the negative-ion chemistry. Hydrogenous compounds appear to be of indirect importance because they represent only perturbations introduced in the chemistry of oxygen. The role played by neutral clusters is unknown.

2.2 Odd Allotropes of Oxygen

The experimental knowledge about O and O_3 distribution at D-region altitudes is very limited. Only one nighttime preliminary profile of mesospheric oxygen concentration has been published (Fedynskii et al, 1967). Daytime ozone measurements have been carried out by Johnson et al, (1954) and by Rawcliffe et al, (1963). Nighttime profiles have been obtained by Carver et al. (1966), Mikirov (1965) and Reed (1968). Figure 2 summarizes these experimental results.

Theoretical computations of O and O_3 distribution are based upon the knowledge about: fluxes of the solar radiation capable of photodissociating

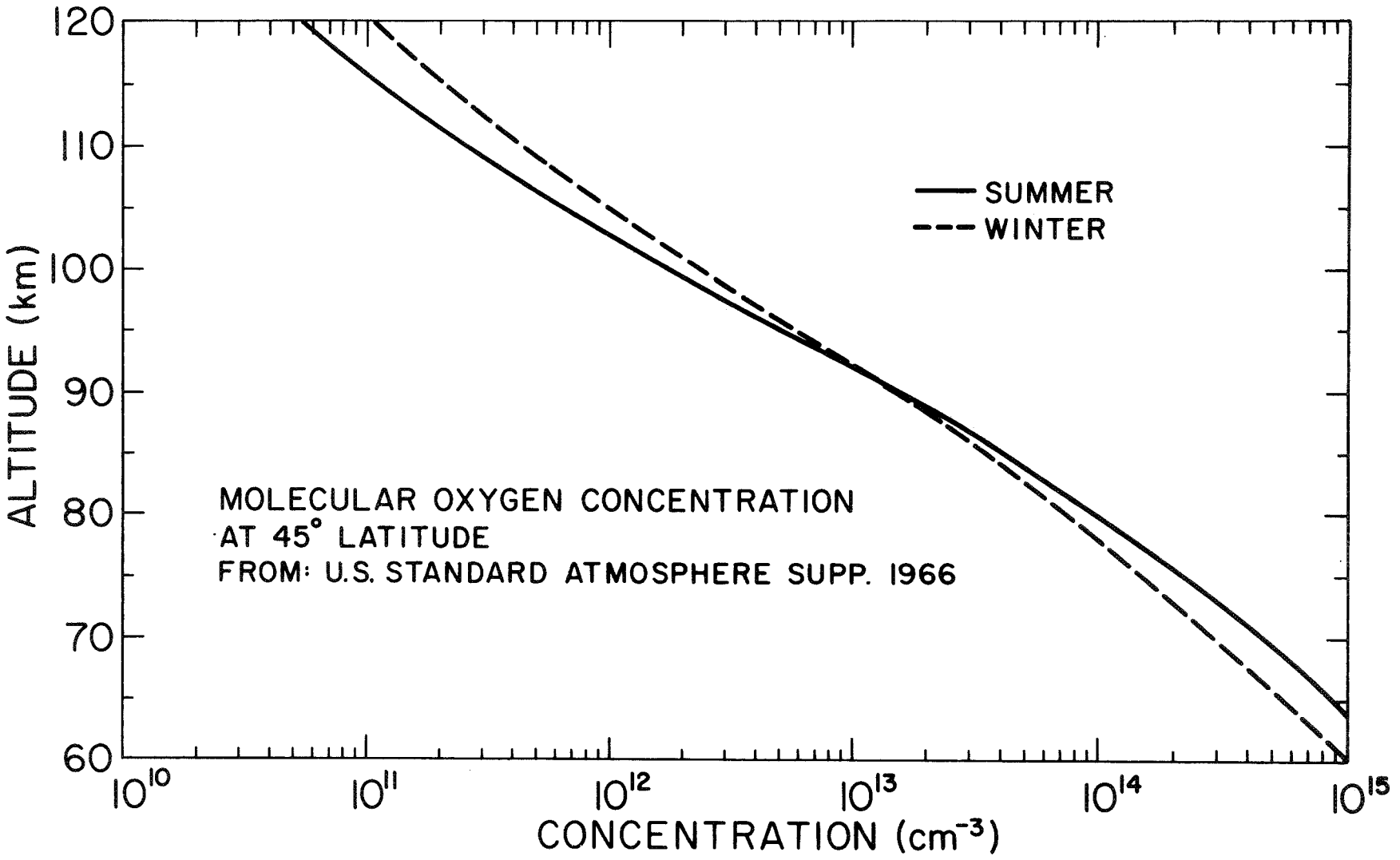

Figure 1. Molecular oxygen concentration at 45° latitude derived from U.S. Standard Atmosphere Supplement 1966. Full line indicates summer conditions; broken line indicates winter conditions.

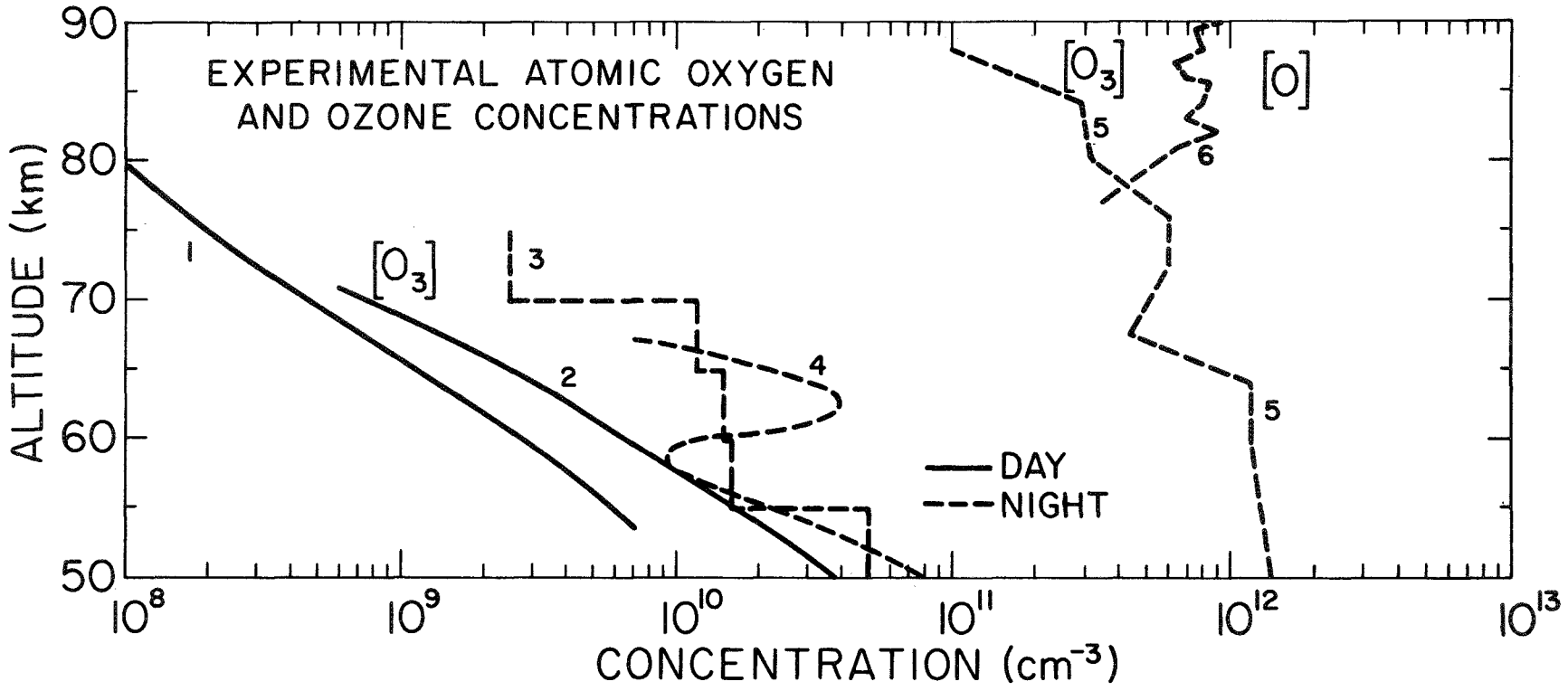

Figure 2. Experimental profiles of atomic oxygen and ozone concentrations. 1. Daytime ozone concentration by Johnson, et al. (1954); 2. Daytime ozone concentration by Rawcliffe, et al. (1963); 3. Nighttime ozone concentration by Carver, et al. (1966); 4. Nighttime ozone concentration by Reed (1968); 5. Nighttime ozone concentration by Mikirov (1965) and 6. Atomic oxygen nighttime concentration by Fedynskii, et al. (1967).

O_2 and O_3, dissociation cross sections as a function of the radiation wavelength, and rates of the chemical reactions involved. The latter represents the less known factor.

The basic photochemical reactions of atmospheric oxygen are:

$$O_2 + h\nu \xrightarrow{j_2} O + O \quad (1375 < \lambda < 2424\text{Å}) \tag{1}$$

$$O_3 + h\nu \xrightarrow{j_3} O + O_2 \quad (1375 < \lambda < 7500) \tag{2}$$

$$O + O + M \xrightarrow{k_3} O_2 + M \tag{3}$$

$$O + O_2 + M \xrightarrow{k_4} O_3 + M \tag{4}$$

$$O + O_3 \xrightarrow{k_5} O_2 + O_2 \tag{5}$$

Cross sections and fluxes of radiation involved in reactions (1) and (2) are shown in Figures 3 and 4.

The diversity of published laboratory values for the rate coefficients of (3), (4) and (5) is very wide. It reflects the complications introduced in the experimental determinations by the effect of hydrogenous and nitrogenous trace impurities and the formation of metastable species (Schofield, 1967).

A recent discussion of experimental studies of reactions (3), (4) and (5) has been given by Kaufman (1967). This author adopts for the range between 190 and 400°K, the value of $k_3 = 3.0 \times 10^{-33} \left(\frac{T}{300}\right)^{-(2.6 \pm 0.4)}$ obtained by combining several data when $M \equiv N_2$. Also $k_5 = (1.4 \pm 0.3) \times 10^{-12} \exp^{-\frac{(3.0 + 0.4)}{RT}}$ is adopted by the same author. It must be noted that some discrepancies among different experimental studies of these reactions still exists. Table 1 shows the individual results of some of these studies

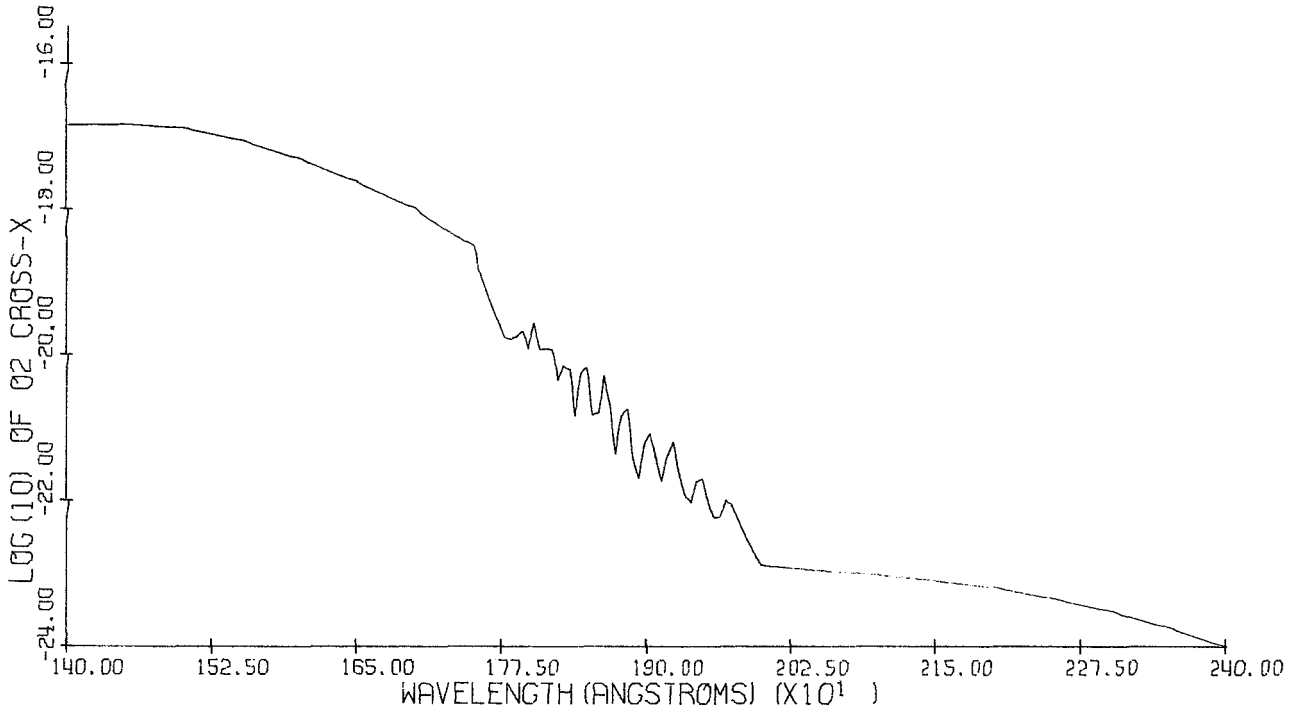

Figure 3a. O_2 absorption cross sections as a function of radiation wavelength (see Appendix for references).

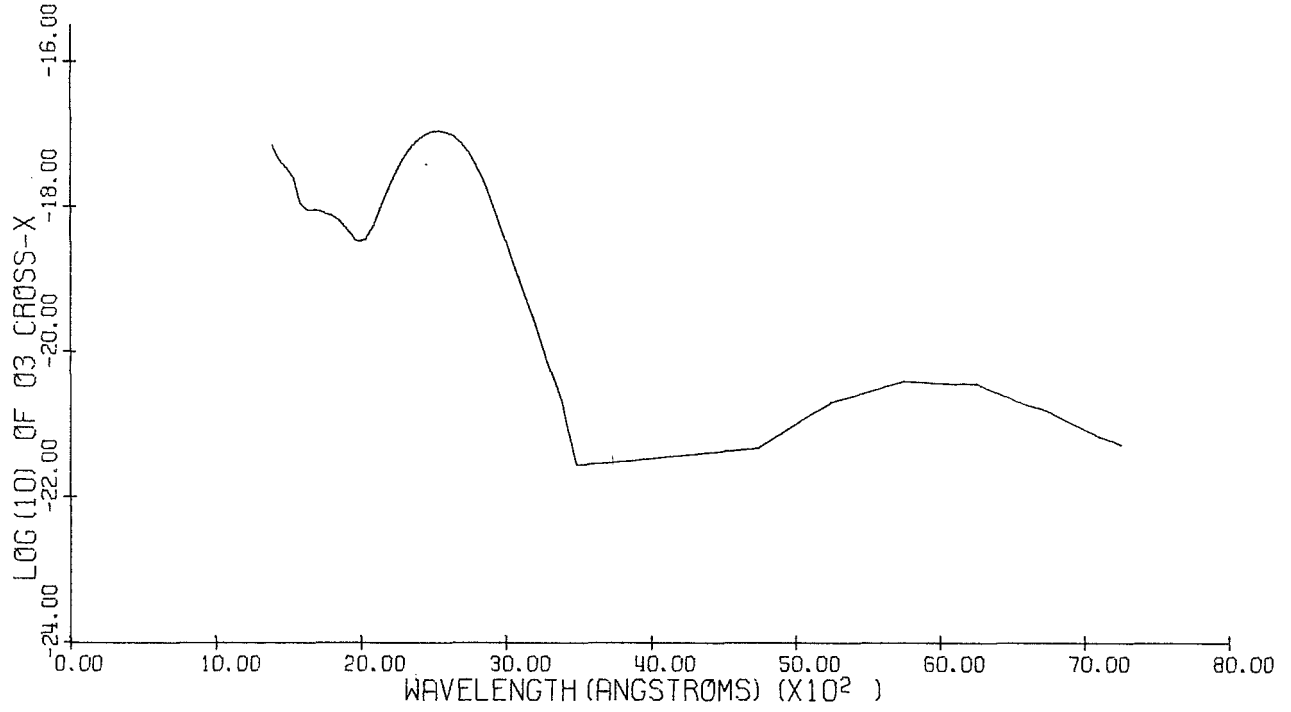

Figure 3b. Ozone absorption cross sections as a function of radiation wavelength (see Appendix for references).

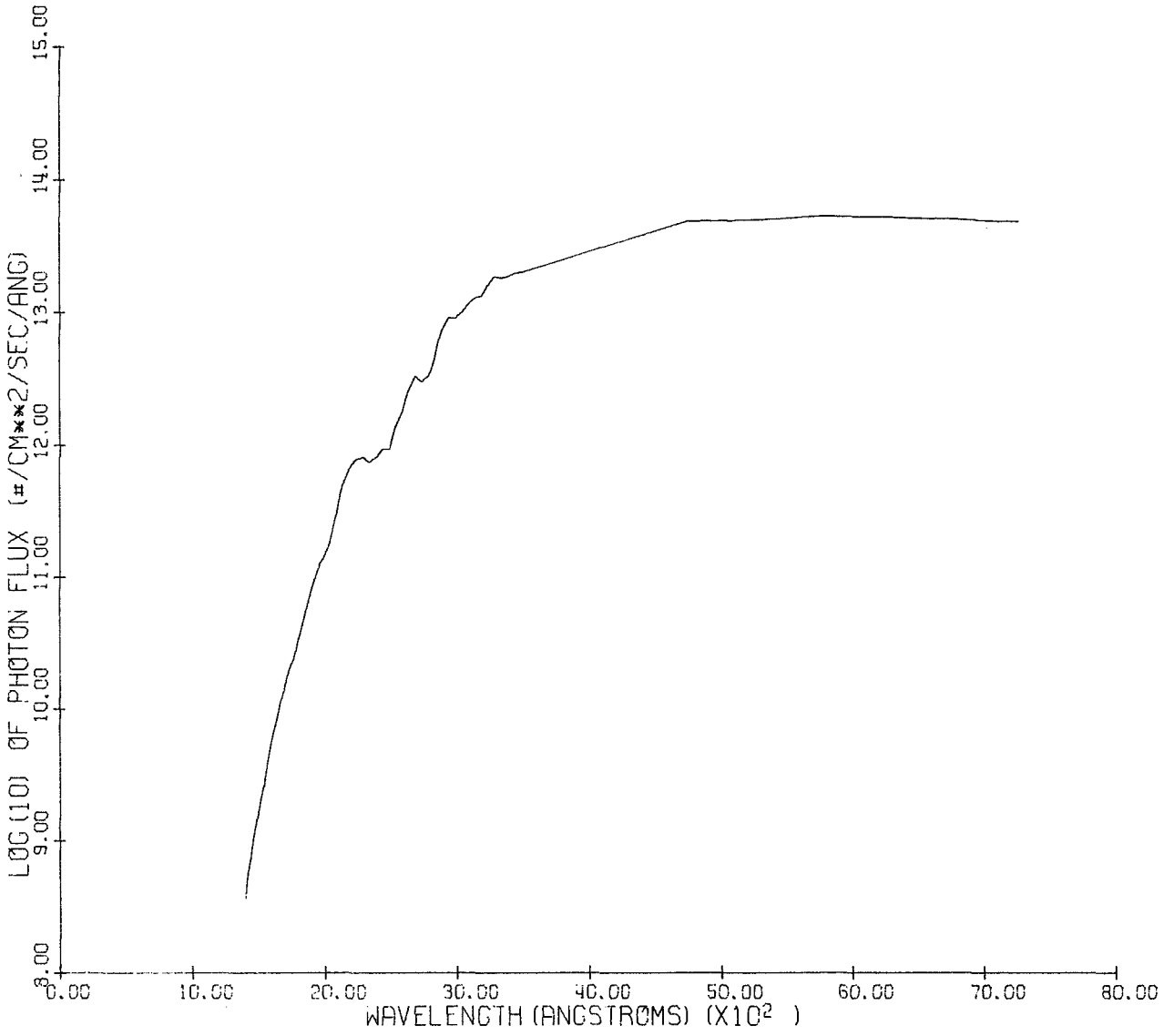

Figure 4. Solar flux radiation as a function of wavelength (see Appendix for references).

TABLE 1

Reaction rate coefficients for oxygen including Kaufman's adopted values

Reaction	Rate Coefficient	Author	Comments
$O + O + M \xrightarrow{k_5} O_2 + M$	2.8×10^{-33} (cm^6 sec^{-1})	Morgan and Schiff (1963)	T = 294°K, M ≡ N_2
	1.5×10^{-34}	Young and Black (1966)	T = 300°K, M ≡ O
	$3.0 \times 10^{-33} (\frac{T}{300})^{-2.9 \pm 0.4}$	Campbell and Thrush (1968)	190 <T< 350°K, M ≡ N_2
	$3.0 \times 10^{-33} (\frac{T}{300})^{-2.9 \pm 0.4}$	Kaufman (1967)	adopted by M ≡ N_2
$O + O_2 + M \xrightarrow{k_4} O_3 + M$	$8.2 \times 10^{-35} \exp(\frac{890}{RT})$ (cm^6 sec^{-1})	Benson and Axworthy (1965)	near T = 360°K, M ≡ O_2
	$(2.6 \pm 0.3) \times 10^{-35}$ $\exp(\frac{1700 \pm 300}{RT})$	Jones and Davidson (1962)	M ≡ N_2
	6.5×10^{-34}	Kaufman and Kelso (1964)	T = 300°K, M ≡ O_2
	5.5×10^{-34}	Kaufman and Kelso (1964)	T = 300°K, M ≡ N_2
	$2.5 \times 10^{-35} \exp(\frac{1800 \pm 400}{RT})$	Clyne et al. (1965)	188 <T< 373°K, M ≡ Ar
	$5.5 \times 10^{-34} (\frac{T}{300})^{-2.6 \pm .4}$	Kaufman (1967)	adopted by, M ≡ N_2
$O + O_3 \xrightarrow{k_5} O_2 + O_2$	$5.6 \times 10^{-11} \exp(-\frac{5700}{RT})$ (cm^2 sec^{-1})	Benson and Axworthy (1965)	340 <T< 390°K
	3.9×10^{-14}	Phillips and Schiff (1962)	Considered questionable value by Schofield (1967)
	8.0×10^{-15}	Mathias and Schiff (1964)	T = 300°K
	$(1.4 \pm 0.3) \times 10^{-12}$ $\exp(-\frac{3000 \pm 400}{RT})$	Kaufman (1967)	adopted by

R = 1.987 cal/(°K mole)

for the range of atmospheric temperatures, together with the data adopted by Kaufman (1967).

Theoretical models of O and O_3 have been calculated by several authors. Some of them considered a photochemical reaction scheme based upon an oxygen alone atmosphere as represented by reactions (1) and (5), (Craig, 1950; Hunt, 1966a; London, 1967; Maeda and Aikin, 1968). However, some of these authors are mainly concerned with stratospheric ozone. It must be noted that the rate coefficients used in the above-mentioned studies are notably different from the values adopted by Kaufman (1967) using all experimental data available at this time.

Models of O and O_3 that take into account reactions of hydrogenous compounds in the chemical scheme have been published by Hampson (1965) and Hunt (1966b). However, they have used reaction rate coefficients that differ sensibly from the ones that are considered correct at this time. Of particular importance, besides the basic oxygen reactions rates already discussed, is the rate coefficient of reaction:

$$O(^1D) + M \xrightarrow{k_6} O(^3P) + M \quad . \qquad (6)$$

Hunt (1966a) assumed a value of $k_6 - 10^{-12}$ ($cm^3\ sec^{-1}$). A more realistic one appears to be: $k_6 = 5 \times 10^{-11}$ as deduced from McGrath and McGarvey (1967).

A more sophisticated approach is to consider an oxygen-hydrogen atmosphere including also the dynamics terms. Konashenok (1967) and Hesstvedt (1968) introduced vertical eddy transport in their calculations. From the work of these authors it is clear that the dynamical terms can change the vertical and geographic distribution of atomic oxygen and ozone. It must be

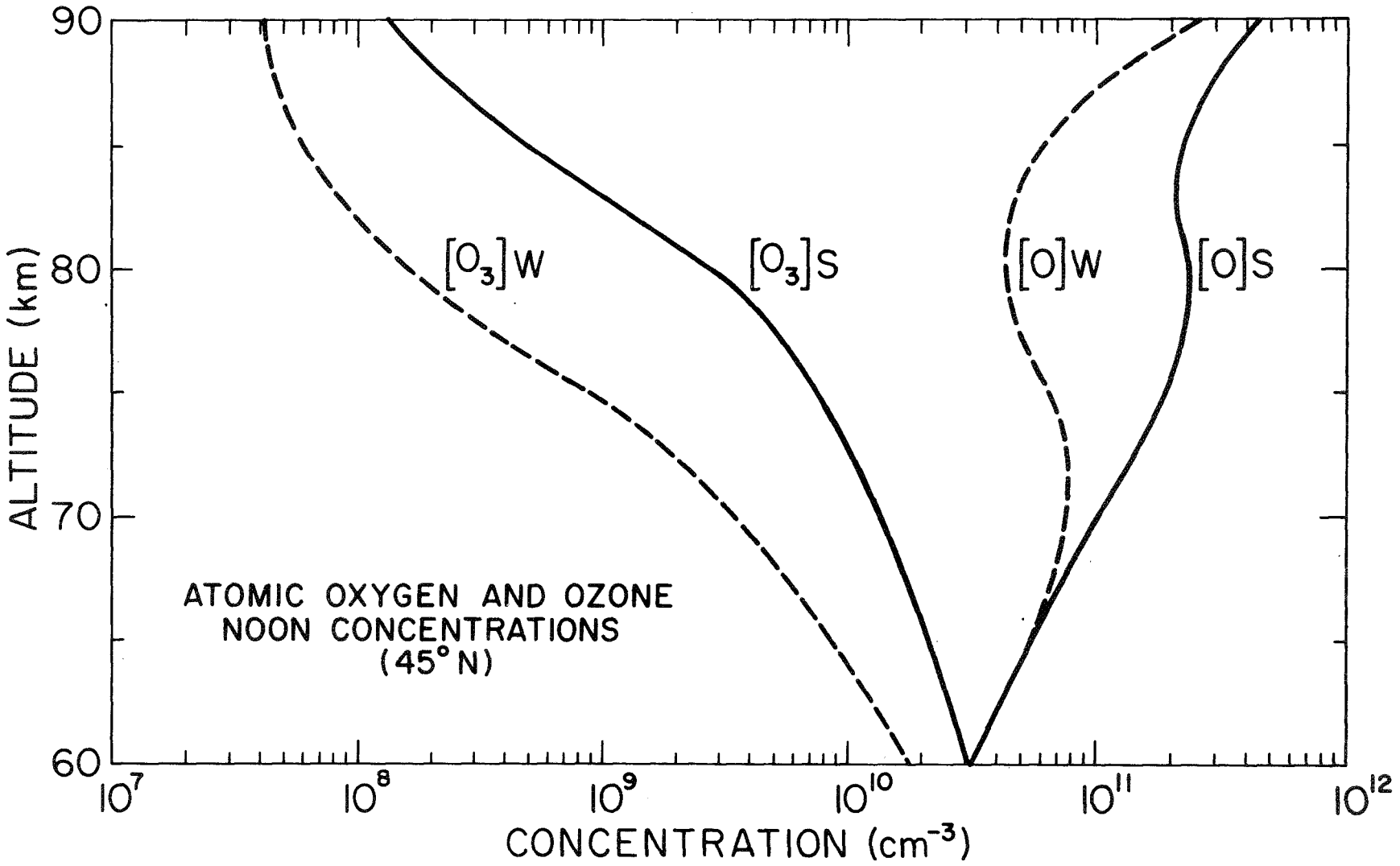

Figure 5. Theoretical profiles of noon atomic oxygen and ozone concentration at 45° N. Full line indicates summer profiles; broken line indicates winter profiles. These values were computed for oxygen alone atmosphere.

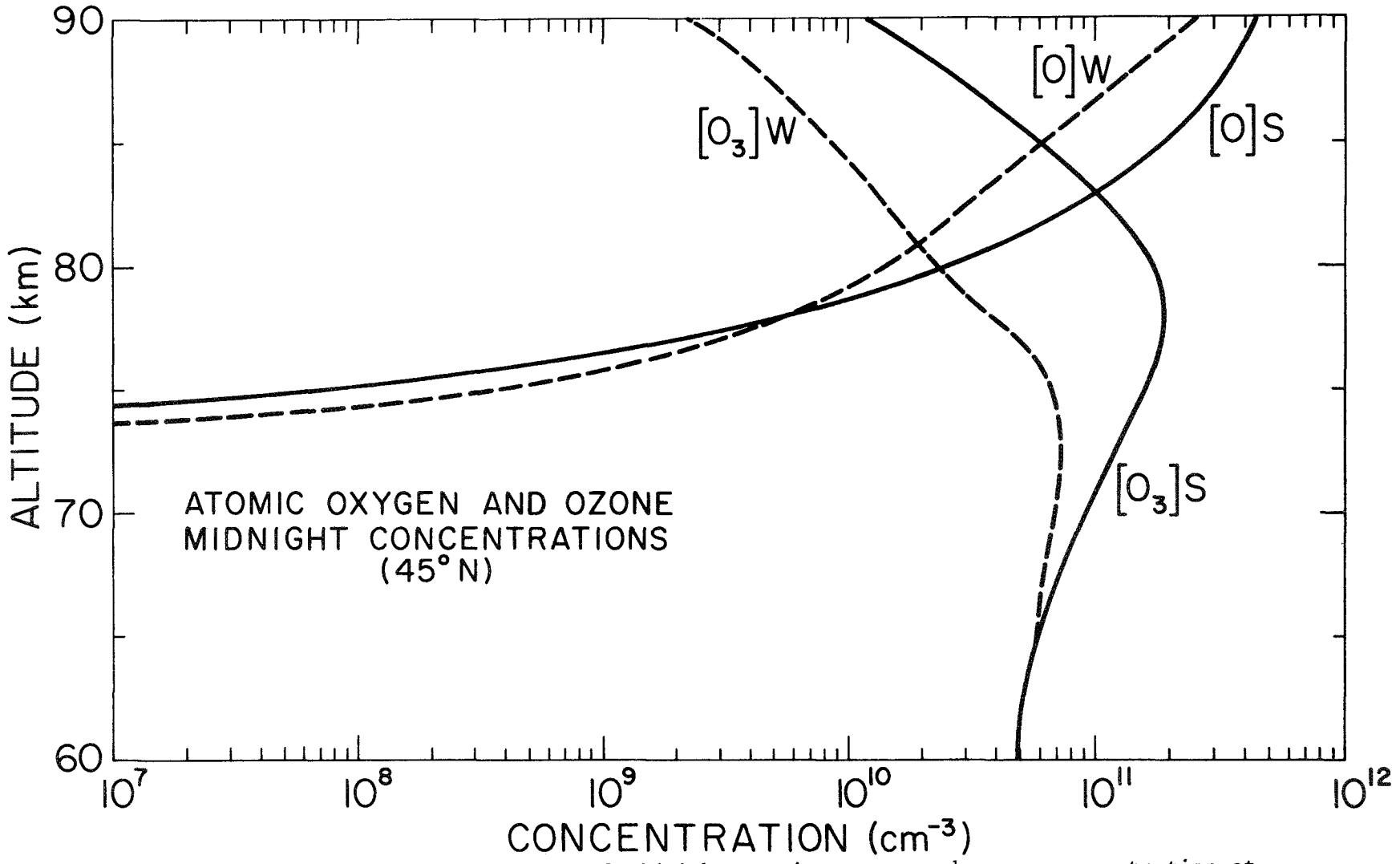

Figure 6. Theoretical profiles of midnight atomic oxygen and ozone concentration at 45° N. Full line indicates summer profiles; broken line indicates winter profiles. These values were computed for oxygen alone atmosphere.

noted however that the reaction rate coefficients of reactions (3) and (5) adopted in all the studies mentioned above, differ notably from the Kaufman (1967) values which, at this time, should be considered more representative.

It is convenient to compute the temporal and spatial variations of O and O_3 based on the Kaufman rate coefficients for the reactions (3) and (5) and also on recent values of solar fluxes. In this way a basic photochemical model and a function of time and latitude is obtained. It can be changed as a second step, by introducing hydrogenous compound reactions and dynamical terms. Time variations as a function of height, latitude and season are computed by solving the continuity equations in the differential forms:

$$\frac{d[O]}{dt} = 2j_2\,[O_2] + j_3[O_3] - 2k_3\,[O]^2[M] - k_4\,[O][O_2][M] - k_5\,[O][O_3] \qquad (7)$$

$$\frac{d[O_3]}{dt} = k_4\,[O][O_2][M] - k_5\,[O][O_3] - j_3\,[O_3] \quad . \qquad (8)$$

The computer programs used and the input values of cross sections, solar radiation fluxes, atmospheric temperature, and densities adopted in the calculations are given in the Appendix. Detailed tabulation of the output data (atomic oxygen and ozone concentrations) are also given there. Figures 5 and 6 show the computed O and O_3 profiles for 45° of latitude north, summer and winter, and noon and midnight. Figures 7, 8 and 9 show the latitudinal variation of atomic oxygen and ozone concentrations at 70, 80 and 90 km. A full discussion of these data will be given elsewhere.

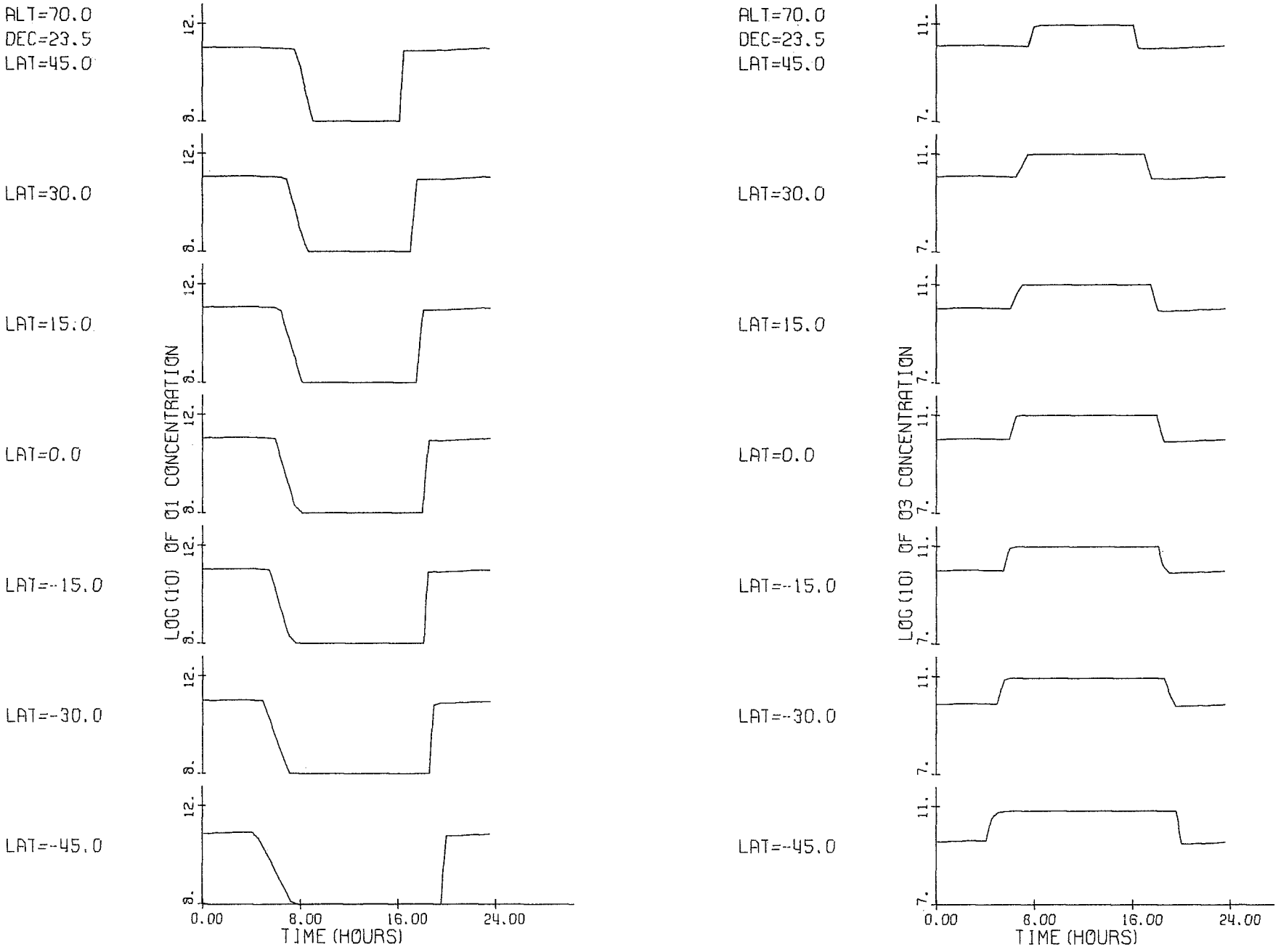

Figure 7. Theoretical values of diurnal latitudinal and seasonal variation of atomic oxygen and ozone for an oxygen alone atmosphere (70 km).

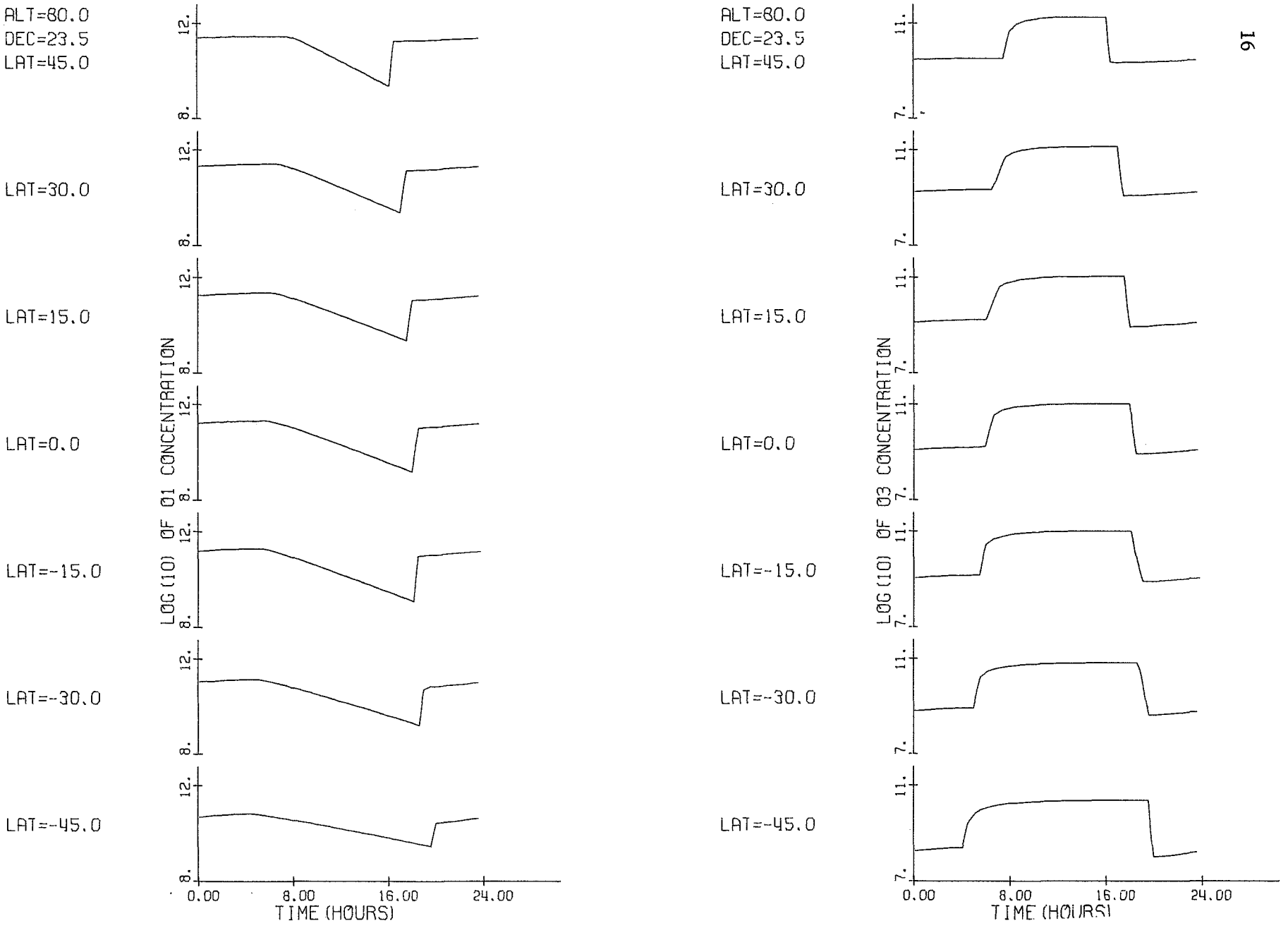

Figure 8. Theoretical values of diurnal latitudinal and seasonal variation of atomic oxygen and ozone for an oxygen alone atmosphere (80 km).

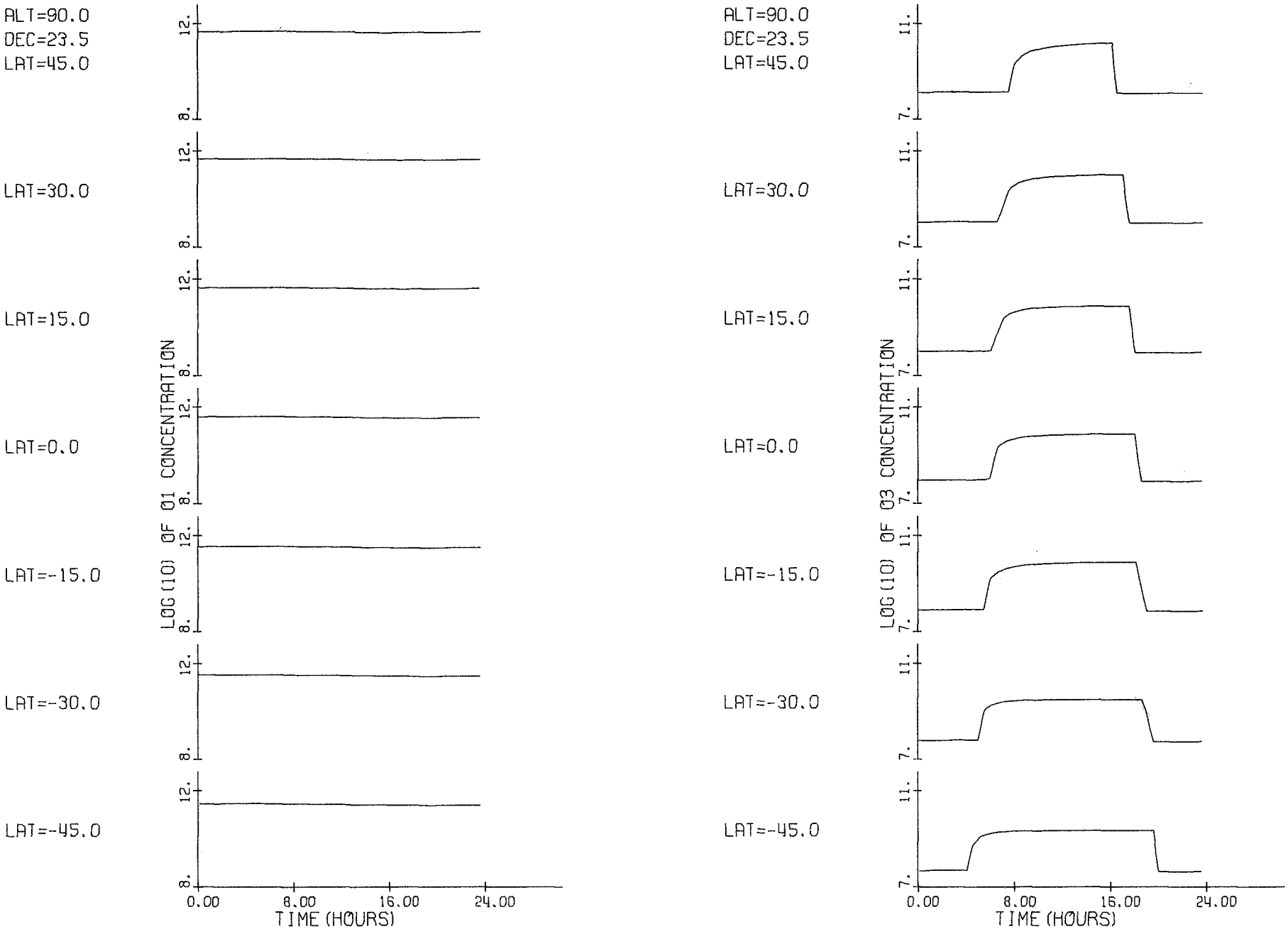

Figure 9. Theoretical values of diurnal latitudinal and seasonal variation of atomic oxygen and ozone for an oxygen alone atmosphere (90 km).

2.3 Nitrogen Oxides

Minor consitutents of great importance to the chemical aeronomy and, in particular, to the D-region ionization are nitric oxide and, in a minor scale, nitrogen dioxide. NO is the relevant specie to the chemistry of the D region as considered by Nicolet and Aikin (1960). Their paper represents one of the first attempts to explain theoretically what was known at the end of the fifties about the D region. These authors introduced the hypothesis that the basic process of formation during low solar activity was the ionization of NO by Lyman-alpha solar radiation with a production peak between 75 and 80 km. Until 1964 no direct experimental data on the nitric oxide distribution were published. The only methods used to derive NO concentration were the indirect ionospheric estimates as the ones obtained by Mitra (1966) and Wagner (1966) for D-region heights. A final model deduced using the same methods has been published recently by Mitra (1968). His NO distribution is expressed by:

$$[NO] = 4 \times 10^{-1} \exp\left(-\frac{3700}{T}\right) [O_2] + 5 \times 10^{-7} [O] \qquad (9)$$

Figure 10 shows Mitra's (1968) distribution of NO.

Direct photometric measurements of the NO airglow were made by Barth (1964, 1966) from Wallops Island during low solar activity. The data obtained from a rocket flight in November 1963 shows an NO concentration of 6.2×10^7 cm^{-3} at 75 km and 6.0×10^7 at 95 km. These values are much higher than the ones deduced by indirect ionospheric methods. For some time the Barth (1966) values were considered doubtful, but a recent rocket photometric experiment by Pearce (1968) again shows very high values of nitric oxide concentration at all heights in the mesosphere. His values are also plotted in Figure 10.

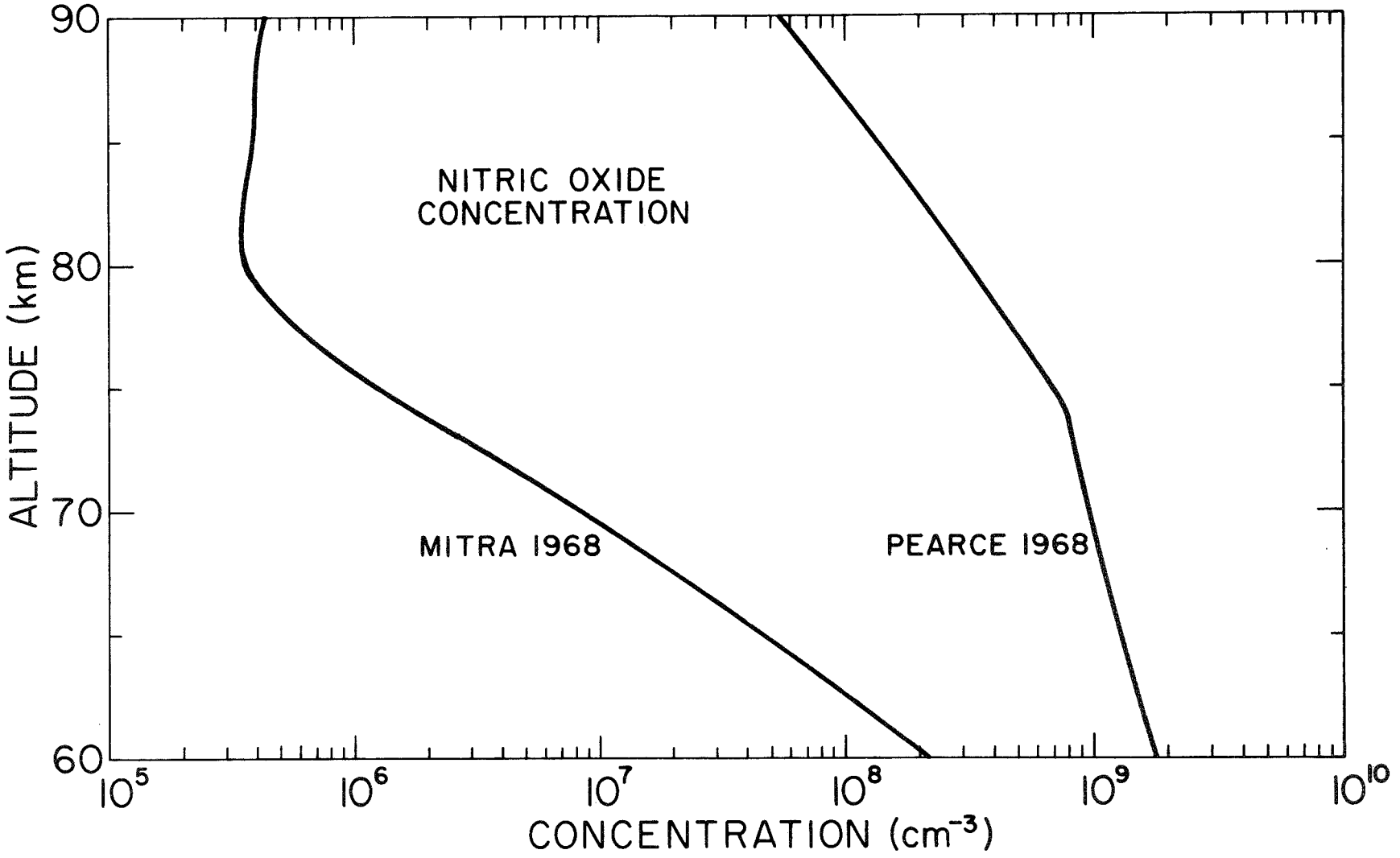

Figure 10. Nitric oxide concentration as a function of height by Mitra (1968) and Pearce (1968).

The more comprehensive theoretical study of the NO distribution has been published by Nicolet (1965a,b). This author shows the importance of atomic oxygen and ozone as reactants in the chemistry of the oxides of nitrogen in the atmosphere. He shows also that in order to conciliate the values given by Barth (1964) it was necessary to introduce ionic reactions in the chemical scheme.

Nitrogen dioxide distribution in the atmosphere have not been determined experimentally. However its chemistry is strongly related to that of nitric oxide.

The basic reaction scheme of the oxides of nitrogen appears to be (Nicolet, 1965a,b) as follows:

$$N_2 + h\nu \rightarrow N_2(a^1 \pi g) \quad (1200 < \lambda < 1250)$$

$$\xrightarrow{j_{10}} N + N \qquad (10)$$

$$N + O_3 \xrightarrow{k_{11}} NO + O_2 \qquad (11)$$

$$N + O + M \xrightarrow{k_{12}} NO + M \qquad (12)$$

$$N + O_2 \xrightarrow{k_{13}} NO + O \qquad (13)$$

$$NO + h\nu \xrightarrow{j_{14}} N + O \qquad (14)$$

$$N + NO \xrightarrow{j_{15}} O + N_2 \qquad (15)$$

$$NO + O_3 \xrightarrow{k_{16}} NO_2 + O_2 \qquad (16)$$

$$NO + h\nu \xrightarrow{I_{17}} NO^+ + e \qquad (17)$$

Rate coefficients for these reactions are given in Table 2.

TABLE 2

Reaction rate coefficients for the oxides of nitrogen

Reaction	Reaction Rate Coefficient	Source
$N + O_3 \xrightarrow{k_{11}} NO + O_2$	5.7×10^{-13}	Phillips and Schiff (1962)
$N + O + M \xrightarrow{k_{12}} NO + M$	$1.1 \times 10^{-33} (\frac{T}{300})^{-0.5 \pm 0.2}$	Kaufman (1968)
$N + O_2 \xrightarrow{k_{13}} NO + O$	$(1.4 \pm 0.2) \times 10^{-11}$ $\exp - (\frac{7100 \pm 400}{RT})$	Clyne and Thrush (1961)
$N + NO \xrightarrow{k_{15}} O + N_2$	$(2.2 \pm 0.6) \times 10^{-11}$	Phillips and Schiff (1962)
$NO + O_3 \xrightarrow{k_{16}} NO_2 + O_2$	$9.5 \times 10^{-13} \exp-(\frac{2450 \pm 150}{RT})$	Clyne *et al.* (1964)
	$R = 1.987$ K cal (°K mole)	

Mesospheric distribution of NO obtained by using the above-mentioned radiation scheme give values much lower than the experimental data obtained by Barth (1966) and Pearce (1968). A possible way of explaining high values of NO concentration around 80 km is by taking into account vertical downward motions of NO from the lower thermosphere as discussed recently by Geisler and Dickinson (1968). Large amounts of nitric oxide can be produced below 120 km by the ion-molecule reaction:

$$O_2^+ + N_2 \xrightarrow{k_{18}} NO^+ + NO \qquad (18)$$

as shown by Ryan (1968).

2.4 Hydrogenous Compounds

The basic hydrogenous compound in the atmosphere below 90 km is water vapor. The only experimental data available on the concentration of water vapor are the data by Fedynskii et al. (1967) which show very large values in the mesosphere up to an altitude of approximately 85 km. Water vapor is dissociated by solar radiation of wavelength less than 2400Å:

$$H_2O + h\nu \xrightarrow{j_{19}} OH + H \quad . \qquad (19)$$

Both atomic hydrogen and hydroxyl are chemically very active and are capable of undergoing a very complex series of reactions with atomic oxygen and ozone. The problem of the presence and distribution of hydrogenous compounds in the mesosphere and stratosphere has been studied in detail by Hesstvedt (1964, 1965, 1968). The chemistry of water vapor is closely related to the chemistry of oxygen. For example, the reaction:

$$H + O_3 \overset{k_{20}}{\rightarrow} OH + O_2 \qquad (20)$$

is capable of reducing the concentration of ozone in the mesosphere as indicated originally by Nicolet (1964) and shown by Hunt (1966b).

Other basic reactions of hydrogen and hydrogenous compounds are:

$$OH + O \overset{k_{21}}{\rightarrow} H + O_2 \qquad (21)$$

$$H + O_2 + M \overset{k_{22}}{\rightarrow} HO_2 + M \qquad (22)$$

$$HO_2 + O \overset{k_{23}}{\rightarrow} OH + O_2 \qquad (23)$$

$$HO_2 + h\nu \overset{k_{24}}{\rightarrow} OH + O \qquad (24)$$

$$HO_2 + O_3 \overset{k_{25}}{\rightarrow} OH + 2\,O_2 \qquad (25)$$

Table 3 gives the rate coefficients of these reactions. Hydrogen peroxide is an additional compound that could be present in the mesosphere but in very small concentration. Its presence gives rise to a large number of secondary reactions. A very detailed chemical scheme has been given recently by Hesstvedt (1968). In the same paper, theoretical models of hydrogen and hydrogenous compounds, distributions are shown. As a comment to these models,it should be noted that when dynamical vertical transport is taken into account, the dominant hydrogenous constituent is water vapor up to a height of about 85 km. This fact indicates that H and OH (both very active and important for the oxygen chemistry) are less abundant than expected, reducing their effect on the distribution of other species.

TABLE 3

Reaction rate coefficients for hydrogen and hydrogeneous compounds

Reaction	Reaction Rate Coefficient	Source
$H + O_3 \xrightarrow{k_{20}} OH + O_2$	$(2.6 \pm 0.5) \times 10^{-11}$	Phillips and Schiff (1962)
$OH + O \xrightarrow{k_{21}} H + O_2$	$(5 \pm 2) \times 10^{-11}$	Kaufman (1968)
$H + O_2 + M \xrightarrow{k_{22}} HO_2 + M$	$3 \times 10^{-32} (\frac{273}{T})^{1.3}$	Schofield (1967)
$HO_2 + O \xrightarrow{k_{23}} OH + O_2$	$\geq 10^{-11}$	Kaufman (1964)
$HO_2 + O_3 \xrightarrow{k_{25}} OH + 2O_2$	$\sim 10^{-14}$ (estimate)	Hunt (1963)

2.5 Carbon Dioxide

The importance of carbon dioxide in the heat balance of the region below 90 km has been recognized for a long time (Gowan 1947a,b). In their study of the photochemistry of the atmospheric CO_2, Bates and Witherspoon (1952) deduced that carbon dioxide should be in constant mixing ratio up to 100 km, approximately. A recent discussion of the role of CO_2 in the mesosphere has been given by Craig (1965). However, no detailed calculations have been made of the distribution variations that can be expected. Also, no direct measurements of this constituent above the troposphere are available at this time.

The photochemistry of CO_2 can be expressed basically by the reactions:

$$CO_2 + h\nu \xrightarrow{j_{27}} CO + O \quad (\lambda<1690\text{Å}) \tag{27}$$

$$CO + O + M \xrightarrow{k_{28}} CO_2 + M \tag{28}$$

Carbon dioxide absorption cross sections are smaller by an order of magnitude with respect to the equivalent molecular oxygen cross sections. The rate coefficient k_{28} is still doubtful, (Kaufman, 1968) but is considered very slow. At 293°K Clyne and Thrush (1962) found $K_{28} < 8 \times 10^{-35}$.

In summary, it can be said that the chemistry of atmospheric carbon oxides is at this time practically unknown.

3. RATES OF IONIZATION

3.1 Introduction

Several sources of ionization can act in the atmosphere below 90 km. The most important one is considered to be, at this time, solar Lyman-alpha radiation ionizing nitric oxide. However, the uncertainties about the mesospheric concentration of this constituent which were mentioned in the last chapter, make difficult a correct estimate of the relative importance of Lyman-alpha and other radiation in the ionization of the D region. Solar X-rays and ultraviolet radiation of 1027-1118Å wavelengths between 85 and 90 km, and cosmic rays below 70 km, are capable of ionizing the atmospheric gas. At night, scattered Lyman-alpha radiation and precipitated electrons could be effective sources of ionization between 70 and 90 km.

3.2 Ionization by Solar Lyman-Alpha

A very intense radiation is emitted from the sun at a wavelength of 1215.7Å. Its photon flux is equal, for average low solar activity, to 2.7 photons cm^{-2} sec^{-1} equivalent to 6 erg cm^{-2} sec^{-1}. The hydrogen Lyman-alpha line originates in the absorbing region between the photosphere and the chromosphere. The kinetic energy of solar protons in that region is lost through the radiative recombination with electrons. Lyman-alpha radiation is mostly absorbed by O_2 and an interesting fact is that one of the absorption "windows" of molecular oxygen atmosphere corresponds to the same wavelength as shown in Figure 11. The corresponding absorption cross section is $\sigma_{O2} = 1.04 \times 10^{20}$ cm^2 (Watanabe, 1958), Lyman-alpha radiation can penetrate as low as 65-70 km. The only atmospheric constituent that can be ionized by this radiation, below 90 km, is nitric oxide, and it becomes a strong

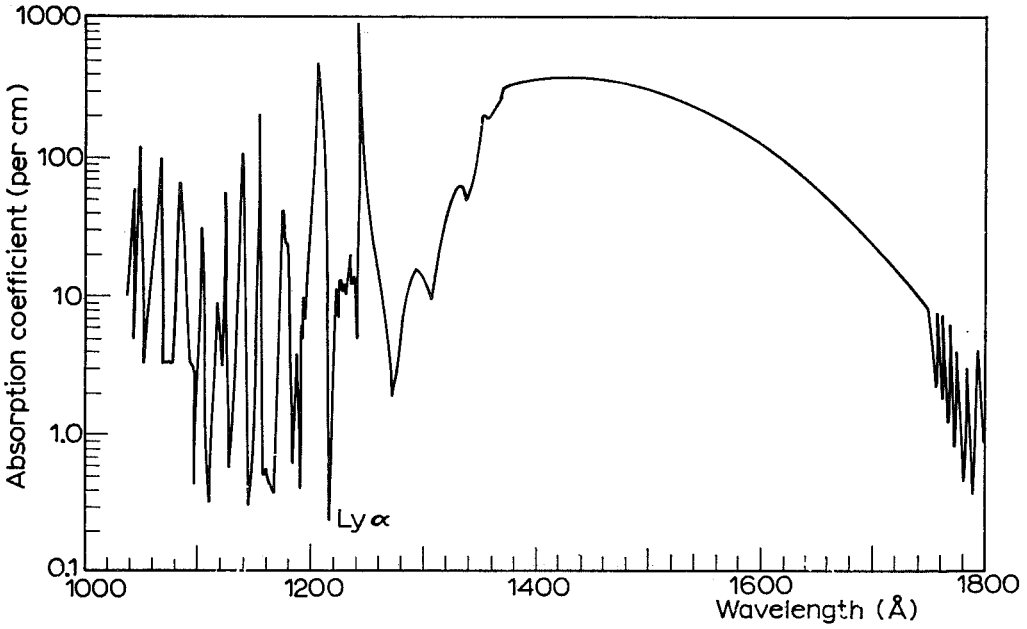

Figure 11. Absorption coefficient of molecular oxygen in the far ultraviolet (Watanabe, et al., 1953).

source of ionization in the D region. NO ionization cross section is $\sigma'_{NO} = 2 \times 10^{-18}$ cm^2 (Watanabe, 1954). With cross section and flux data it is possible to compute the rate of NO ionization by Lyman-alpha. This is done by using the expression:

$$q_{L\alpha}(h) = \sigma'_{NO}[NO] \exp(- \sec \chi \, \sigma_{O_2} \int_h^\infty d[O_2] \, d\, h) \qquad (29)$$

where $q_{L\alpha}$ indicates the rate of ionization, h the altitude, brackets indicate concentration, and χ is the solar zenith angle. Sec χ is substituted by the Chapman function for angles greater than 80°.

By using Mitra (1968) and Pearce (1968) nitric oxide distributions shown in Figure 3, different rates are computed and are drawn in Figure 12. The Pearce data results in a very large rate of ionization which overdraw the effects of X-rays and in part, of cosmic rays as effective sources of ionization as will be seen below.

3.3 Ionization by X-Rays

Quasi-thermal X-ray emissions of wavelength < 100Å originates in the corona of the sun. This radiation is highly variable as is shown in Figure 13, reproduced from de Jager (1967).

Solar X-rays of wavelength between 1 and 40Å can penetrate in the D region down to an altitude of 50 km, ionizing all the constituents of the mesosphere. However, the low photon fluxes available during low solar activity are not capable of producing important ionization below 85 km. Under such conditions the X-ray contribution to the formation of the D region is limited to its upper part. During solar flares when the X-ray fluxes increase by several orders of magnitude, this radiation increases greatly the ionization of all the D region.

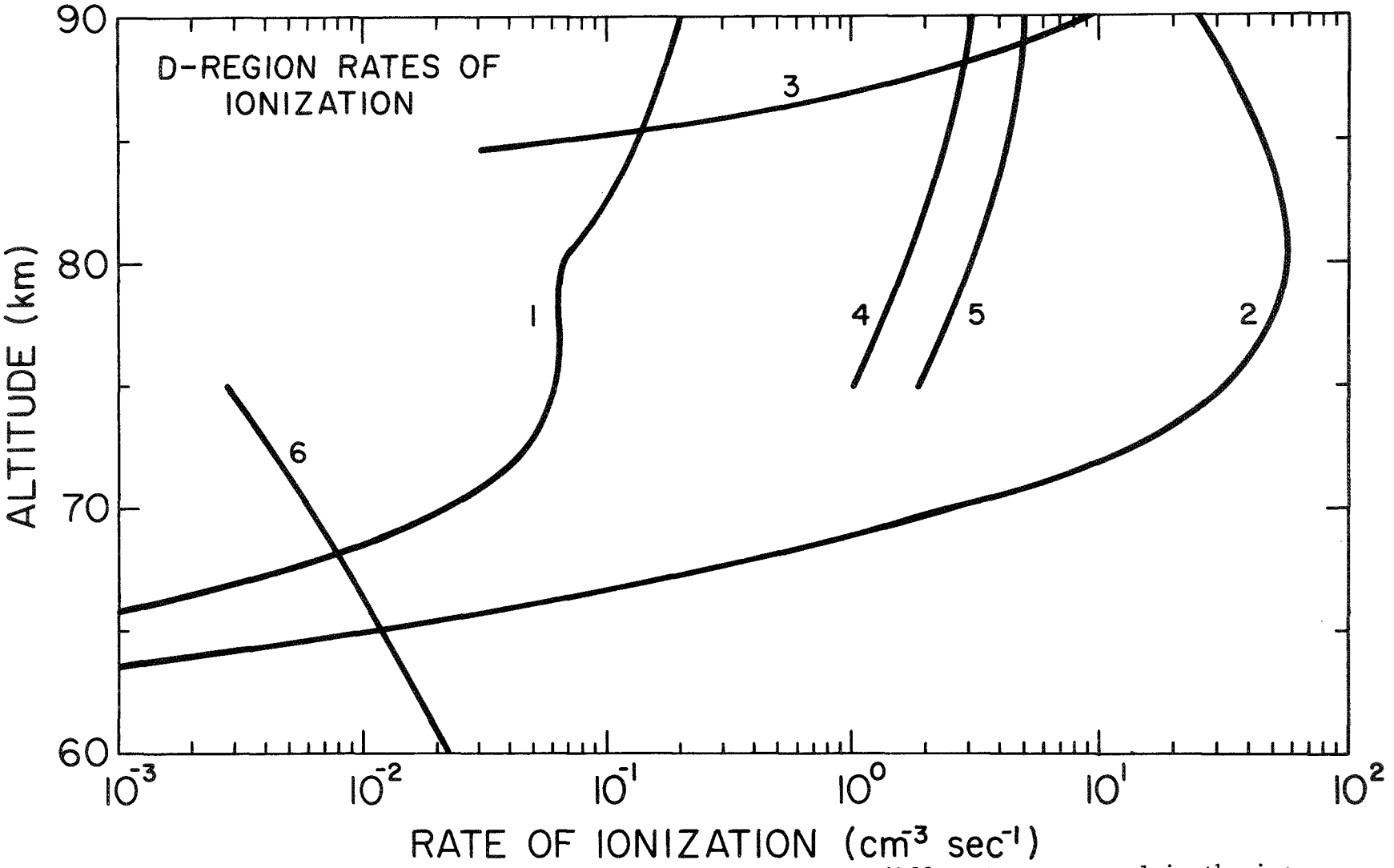

Figure 12. Daytime D-region rates of ionization due to different sources. 1 is the ion-pair production by Lα radiation on NO concentration given by Mitra (1968). 2 is ionization of NO with Pearce (1968) distribution. 3 is x-ray ion-pair production from Ohshio, et al. (1966) and Hinterreger, et al. (1965). 4 and 5 are rates of ionization of $O_2(^1\Delta g)$ given by Hunten and McElroy (1968).

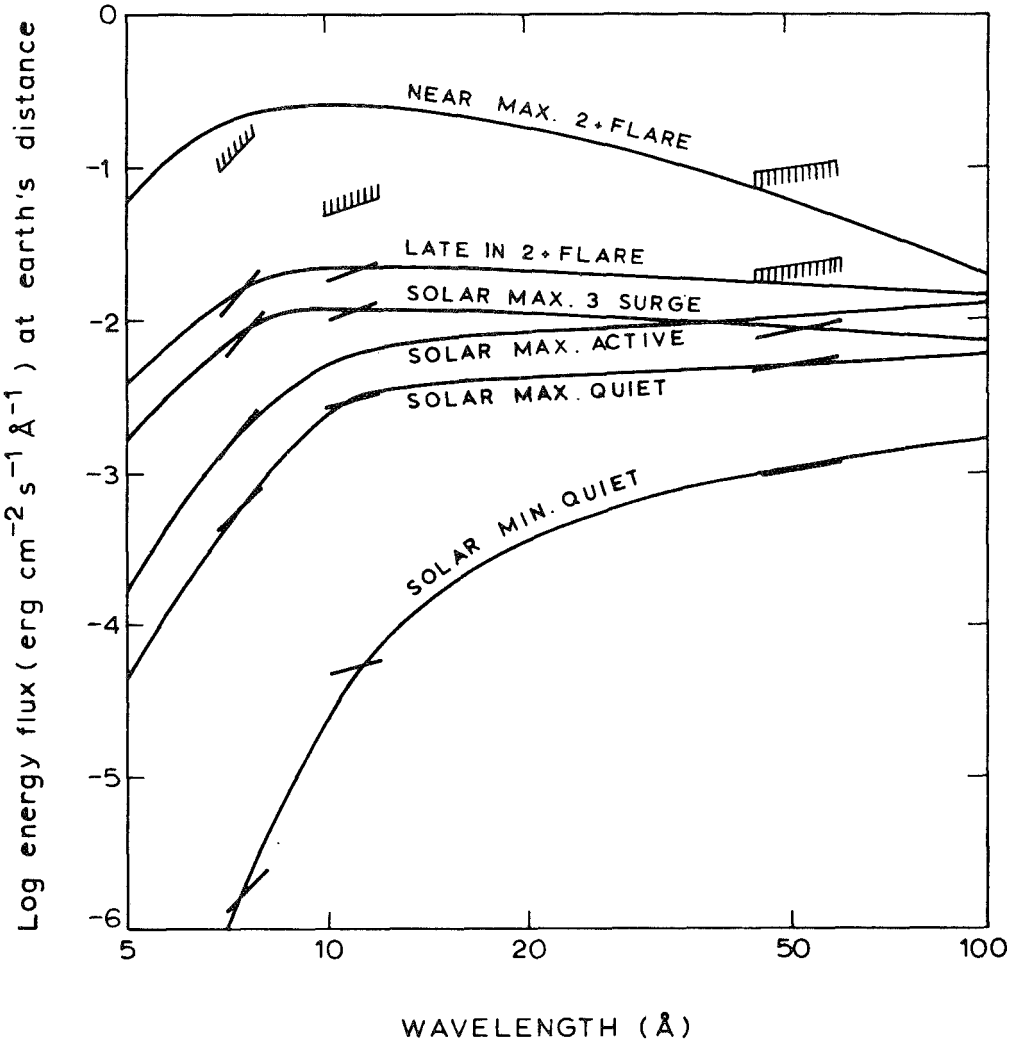

Figure 13. Solar x-ray emission for various solar conditions. The curves drawn are based on measurements in three wavelength bands, as indicated by the heavy bar segments. The slopes of the bar segments are the slopes of the assumed x-ray emission functions used to reduce the photometer responses to the plotted energy fluxes. The energy fluxes refer to values observed at the earth's distance above the atmosphere (from H. Friedman, 1963).

A summary of the absorption and ionization cross sections for X-rays and O_2 and N_2 has been given by Hinterreger et al. (1965) and are reproduced in Table 4, together with their estimates of photon fluxes for quiet conditions of low solar activity. From these data the rate of ionization due to X-rays of wavelength from 1 to 40Å, can be computed by using the expression:

$$q_{XR}(h, \chi) = \sum_i \sum_j \sigma_{ij} [X]_j \exp - \sec \chi_j \sum \sigma_{ij} \int_h^\infty [X]_j \, dh \qquad (31)$$

where i represents wavelength, j constituent, and the other symbols have been defined above. Ohshio et al. (1966) using Hinterreger et al. (1965) cross sections, computed the rate of ionization produced by a unit photon flux for all solar radiation. They included the band from 1 to 40Å X-rays. With their data and the fluxes of Table 4, the rate of ionization for undisturbed low solar activity are also shown in Figure 7.

3.4 Ionization of Metastable Molecular Oxygen

Recently (Hunten and McElroy, 1968) it has been suggested that a major source of ionization in the upper D region could be the ionization of the metastable species $O_2(^1\Delta g)$ by solar ultraviolet radiation on the wavelength band 1027-1184Å. Ionization of the metastable molecular oxygen requires less energy than the non-excited O_2. Experimental measurements of $O_2(^1\Delta g)$ shows that its concentration is large in the mesosphere as is shown in Figure 14, taken from Hunten and McElroy, (1968). The rate of ionization obtained by the same authors is also shown in Figure 12.

3.5 Ionization by Precipitated Electrons

It is known that the auroral excitation and ionization in the lower ionosphere is produced mostly by the precipitation of energetic electrons in the atmosphere (Hultqvist, 1965 and references therein). Electrons

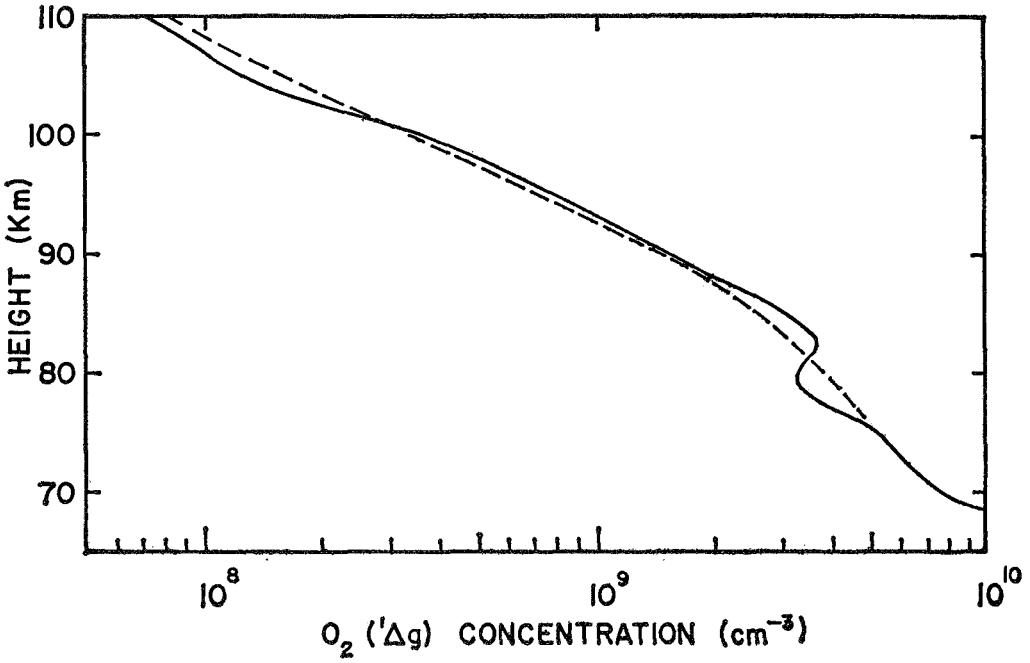

Figure 14. The concentrations of $O_2(^1\Delta g)$ above 70 km, from the dayglow measurement of Evans, et al. (1968). The smooth version shown dashed was used for the calculations in this paper.

TABLE 4

Absorption and ionization coefficients for O_2 and N_2 in the X-ray region

Wavelength Region or line (Å)	Photon Energy (eV)	Flux (10^9 ph cm^{-2} s^{-1})	Flux (erg cm^{-2} s^{-1})	Effective Cross Sections (10^{-18} cm^2) Total O_2	Total N_2	Ionization O_2	Ionization N_2
41 - 31	300-400	0.15	0.083	0.2	0.07	0.2	0.07
31 - 22.8	400-540	5×10^{-3}	0.005	0.09	1.0	0.09	1.0
22.8 - 15	540-830	3×10^{-3}	0.003	0.7	0.36	0.7	0.36
15 - 10	830-1240	5×10^{-4}	0.001	0.27	0.15	0.27	0.15
10 - 5	1240-2480	1.5×10^{-4}	0.001	0.075	0.045	0.075	0.045
5 - 3	2480-4140	2×10^{-6}	$<10^{-5}$	0.012	0.0065	0.012	0.0065
3 - 1	4140-12400	10^{-8}	$<10^{-7}$	0.002	0.0015	0.002	0.0015

precipitating in the region of the South Atlantic anomaly (Ghielmetti et al., 1965; Paulikas et al., 1966 and references therein) can be a substantial source of ionization in that area, both at night and in the day (Zmuda, 1966).

In July 1964, O'Brien et al. (1965) measured for the first time simultaneously, both the flux of precipitating electrons ($E \geq 40$ keV) and nightglow emissions including the 3914Å line using rocket techniques. On that occasion, they recorded a flux of 40 electron cm^{-2} sec^{-1}. Tulinov (1967) and Tulinov et al. (1969) have measured directly the flux of daytime and nighttime energetic particles with a system of Geiger counters aboard rockets. Values of particles fluxes as a function of latitude obtained are shown in Figure 15. The same author computed the rate of ionization that is drawn in Figure 16. The figure also shows the rate of ionization computed by using O'Brien et al. (1965) particle flux and assumed spectrum. This computation has been carried out by using the formulation of Lazarev (1967) which is essentially the same as developed by Rees (1963) but more adequate for a complete computation.

It has been shown (Radicella, 1968) that nighttime ionization in the upper D region can be explained assuming ionization by electron precipitation. His computations were based upon a chemical scheme that will be discussed in the next chapter and on the rate of nighttime ionization given by Ivanov-Kholodyny (1965). By using the same formulation given by Radicella (1968) and the rate of ionization obtained from O'Brien et al. (1965) data, the electron density shown in Figure 17 is computed. The figure also shows an experimental profile measured by Mechtly and Smith (1968a). It can be seen that measured electron precipitation can produce at night the necessary ionization in the upper D region.

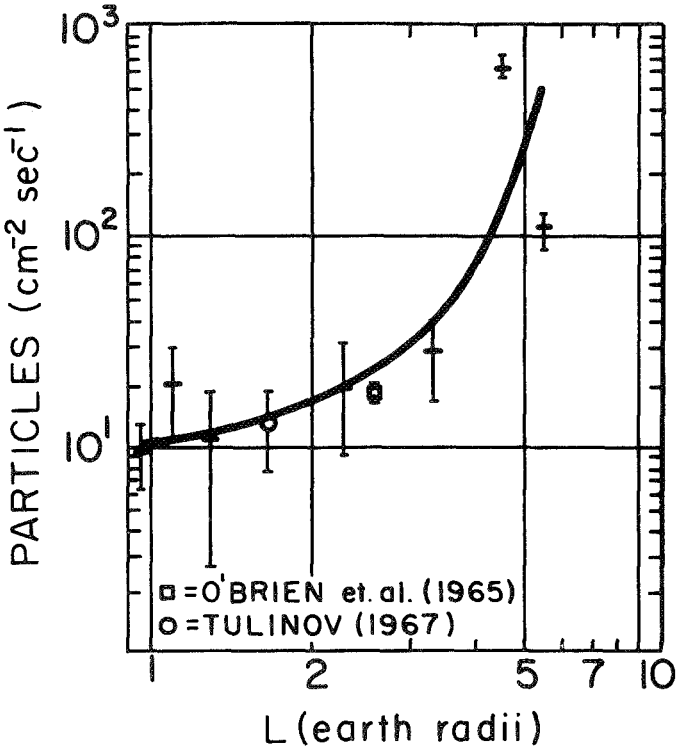

Figure 15. Flux measurements of precipitating energetic particles.

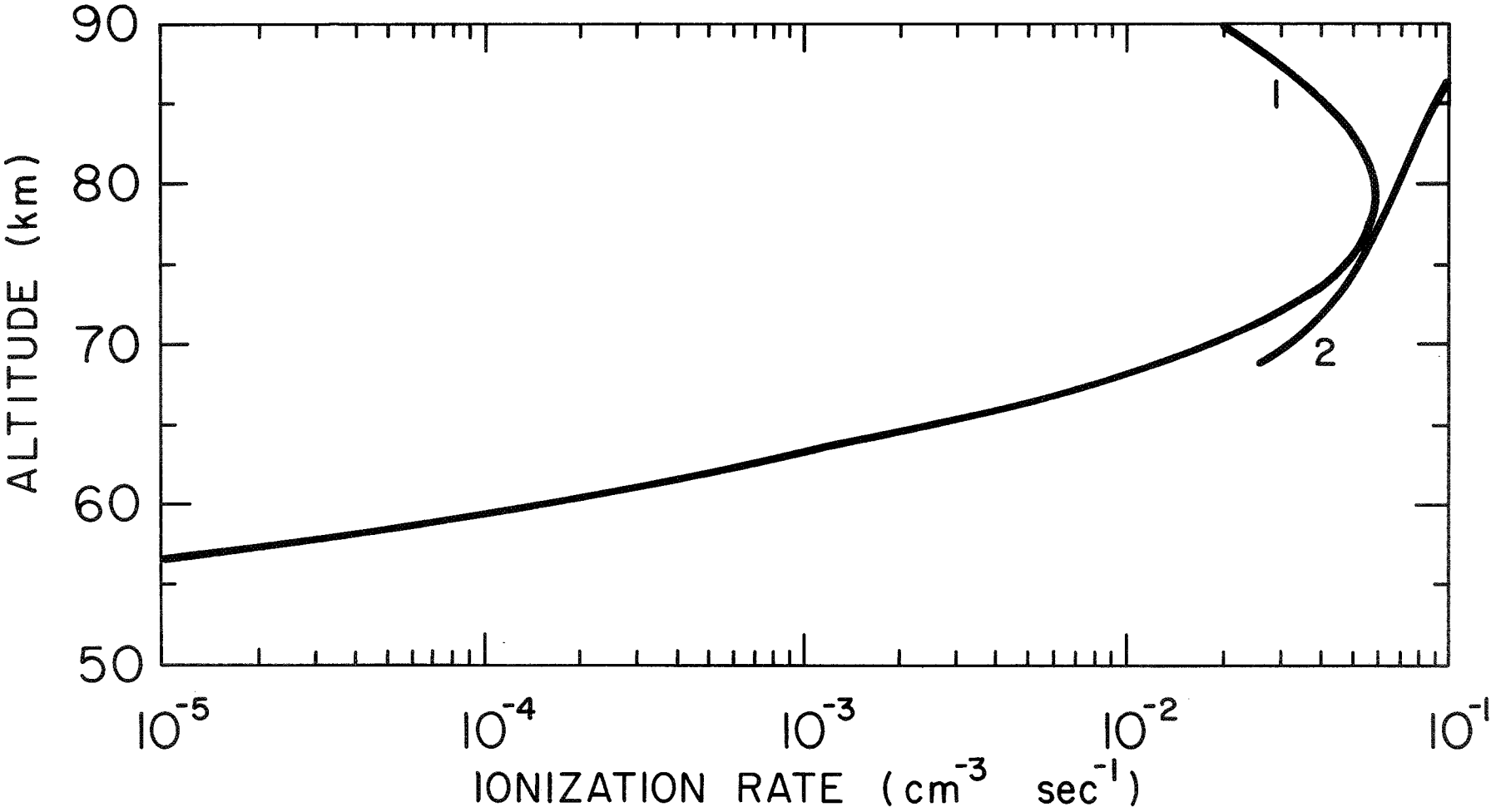

Figure 16. 1 Rate of ionization computed from O'Brien, et al. (1965) measured electron fluxes and estimated spectrum. 2 Tulinov, et al. (1968) rate of ionization from precipitated electrons.

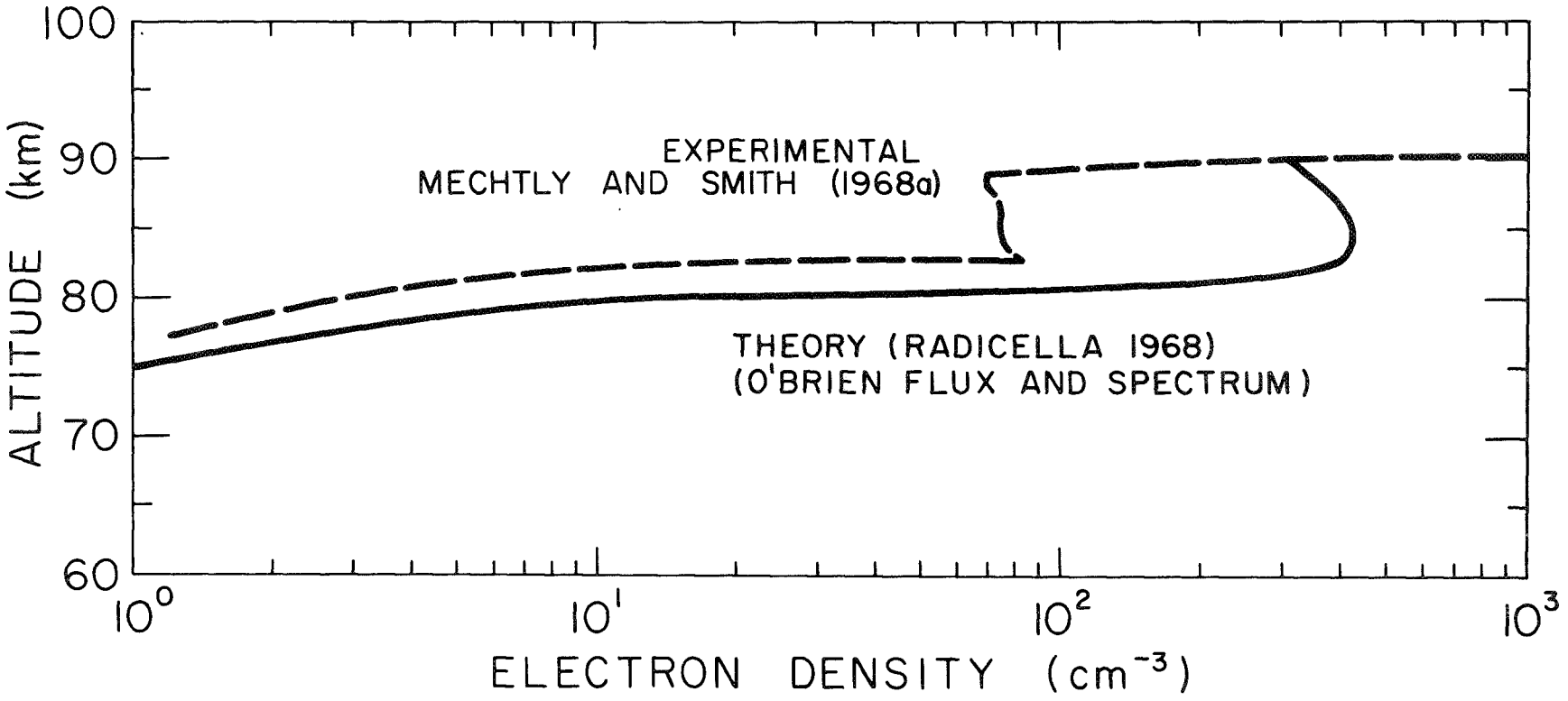

Figure 17. Comparison of experimental and theoretical electron densities in the nighttime D region.

3.6 Ionization by Cosmic Rays

Almost forty years ago Hulburt (1930) used Millikan's measurements to compute ionization by cosmic radiation in the region below 60 km. Nicolet and Aikin (1960), in their early theory of the D region, attributed the ionization of the lower part of that region to galactic cosmic rays. Values of the rate of ionization produced by galactic cosmic rays is shown also in Figure 7. The computed values were obtained by using the empirical relation given by Arnold and Pierce (1963):

$$q = 1.5 \times 10^{-18}[M] \cos^{-4} \theta[1 - \frac{3}{22}(y = 1964)] \qquad (32)$$

where

q = ion pair production (cm^{-3} sec^{-1})

θ = geomagnetic latitude

y = year

$[M]$ = neutral gas density.

4. NEGATIVE-ION CHEMISTRY IN THE D REGION

4.1 Laboratory Measurements of Negative-Ion Reaction Rates

On the basis of the known laboratory measurements of attachment reactions and mesospheric composition it appears that the basic process of negative-ion formation in the D region is:

$$e + O_2 + O_2 \xrightarrow{k_{33}} O_2^- + O_2 \qquad (33)$$

with a rate coefficient (Phelps, 1967):

$$k_{33} = 1.4 \times 10^{-29} \left(\frac{300}{T}\right) e^{-\frac{600}{T}} .$$

Other three-body attachment reactions involving minor constituents are unimportant. Reaction:

$$e + O_3 \xrightarrow{k_{34}} O^- + O_2 \qquad (34)$$

is very slow (Fehsenfeld and Ferguson, 1968) and as a result, O^- is not considered as an initial negative ion of importance. It should be considered also that binary attachment reactions involving heavy neutrals like NO_3 could have rate coefficients as high as 10^{-7} cm^{-3} sec^{-1}.

Molecular oxygen negative ions are short lived because electrons can be detached from them by collision with atomic and excited species, and because they can charge exchange with neutral molecular species.

The only abundant atomic species in the D region is atomic oxygen which reacts rapidly with O_2^-:

$$O_2^- + O \xrightarrow{k_{35}} O_3 + e \qquad (35)$$

where $k_{34} = 3 \times 10^{-10}$ (Fehsenfeld et al., 1967). Also the excited species $O_2(^1\Delta g)$ detaches electrons through:

$$O_2^- + O_2(^1\Delta g) \xrightarrow{k_{36}} 2\ O_2 + e \qquad (36)$$

where $k_{36} = 2 \times 10^{-10}$ (E. E. Ferguson, 1968 private communication).

Recently, several charge exchange reactions have been measured in the laboratory. In particular:

$$O_2^- + O_3 \xrightarrow{k_{37}} O_3^- + O_2 \qquad (37)$$

$$O_2^- + NO_2 \xrightarrow{k_{38}} NO_2^- + O_2 \qquad (38)$$

where $k_{37} = 3 \times 10^{-10}$ (Fehsenfeld et al., 1967) and $k_{38} = 1 \times 10^{-9}$ (Fehsenfeld and Ferguson, 1968; Rutherford and Turner, 1967).

The reaction:

$$O_2^- + NO \xrightarrow{k_{39}} NO_2^- + O \qquad (39)$$

suggested by Nicolet (1965b) has been found to be slow in laboratory measurements, Ferguson (1967). At this time, reaction (35) appears as the basic charge exchange for O_2^-. Reaction 36 could be important only at night below 70 km where it will eventually provide an effective process in formation of NO_2^-.

Possible three-body reactions leading to the formation of heavy and stable negative ions should be investigated in the laboratory because of their potential importance at D-region heights. Experimental observations of negative ions spectra Narcisi (1968), for example, suggest the presence of heavy negative ions below 100 km.

Negative ion O_3^- can exchange its charge with molecular species:

$$O_3^- + CO_2 \xrightarrow{k_{40}} CO_3^- + O_2 \qquad (40)$$

$$O_3^- + NO \xrightarrow{k_{41}} NO_3^- + O \qquad (41)$$

where $k_{40} = 4 \times 10^{-10}$ and $k_{41} = 1 \times 10^{-11}$ at room temperature, as found by Fehsenfeld et al., (1967). Reaction (40) is always more effective than reaction (41) because the ratio $[CO_2]/[NO]$ is much larger than one below 90 km, also if the large values estimated by Barth (1966) and Pearce (1968) are accepted.

NO_3^- is a stable negative ion. This is not the case with CO_3^- which can react with atomic oxygen regenerating O_2^- as shown by Fehsenfeld et al., (1967)

$$CO_3^- + O \xrightarrow{k_{42}} O_2^- + CO_2 \qquad (42)$$

where $k_{42} = 8 \times 10^{-11}$.

Another possible reaction is:

$$CO_3^- + NO \xrightarrow{k_{43}} NO_2^- + CO_2 \qquad (43)$$

where $k_{11} = 9 \times 10^{-12}$ (Fehsenfeld et al., 1967). Reaction (42) is more effective than (43) if:

$$[O] >> \frac{k_{43}}{k_{42}} [NO] \cong 10^{-1} [NO] \quad .$$

It can be said safely that above 55 km during daytime and above 70 km at night, reaction (42) is the main charge exchange process of CO_3^-. However,

the formation of O_2^- by (42) and the rapid detachment that takes place through reactions (35) and (36), tend to produce an excess of electrons below 90 km during both daytime and nighttime, contrary to the experimental evidence. To avoid this difficulty in studying nighttime D region, Radicella (1968) postulated another fast charge exchange reaction dealing with a stable negative ion, suggested originally by Whitten and Poppoff (1964):

$$O_3^- + N_2 \xrightarrow{k_{44}} NO_2^- + NO \quad , \tag{44}$$

assuming $k_{44} = 10^{-13 \pm 1}$. However, F. C. Fehsenfeld (private communication 1968) studied this reaction in the laboratory and found it to be very slow ($k_{44} < 10^{-15}$ cm^{-3} sec^{-1}) at room temperature.

It must be noticed, however, that the final implicit equation used by Radicella (1968) in order to compute nighttime electron-density profiles for steady-state conditions (see his Appendix 2, Equation A12) is independent of the particular reaction that produces the stable negative ion. That equation is formally identical with equation below.

Final processes that involve electrons and stable negative ions in the D region are recombination and mutual neutralization. The rate coefficient for dissociative recombination:

$$e + XY^+ \xrightarrow{k_{13}} X + Y \tag{45}$$

has been analyzed recently by Biondi (1967).

A value of $k_{45} = 7 \times 10^{-7}$ at 200°K (D-region temperature) with a temperature dependence of the type T^{-1} appears to be reasonable, when $XY^+ \equiv NO^+$.

The present experimental knowledge about the rate of mutual neutralization:

$$M^- + XY^+ \xrightarrow{k_{46}} \text{neutrals} \qquad (46)$$

is not very good. However, a rate coefficient $k_{46} = 4 \times 10^{-8}$ for atmospheric ions has been measured by Hirsch et al. (1967) and this value agrees with the theoretical estimate of $k_{46} = 5 \times 10^{-8}$ by Baulknight and Bortner (1964).

A summary of the rate coefficients of negative-ion reactions is given in Table 5. In the above discussion, we confined our attention on a rather reduced number of reactions involving the major constituents and the minor constituents of larger concentration. A simple inspection of the rate coefficients for the many negative-ion reactions involving the known minor atmospheric consituents including hydrogenous compounds. (DASA Reaction Rate Handbook: 1967) shows that they are of very little importance in the negative-ion chemistry of the normal D region.

4.2 General Schemes of D-Region Negative-Ion Chemistry

Let reaction (33) be the initial step in the formation of negative ions. Time variations of the ionic species at a given altitude can be written:

$$\frac{d[e]}{dt} = \sum q + \delta[O_2^-][P_1] - \beta[e][M]^2 - \alpha_e[e][XY^+] \qquad (47)$$

$$\frac{d[O_2^-]}{dt} = \beta[e][M]^2 - \delta[O_2^-][P_1] - \gamma\,[O_2^-][P_2] \qquad (48)$$

$$\frac{d[M^-]}{dt} = \gamma\,[O_2^-][P_2] - \alpha_i[XY^+][M^-] \qquad (49)$$

where brackets indicate concentrations, e indicates electron, P_1, P_2.... are neutral molecules or atoms, M is the atmospheric gas as a whole, N^- is the final molecular stable negative ion, XY^+ is the general molecular positive ion, and $\sum q$ is the ion pair porduction rate due to the sum of all possible sources of ionization. α_e, α_i, β, γ, δ are, respectively, rate coefficients of recombination, mutual neutralization, attachment, charge exchange and detachment. It can be assumed also that:

$$[XY^+] \approx [e] + [N^-] \tag{50}$$

because the stable negative ion will be always more abundant than other intermediate negative ions like O_2^-. When:

$$\frac{d[e]}{dt} = \frac{d[O_2^-]}{dt} = \frac{d[M^-]}{dt} = 0 \tag{51}$$

is assumed, i.e. when steady-state conditions are considered, solutions of Equations (47), (48) and (49) will not be changed if intermediate charge exchange reactions take place. The steady-state solution of Equation (48) gives:

$$[O_2^-] = \frac{\beta[M]^2[e]}{\gamma[P_1]+\delta[P_2]} \quad . \tag{52}$$

By substitution in 47 the following equation is obtained:

$$\sum q - \frac{\gamma[P_2]}{\delta[P_1]+\gamma[P_2]} \beta[M]^2[e] - \alpha_e[XY^+][e] = 0 \tag{53}$$

or:

$$\sum q - \beta_{eff}[e] - \alpha_e[XY^+][e] = 0 \tag{54}$$

where:

$$\beta_{eff} = \frac{\gamma[P_2]}{\delta[P_1]+\gamma[P_2]}\,\beta[M]^2 \tag{55}$$

can be called an "effective attachment factor". Taking into account Equation (50), it can be written:

$$\sum q - (\beta_{eff} + \alpha_e[N^-])[e] - \alpha_e[e]^2 = 0 \tag{56}$$

$$\beta_{eff}[e] - \alpha_i[e][N^-] - \alpha_i[N^-]^2 = 0 \quad . \tag{57}$$

This system of equations can be solved in terms of e and N^- if the ion-pair function and coefficients are known. An implicit equation in β_{eff} is written as follows:

$$[e] = \frac{\sum q}{\alpha_e \left\{ \frac{[e]}{2} + \sqrt{\frac{[e]^2}{4} + \beta_{eff}\frac{[e]}{\alpha_i}} \right\} + \beta_{eff}} \tag{58}$$

which is formally equal to Equation A12 of Radicella (1968). If the electron density is known an implicit equation in β_{eff} is:

$$\beta_{eff} = \frac{\sum q}{[e]} - \alpha_e \left\{ \frac{[e]}{2} + \sqrt{\frac{[e]^2}{4} + \beta_{eff}\frac{[e]}{\alpha_i}} \right\} \tag{59}$$

Equations (47) to (49) have been written considering only the detachment process with a rate $\delta[P_1][O_2^-]$. If an additional process with a rate $\delta'[P_1'][O_2^{1}]$ is taken into account, reactions (56) and (57) are formally maintained, but now is:

$$\beta_{ef} = \frac{\gamma[P_2]}{\delta[P_1] + \delta'[P_1'] + \gamma[P_2]} \beta[M]^2 \qquad (60)$$

If the charge exchange with rate $\gamma[P_2][O_2^-]$ is such that:

$$\gamma\ [P_2] >> \delta\ [P_1]$$

Equation (23) reduces to:

$$\beta_{eff} = \beta[M]^2 \qquad (61)$$

Another possibility appears if the charge exchange reaction or chain of reactions is not capable of producing a large concentration of stable negative ions. The effect will be:

$$\beta_{eff} << \beta\ [M]^2 \qquad (62)$$

that is equivalent, in terms of electron density, to reducing Equation (26) to:

$$[e] = \sqrt{\frac{\Sigma q}{\alpha_e}} \quad . \qquad (63)$$

A final case results if an additional attachment process is postulated with a rate $\beta^1[X]$, where X is an unknown constituent, and such that Equation (23) becomes:

$$\beta_{eff} = \beta'[X] + \frac{\gamma[P_2]}{\delta[P_1] + \gamma[P_2]} \beta[M]^2 \approx \beta'[X] \quad . \qquad (64)$$

From the above discussion it is clear that each of the different forms of β_{eff} reflects a different negative-ion scheme. It is possible now to analyze

the problem of the apparent contradictions between daytime-measured electron densities and NO concentration. If measured NO concentration (Pearce, 1968) is accepted together with reactions (33), (34), (35), (36), (37), (40), (41), (42), (43), (45), and (46), which represent the most accepted set, and which will refer as the "basic schemes", the effective attachment factor will be written as:

$$\beta_{eff} = 1 \frac{\dfrac{k_{43}[NO]}{k_{43}[NO] + k_{42}[O]}}{\dfrac{[O] + \frac{2}{3}[O_2(^1\Delta g)]}{[O_3]} + \dfrac{k_{43}[NO]}{k_{43}[NO] + k_{42}[O]}} k_{33}[O_2]^2 \qquad (65)$$

As it is mentioned before, during daytime, above 55-60 km, and at night above 70-75 km:

$$k_{42}[O] >> k_{43}[NO] \quad ,$$

Then:

$$\beta_{eff} \approx \frac{\dfrac{k_{43}[NO]}{k_{42}[O]}[O_3]}{[O] + \frac{2}{3}[O_2(^1\Delta g)] + \dfrac{k_{43}[NO]}{k_{42}[O]}[O_3]} k_{33}[O_2]^2 \qquad (66)$$

where:

$$\frac{\dfrac{k_{43}[NO]}{k_{42}[O]}[O_3]}{[O] + \frac{2}{3}[O_2(^1\Delta g)] + \dfrac{k_{43}[NO]}{k_{42}[O]}[O_3]} << 1 \quad . \qquad (67)$$

This case corresponds then to the condition given by Equation (63). The electron distribution can be computed by using Equations (58) and (66) and the ion-pair production rate given in Chapter 2 when Pearce (1968) NO

concentration is adopted. The result is shown in Figure 18 together with experimental data and it can be seen that below 85 - 90 km the electron density is much larger than expected on the basis of experimental evidence (Mechtly and Smith, 1968b).

By using the basic sequence plus an additional fast charge exchange of the type given by Radicella (1968):

$$O_3^- + X \xrightarrow{k_{36}} X^- + O_3 \tag{68}$$

where:

$$k_{68}[X] >> k_{46}[CO_2] \quad .$$

The effective attachment factor will be:

$$\beta_{eff} = \frac{[O_3]}{[O] + [O_3] + \frac{2}{3}[O_2(^1\Delta g)]} \; k_{33}[O_2]^2 \tag{69}$$

which is equivalent to Equation (60). Again by using (58) and (69) the electron density is computed and it is shown in Figure 19. Once more, this theoretical computation shows a larger electron density than what expected experimentally. This is also the case if a fast charge exchange reaction of the type:

$$O_2^- + X \xrightarrow{k_{70}} X^- + O_2 \tag{70}$$

such that:

$$k_{70}[X] >> k_{35}([O] + \frac{2}{3}[O_2(^1\Delta g)])$$

is accepted. The effective attachment factor reduces then to:

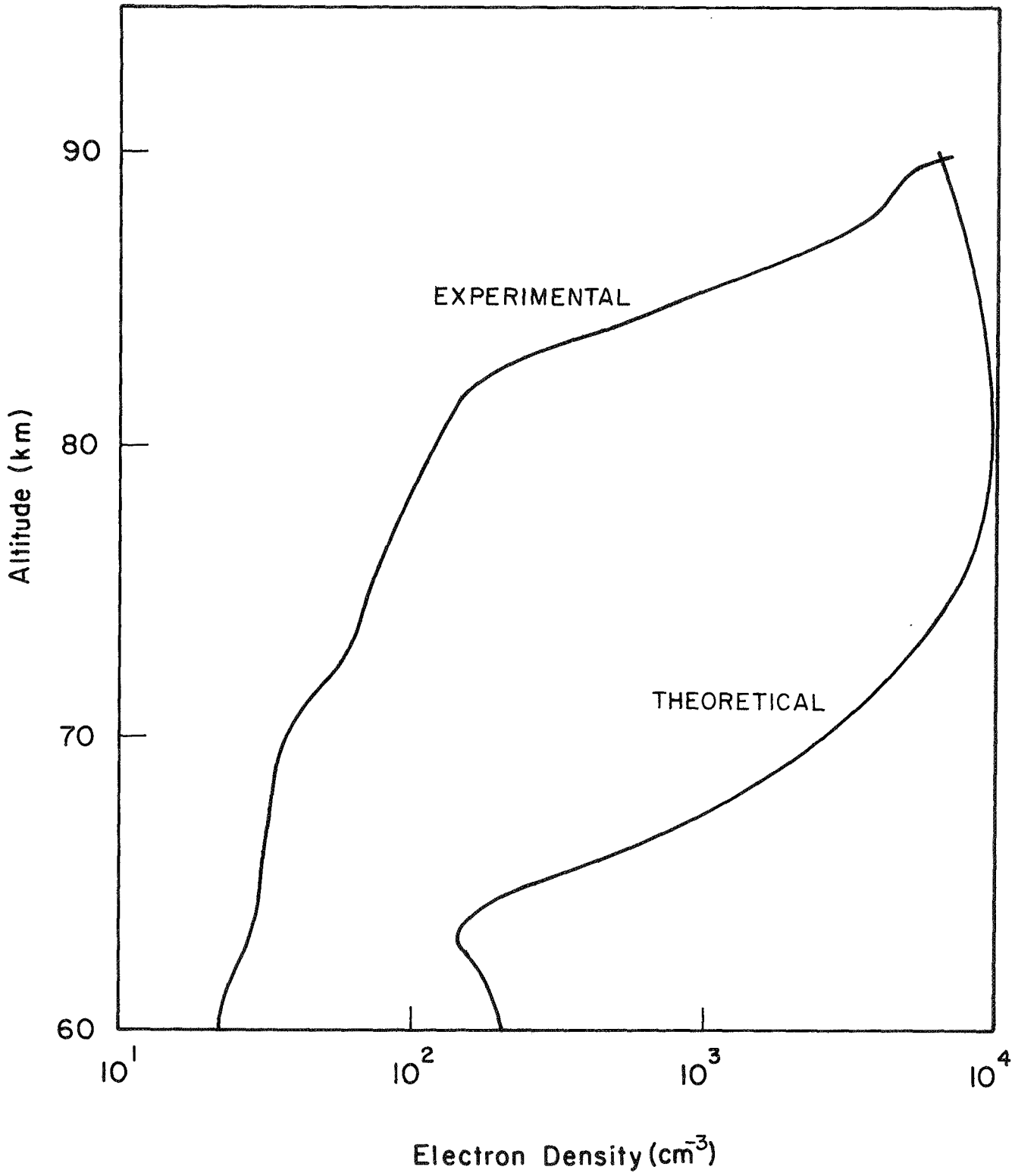

Figure 18. Comparison of daytime electron densities. Experimental by Mechtly and Smith (1968b); theoretical from Equations (58) and (66) and NO concentration by Pearce (1968).

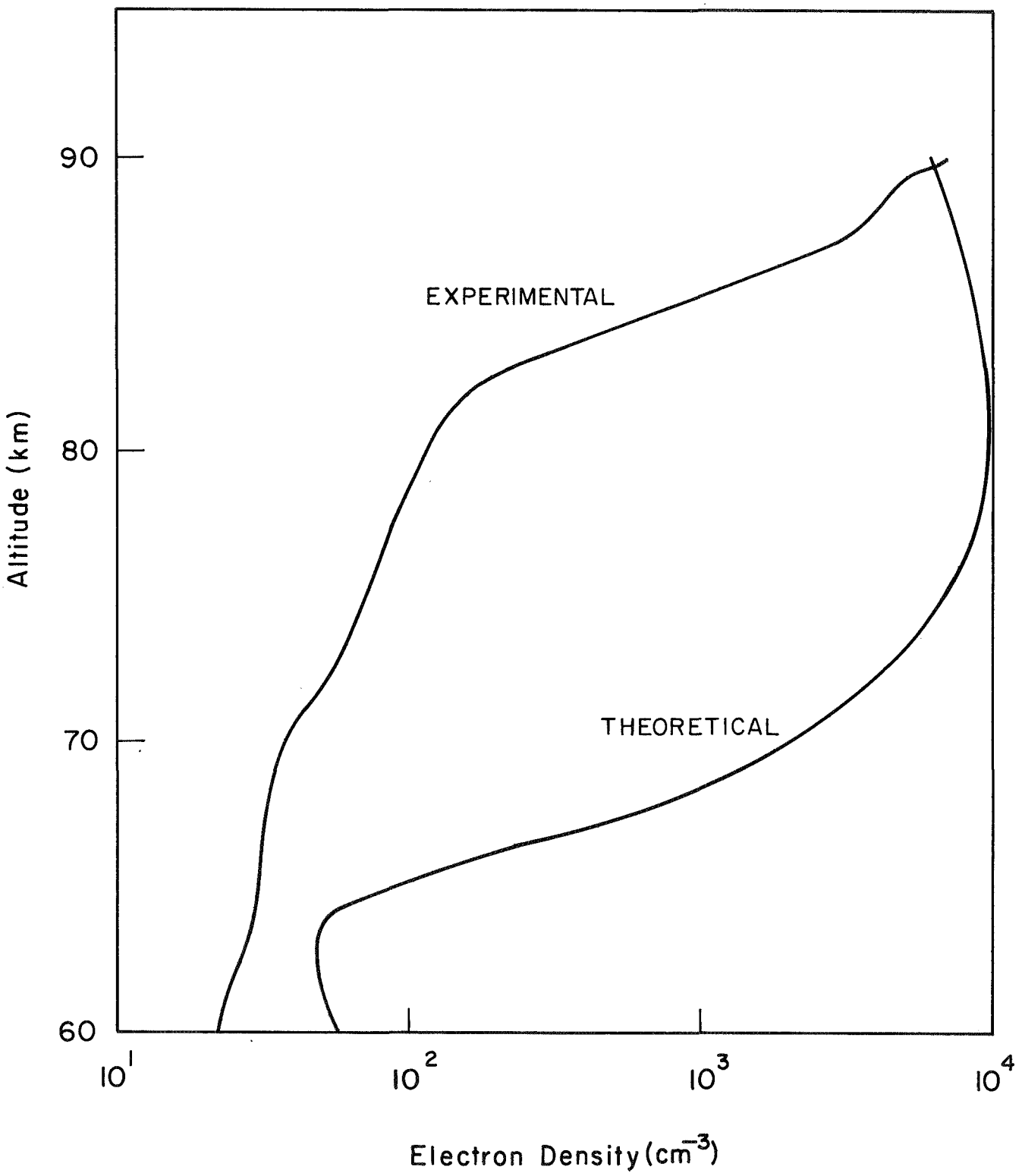

Figure 19. Comparison of daytime electron densities. Experimental by Mechtly and Smith (1968b); theoretical from Equations (58) and (69) and NO concentration by Pearce (1968).

$$\beta_{eff} = k_{33}[O_2]^2 \tag{71}$$

which is formally equal to Equation (61). The computed electron density for this case is shown in Figure 20 and again no agreement is reached with the experimental data.

The only possibility left in order to obtain an agreement between the experimental electron density and the measured NO concentration is to search for new attachment reactions faster than the attachment to O_2 between 70 and 90 km. This is done by means of β_{eff}. It can be computed by using Equation (59), daytime experimental values of [NO] and [e], and accepted deionization coefficients. The effective attachment factor can be also derived theoretically from (69) and (71). Figure 21 shows these computed values of β_{eff}. It can be seen that the profile based upon experimental data, is quite different from the two theoretical profiles. The only way to conciliate experimental values of [NO] and [e] and theoretical computation is to postulate a binary attachment reaction of the type:

$$e + ZW \xrightarrow{k_{49}} Z^- + Y \tag{72}$$

where Z^- is a stable negative ion and such that:

$$k_{72}[ZW] >> k_{33}[O_2]^2$$

or:

$$\beta_{eff} = k_{72}[ZW]$$

which corresponds to Equation (64).

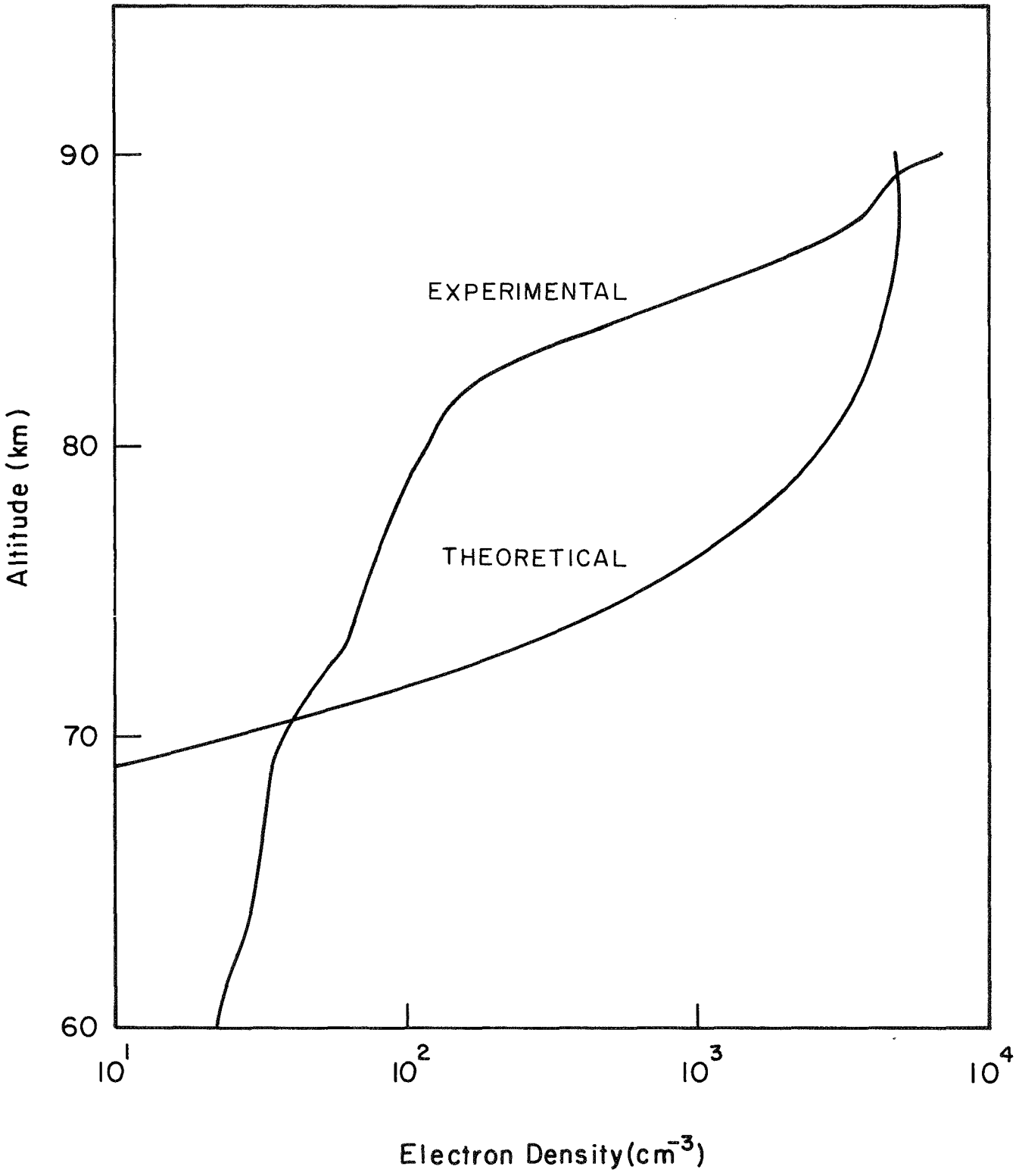

Figure 20. Comparison of daytime electron densities. Experimental by Mechtly and Smith (1968b); theoretical from Equations (58) and (71) and NO concentration by Pearce (1968).

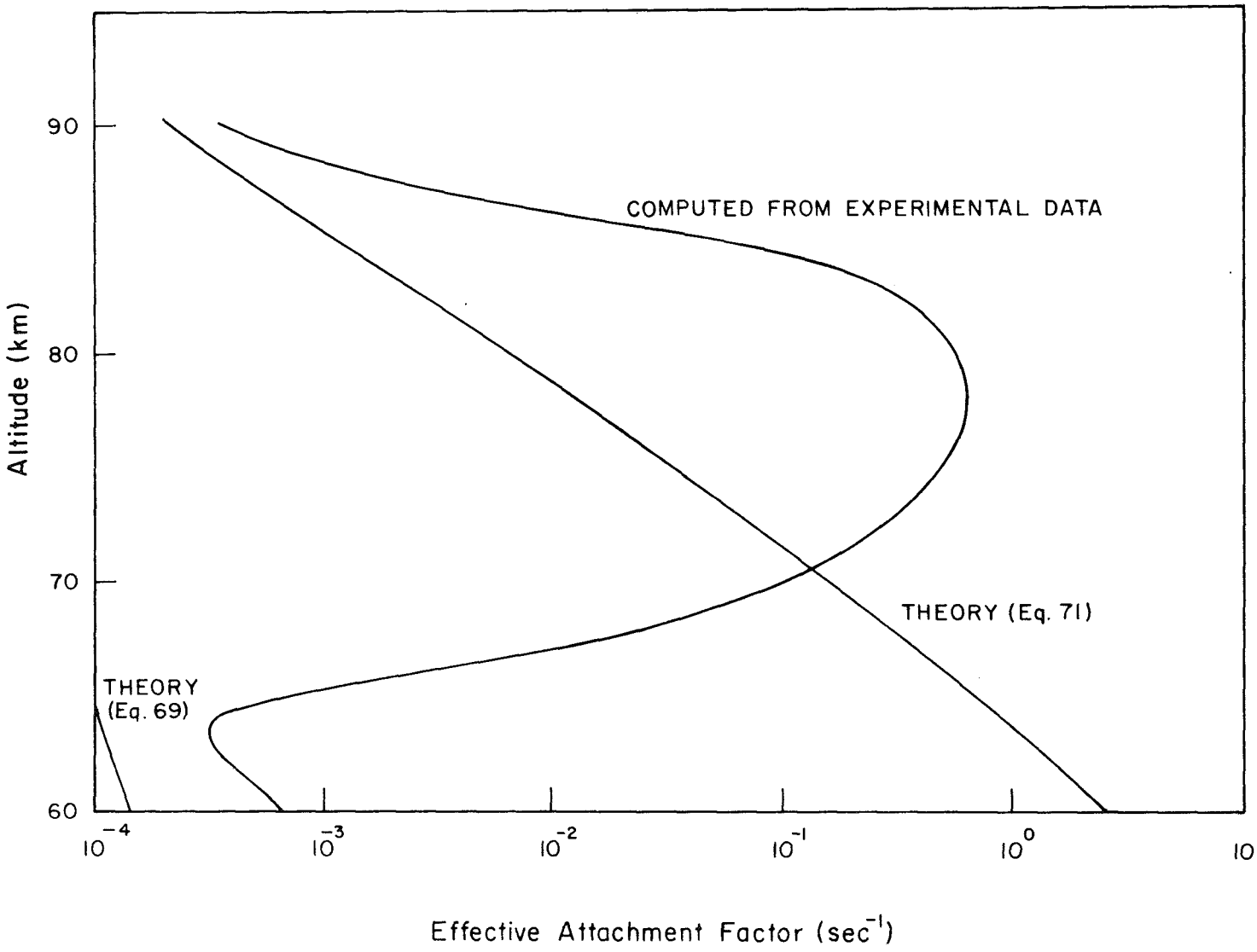

Figure 21. Comparison of effective attachment values. Computed from experimental data of Mechtly and Smith (1968b) and Pearce (1968) and from Equations (69) and (71).

Accepting reaction (72) where [ZW] could be a heavy neutral, and a tentative rate coefficient $k_{72} \sim 10^{-7}$ cm^{-3} sec^{-1}, β_{eff} experimental in Figure 21 will indicate that the specie [ZW] would be a minor constituent with a peak concentration of $\sim 5 \times 10^{6}$ at around 80 km. Such a minor contamination at that height could be accepted, but its eventual nature is at this time unpredictable. Possible conglomerates of neutral particle in the region of low temperature could form heavy neutrals.

In summary it can be said, that the negative-ion chemistry can be represented by an effective attachment coefficient β_{eff} as shown by Equation (54) which takes different forms depending upon the negative-ion processes involved. To conciliate the high values of [NO] given by Pearce (1968) with experimental values of electron density and recombination, and mutual neutralization rates, a new attachment process must be postulated. This should be able to form a stable negative ion and could be a fast binary reaction involving heavy neutral molecular compounds or conglomerates formed under the low temperature conditions of the D region. However, further complications appear in the lower mesosphere where the experimental values of β_{eff} suggest the existence of fast detachment reactions.

APPENDIX I

1. SOURCES OF DATA

1.1 Introduction

The computations for the oxygen atmosphere were based on Equations (7) and (8) of the text. The values of k_3, k_4 and k_5 were taken from the Kaufman adopted data in Table 1.

The O_2 and O_3 absorption cross sections and the solar photon flux are tabulated in Table A1. The same data is shown graphically in Figures 3 and 4 of the text. A list of the references from which the cross sections and fluxes were taken is given in Table A2. The solar flux is the unattenuated photon flux outside the earth's atmosphere. The data numbers in Table A2 refer to those in Table A1. Below 2425Å the O_2 absorption cross sections are very small according to Hunt (1963) SAD 123, so corrections below 2425 Å are assumed to be zero for these calculations. Between 1775 Å and 1975 Å the solar flux was read from a graph in the Handbook of Physics at 5 Å intervals. These values were then averaged over 50 Å intervals to give an average flux for each 50 Å interval.

1.2 Neutral Atmosphere Parameters [O2], [M]

The attenuation of solar radiation as it passes through the atmosphere depends on the number of absorbing molecules between the altitude of interest and the outside of the earth's atmosphere. For these calculations O_2 was assumed to be the only species which significantly attenuated the solar flux. From 300 to 120 km, the values of $[O_2]$ were obtained from the U.S. Standard Atmosphere Supplement 1966 for the 3 cases: Winter Model, Exospheric Temperature = 1000°K, Summer Model, Exospheric Temperature = 1000°K, and Spring/Fall Model, Exospheric Temperature = 1000°K.

Below 120 km it was necessary to convert the absolute atmospheric density

Table A1

DATUM NUMBER	CENTRAL WAVELENGTH (Å)	WAVELENGTH INTERVAL (Å)	PHOTON FLUX PER INTERVAL (phot. cm^{-2} sec^{-1} $\Delta Å^{-1}$)	PHOTON FLUX PER ANGSTROM (phot. cm^{-2} sec^{-1} $Å^{-1}$)	O2 ABSORB. CROSS-X (cm^{-2})	O3 ABSORB. CROSS-X (cm^{-2})
1	1215.	1.0	2.700D 11	2.700E 11	1.100D-20	3.500D-17
2	1400.	50.0	1.830D 10	3.660E 08	1.450D-17	7.000D-18
3	1450.	50.0	3.700D 10	7.400E 08	1.480D-17	4.500D-18
4	1500.	50.0	7.300D 10	1.460E 09	1.280D-17	3.500D-18
5	1550.	50.0	1.330D 11	2.660E 09	8.800D-18	2.500D-18
6	1600.	50.0	2.600D 11	5.200E 09	4.870D-18	1.100D-18
7	1650.	50.0	4.200D 11	8.400E 09	2.370D-18	9.000D-19
8	1700.	50.0	7.000D 11	1.400E 10	1.020D-18	9.000D-19
9	1750.	50.0	1.060D 12	2.120E 10	3.080D-19	8.500D-19
10	1775.	2.5	6.088D 10	2.435E 10	2.530D-20	8.000D-19
11	1780.	5.0	1.275D 11	2.550E 10	1.700D-20	7.900D-19
12	1785.	5.0	1.328D 11	2.656E 10	1.630D-20	7.900D-19
13	1790.	5.0	1.394D 11	2.788E 10	1.770D-20	7.800D-19
14	1795.	5.0	1.407D 11	2.814E 10	2.080D-20	7.800D-19
15	1800.	5.0	1.515D 11	3.030E 10	1.200D-20	7.700D-19
16	1805.	5.0	1.587D 11	3.174E 10	2.670D-20	7.700D-19
17	1810.	5.0	1.660D 11	3.320E 10	1.170D-20	7.600D-19
18	1815.	5.0	1.733D 11	3.466E 10	1.190D-20	7.500D-19
19	1820.	5.0	1.806D 11	3.612E 10	1.180D-20	7.400D-19
20	1825.	5.0	1.880D 11	3.760E 10	4.500D-21	7.300D-19
21	1830.	5.0	1.977D 11	3.954E 10	7.040D-21	7.200D-19
22	1835.	5.0	2.061D 11	4.122E 10	6.340D-21	7.100D-19
23	1840.	5.0	2.150D 11	4.300E 10	1.430D-21	7.000D-19
24	1845.	5.0	2.248D 11	4.496E 10	5.630D-21	6.900D-19
25	1850.	5.0	2.347D 11	4.694E 10	6.640D-21	6.800D-19
26	1855.	5.0	2.447D 11	4.894E 10	1.480D-21	6.700D-19
27	1860.	5.0	2.570D 11	5.140E 10	1.570D-21	6.550D-19
28	1865.	5.0	2.671D 11	5.342E 10	5.070D-21	6.400D-19
29	1870.	5.0	2.819D 11	5.638E 10	2.030D-21	6.250D-19
30	1875.	5.0	2.921D 11	5.842E 10	4.400D-22	6.100D-19
31	1880.	5.0	3.070D 11	6.140E 10	1.450D-21	5.950D-19
32	1885.	5.0	3.197D 11	6.394E 10	1.770D-21	5.800D-19
33	1890.	5.0	3.348D 11	6.696E 10	3.560D-22	5.650D-19
34	1895.	5.0	3.500D 11	7.000E 10	2.060D-22	5.500D-19
35	1900.	5.0	3.628D 11	7.256E 10	6.370D-22	5.300D-19
36	1905.	5.0	3.781D 11	7.562E 10	8.280D-22	5.200D-19
37	1910.	5.0	3.935D 11	7.870E 10	3.980D-22	5.100D-19
38	1915.	5.0	4.138D 11	8.276E 10	1.880D-22	5.000D-19
39	1920.	5.0	4.293D 11	8.586E 10	4.300D-22	4.800D-19
40	1925.	5.0	4.450D 11	8.900E 10	6.450D-22	4.700D-19
41	1930.	5.0	4.655D 11	9.310E 10	2.280D-22	4.600D-19
42	1935.	5.0	4.862D 11	9.724E 10	1.200D-22	4.500D-19
43	1940.	5.0	4.972D 11	9.944E 10	9.440D-23	4.400D-19
44	1945.	5.0	5.278D 11	1.056E 11	1.800D-22	4.300D-19
45	1950.	5.0	5.438D 11	1.088E 11	1.980D-22	4.200D-19
46	1955.	5.0	5.649D 11	1.130E 11	8.870D-23	4.100D-19
47	1960.	5.0	5.860D 11	1.172E 11	5.850D-23	3.900D-19
48	1965.	5.0	5.974D 11	1.195E 11	5.970D-23	3.750D-19
49	1970.	5.0	6.286D 11	1.257E 11	1.030D-22	3.600D-19
50	1975.	2.5	3.250D 11	1.300E 11	8.850D-23	3.450D-19
51	2000.	50.0	7.035D 12	1.407E 11	1.300D-23	3.300D-19
52	2050.	50.0	9.271D 12	1.854E 11	1.100D-23	3.520D-19
53	2100.	50.0	1.530D 13	3.060E 11	9.600D-24	5.490D-19
54	2150.	50.0	2.593D 13	5.186E 11	7.900D-24	9.860D-19
55	2200.	50.0	3.427D 13	6.854E 11	6.400D-24	1.750D-18
56	2250.	50.0	3.957D 13	7.914E 11	4.600D-24	2.890D-18
57	2300.	50.0	4.161D 13	8.322E 11	3.100D-24	4.450D-18
58	2350.	50.0	3.779D 13	7.558E 11	1.800D-24	6.250D-18
59	2400.	50.0	4.100D 13	8.200E 11	1.000D-24	8.050D-18
60	2450.	50.0	4.802D 13	9.604E 11	0.0	9.800D-18
61	2500.	50.0	4.774D 13	9.548E 11	0.0	1.090D-17
62	2550.	50.0	7.176D 13	1.435E 12	0.0	1.130D-17
63	2600.	50.0	9.146D 13	1.829E 12	0.0	1.080D-17
64	2650.	50.0	1.332D 14	2.664E 12	0.0	9.560D-18
65	2700.	50.0	1.696D 14	3.392E 12	0.0	7.770D-18
66	2750.	50.0	1.520D 14	3.040E 12	0.0	5.700D-18
67	2800.	50.0	1.688D 14	3.376E 12	0.0	3.840D-18
68	2850.	50.0	2.435D 14	4.870E 12	0.0	2.440D-18
69	2900.	50.0	3.789D 14	7.578E 12	0.0	1.390D-18
70	2950.	50.0	4.670D 14	9.340E 12	0.0	7.440D-19
71	3000.	50.0	4.598D 14	9.196E 12	0.0	3.840D-19
72	3050.	50.0	5.134D 14	1.027E 13	0.0	1.960D-19
73	3100.	50.0	5.920D 14	1.184E 13	0.0	1.020D-19
74	3150.	50.0	6.490D 14	1.298E 13	0.0	5.360D-20
75	3200.	50.0	6.834D 14	1.367E 13	0.0	2.940D-20
76	3250.	50.0	8.329D 14	1.666E 13	0.0	1.460D-20
77	3300.	50.0	9.535D 14	1.907E 13	0.0	7.040D-21
78	3350.	50.0	9.343D 14	1.869E 13	0.0	3.820D-21
79	3400.	50.0	9.482D 14	1.896E 13	0.0	1.940D-21
80	3450.	50.0	1.014D 15	2.028E 13	0.0	7.040D-22
81	3500.	50.0	1.038D 15	2.076E 13	0.0	2.740D-22
82	4750.	500.0	2.506D 16	5.012E 13	0.0	4.800D-22
83	5250.	500.0	2.575D 16	5.150E 13	0.0	2.060D-21
84	5750.	500.0	2.757D 16	5.514E 13	0.0	3.980D-21
85	6250.	500.0	2.698D 16	5.396E 13	0.0	3.660D-21
86	6750.	500.0	2.602D 16	5.204E 13	0.0	1.530D-21
87	7250.	500.0	2.474D 16	4.948E 13	0.0	5.230D-22

TABLE A2

Ø2 Absorption Cross Sections

Data Numbers	Wavelength	Source
1-50	1215Å, 1375Å-1975Å	A
51-87	1975Å-3525Å, 4500Å-7500Å	B

Ø3 Absorption Cross Sections

Data Numbers	Wavelength	Source
1-10	1215Å, 1375Å-1775Å	C
15,25,35,45	1800Å, 1850Å, 1900Å, 1950Å	D
51-87	1975Å-3525Å, 4500Å-7500Å	D

Between 1775Å and 1975Å, all cross sections not listed in this table are smooth curve interpolations of Hunt's data.

Solar Flux

Data Numbers	Wavelength	Source
1-50	1215Å, 1375Å-1975Å	E
51-81	1975Å-3525Å	F
82-87	4500Å-7500Å	G

TABLE A2 SUPPLEMENT

A. Huffman, Robert E., DASA Reaction Rate Handbook, October 1967, Chapter 10, PHOTOCHEMICAL PROCESSES, page 10-7, Values read from graph, General Electrical Company Missile and Space Division, Space Sciences Lab., Philadelphia, Penn.

B. Hunt, B. G., Technical Note SAD 123, Weapons Research Establishment, June 1963, Adelaide, South Australia, page 22.

C. Craig, Richard A., The Upper Atmosphere, Meteorology and Physics, 1965, Academy Press, N.Y., Ed. J. Van Mieghem, page 168 read from graph, Chapter 4, The Sun's Radiation and the Upper Atmosphere.

D. Hunt, SAD 123, page 24.

E. Handbook of Geophysics, Data Numbers 1-9 from page 16-16, Data numbers 9-50 read from graph page 16-11.

F. Tousey, Richard, Space Science Reviews, Vol. 2, 1963, The Extreme Ultraviolet Spectrum of the Sun, page 22.

G. Handbook Geophysics, page 165.

given in the U. S. Standard Atmosphere Supplement 1966 to $[O_2]$ and [M] by using the mean molecular weight and the percent composition of O_2. Below 90 km the densities were converted to $[O_2]$ and [M] by assuming a constant mean molecular weight of 28.96 (CIRA 1965) and constant ratio of $[O_2]$ to [M] of .2091 for all seasons. This ratio was calculated from the 90 km values of $[N_2]$, $[O_2]$, [O], and [A] given in CIRA 1965 page 12. At 120 km the mean molecular weight and percent composition of O_2 to M for each season was calculated from data in the U. S. Standard Atmosphere Supplement 1966. Between 90 and 120 km the mean molecular weight and the percent composition were assumed to vary linearly with altitude so as to match the boundary values of 90 and 120 km. The boundary values of composition and mean molecular mass at 90 km and 120 km are given in Table A3. The resultant values of $[O_2]$ were then used to calculate the integral $\int_z^{300\ km}[O_2]dh$ which is used in the calculation of the photodissociation rates. Above 300 km $[O_2]$ contributed negligibly to the integral.

The photodissociation rate J_k of the kth constituent was calculated according to the formula:

$$J_k = \sum_\lambda \sigma k\lambda\ R_\lambda\ \exp(-\sec\chi\ \sigma_\lambda(O_2)\ \int^{300\ km}[O_2]dh)$$

where: $\sigma k\lambda$ = the average value of the photodissociation cross section of the kth constituent in the λth wavelength interval

R_λ = the total solar photon flux with wavelength in the λth interval

$\sec\chi$ = the secant of the solar zenith angle χ

$\sigma_\lambda(O_2)$ = the average absorption cross section of O_2 in the λth interval

$\int_z^{300\ km}[O_2]dh$ = the integral of the O_2 concentration from 300 km to Z, the altitude of interest.

TABLE A3

90 km	Mean Molecular Mass	Composition
Summer	28.96	20.91%
Winter	28.96	20.91%
Spring/Fall	28.96	20.91%

120 km	Mean Molecular Mass	Composition
Summer	26.76	13.17%
Winter	27.12	14.40%
Spring/Fall	26.90	13.61%

In the calculation of the photodissociation rates, it was assumed that only O_2 significantly attenuated solar radiation. It was also assumed that the quantum efficiency for O_2 and O_3 was unity; i.e. every photon absorbed by the molecule resulted in the dissociation of that molecule. Thus, the absorption cross sections are the same as the photodissociation cross sections.

1.3 Initial Values for the Oxygen Atmosphere

Initial values of O and O_3 were calculated for latitudes ranging from 45°N to 45°S in 15° intervals with a constant solar declination of 23.5°N. The appropriate temperature profiles for the rate coefficients, as well as $[O_2]$, and the $[O_2]$ integrals, were obtained from the data in U.S. Standard Atmosphere Supplement 1966. The solar zenith angle used in computing the photodissociation rates was calculated from the formula:

$$\cos\chi = \sin(\text{latitude})\sin(\text{declination}) + \cos(\text{latitude})\cos(\text{declination})$$

The steady state concentrations of O and O_3 were approximated by:

$$[O] = \left[\frac{J_2[O_2]}{[M](k_3 + \frac{k_4 k_5 [O_2]}{2J_3})}\right]^{1/2}$$

$$[O_3] = \frac{k_4[O][O_2][M]}{J_3}$$

k_3, k_4, k_5 are the Kaufman reaction rates given in Table 1 of the text.

J_2, J_3 = photodissociation rates of O_2 and O_3 respectively.

$[O]$, $[O_2]$, $[M]$, $[O_3]$ are the concentrations of O, O_2, M, and O_3, respectively.

1.4 Time-Dependent Oxygen Atmosphere

The time-dependent oxygen atmosphere used the values of $[O]$ and $[O_2]$ from the steady-state approximation as initial values. The basic data for reaction rates, temperatures, cross-sections, solar fluxes, and $[O_2]$ profiles were identical in both models. The time dependence was incorporated into the

solar zenith angle χ in the form $\cos\chi$ = sin(latitude) sin(declination) + cos(latitude) cos(declination) cos(hour angle) where the hour angle uniformly increased at the rate of 24 hours per day. An approximation to the Chapman function was used for the solar zenith angle χ between 80° and 90° to lessen errors due to the curvature of the atmosphere. The values of the Chapman function $Ch(\chi,x)$ were taken from M.V. Wiles. (In this notation χ = solar zenith angle, and $x = \frac{h+Re}{H}$ where h is the altitude of observation above the earth's surface, Re is the radius of the earth, and H is the scale height of O_2 at that altitude.) At the altitudes and densities involved, the resultant values of x were quite large, of the order of 1000. To approximate the Chapman function, the region between 80° and 90° was broken into 1° intervals. Within each interval the Chapman function was approximated quite well as a linear function of x about the value at x = 1000. When $\chi \geq 90°$ all dissociation rates were set to zero because the solar radiation must pass through very dense layers of O_2 for larger values of χ. Near sunrise and sunset the equations are only rough approximations because only absorption by O_2 is considered. In reality at sunset the sun's rays must pass through dense layers of the atmosphere so that absorption by constituents such as O_3 also becomes important. The results of the time-dependent oxygen atmosphere are depicted graphically in Figures A1 through A24. Numerical tabulations of the O and O_3 variation during a 24 hour period are given in Table A4 to A37. Profiles were computed and plotted for 90 km, 80 km, 70 km, and 60 km for each of the latitudes 45°, 30°, 15°, 0°, -15°, -30°, -45° for a constant solar declination of +23.5°, corresponding to a summer solstice in the + latitudes. In addition, profiles were computed at 85 km, 75 km, and 65 km for ±45° latitude and declination of 23.5°. The solutions for each latitude and altitude were generated until the concentration

of O_3 at successive noons was within 5% of each other or until a maximum time of 6 days was reached. At all altitudes, except 90 km, the solutions stabilized to within 5% at successive noons before six days passed, and at 90 km the profiles indicate that stabilization would have been reached within another 24 hour period.

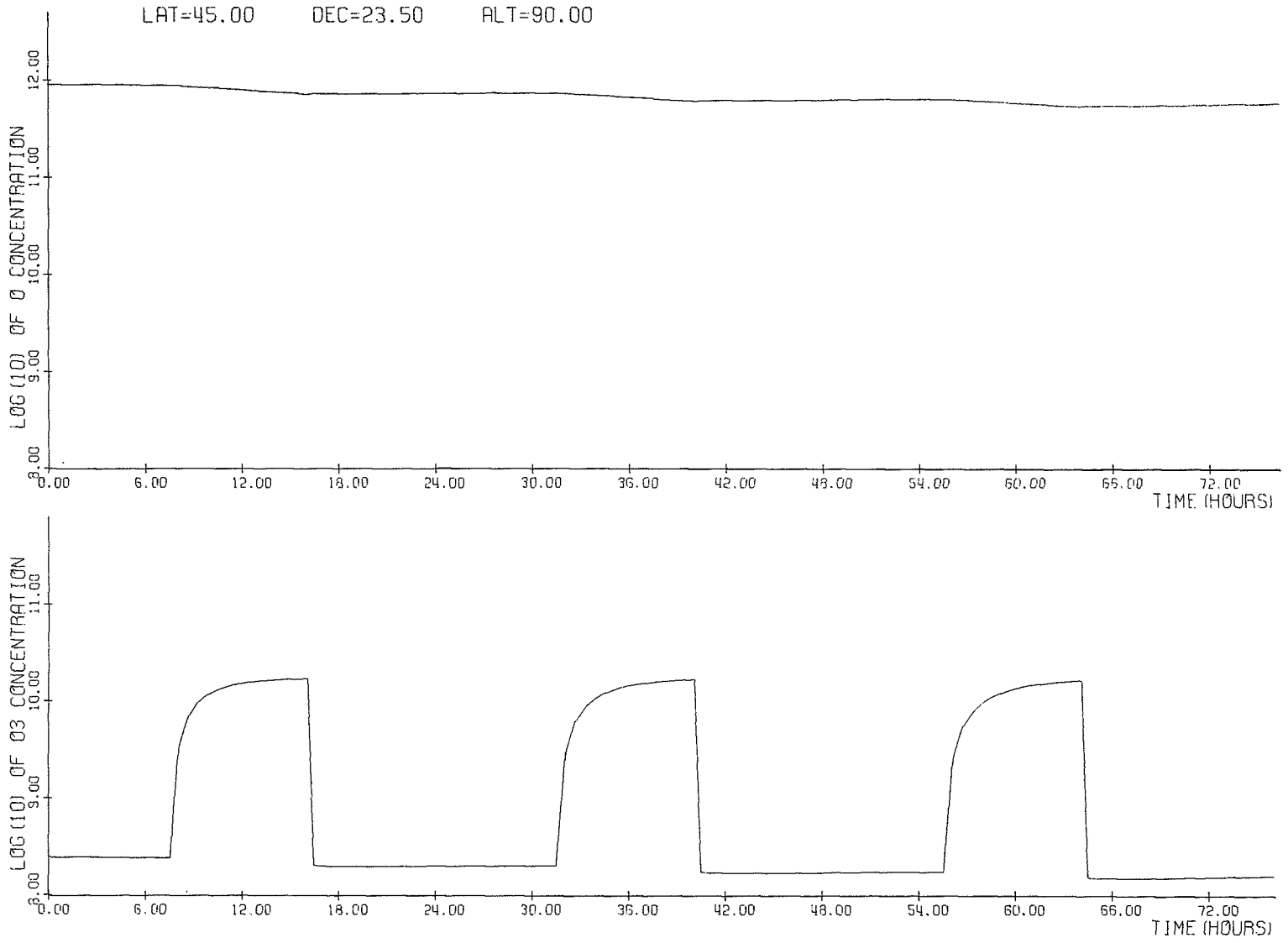
LAT=45.00 DEC=23.50 ALT=90.00
LOG(10) OF O CONCENTRATION
12.00
11.00
10.00
9.00
8.00
0.00 6.00 12.00 18.00 24.00 30.00 36.00 42.00 48.00 54.00 60.00 66.00 72.00
TIME (HOURS)
LOG(10) OF O3 CONCENTRATION
11.00
10.00
9.00
8.00
0.00 6.00 12.00 18.00 24.00 30.00 36.00 42.00 48.00 54.00 60.00 66.00 72.00
TIME (HOURS)

Figure A1

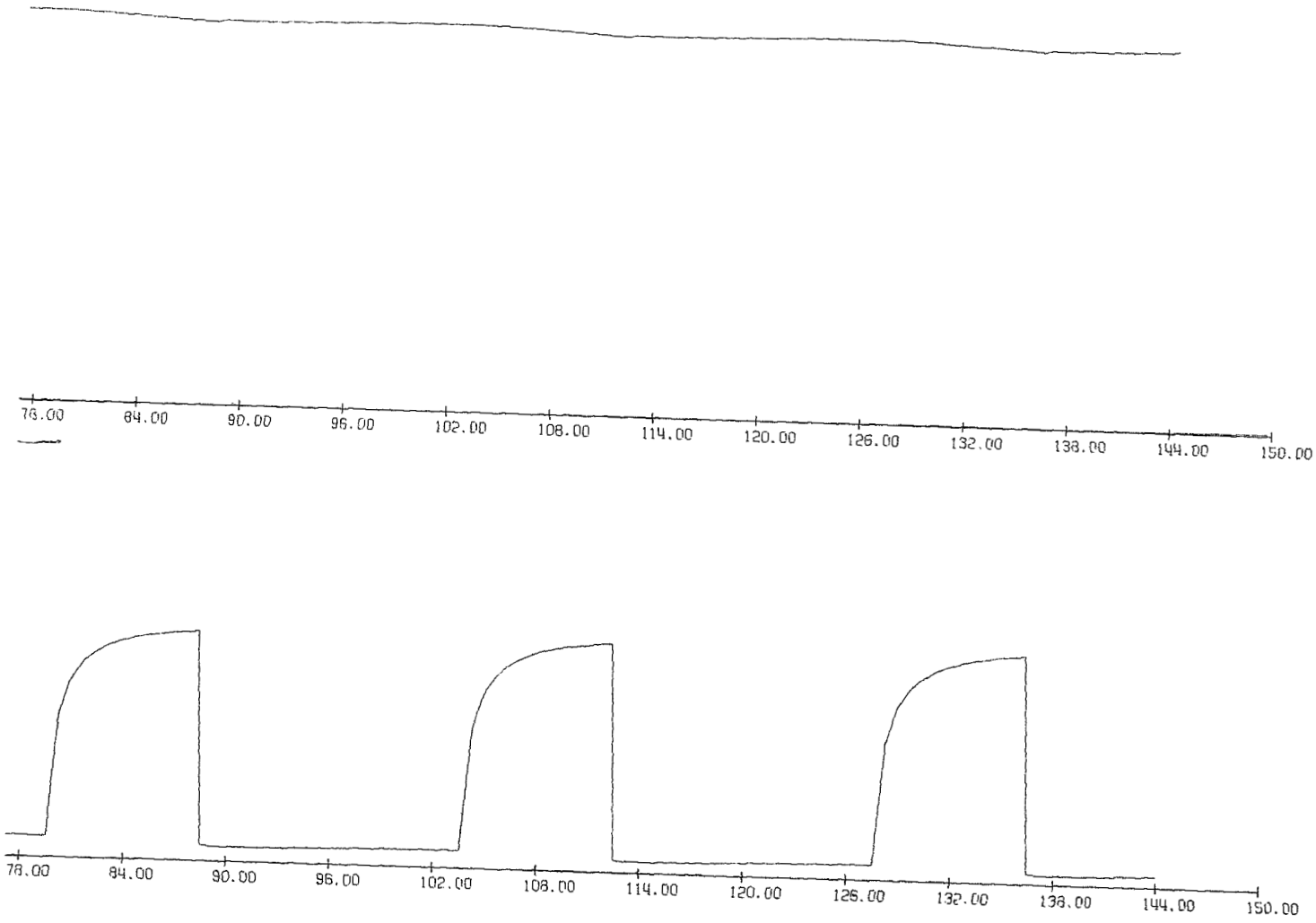

Figure A1 (continued)

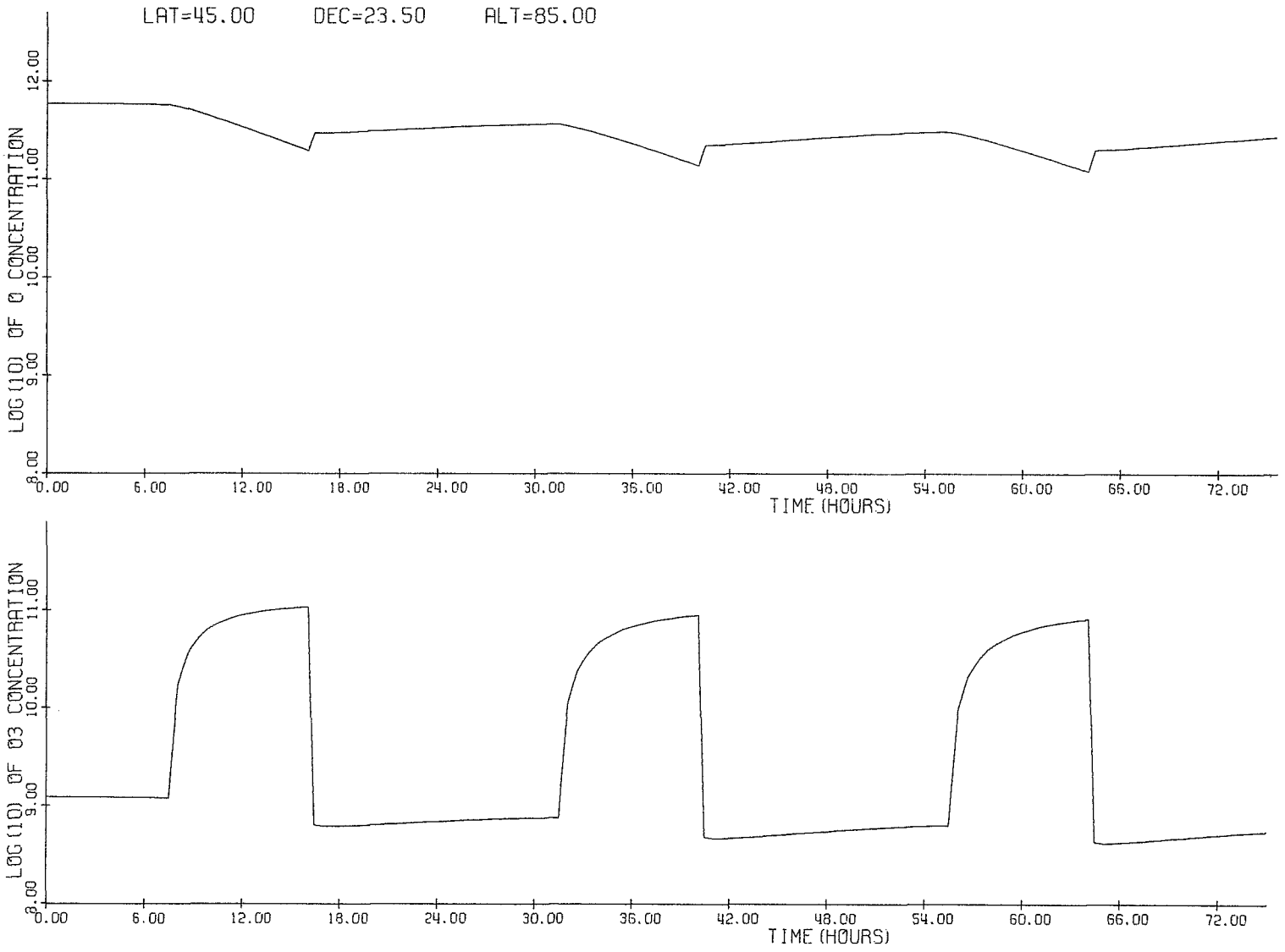
LAT=45.00 DEC=23.50 ALT=85.00
LOG(10) OF O CONCENTRATION
12.00
11.00
10.00
9.00
8.00
0.00 6.00 12.00 18.00 24.00 30.00 36.00 42.00 48.00 54.00 60.00 66.00 72.00
TIME (HOURS)
LOG(10) OF O3 CONCENTRATION
11.00
10.00
9.00
8.00
0.00 6.00 12.00 18.00 24.00 30.00 36.00 42.00 48.00 54.00 60.00 66.00 72.00
TIME (HOURS)

Figure A2

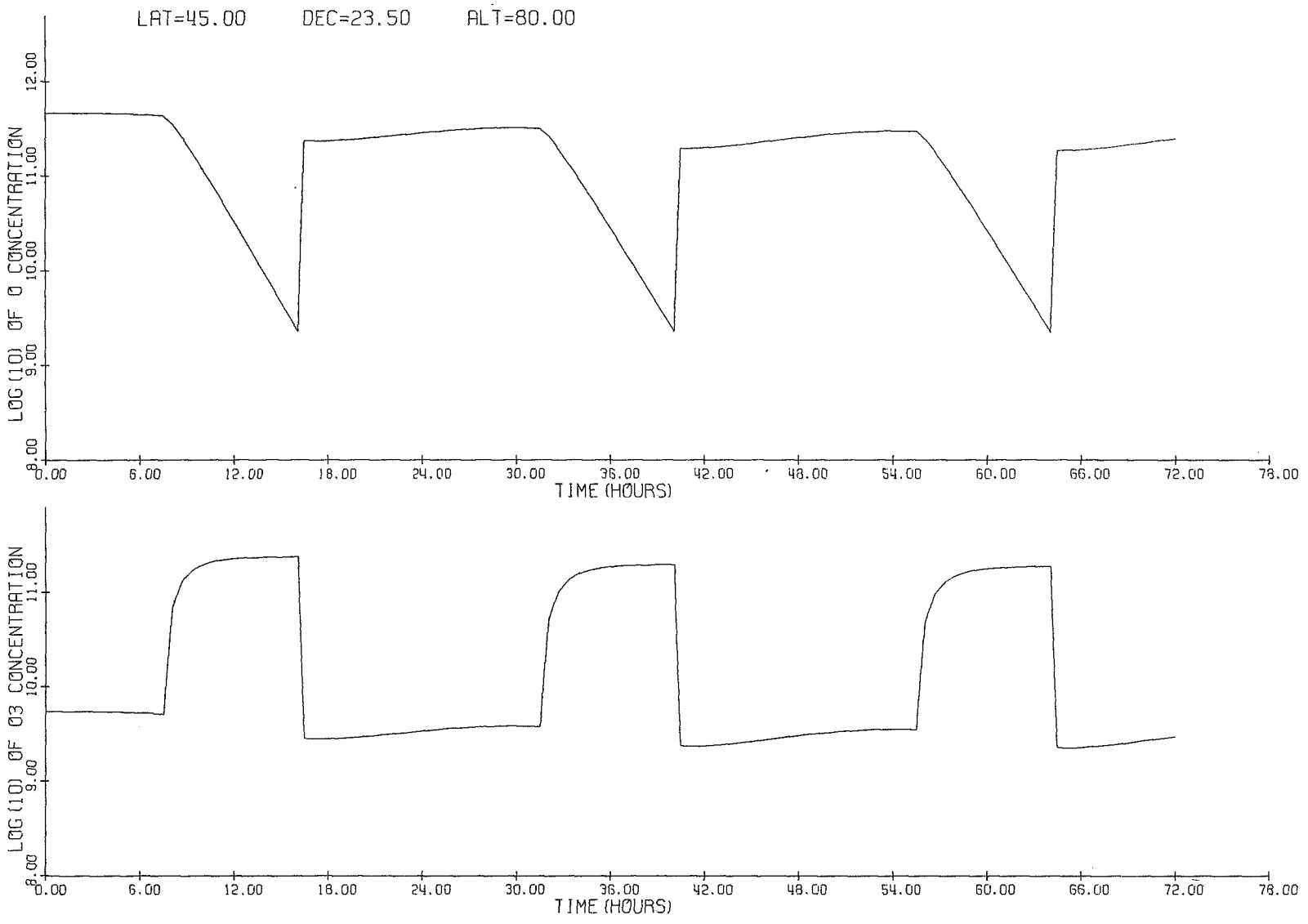
LAT=45.00 DEC=23.50 ALT=80.00
LOG(10) OF O CONCENTRATION
12.00
11.00
10.00
9.00
8.00
0.00 6.00 12.00 18.00 24.00 30.00 36.00 42.00 48.00 54.00 60.00 66.00 72.00 78.00
TIME (HOURS)
LOG(10) OF O3 CONCENTRATION
11.00
10.00
9.00
8.00
0.00 6.00 12.00 18.00 24.00 30.00 36.00 42.00 48.00 54.00 60.00 66.00 72.00 78.00
TIME (HOURS)

Figure A3

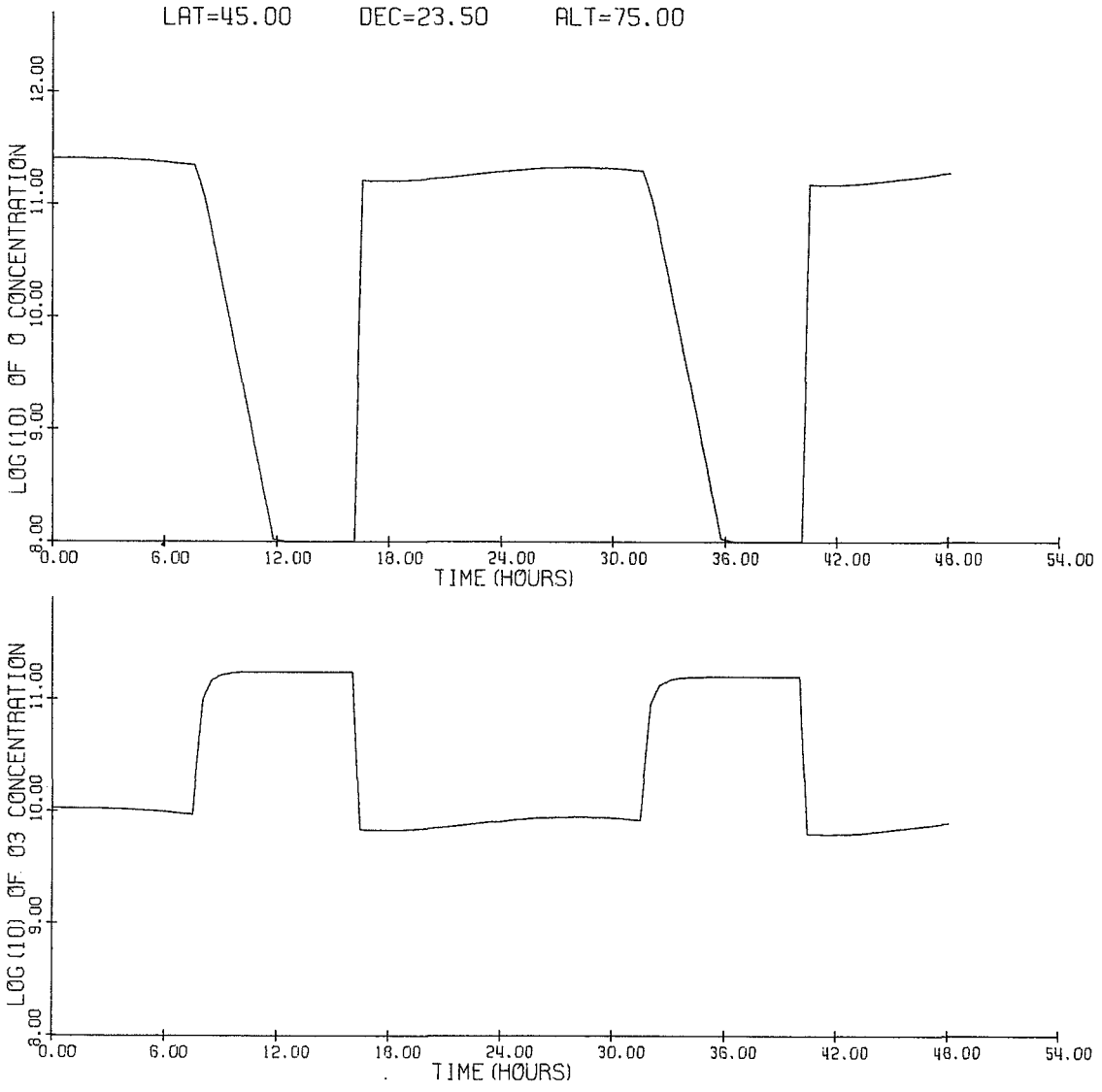

Figure A3 (continued)

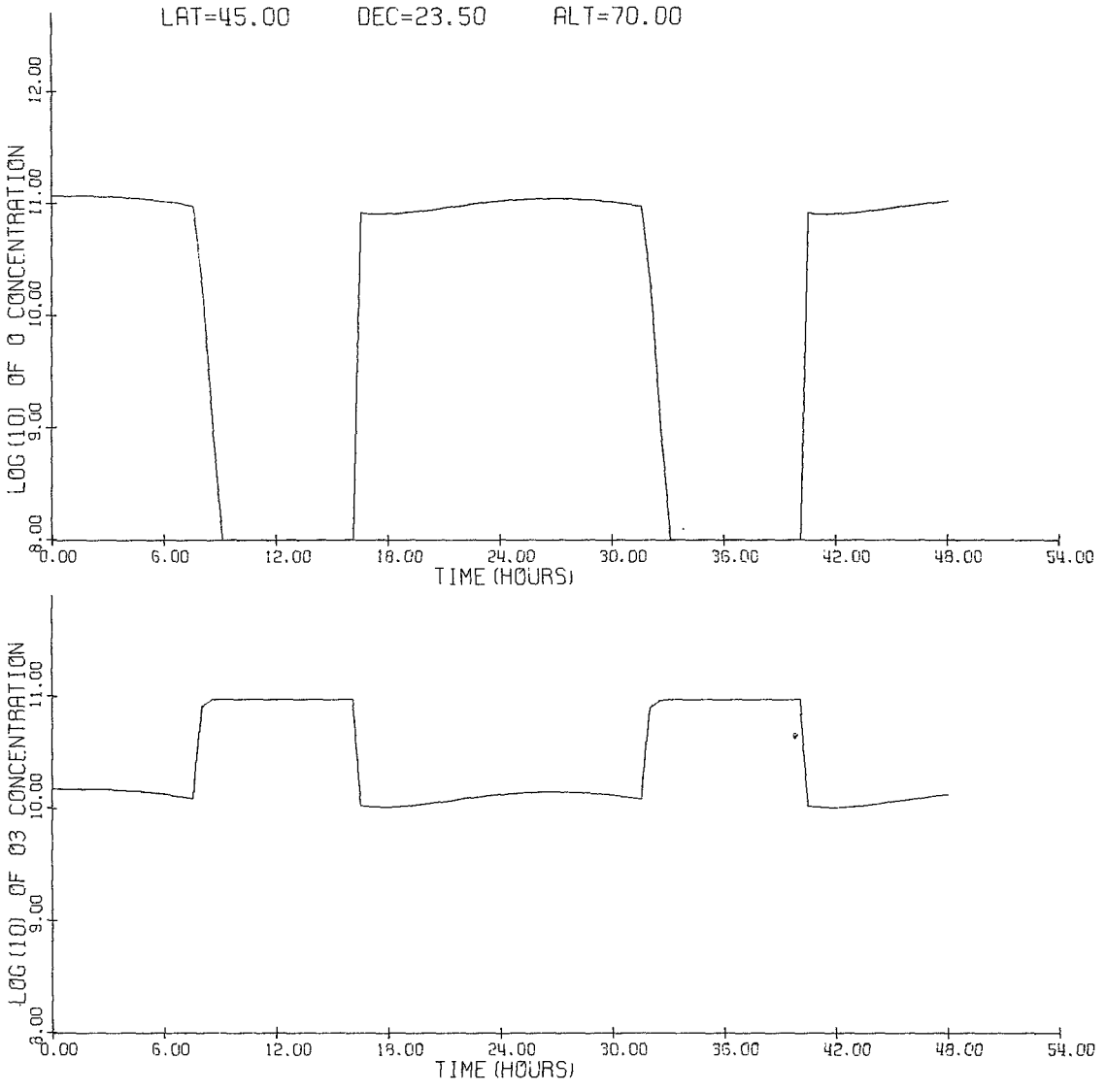
LAT=45.00 DEC=23.50 ALT=70.00
LOG(10) OF O CONCENTRATION
12.00
11.00
10.00
9.00
8.00
0.00 6.00 12.00 18.00 24.00 30.00 36.00 42.00 48.00 54.00
TIME (HOURS)
LOG(10) OF O3 CONCENTRATION
11.00
10.00
9.00
8.00
0.00 6.00 12.00 18.00 24.00 30.00 36.00 42.00 48.00 54.00
TIME (HOURS)

Figure A4

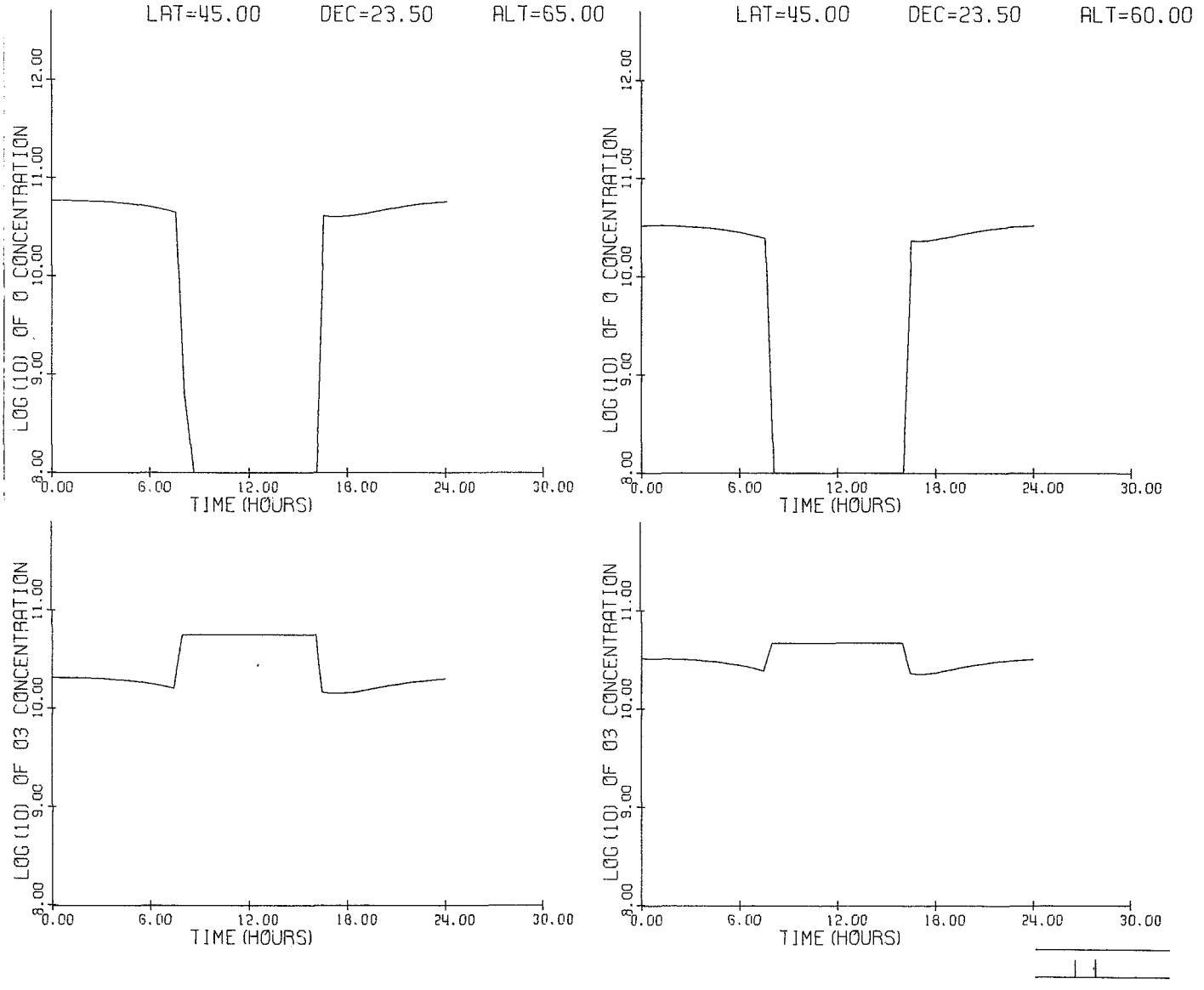

Figure A4 (continued)

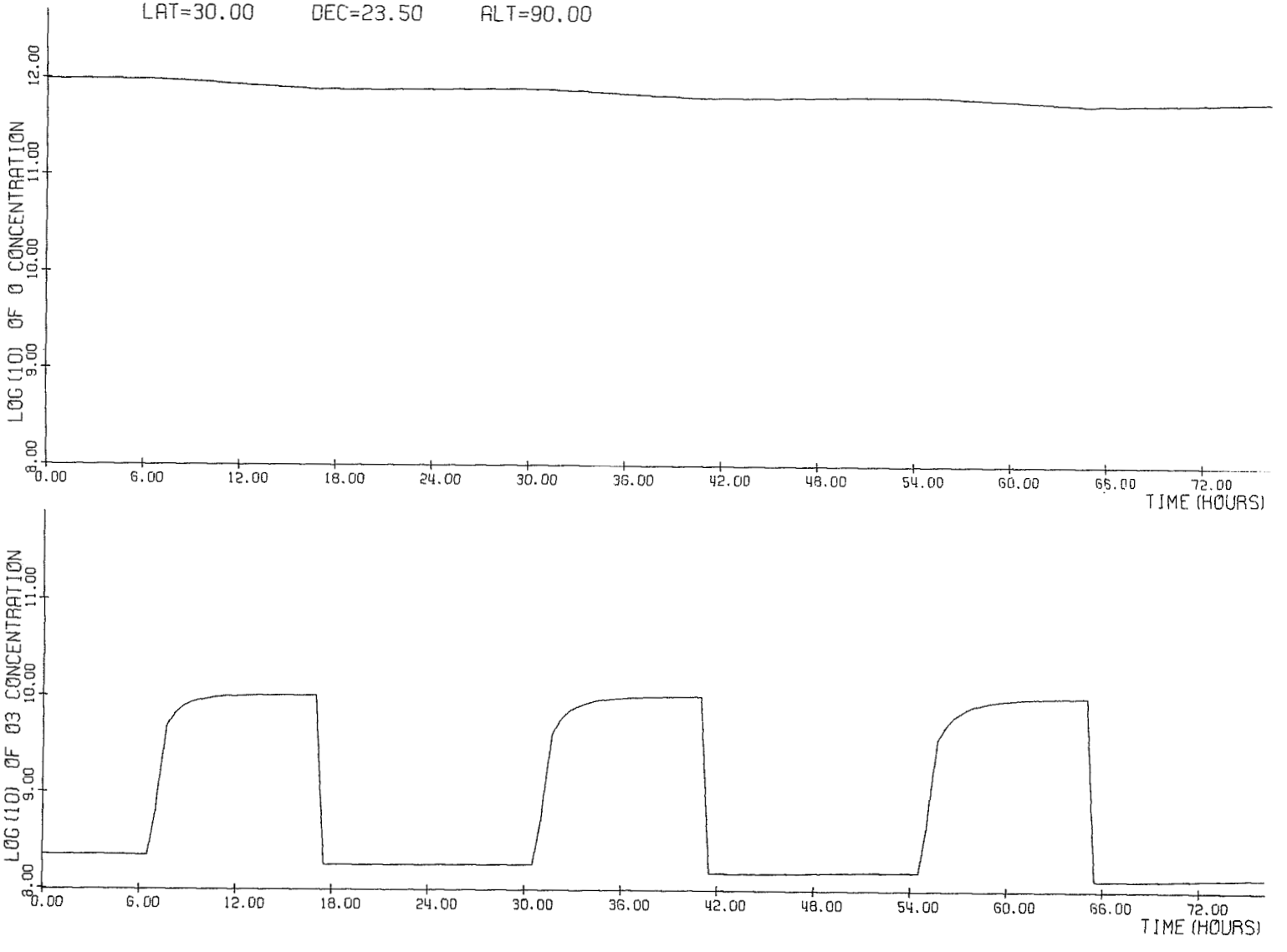
LAT=30.00 DEC=23.50 ALT=90.00
LOG(10) OF O CONCENTRATION
12.00
11.00
10.00
9.00
8.00
0.00
6.00
12.00
18.00
24.00
30.00
36.00
42.00
48.00
54.00
60.00
66.00
72.00
TIME (HOURS)
LOG(10) OF O3 CONCENTRATION
11.00
10.00
9.00
8.00
0.00
6.00
12.00
18.00
24.00
30.00
36.00
42.00
48.00
54.00
60.00
66.00
72.00
TIME (HOURS)

Figure A5

78.00
84.00
90.00
96.00
102.00
108.00
114.00
120.00
126.00
132.00
138.00
144.00
150.00

78.00
84.00
90.00
96.00
102.00
108.00
114.00
120.00
126.00
132.00
138.00
144.00
150.00

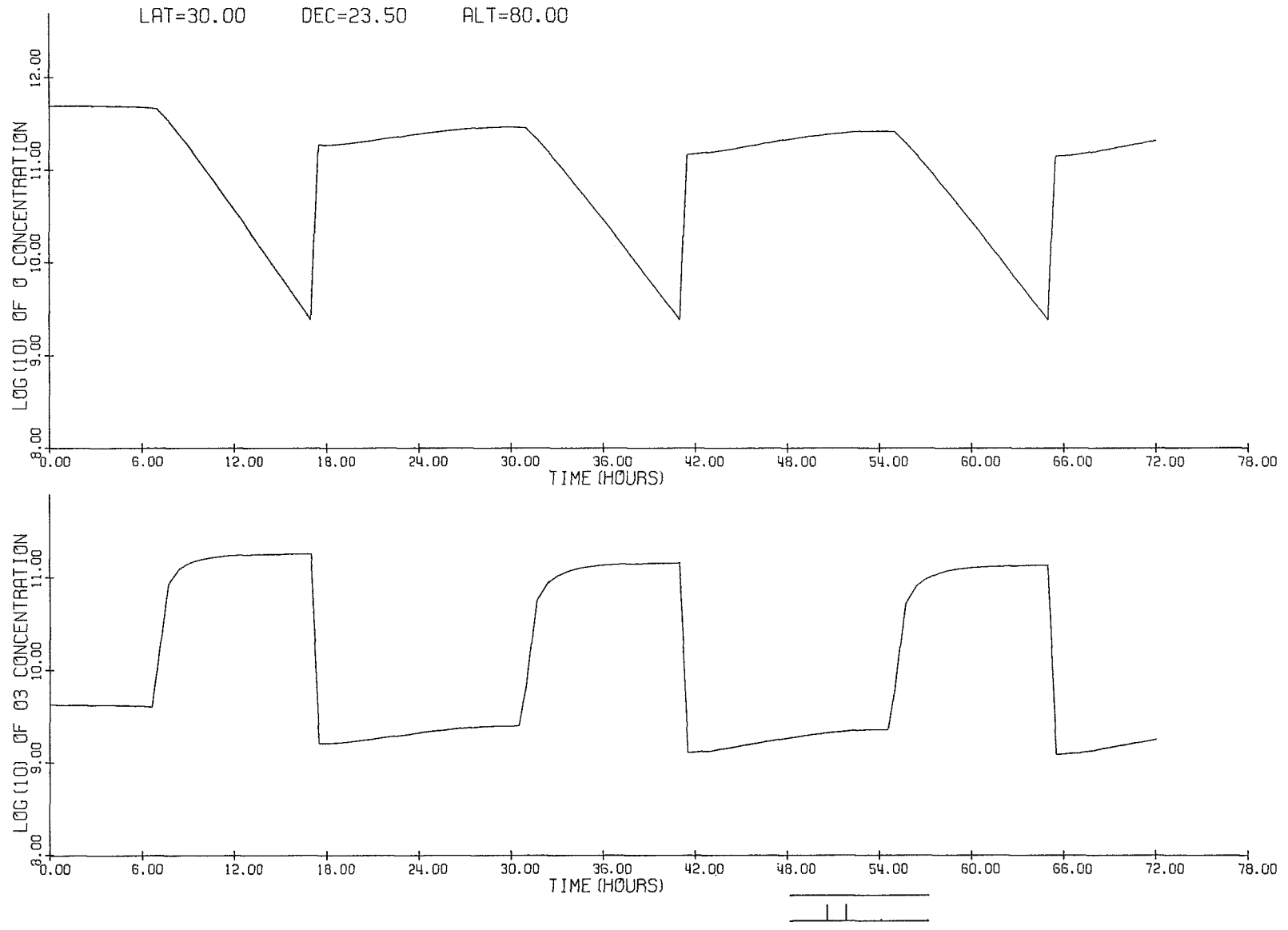
LAT=30.00 DEC=23.50 ALT=80.00
LOG(10) OF O CONCENTRATION
12.00
11.00
10.00
9.00
8.00
0.00 6.00 12.00 18.00 24.00 30.00 36.00 42.00 48.00 54.00 60.00 66.00 72.00 78.00
TIME (HOURS)
LOG(10) OF O3 CONCENTRATION
11.00
10.00
9.00
8.00
0.00 6.00 12.00 18.00 24.00 30.00 36.00 42.00 48.00 54.00 60.00 66.00 72.00 78.00
TIME (HOURS)
PUTER PRODUCTS, INC. ANAHEIM, CALIFORNIA CHART NO. 400
MADE IN U.S.A.

Figure A6

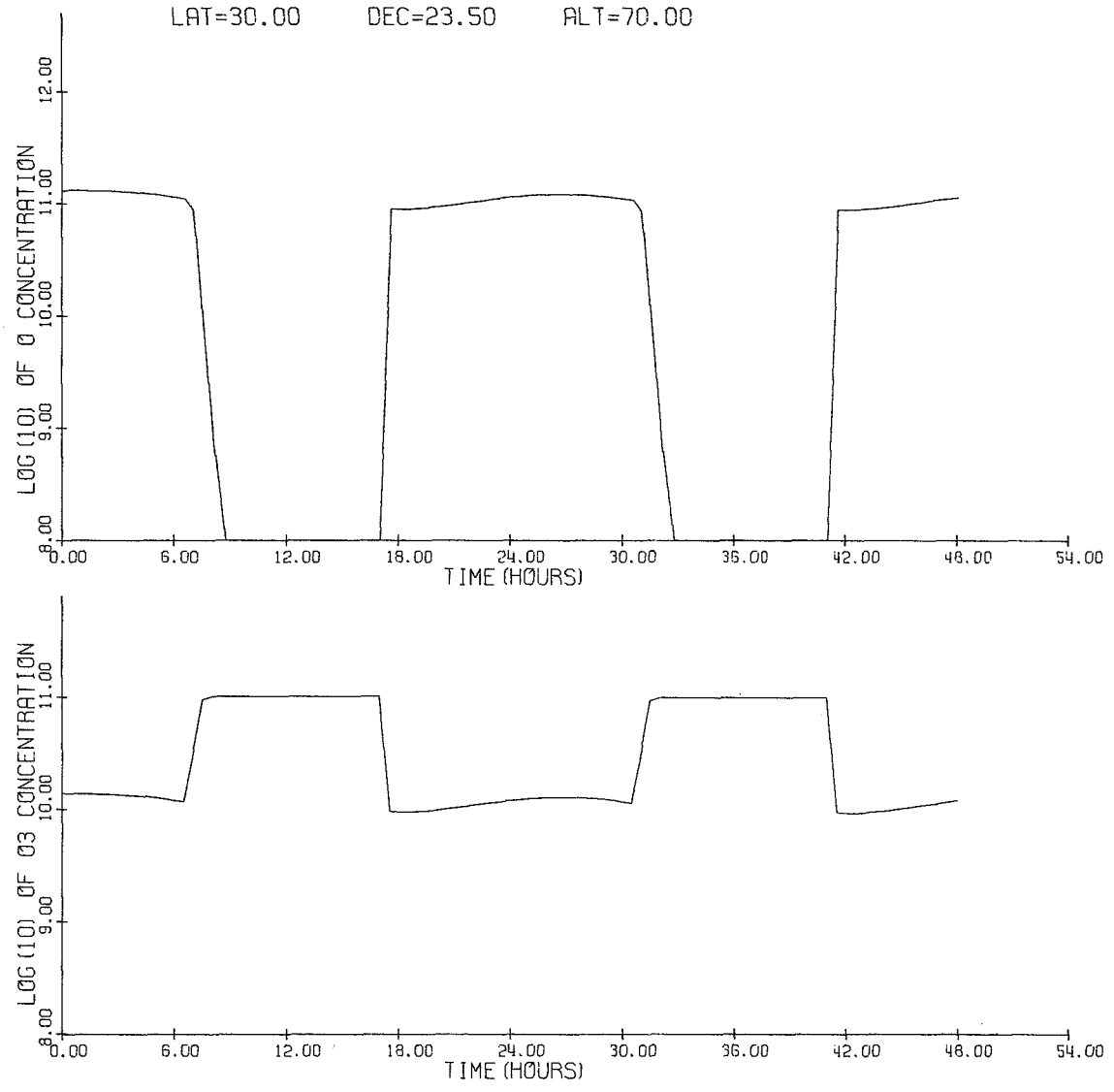
LAT=30.00 DEC=23.50 ALT=70.00
LOG(10) OF O CONCENTRATION
12.00
11.00
10.00
9.00
8.00
0.00
6.00
12.00
18.00
24.00
30.00
36.00
42.00
48.00
54.00
TIME (HOURS)
LOG(10) OF O3 CONCENTRATION
11.00
10.00
9.00
8.00
0.00
6.00
12.00
18.00
24.00
30.00
36.00
42.00
48.00
54.00
TIME (HOURS)

Figure A7

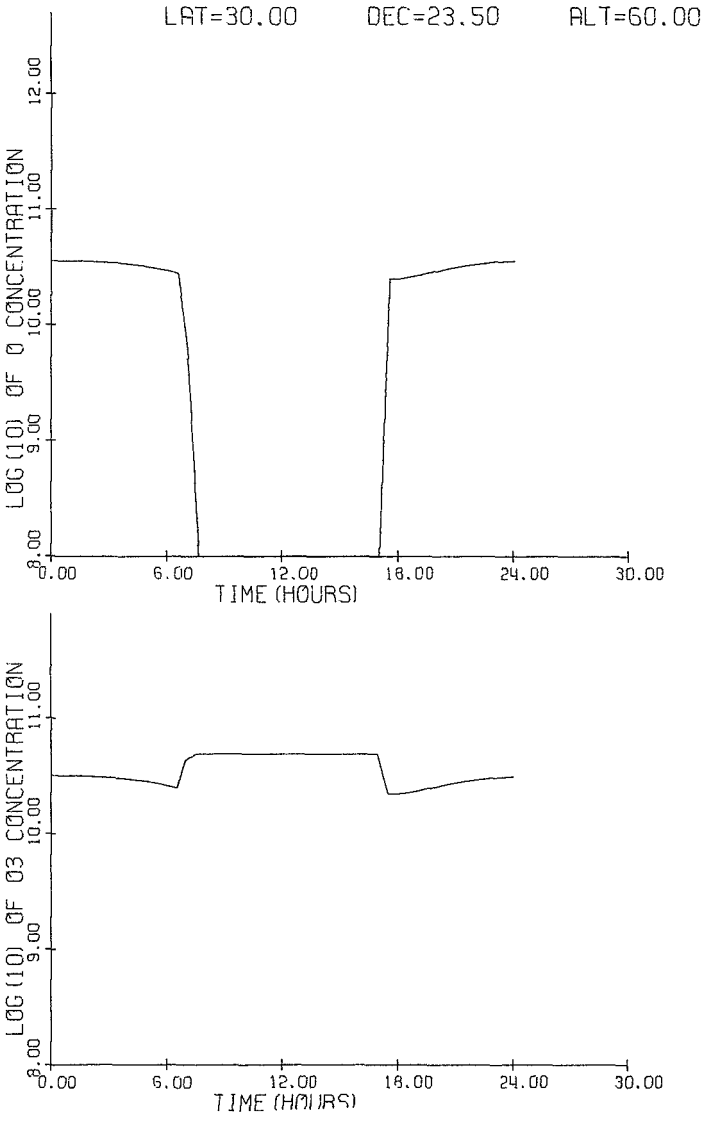

Figure A7 (continued)

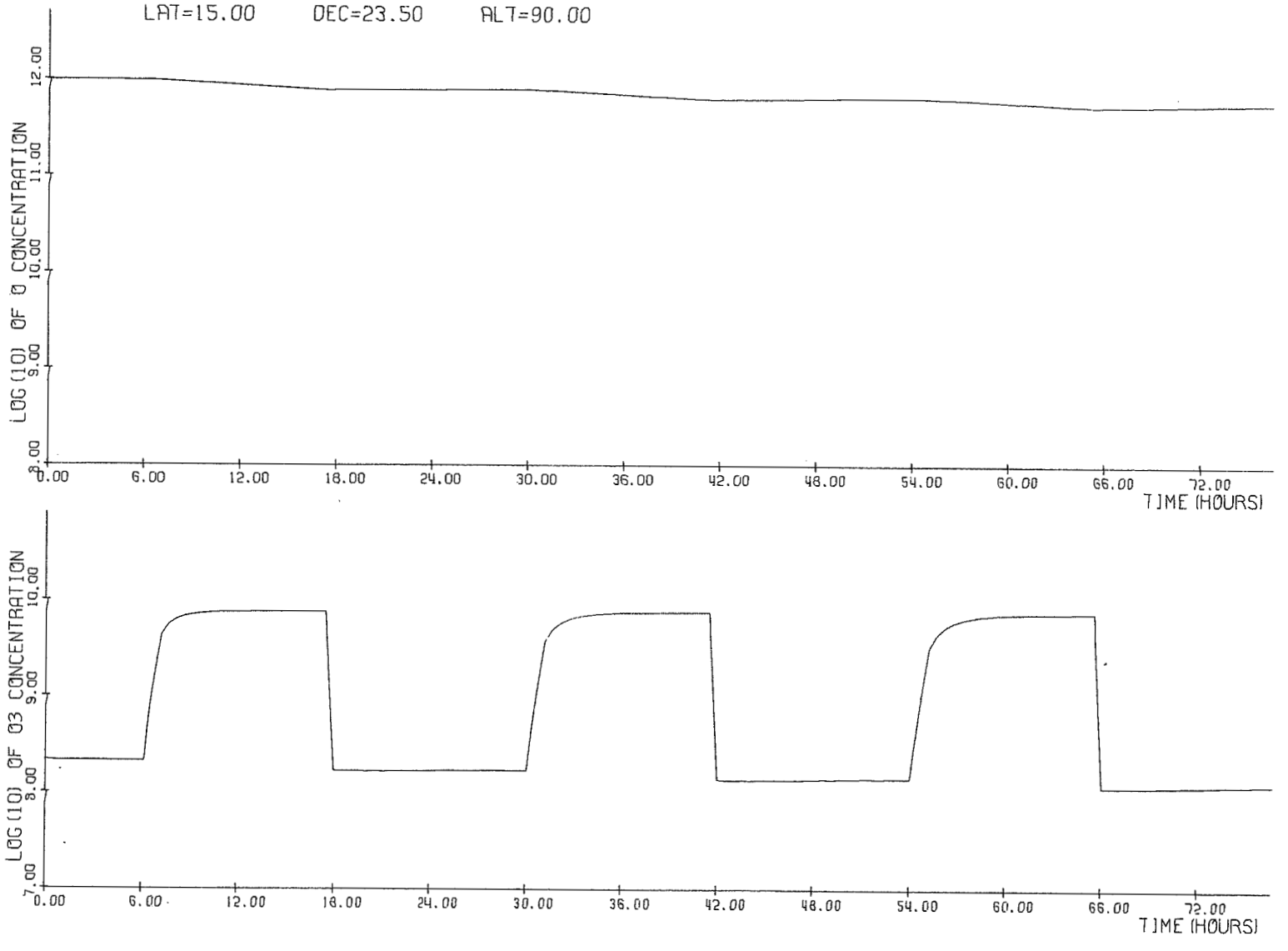
LAT=15.00 DEC=23.50 ALT=90.00
LOG(10) OF O CONCENTRATION
12.00
11.00
10.00
9.00
8.00
0.00 6.00 12.00 18.00 24.00 30.00 36.00 42.00 48.00 54.00 60.00 66.00 72.00
TIME (HOURS)
LOG(10) OF O3 CONCENTRATION
10.00
9.00
8.00
7.00
0.00 6.00 12.00 18.00 24.00 30.00 36.00 42.00 48.00 54.00 60.00 66.00 72.00
TIME (HOURS)

Figure A8

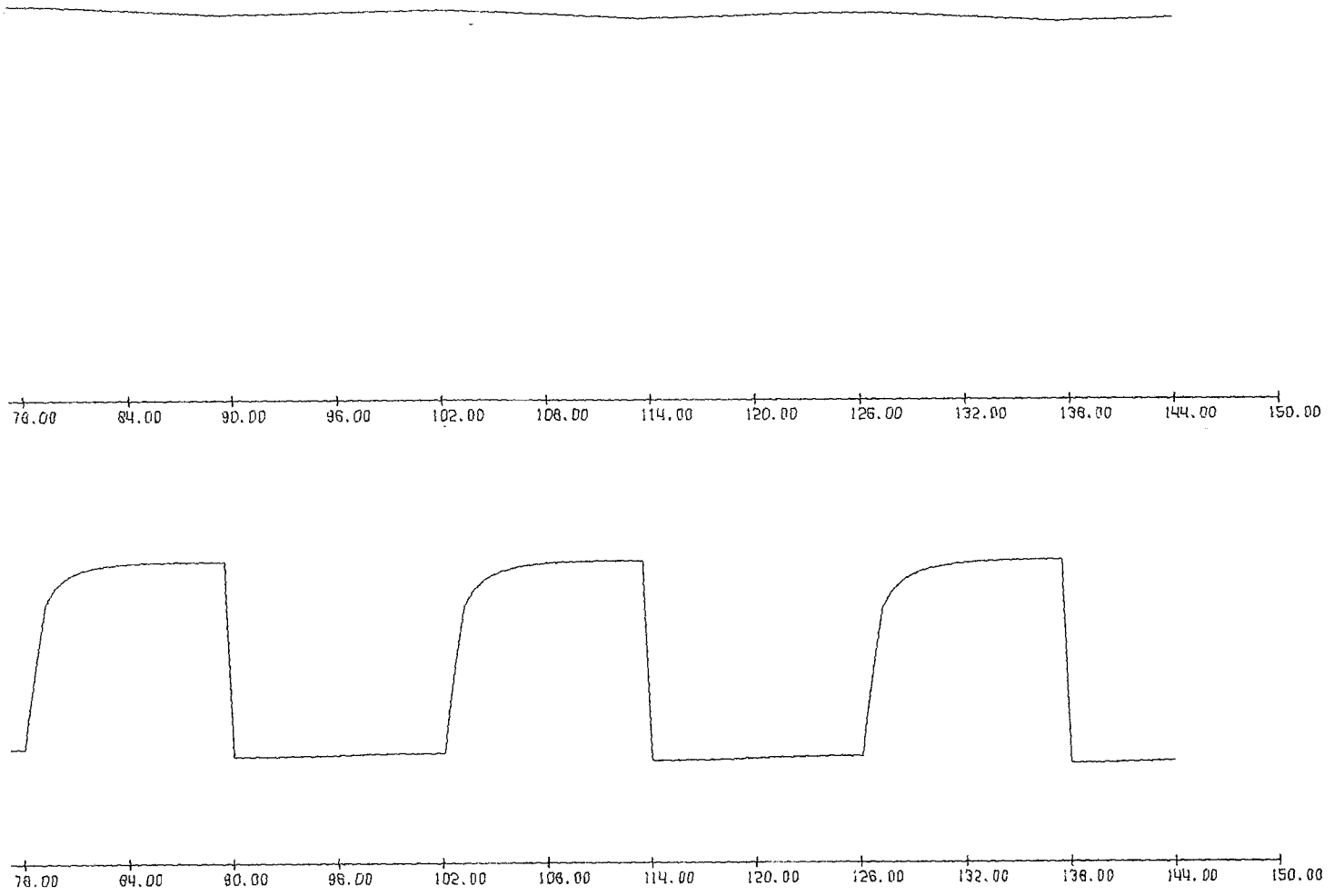

Figure A8 (continued)

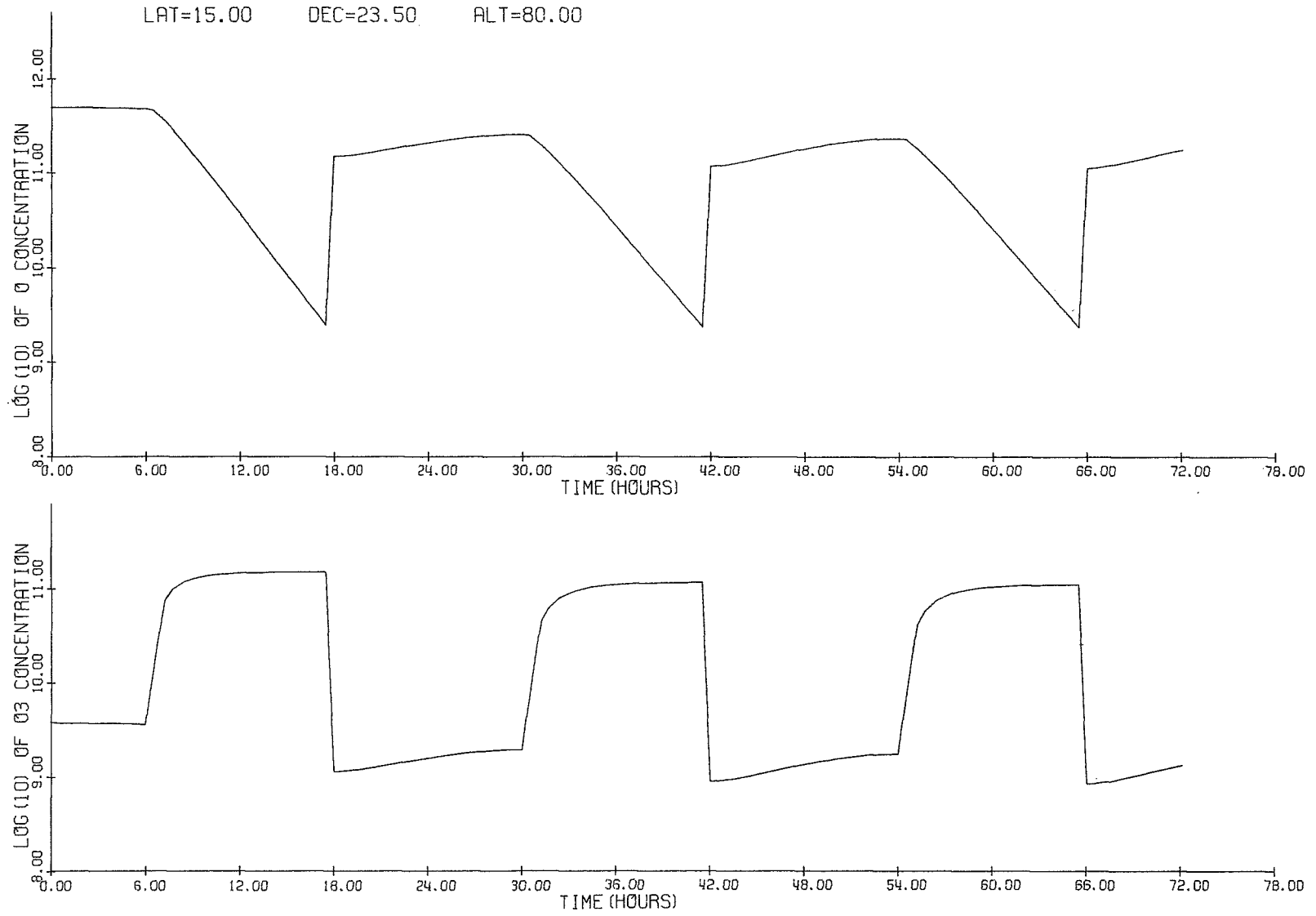
LAT=15.00 DEC=23.50 ALT=80.00
LOG(10) OF O CONCENTRATION
12.00
11.00
10.00
9.00
8.00
0.00 6.00 12.00 18.00 24.00 30.00 36.00 42.00 48.00 54.00 60.00 66.00 72.00 78.00
TIME (HOURS)
LOG(10) OF O3 CONCENTRATION
11.00
10.00
9.00
8.00
0.00 6.00 12.00 18.00 24.00 30.00 36.00 42.00 48.00 54.00 60.00 66.00 72.00 78.00
TIME (HOURS)

Figure A9

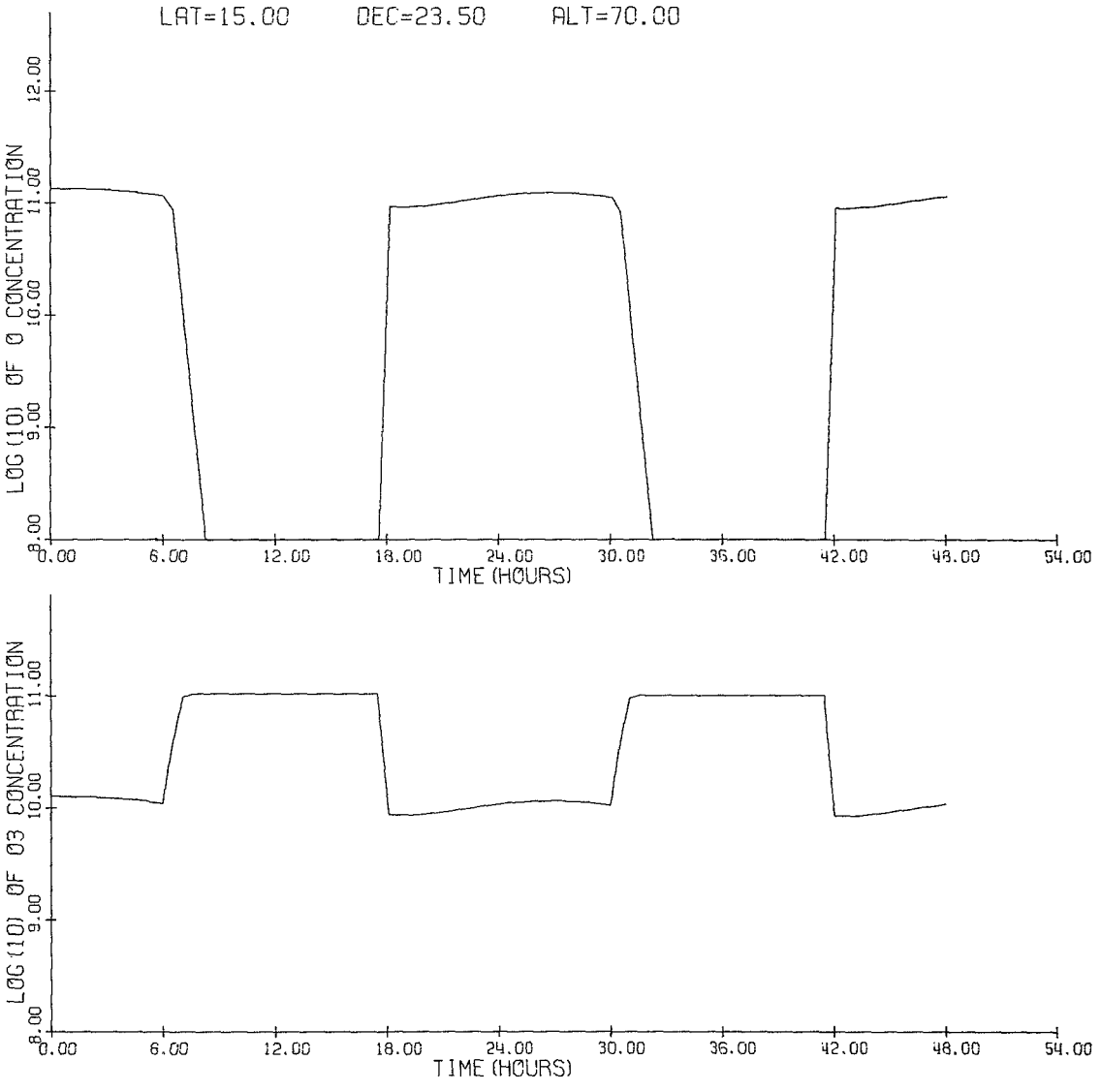
LAT=15.00 DEC=23.50 ALT=70.00
LOG(10) OF O CONCENTRATION
12.00
11.00
10.00
9.00
8.00
0.00
6.00
12.00
18.00
24.00
30.00
36.00
42.00
48.00
54.00
TIME (HOURS)
LOG(10) OF O3 CONCENTRATION
11.00
10.00
9.00
8.00
0.00
6.00
12.00
18.00
24.00
30.00
36.00
42.00
48.00
54.00
TIME (HOURS)

Figure A10

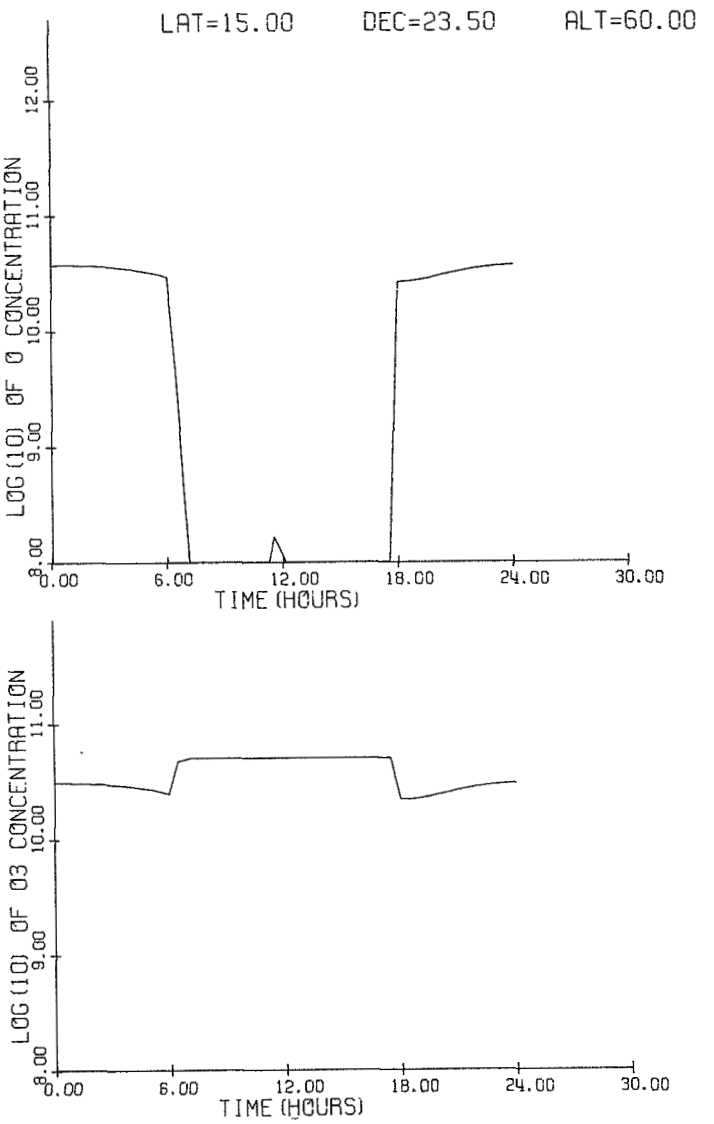

Figure A10 (continued)

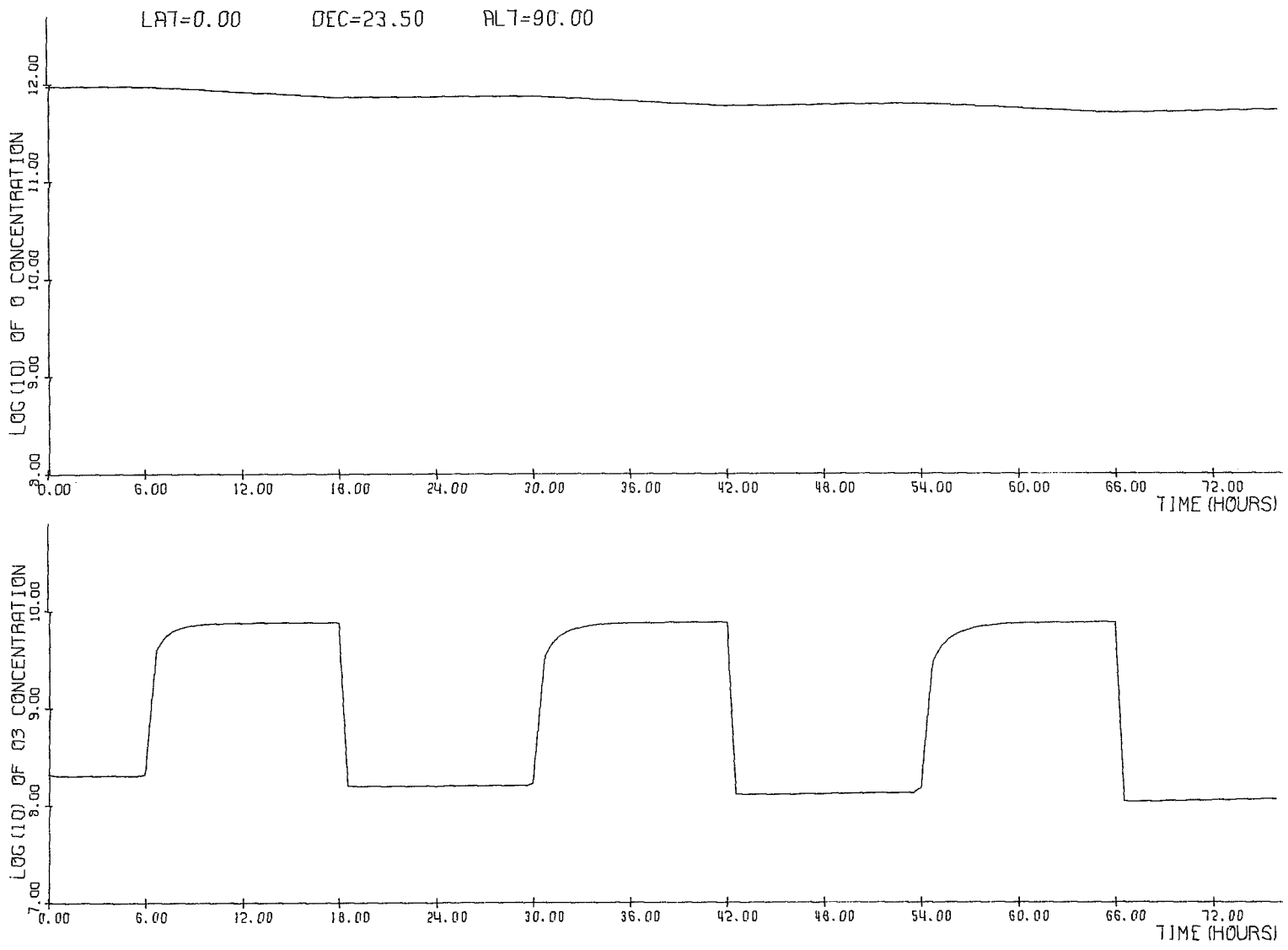
LAT=0.00 DEC=23.50 ALT=90.00
LOG(10) OF O CONCENTRATION
12.00
11.00
10.00
9.00
8.00
0.00 6.00 12.00 18.00 24.00 30.00 36.00 42.00 48.00 54.00 60.00 66.00 72.00
TIME (HOURS)
LOG(10) OF O3 CONCENTRATION
10.00
9.00
8.00
7.00
0.00 6.00 12.00 18.00 24.00 30.00 36.00 42.00 48.00 54.00 60.00 66.00 72.00
TIME (HOURS)

Figure A11

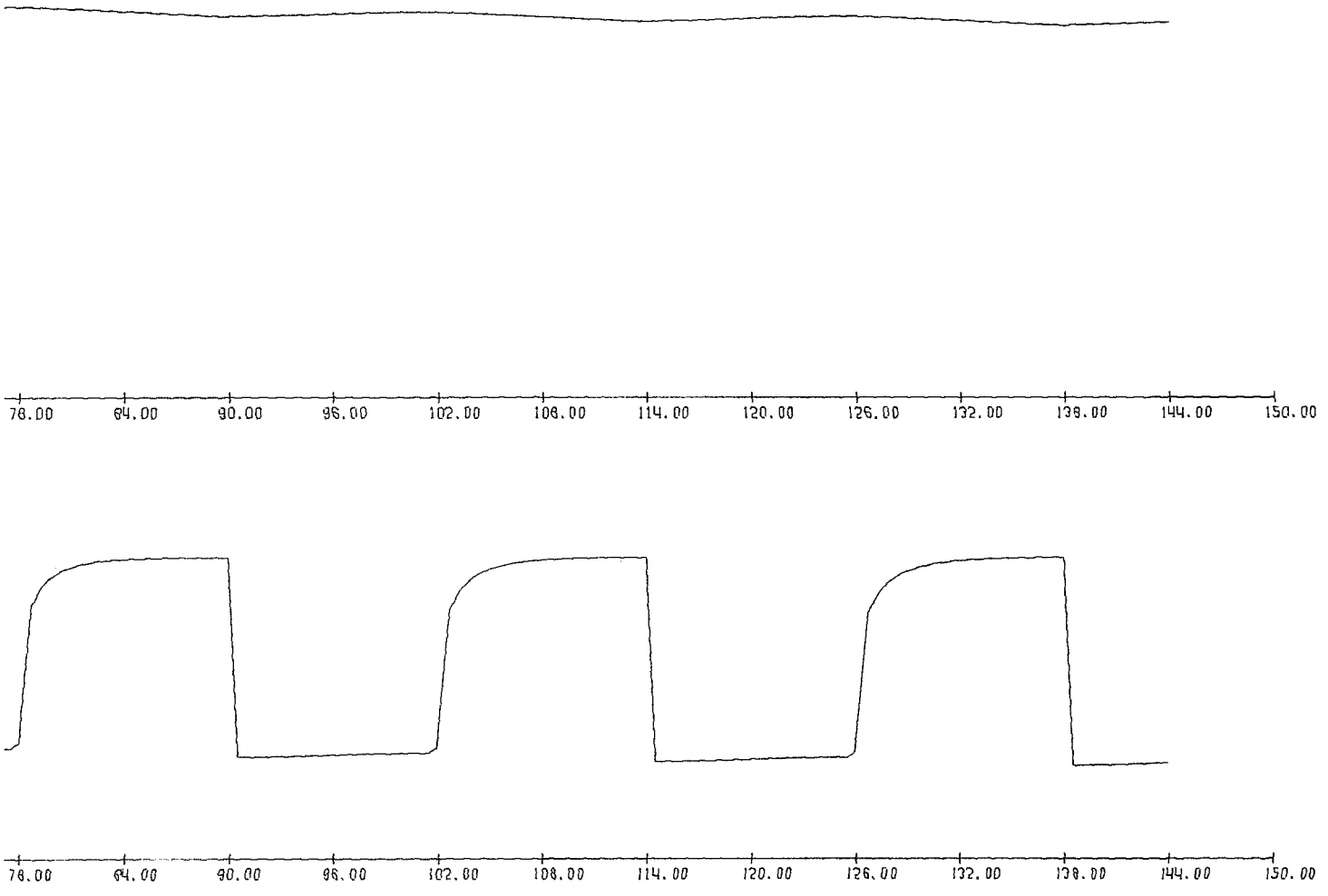

Figure A11 (continued)

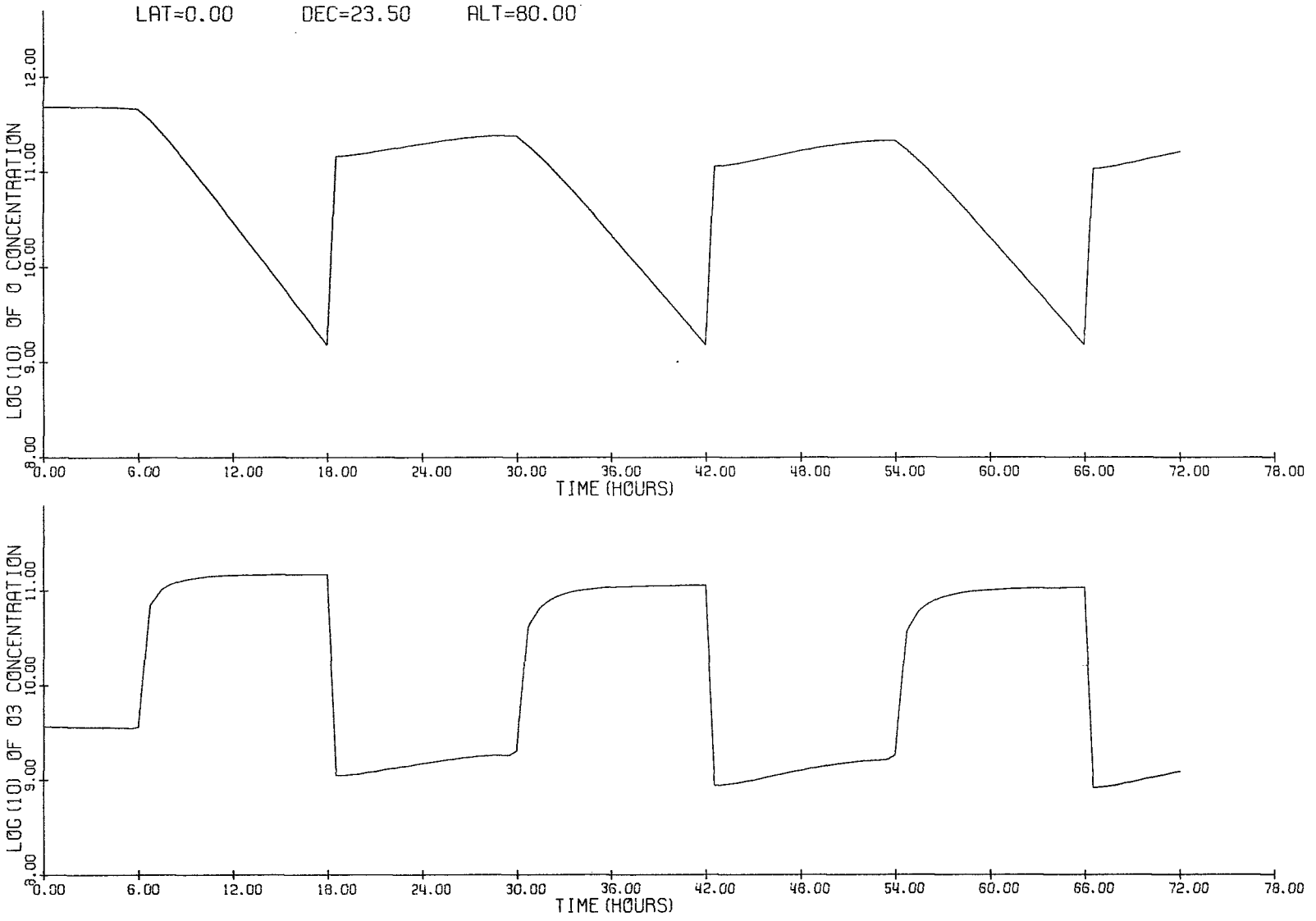
LAT=0.00 DEC=23.50 ALT=80.00
LOG(10) OF O CONCENTRATION
12.00
11.00
10.00
9.00
8.00
0.00 6.00 12.00 18.00 24.00 30.00 36.00 42.00 48.00 54.00 60.00 66.00 72.00 78.00
TIME (HOURS)
LOG(10) OF O3 CONCENTRATION
11.00
10.00
9.00
8.00
0.00 6.00 12.00 18.00 24.00 30.00 36.00 42.00 48.00 54.00 60.00 66.00 72.00 78.00
TIME (HOURS)

Figure A12

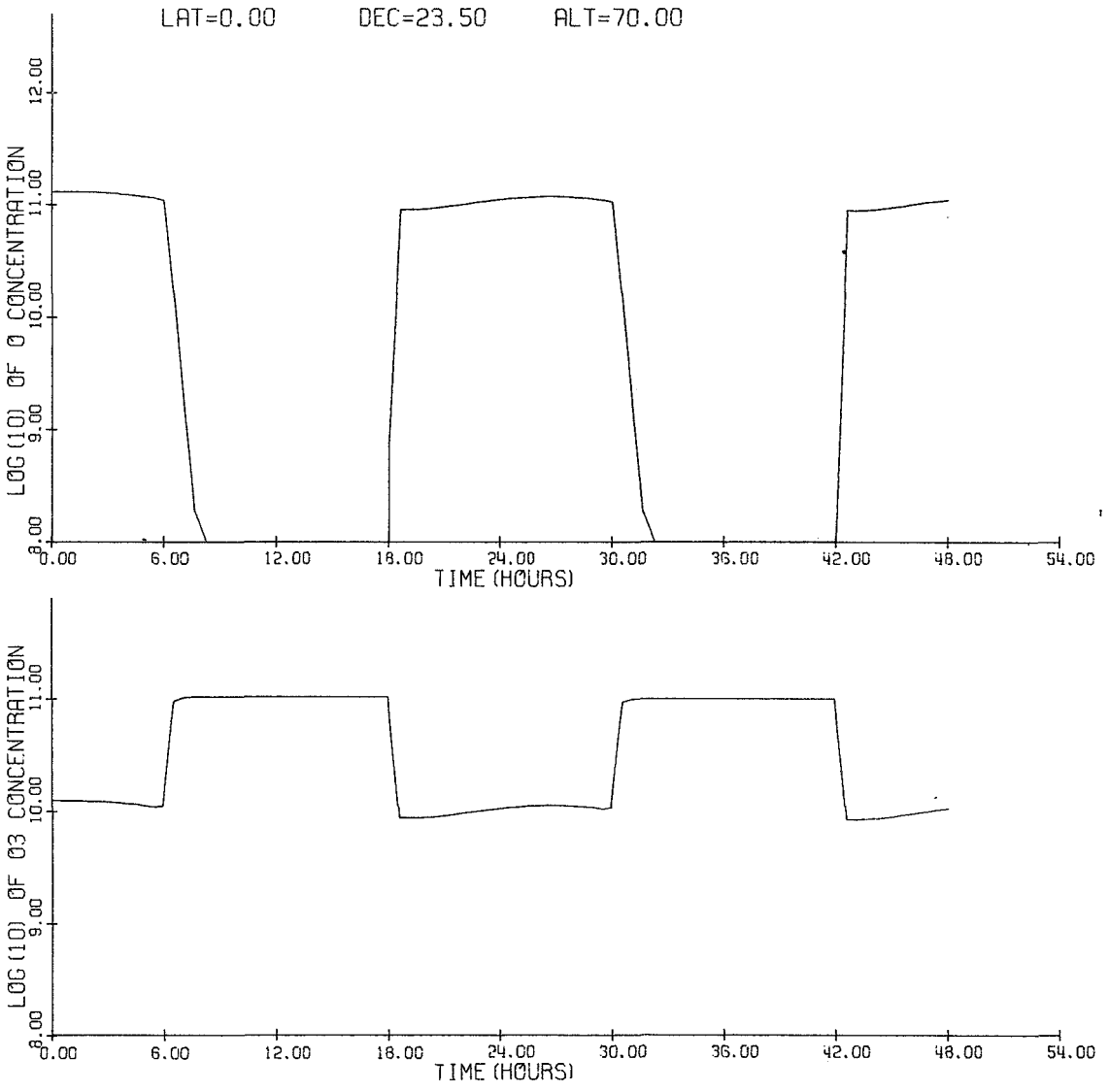
LAT=0.00
DEC=23.50
ALT=70.00
LOG(10) OF O CONCENTRATION
12.00
11.00
10.00
9.00
8.00
0.00
6.00
12.00
18.00
24.00
30.00
36.00
42.00
48.00
54.00
TIME (HOURS)
LOG(10) OF O3 CONCENTRATION
11.00
10.00
9.00
8.00
0.00
6.00
12.00
18.00
24.00
30.00
36.00
42.00
48.00
54.00
TIME (HOURS)

Figure A13

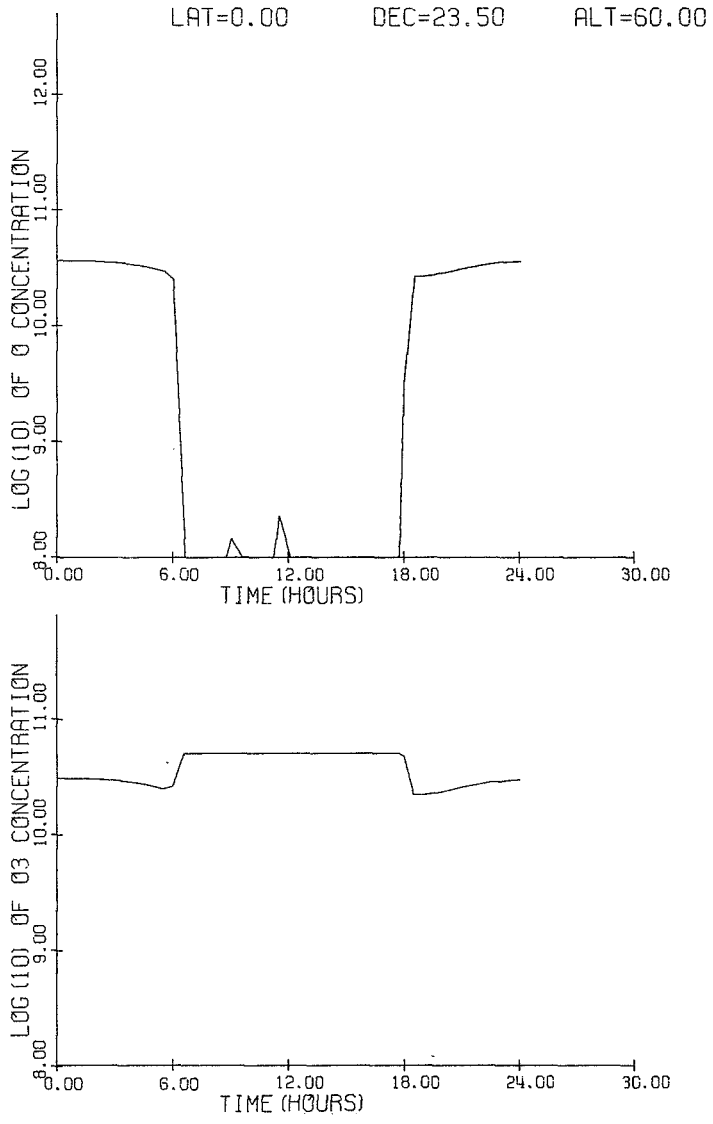

Figure A13 (continued)

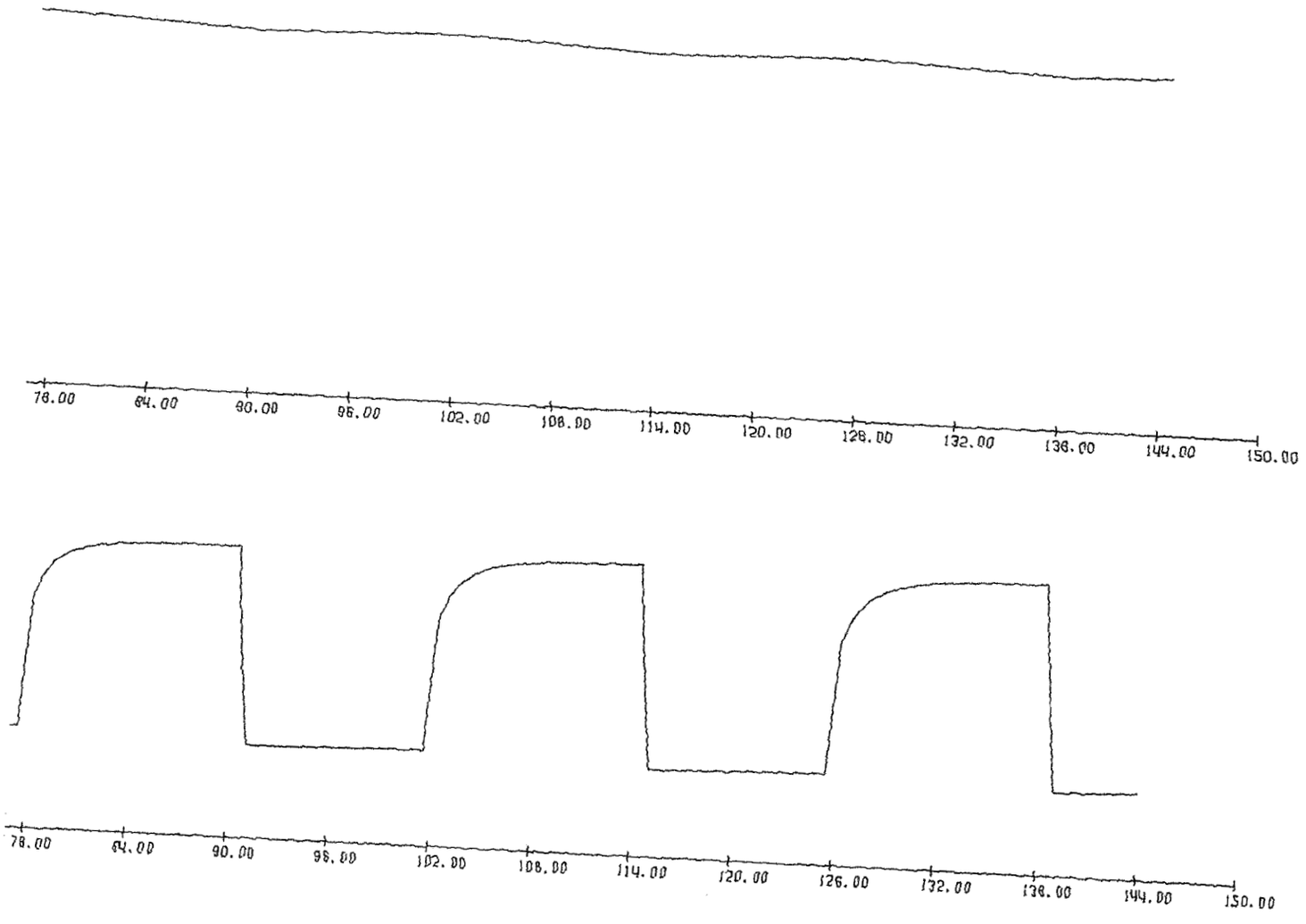
78.00
84.00
90.00
96.00
102.00
108.00
114.00
120.00
126.00
132.00
138.00
144.00
150.00
78.00
84.00
90.00
96.00
102.00
108.00
114.00
120.00
126.00
132.00
138.00
144.00
150.00

Figure A14

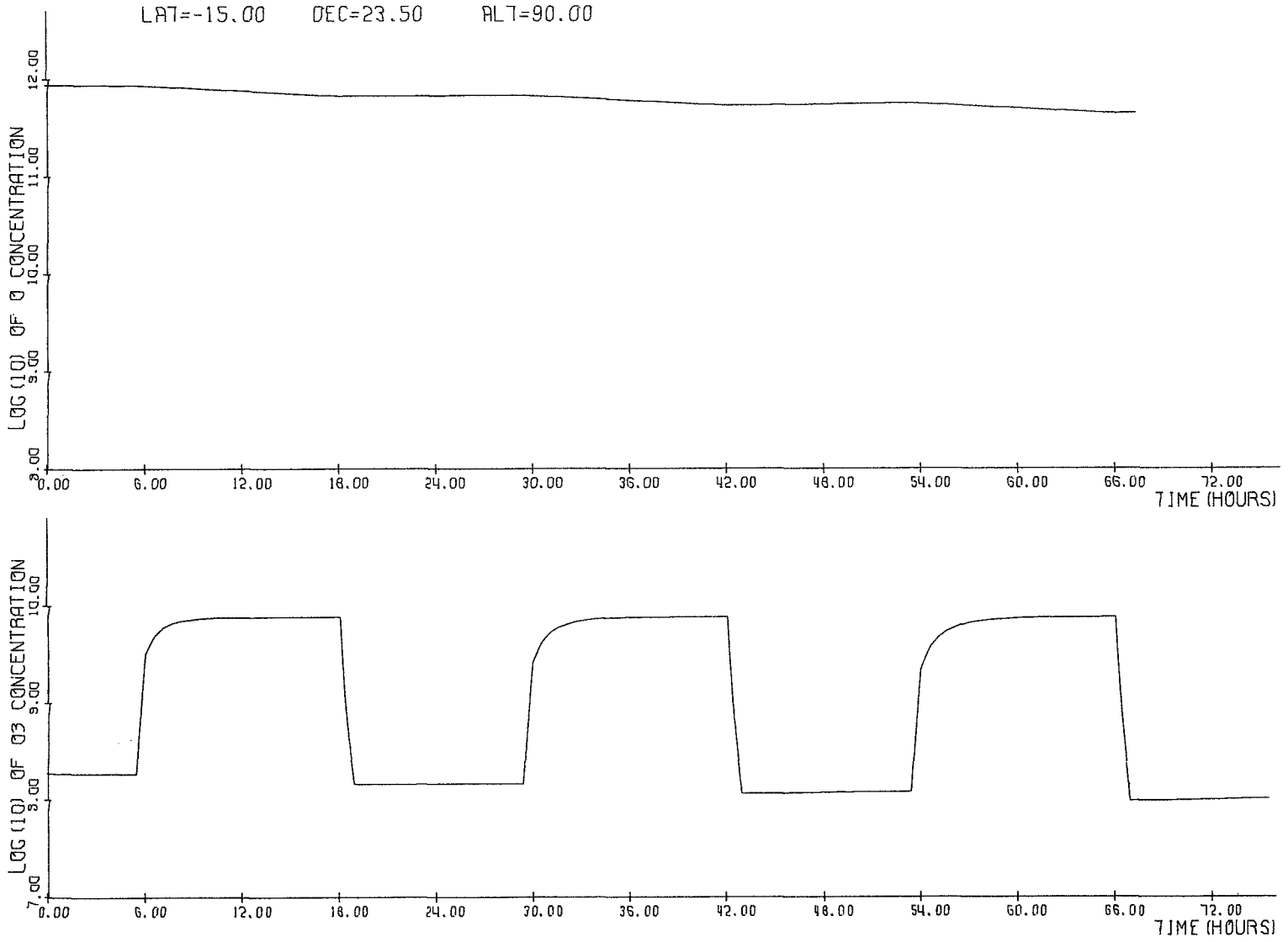

Figure A14 (continued)

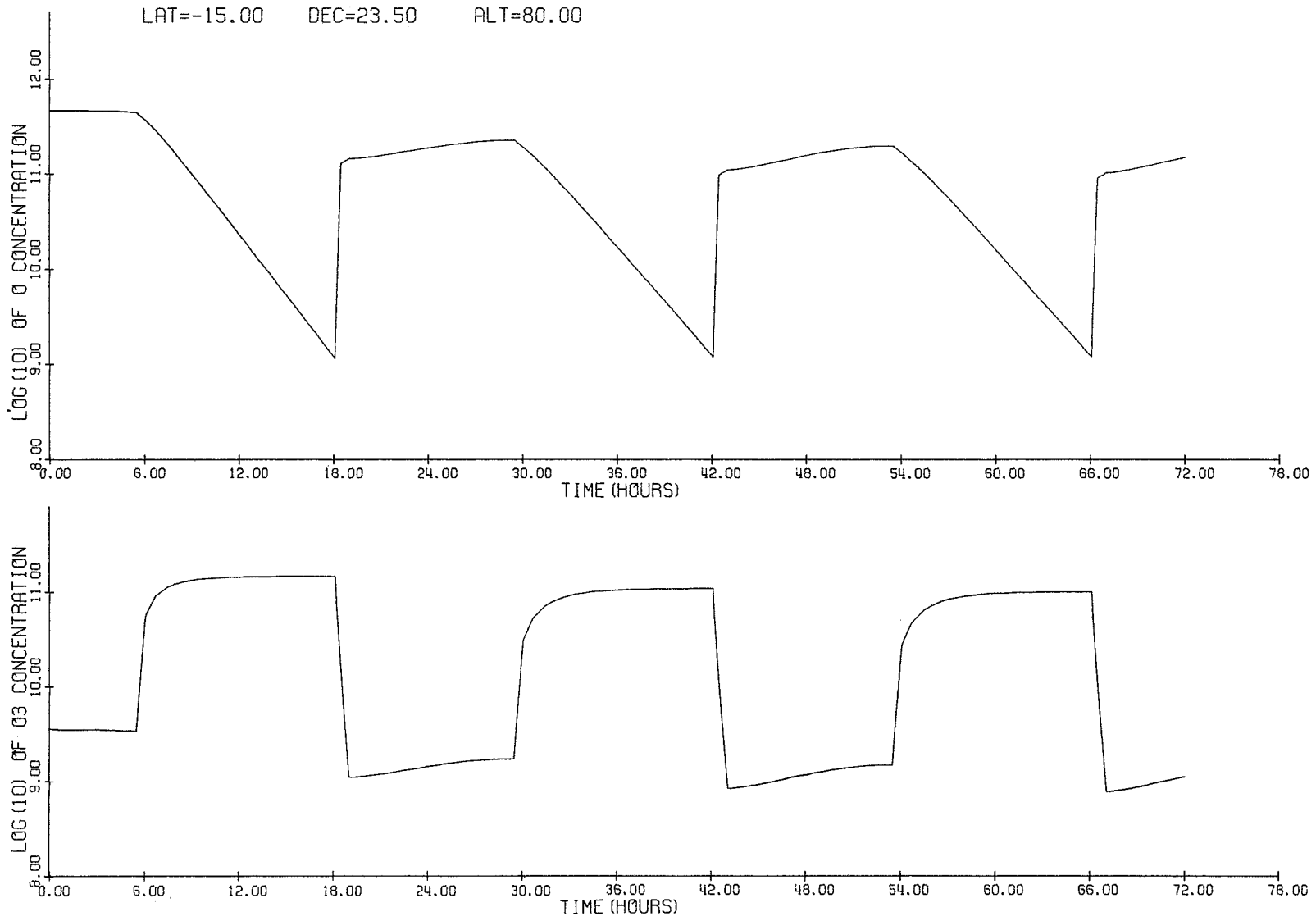
LAT=-15.00 DEC=23.50 ALT=80.00
LOG(10) OF O CONCENTRATION
12.00
11.00
10.00
9.00
8.00
0.00 6.00 12.00 18.00 24.00 30.00 36.00 42.00 48.00 54.00 60.00 66.00 72.00 78.00
TIME (HOURS)
LOG(10) OF O3 CONCENTRATION
11.00
10.00
9.00
8.00
0.00 6.00 12.00 18.00 24.00 30.00 36.00 42.00 48.00 54.00 60.00 66.00 72.00 78.00
TIME (HOURS)

Figure A15

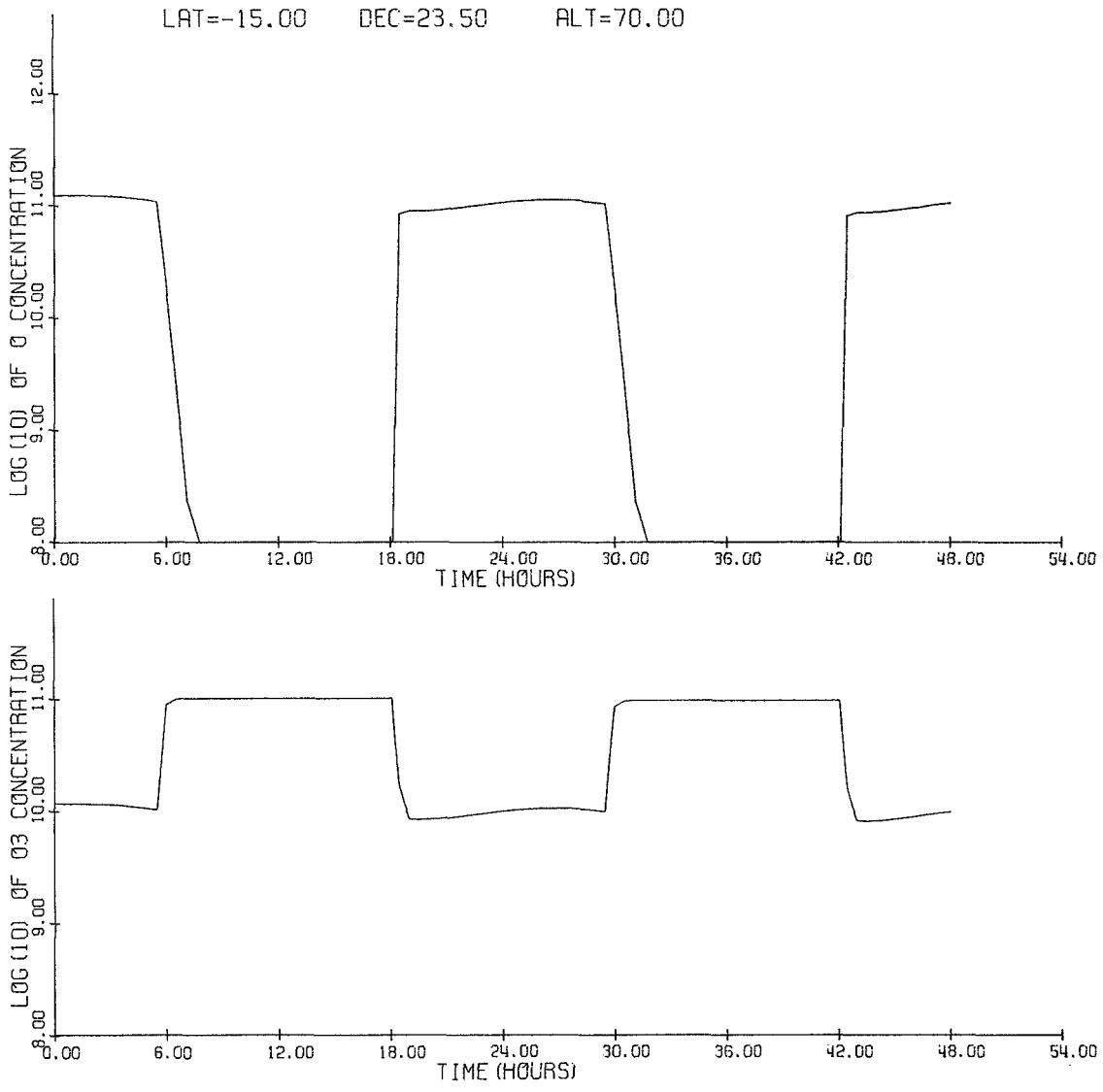
LAT=-15.00 DEC=23.50 ALT=70.00
LOG(10) OF O CONCENTRATION
12.00
11.00
10.00
9.00
8.00
0.00
6.00
12.00
18.00
24.00
30.00
36.00
42.00
48.00
54.00
TIME (HOURS)
LOG(10) OF O3 CONCENTRATION
11.00
10.00
9.00
8.00
0.00
6.00
12.00
18.00
24.00
30.00
36.00
42.00
48.00
54.00
TIME (HOURS)

Figure A16

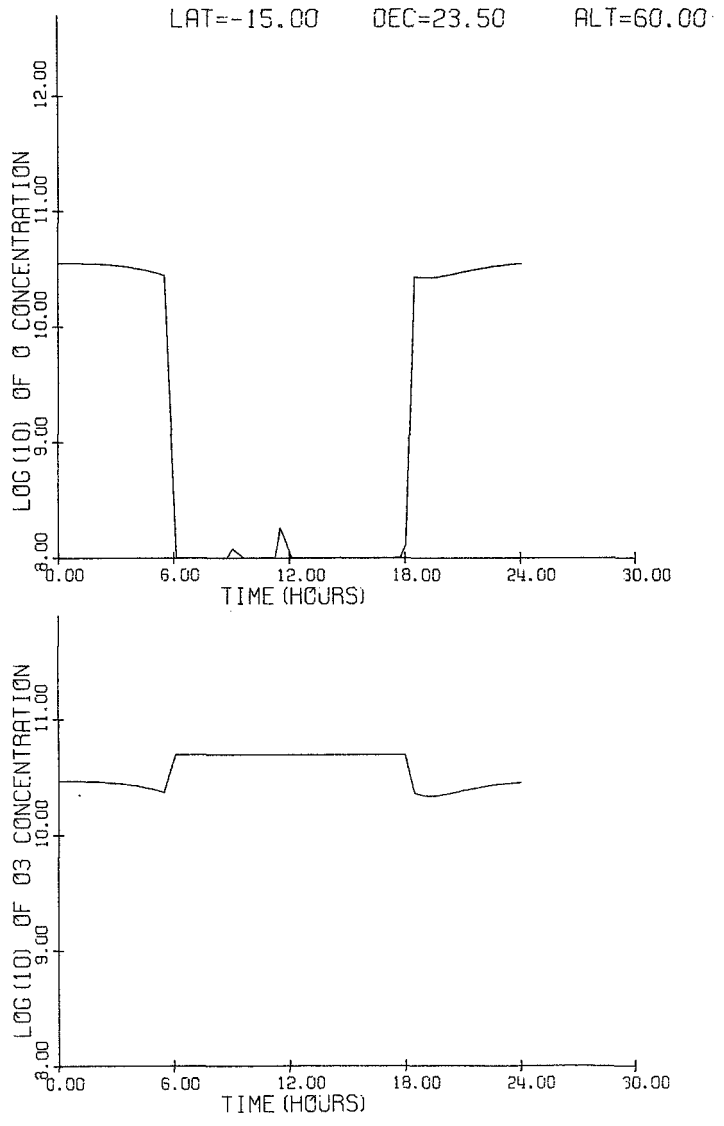

Figure A16 (continued)

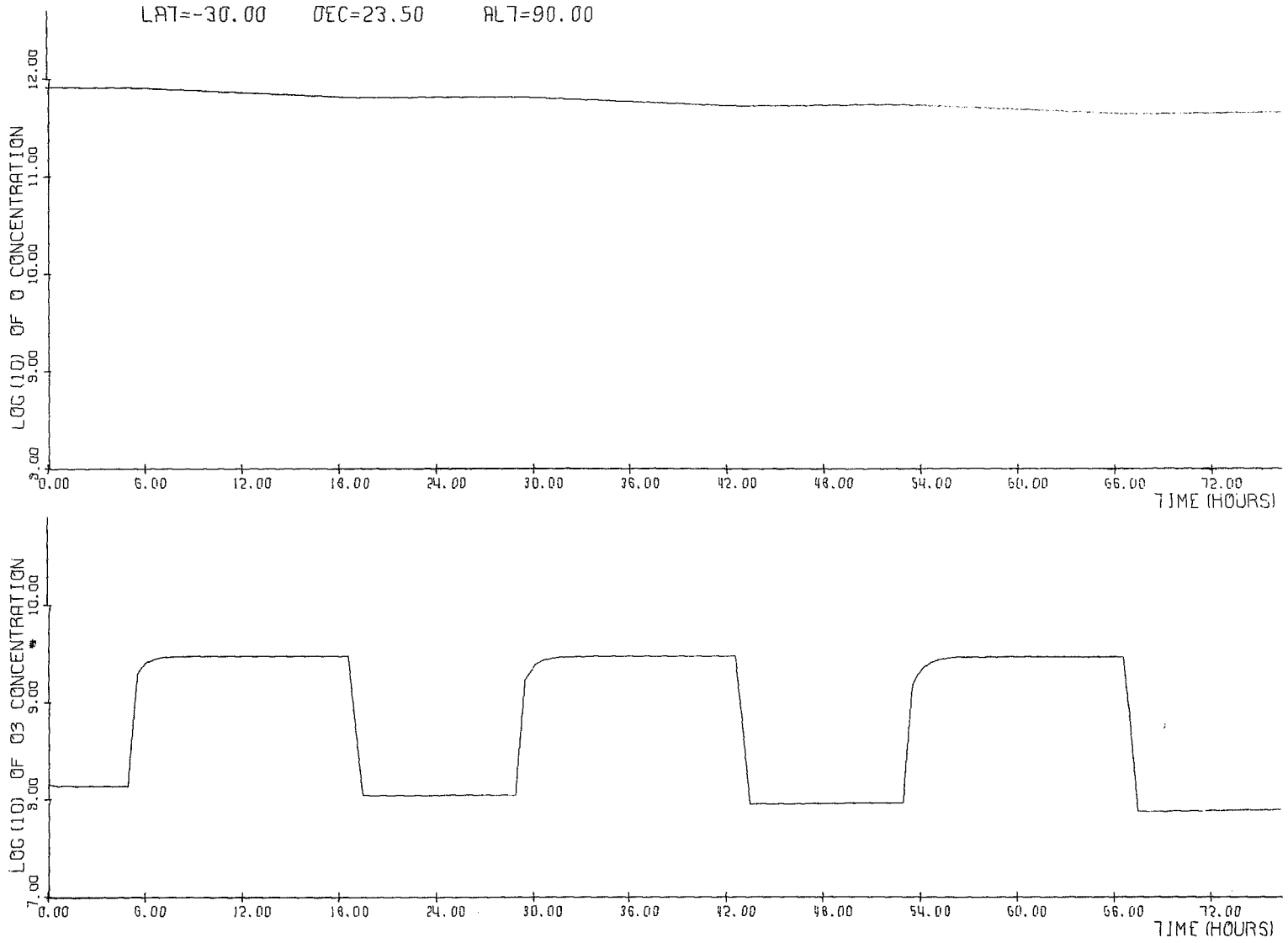
LAT=-30.00 DEC=23.50 ALT=90.00
LOG(10) OF O CONCENTRATION
12.00
11.00
10.00
9.00
8.00
0.00 6.00 12.00 18.00 24.00 30.00 36.00 42.00 48.00 54.00 60.00 66.00 72.00
TIME (HOURS)
LOG(10) OF O3 CONCENTRATION
10.00
9.00
8.00
7.00
0.00 6.00 12.00 18.00 24.00 30.00 36.00 42.00 48.00 54.00 60.00 66.00 72.00
TIME (HOURS)

Figure A17

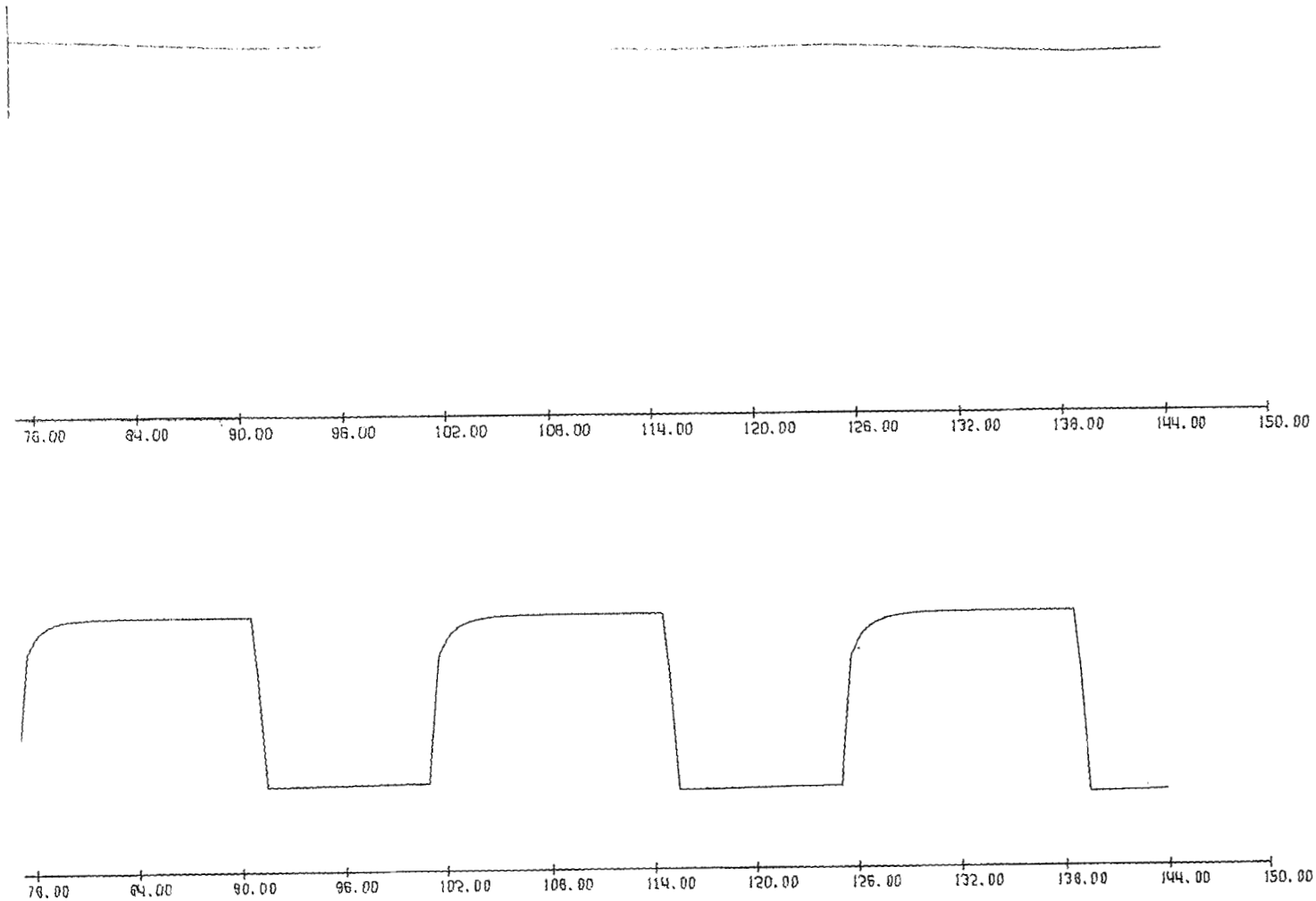

Figure A17 (continued)

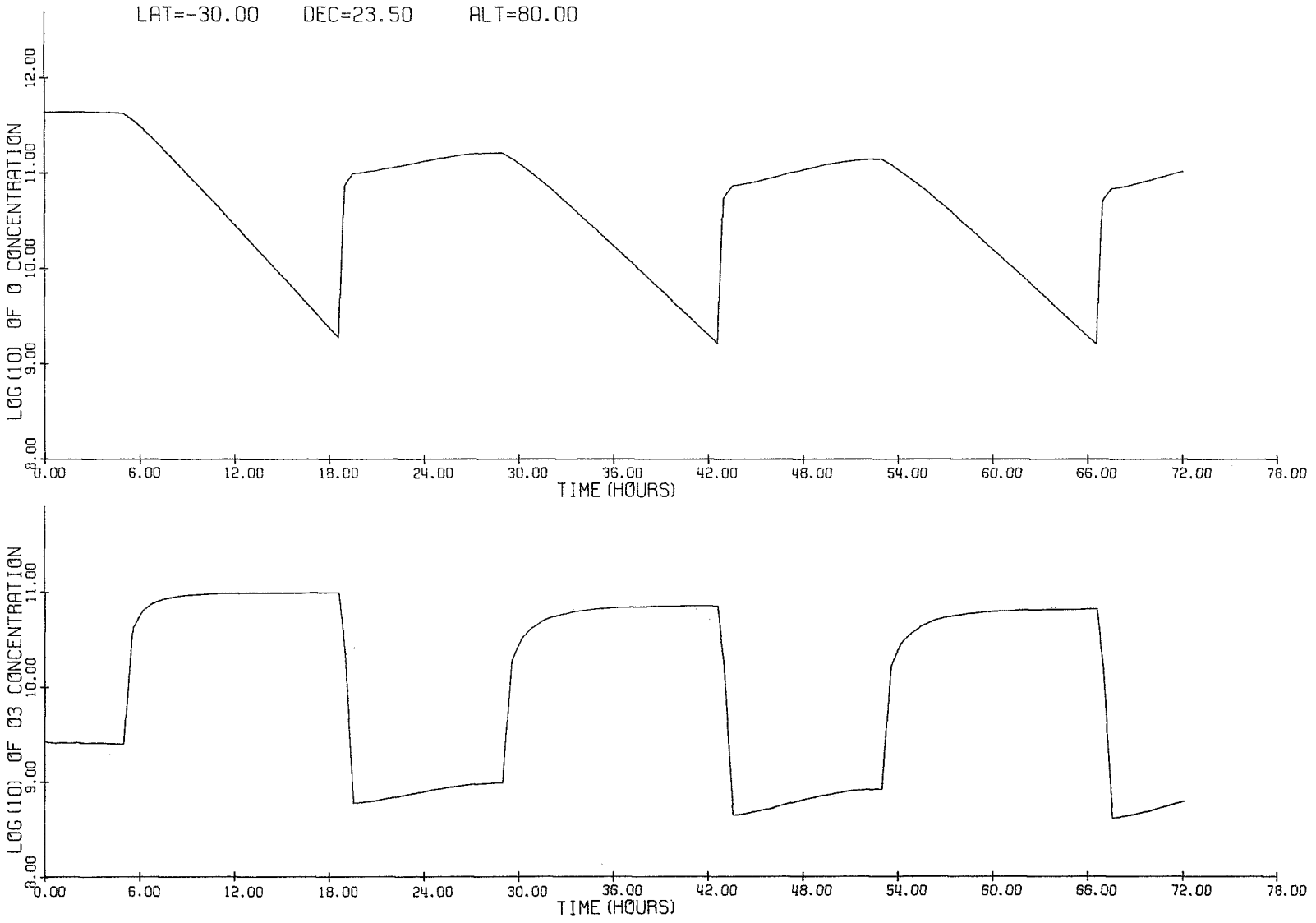
LAT=-30.00 DEC=23.50 ALT=80.00
LOG(10) OF O CONCENTRATION
12.00
11.00
10.00
9.00
8.00
0.00 6.00 12.00 18.00 24.00 30.00 36.00 42.00 48.00 54.00 60.00 66.00 72.00 78.00
TIME (HOURS)
LOG(10) OF O3 CONCENTRATION
11.00
10.00
9.00
8.00
0.00 6.00 12.00 18.00 24.00 30.00 36.00 42.00 48.00 54.00 60.00 66.00 72.00 78.00
TIME (HOURS)

Figure A18

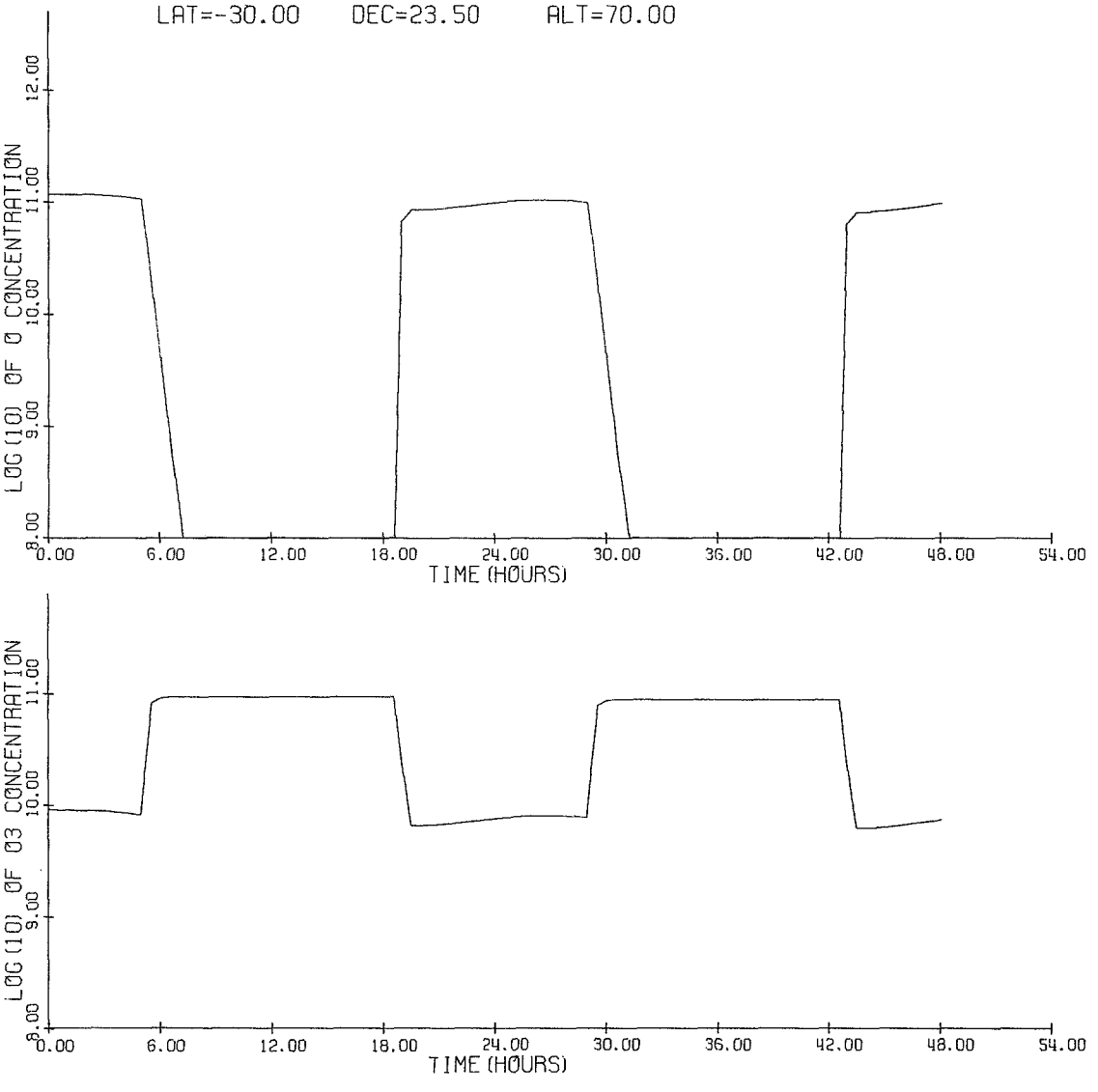
LAT=-30.00 DEC=23.50 ALT=70.00
LOG(10) OF O CONCENTRATION
12.00
11.00
10.00
9.00
8.00
0.00
6.00
12.00
18.00
24.00
30.00
36.00
42.00
48.00
54.00
TIME (HOURS)
LOG(10) OF O3 CONCENTRATION
11.00
10.00
9.00
8.00
0.00
6.00
12.00
18.00
24.00
30.00
36.00
42.00
48.00
54.00
TIME (HOURS)

Figure A19

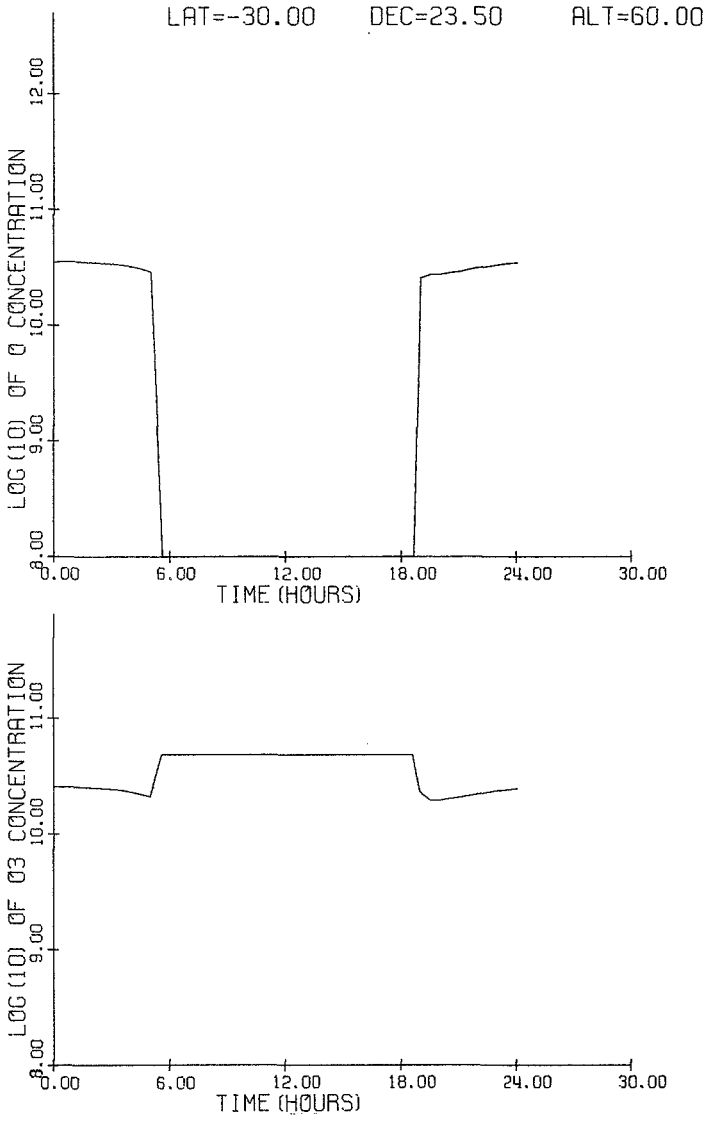

Figure A19 (continued)

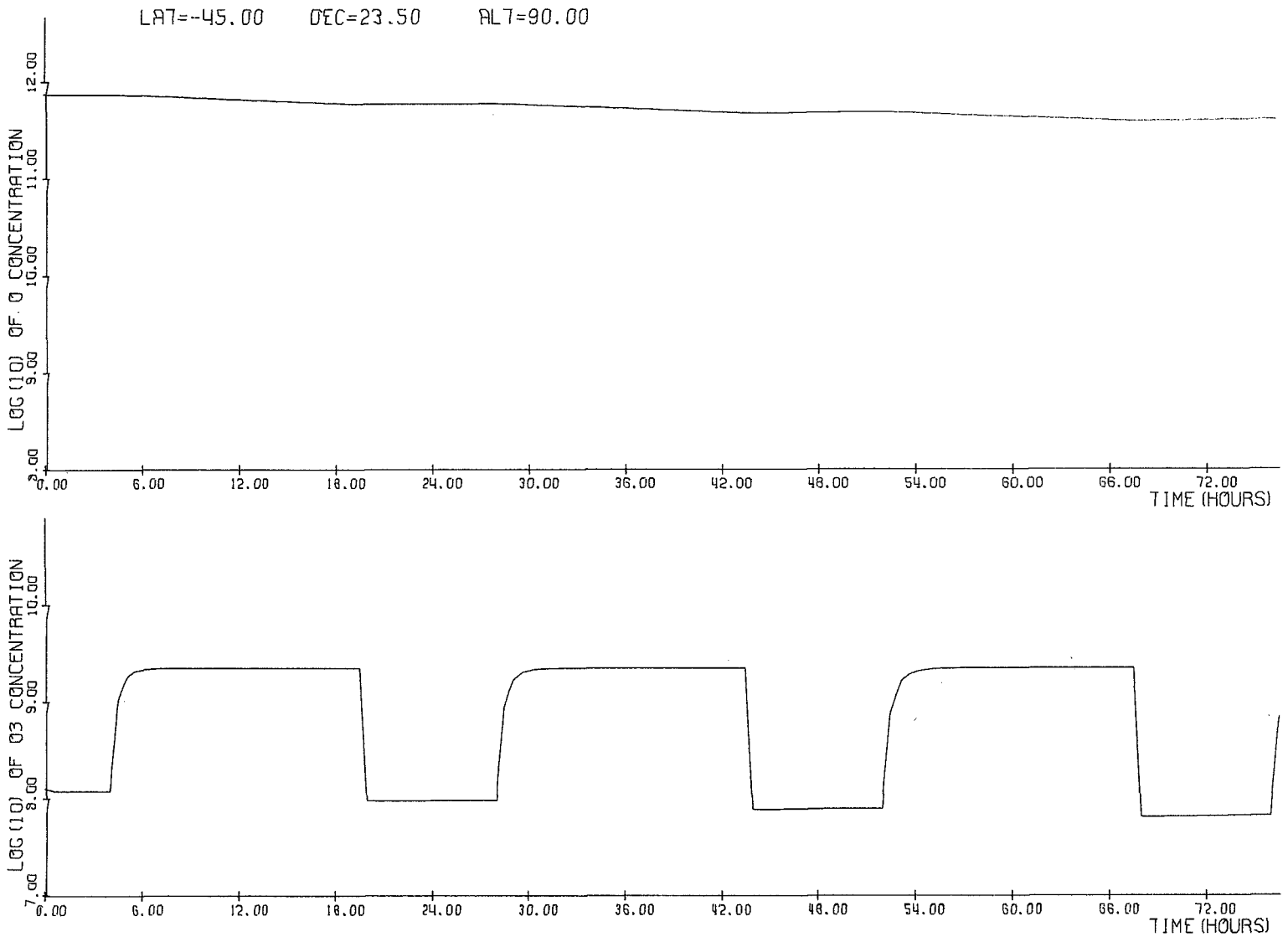
LAT=-45.00 DEC=23.50 ALT=90.00
LOG(10) OF O CONCENTRATION
12.00
11.00
10.00
9.00
8.00
0.00 6.00 12.00 18.00 24.00 30.00 36.00 42.00 48.00 54.00 60.00 66.00 72.00
TIME (HOURS)
LOG(10) OF O3 CONCENTRATION
10.00
9.00
8.00
7.00
0.00 6.00 12.00 18.00 24.00 30.00 36.00 42.00 48.00 54.00 60.00 66.00 72.00
TIME (HOURS)

Figure A20

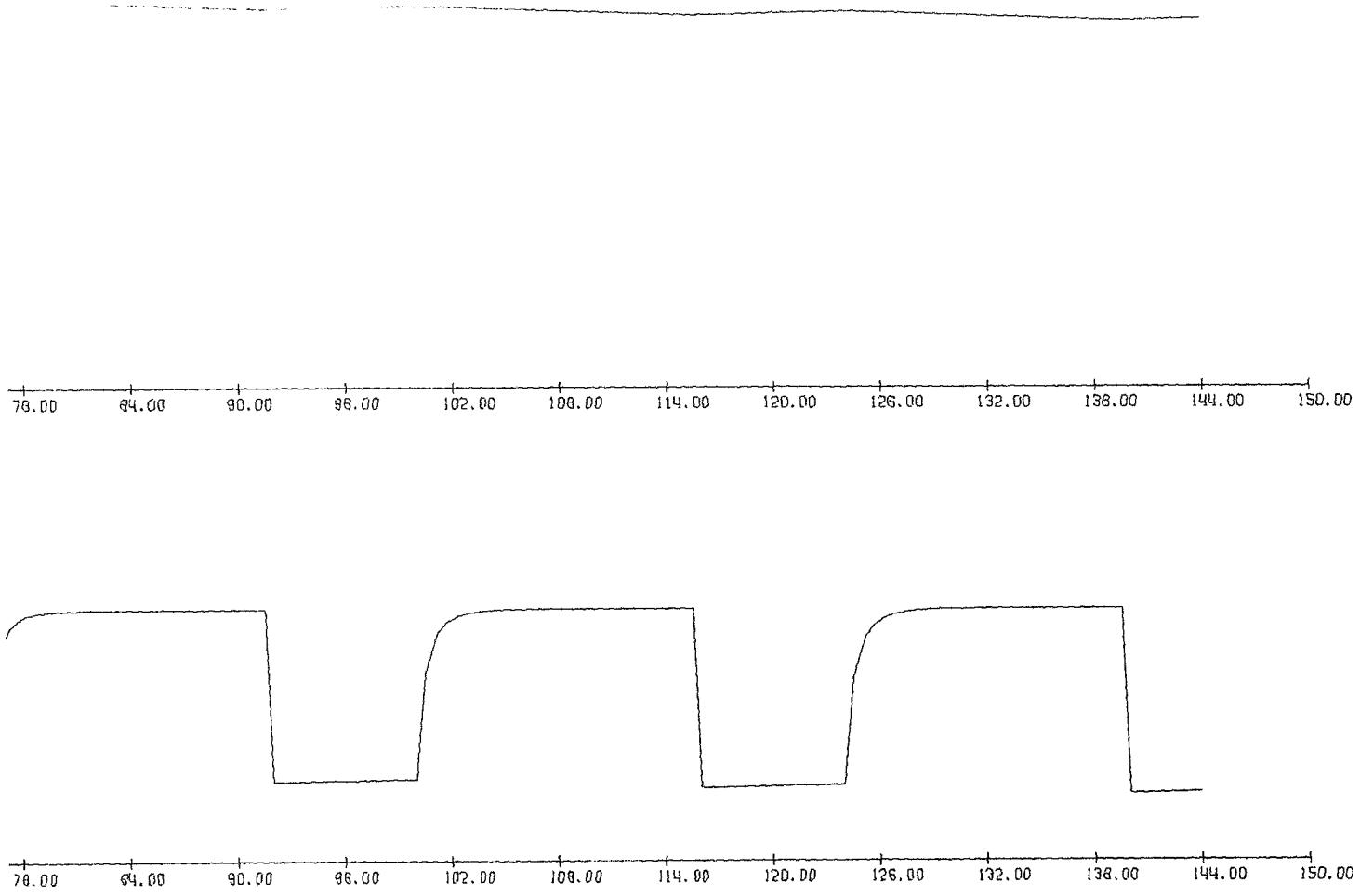

Figure A20 (continued)

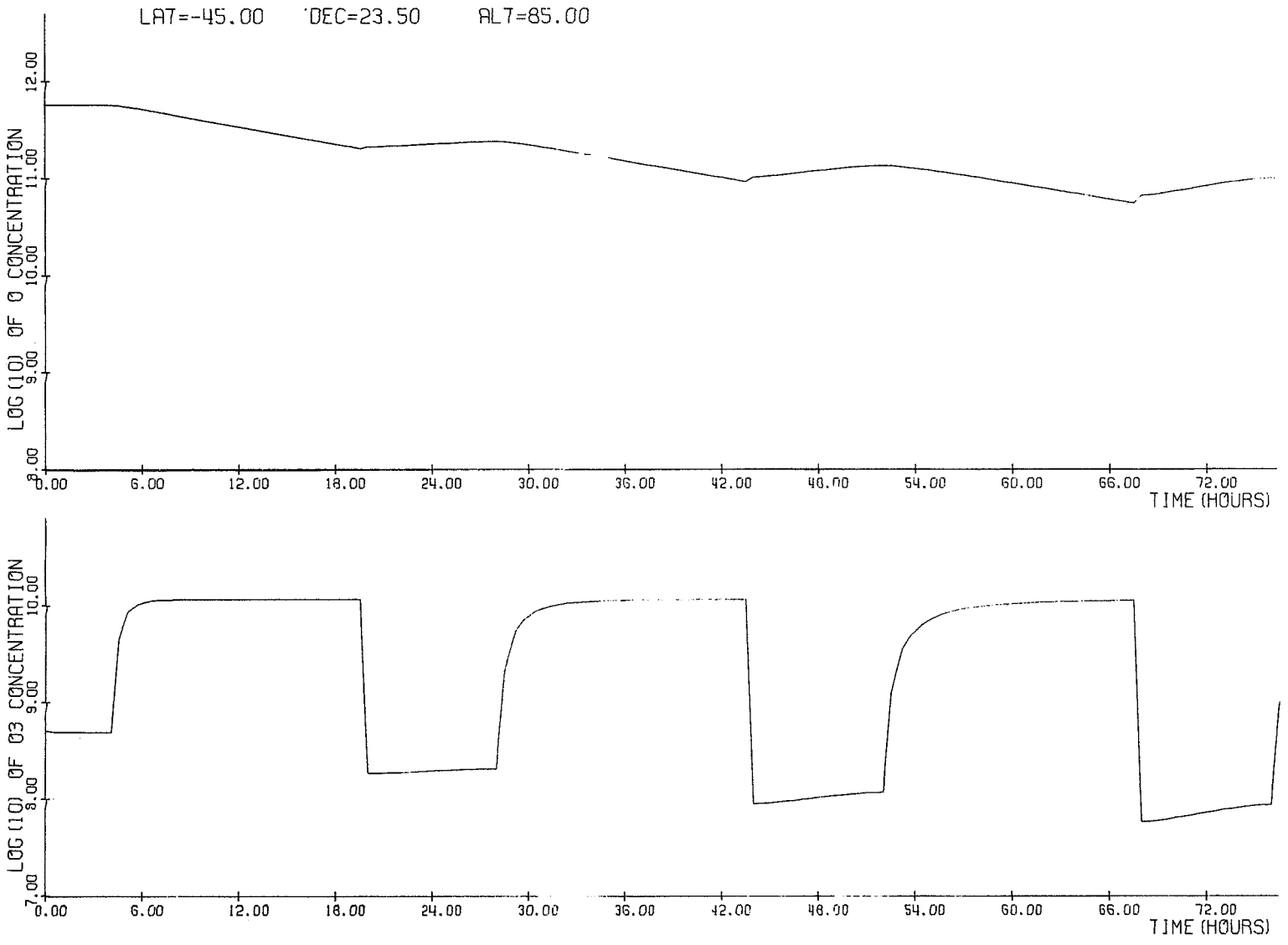
LAT=-45.00 DEC=23.50 ALT=85.00
LOG(10) OF O CONCENTRATION
12.00
11.00
10.00
9.00
8.00
0.00
6.00
12.00
18.00
24.00
30.00
36.00
42.00
48.00
54.00
60.00
66.00
72.00
TIME (HOURS)
LOG(10) OF O3 CONCENTRATION
10.00
9.00
8.00
7.00
0.00
6.00
12.00
18.00
24.00
30.00
36.00
42.00
48.00
54.00
60.00
66.00
72.00
TIME (HOURS)

Figure A21

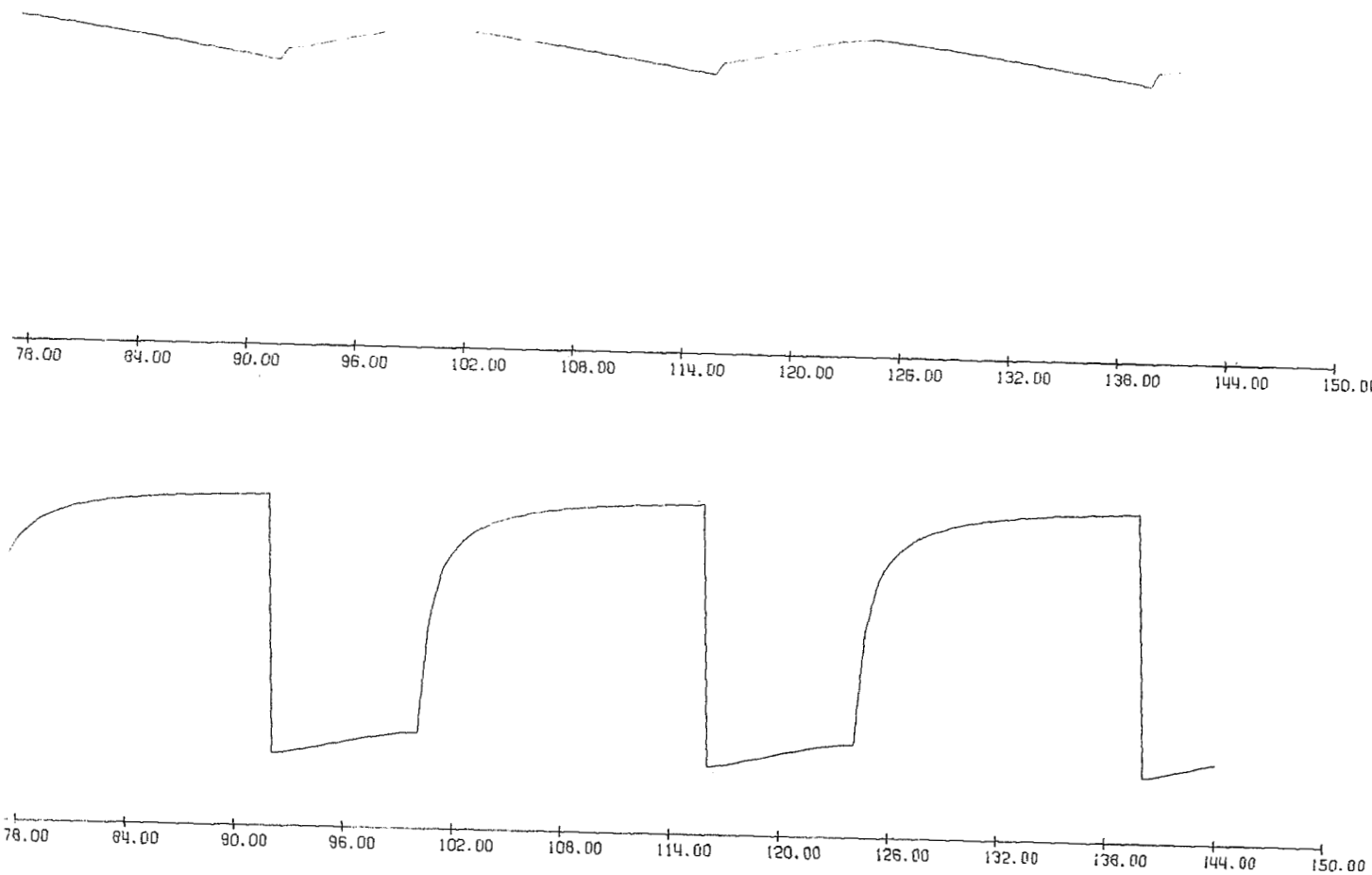

Figure A21 (continued)

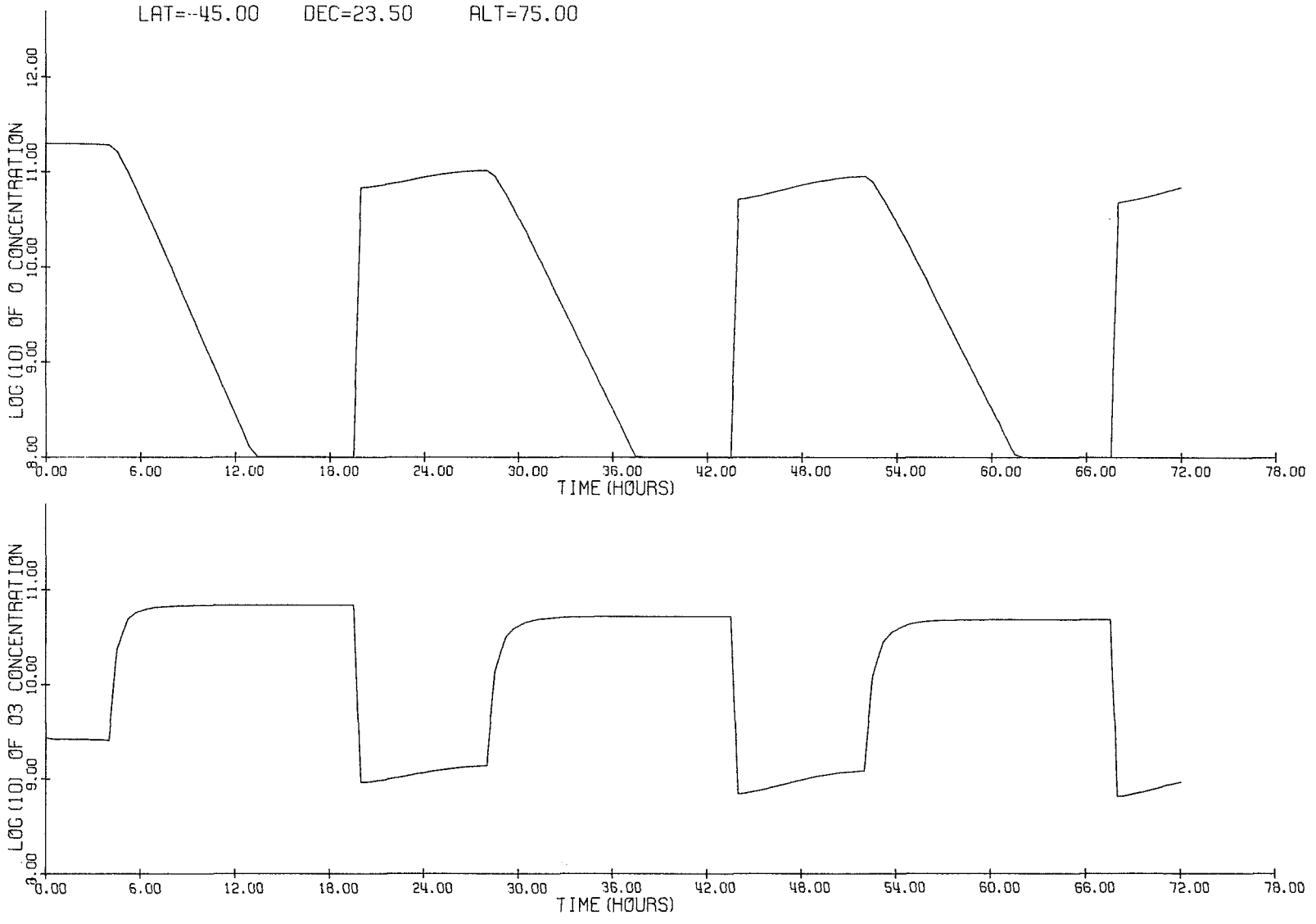
LAT=-45.00 DEC=23.50 ALT=75.00
LOG(10) OF O CONCENTRATION
12.00
11.00
10.00
9.00
8.00
0.00 6.00 12.00 18.00 24.00 30.00 36.00 42.00 48.00 54.00 60.00 66.00 72.00 78.00
TIME (HOURS)
LOG(10) OF O3 CONCENTRATION
11.00
10.00
9.00
8.00
0.00 6.00 12.00 18.00 24.00 30.00 36.00 42.00 48.00 54.00 60.00 66.00 72.00 78.00
TIME (HOURS)

Figure A22

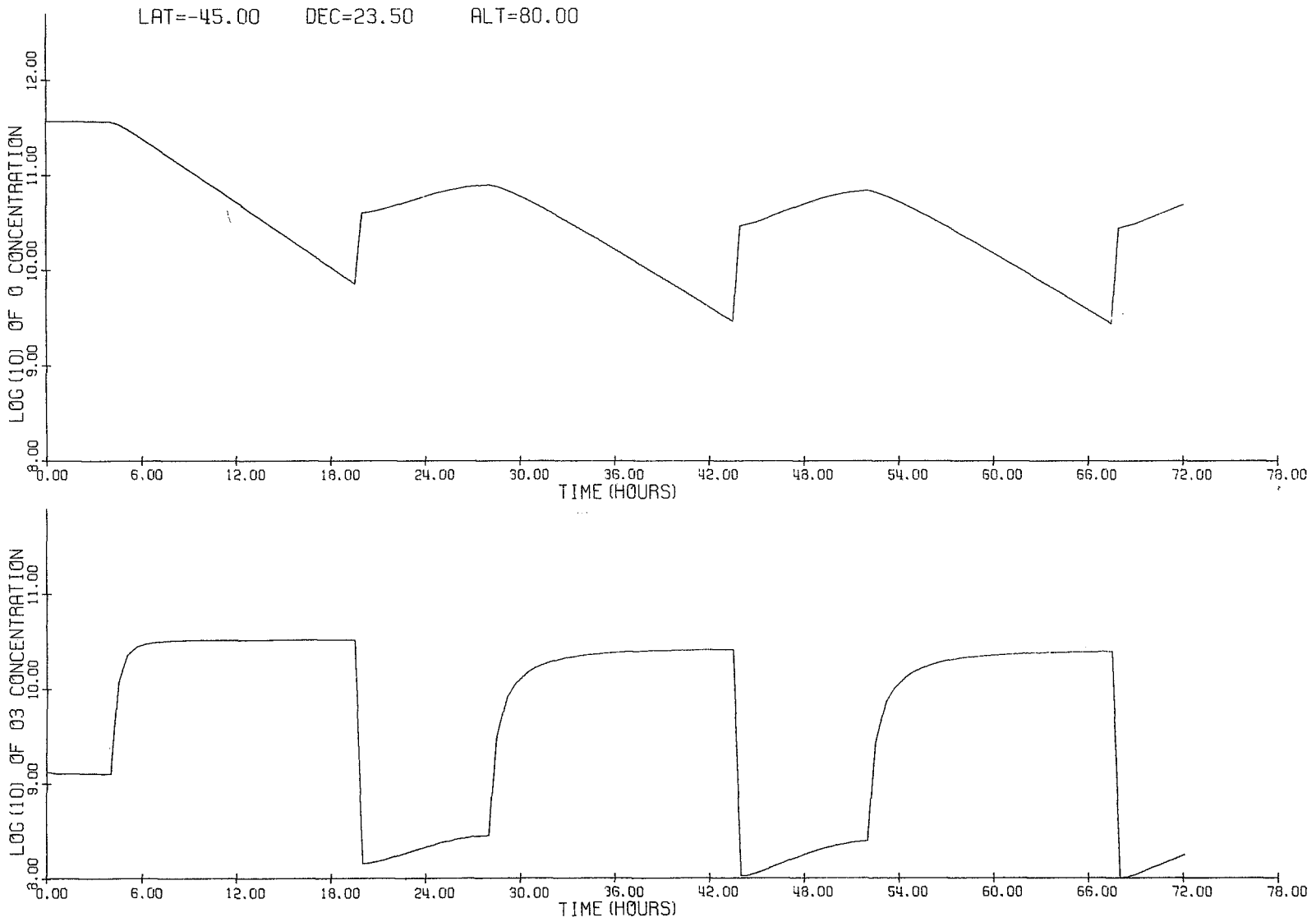

Figure A22 (continued)

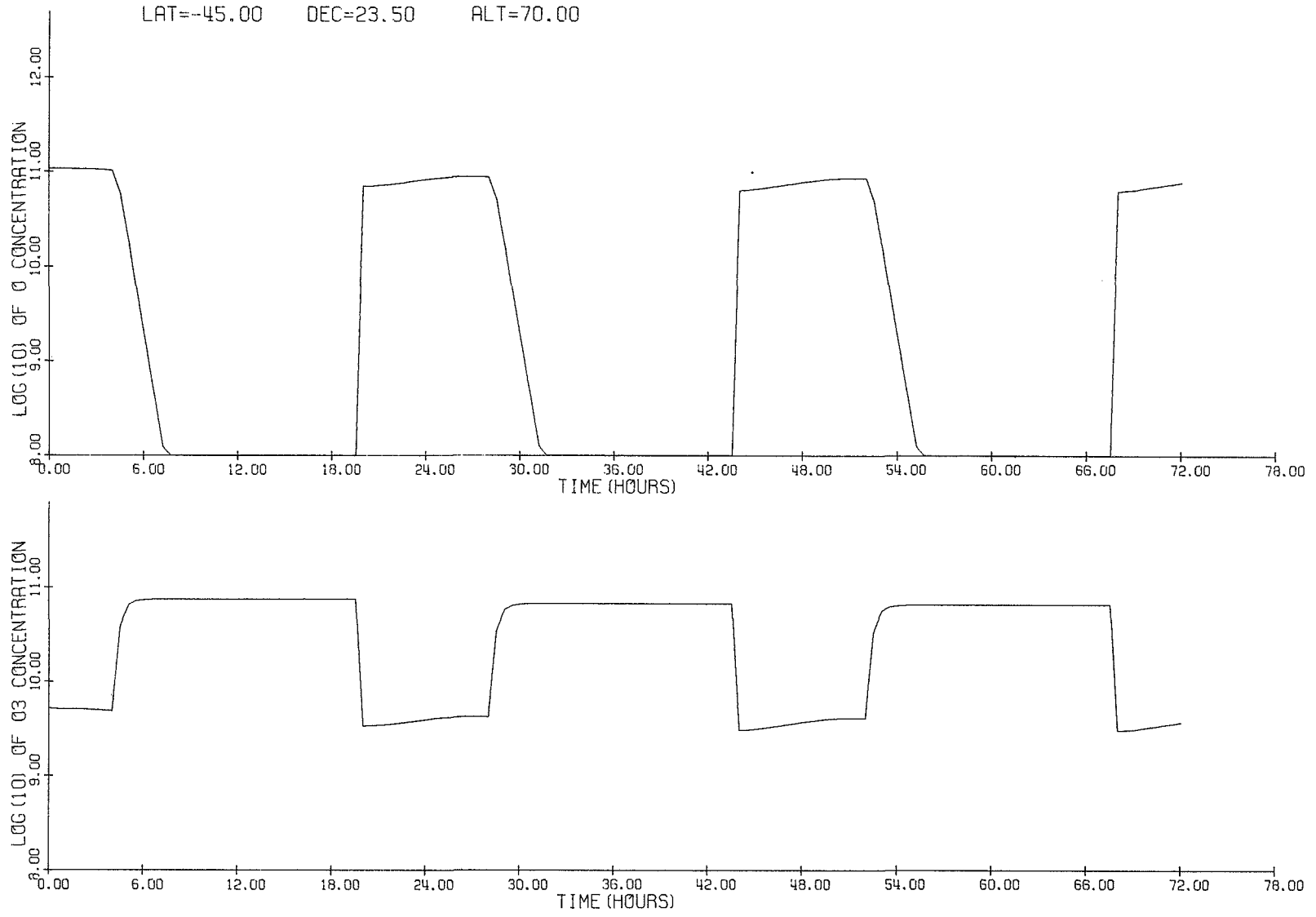
LAT=-45.00 DEC=23.50 ALT=70.00
LOG(10) OF O CONCENTRATION
8.00
9.00
10.00
11.00
12.00
0.00
6.00
12.00
18.00
24.00
30.00
36.00
42.00
48.00
54.00
60.00
66.00
72.00
78.00
TIME (HOURS)
LOG(10) OF O3 CONCENTRATION
8.00
9.00
10.00
11.00
0.00
6.00
12.00
18.00
24.00
30.00
36.00
42.00
48.00
54.00
60.00
66.00
72.00
78.00
TIME (HOURS)

Figure A23

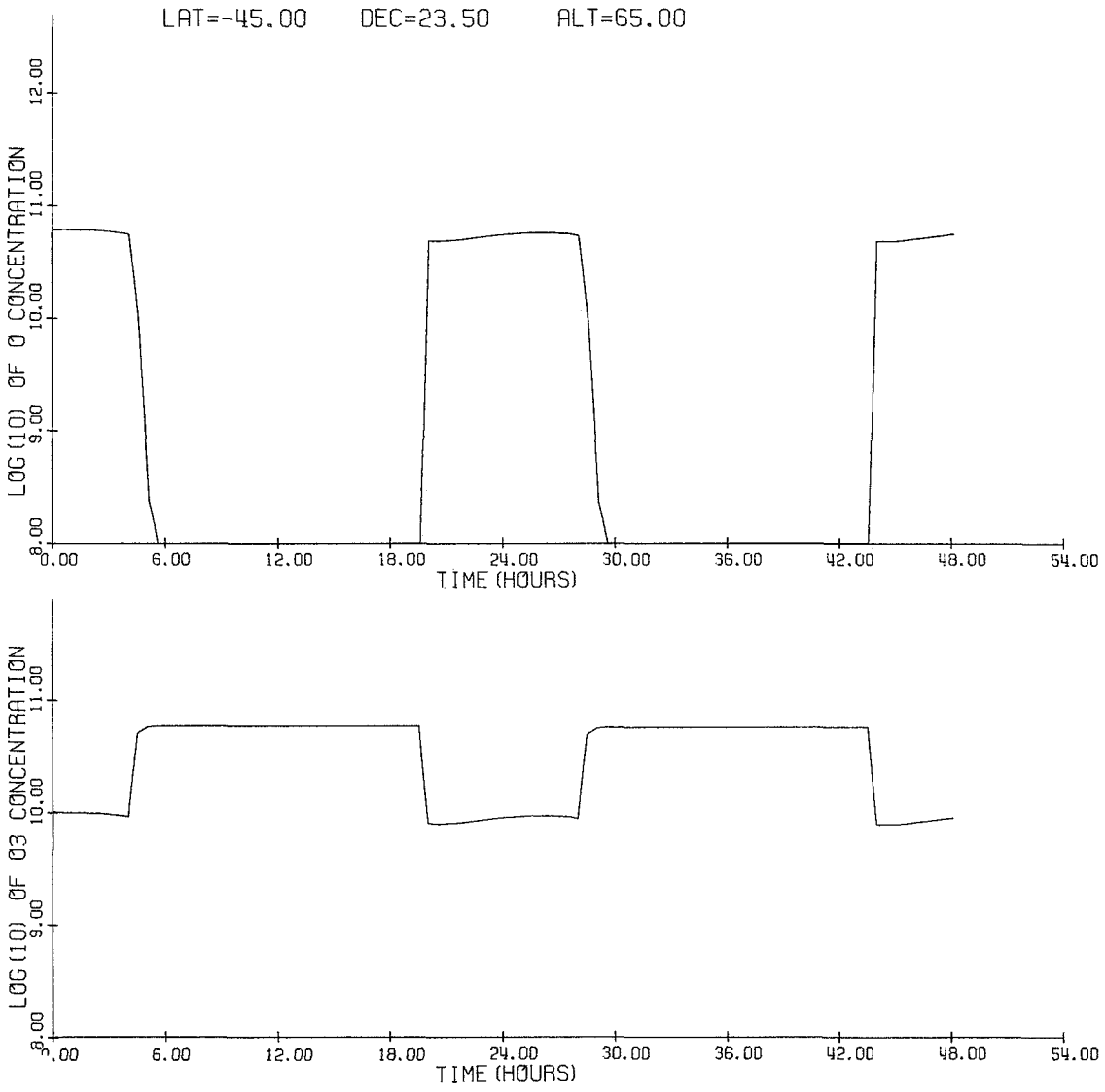
LAT=-45.00 DEC=23.50 ALT=65.00
LOG(10) OF O CONCENTRATION
12.00
11.00
10.00
9.00
8.00
0.00
6.00
12.00
18.00
24.00
30.00
36.00
42.00
48.00
54.00
TIME (HOURS)
LOG(10) OF O3 CONCENTRATION
11.00
10.00
9.00
8.00
0.00
6.00
12.00
18.00
24.00
30.00
36.00
42.00
48.00
54.00
TIME (HOURS)

Figure A24

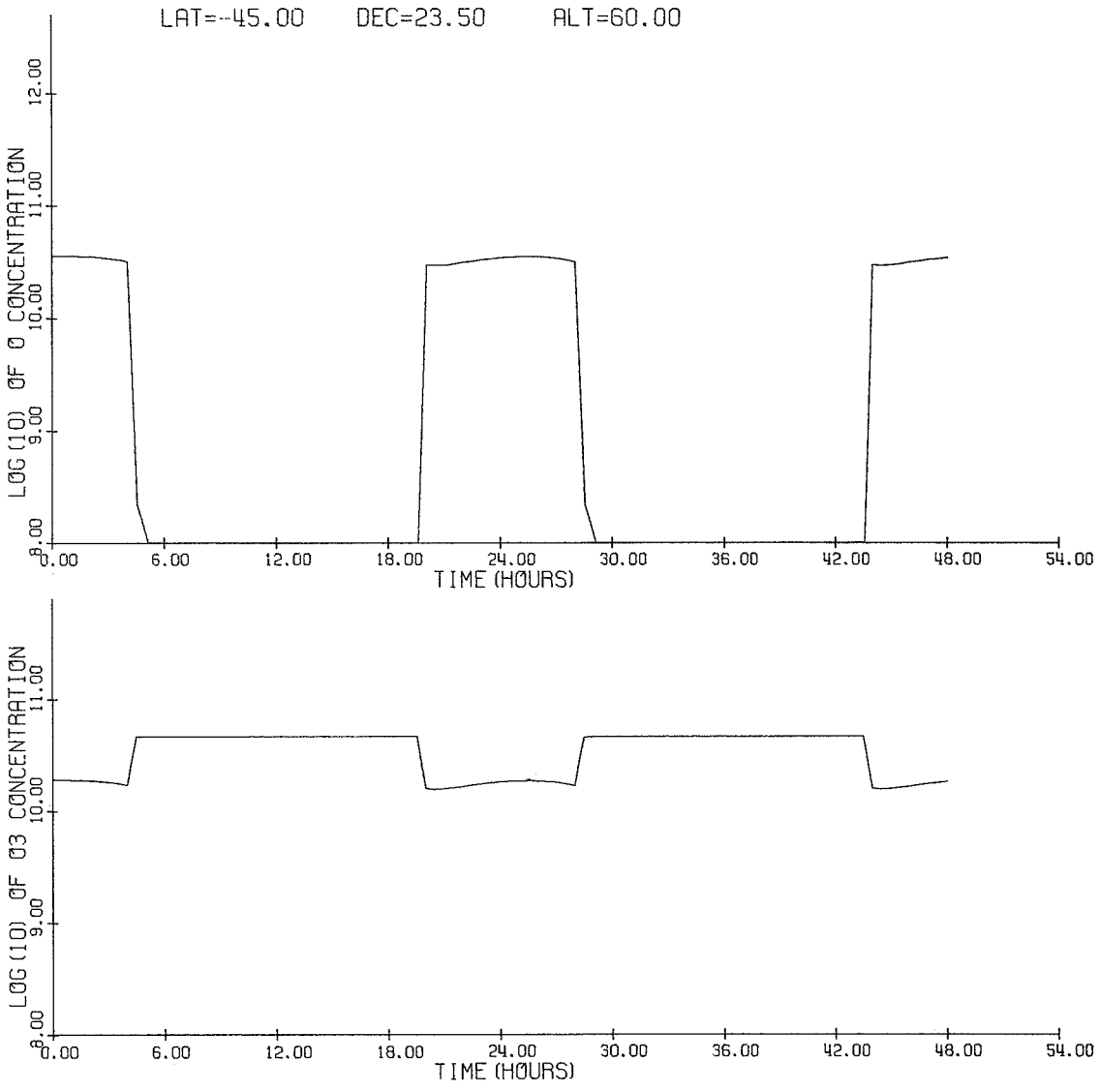

Figure A24 (continued)

Table A4

LATITUDE= 45.0 DEG ALTITUDE= 90.0 KM

DECLINATION=23.5 DEG

TIME(HR-MIN)	N(O)	N(O3)
0- 7	4.786E 11	1.334E 08
0-31	4.898E 11	1.343E 08
1- 7	4.898E 11	1.349E 08
1-31	4.898E 11	1.358E 08
2- 7	4.898E 11	1.361E 08
2-31	4.898E 11	1.368E 08
3- 7	5.012E 11	1.371E 08
3-31	5.012E 11	1.380E 08
4- 7	5.012E 11	1.380E 08
4-31	5.012E 11	1.387E 08
5- 7	5.012E 11	1.384E 08
5-31	5.012E 11	1.390E 08
6- 7	5.012E 11	1.390E 08
6-31	5.012E 11	1.396E 08
7- 7	5.012E 11	1.390E 08
7-33	5.012E 11	1.390E 08
8- 7	5.012E 11	2.065E 09
8-44	4.898E 11	4.603E 09
9-29	4.898E 11	7.096E 09
9-59	4.786E 11	8.472E 09
10-30	4.786E 11	9.660E 09
11- 0	4.786E 11	1.072E 10
11-30	4.677E 11	1.148E 10
12- 0	4.677E 11	1.230E 10
12-30	4.571E 11	1.288E 10
13- 0	4.571E 11	1.349E 10
13-30	4.467E 11	1.413E 10
14- 0	4.467E 11	1.445E 10
14-30	4.365E 11	1.479E 10
15- 0	4.365E 11	1.514E 10
15-30	4.266E 11	1.549E 10
16- 0	4.266E 11	1.585E 10
16- 7	4.266E 11	1.585E 10
16-30	4.365E 11	1.242E 08
17- 7	4.365E 11	1.211E 08
17-37	4.365E 11	1.211E 08
18- 3	4.365E 11	1.213E 08
18-37	4.365E 11	1.216E 08
19- 3	4.365E 11	1.216E 08
19-37	4.467E 11	1.222E 08
20- 3	4.467E 11	1.225E 08
20-33	4.467E 11	1.227E 08
21- 3	4.467E 11	1.233E 08
21-37	4.467E 11	1.242E 08
22- 1	4.467E 11	1.253E 08
22-37	4.571E 11	1.253E 08
23- 3	4.571E 11	1.262E 08
23-37	4.571E 11	1.268E 08

Table A5

LATITUDE= 45.0 DEG ALTITUDE= 85.0 KM

TIME(HR-MIN)	N(O)	N(O3)
0- 7	2.455E 11	5.129E 08
0-31	2.512E 11	5.200E 08
1- 7	2.570E 11	5.284E 08
1-31	2.570E 11	5.358E 08
2- 7	2.630E 11	5.432E 08
2-31	2.630E 11	5.508E 08
3- 7	2.692E 11	5.572E 08
3-31	2.692E 11	5.649E 08
4- 7	2.754E 11	5.715E 08
4-31	2.754E 11	5.781E 08
5- 7	2.818E 11	5.821E 08
5-31	2.818E 11	5.888E 08
6- 7	2.884E 11	5.916E 08
6-31	2.884E 11	5.970E 08
7- 7	2.884E 11	5.957E 08
7-33	2.884E 11	5.957E 08
8- 7	2.754E 11	8.933E 09
8-45	2.630E 11	2.042E 10
9-30	2.455E 11	3.162E 10
10- 0	2.291E 11	3.802E 10
10-30	2.188E 11	4.467E 10
11- 0	2.089E 11	4.898E 10
11-30	1.950E 11	5.370E 10
12- 0	1.862E 11	5.888E 10
12-30	1.778E 11	6.166E 10
13- 0	1.660E 11	6.607E 10
13-30	1.549E 11	6.918E 10
14- 0	1.479E 11	7.079E 10
14-30	1.380E 11	7.413E 10
15- 0	1.318E 11	7.586E 10
15-30	1.230E 11	7.762E 10
16- 0	1.148E 11	7.943E 10
16- 7	1.148E 11	7.943E 10
16-31	1.905E 11	4.140E 08
17- 7	1.905E 11	3.999E 08
17-37	1.950E 11	4.027E 08
18- 3	1.950E 11	4.064E 08
18-37	1.995E 11	4.140E 08
19- 3	1.995E 11	4.178E 08
19-37	2.042E 11	4.256E 08
20- 3	2.089E 11	4.315E 08
20-33	2.138E 11	4.385E 08
21- 7	2.138E 11	4.477E 08
21-31	2.188E 11	4.560E 08
22- 7	2.239E 11	4.634E 08
22-31	2.291E 11	4.710E 08
23- 7	2.291E 11	4.797E 08
23-31	2.344E 11	4.875E 08

Table A6

LATITUDE= 45.0 DEG ALTITUDE= 80.0 KM

DECLINATION=23.5 DEG

TIME(HR-MIN)	N(C)	N(C3)
0- 7	2.570E 11	3.048E 09
0-31	2.630E 11	3.119E 09
1- 7	2.692E 11	3.177E 09
1-33	2.692E 11	3.228E 09
2- 7	2.754E 11	3.289E 09
2-33	2.818E 11	3.342E 09
3- 3	2.884E 11	3.388E 09
3-37	2.884E 11	3.436E 09
4- 1	2.951E 11	3.475E 09
4-37	2.951E 11	3.508E 09
5- 1	2.951E 11	3.540E 09
5-37	2.951E 11	3.540E 09
6- 1	2.951E 11	3.548E 09
6-33	2.951E 11	3.548E 09
7- 7	2.951E 11	3.532E 09
7-33	2.951E 11	3.508E 09
8- 7	2.455E 11	4.786E 10
8-45	1.778E 11	9.550E 10
9-30	1.175E 11	1.318E 11
10- 0	8.710E 10	1.479E 11
10-30	6.607E 10	1.585E 11
11- 0	4.898E 10	1.660E 11
11-30	3.631E 10	1.738E 11
12- 0	2.692E 10	1.778E 11
12-30	1.995E 10	1.820E 11
13- 0	1.479E 10	1.820E 11
13-30	1.096E 10	1.862E 11
14- 0	8.147E 09	1.862E 11
14-30	6.012E 09	1.862E 11
15- 0	4.446E 09	1.862E 11
15-30	3.281E 09	1.862E 11
16- 0	2.421E 09	1.862E 11
16- 7	2.244E 09	1.862E 11
16-31	1.862E 11	2.265E 09
17- 7	1.862E 11	2.234E 09
17-37	1.905E 11	2.249E 09
18- 3	1.905E 11	2.265E 09
18-37	1.950E 11	2.307E 09
19- 3	1.950E 11	2.333E 09
19-37	1.995E 11	2.388E 09
20- 7	2.042E 11	2.438E 09
20-33	2.089E 11	2.489E 09
21- 3	2.138E 11	2.547E 09
21-37	2.188E 11	2.624E 09
22- 1	2.239E 11	2.685E 09
22-37	2.344E 11	2.754E 09
23- 1	2.344E 11	2.825E 09
23-37	2.455E 11	2.897E 09

Table A7

LATITUDE= 45.0 DEG ALTITUDE= 75.0 KM

TIME(HR-MIN)	N(O)	N(O3)
0- 1	1.995E 11	8.166E 09
0-37	2.042E 11	8.414E 09
1- 3	2.042E 11	8.531E 09
1-37	2.089E 11	8.670E 09
2- 3	2.089E 11	8.770E 09
2-33	2.138E 11	8.851E 09
3- 7	2.138E 11	8.933E 09
3-33	2.138E 11	8.954E 09
4- 3	2.138E 11	8.974E 09
4-37	2.138E 11	8.974E 09
5- 3	2.138E 11	8.933E 09
5-33	2.138E 11	8.872E 09
6- 7	2.089E 11	8.770E 09
6-33	2.089E 11	8.690E 09
7- 7	2.042E 11	8.551E 09
7-33	2.042E 11	8.414E 09
8- 7	1.023E 11	9.120E 10
8-37	4.074E 10	1.349E 11
9-15	1.259E 10	1.514E 11
9-45	4.909E 09	1.585E 11
10-15	1.892E 09	1.585E 11
10-45	7.278E 08	1.585E 11
11-15	2.799E 08	1.585E 11
11-45	1.076E 08	1.585E 11
12-30	1.000E 08	1.585E 11
13- 0	1.000E 08	1.585E 11
13-30	1.000E 08	1.585E 11
14- 0	1.000E 08	1.585E 11
14-30	1.000E 08	1.585E 11
15- 0	1.000E 08	1.585E 11
15-30	1.000E 08	1.585E 11
16- 0	1.000E 08	1.585E 11
16- 7	1.000E 08	1.585E 11
16-31	1.514E 11	6.339E 09
17- 1	1.514E 11	6.281E 09
17-37	1.514E 11	6.266E 09
18- 3	1.514E 11	6.281E 09
18-33	1.514E 11	6.324E 09
19- 7	1.549E 11	6.397E 09
19-33	1.549E 11	6.486E 09
20- 3	1.585E 11	6.592E 09
20-37	1.622E 11	6.761E 09
21- 3	1.660E 11	6.887E 09
21-33	1.698E 11	7.063E 09
22- 7	1.738E 11	7.261E 09
22-33	1.778E 11	7.413E 09
23- 7	1.820E 11	7.603E 09
23-33	1.862E 11	7.780E 09

Table A8

LATITUDE= 45.0 DEG ALTITUDE= 70.0 KM

DECLINATION=23.5 DEG

TIME(HR-MIN)	N(O)	N(O3)
0- 1	1.047E 11	1.349E 10
0-31	1.072E 11	1.349E 10
1- 7	1.096E 11	1.380E 10
1-33	1.096E 11	1.413E 10
2- 3	1.096E 11	1.413E 10
2-31	1.096E 11	1.413E 10
3- 1	1.096E 11	1.413E 10
3-31	1.096E 11	1.413E 10
4- 1	1.096E 11	1.413E 10
4-31	1.096E 11	1.380E 10
5- 1	1.072E 11	1.380E 10
5-31	1.047E 11	1.349E 10
6- 1	1.023E 11	1.318E 10
6-31	1.000E 11	1.288E 10
7- 1	9.772E 10	1.259E 10
7-33	9.333E 10	1.202E 10
8- 3	1.660E 10	8.128E 10
8-37	9.057E 08	9.333E 10
9- 7	1.000E 08	9.333E 10
9-45	1.000E 08	9.333E 10
10-15	1.000E 08	9.333E 10
10-45	1.000E 08	9.333E 10
11-30	1.000E 08	9.333E 10
12- 0	1.000E 08	9.333E 10
12-30	1.000E 08	9.333E 10
13- 0	1.000E 08	9.333E 10
13-30	1.000E 08	9.333E 10
14- 0	1.000E 08	9.333E 10
14-30	1.000E 08	9.333E 10
15- 0	1.000E 08	9.333E 10
15-30	1.000E 08	9.333E 10
16- 0	1.000E 08	9.333E 10
16- 7	1.000E 08	9.333E 10
16-31	8.128E 10	1.047E 10
17- 3	8.128E 10	1.023E 10
17-37	7.943E 10	1.023E 10
18- 7	7.943E 10	1.023E 10
18-33	8.128E 10	1.047E 10
19- 3	8.128E 10	1.047E 10
19-31	8.318E 10	1.072E 10
20- 1	8.511E 10	1.096E 10
20-31	8.710E 10	1.122E 10
21- 1	9.12CE 10	1.148E 10
21-31	9.333E 10	1.175E 10
22- 1	9.550E 10	1.230E 10
22-31	9.772E 10	1.259E 10
23- 1	1.000E 11	1.288E 10
23-31	1.023E 11	1.318E 10

Table A9

LATITUDE= 45.0 DEG ALTITUDE= 65.0 KM

TIME(HR-MIN)	N(O)	N(O3)
0- 0	5.888E 10	2.089E 10
0-37	5.888E 10	2.089E 10
1- 3	5.888E 10	2.089E 10
1-31	5.888E 10	2.089E 10
2- 7	5.888E 10	2.042E 10
2-33	5.754E 10	2.042E 10
3- 1	5.754E 10	2.042E 10
3-37	5.623E 10	1.995E 10
4- 3	5.623E 10	1.995E 10
4-31	5.495E 10	1.950E 10
5- 7	5.37CE 10	1.905E 10
5-33	5.248E 10	1.862E 10
6- 1	5.129E 10	1.820E 10
6-37	4.898E 10	1.738E 10
7- 3	4.677E 10	1.660E 10
7-31	4.467E 10	1.585E 10
8- 1	6.397E 08	5.623E 10
8-37	1.000E 08	5.754E 10
9-15	1.000E 08	5.754E 10
9-45	1.000E 08	5.754E 10
10-15	1.000E 08	5.754E 10
10-45	1.000E 08	5.754E 10
11- 7	1.000E 08	5.754E 10
11-45	1.000E 08	5.754E 10
12-15	1.000E 08	5.754E 10
12-45	1.000E 08	5.754E 10
13- 7	1.000E 08	5.754E 10
13-45	1.000E 08	5.754E 10
14-15	1.000E 08	5.754E 10
14-45	1.000E 08	5.754E 10
15- 7	1.000E 08	5.754E 10
15-45	1.000E 08	5.754E 10
16- 7	1.000E 08	5.754E 10
16-31	4.074E 10	1.479E 10
17- 3	3.981E 10	1.413E 10
17-33	3.981E 10	1.413E 10
18- 3	4.074E 10	1.445E 10
18-31	4.169E 10	1.445E 10
19- 7	4.365E 10	1.549E 10
19-31	4.467E 10	1.585E 10
20- 7	4.677E 10	1.660E 10
20-37	4.786E 10	1.698E 10
21- 3	5.012E 10	1.778E 10
21-31	5.129E 10	1.820E 10
22- 7	5.248E 10	1.862E 10
22-33	5.37CE 10	1.905E 10
23- 1	5.495E 10	1.950E 10
23-37	5.623E 10	1.995E 10

Table A10

LATITUDE= 45.0 DEG ALTITUDE= 60.0 KM

DECLINATION=23.5 DEG

TIME(HR-MIN)	N(O)	N(O3)
0- 0	3.311E 10	3.311E 10
0-30	3.311E 10	3.311E 10
1- 0	3.311E 10	3.311E 10
1-30	3.311E 10	3.236E 10
2- 0	3.236E 10	3.236E 10
2-30	3.236E 10	3.236E 10
3- 0	3.236E 10	3.162E 10
3-30	3.162E 10	3.162E 10
4- 0	3.090E 10	3.090E 10
4-30	3.020E 10	3.020E 10
5- 0	2.951E 10	2.951E 10
5-30	2.884E 10	2.884E 10
6- 0	2.818E 10	2.818E 10
6-30	2.692E 10	2.692E 10
7- 0	2.570E 10	2.570E 10
7-31	2.455E 10	2.455E 10
8- 3	1.000E 08	4.677E 10
8-33	1.000E 08	4.677E 10
9- 7	1.000E 08	4.677E 10
9-31	1.000E 08	4.677E 10
10- 7	1.000E 08	4.677E 10
10-31	1.000E 08	4.677E 10
11- 7	1.000E 08	4.677E 10
11-33	1.000E 08	4.677E 10
12- 7	1.000E 08	4.677E 10
12-33	1.000E 08	4.677E 10
13- 7	1.000E 08	4.677E 10
13-33	1.000E 08	4.677E 10
14- 7	1.000E 08	4.677E 10
14-33	1.000E 08	4.677E 10
15- 3	1.000E 08	4.677E 10
15-37	1.000E 08	4.677E 10
16- 1	1.000E 08	4.677E 10
16-31	2.291E 10	2.291E 10
17- 1	2.291E 10	2.239E 10
17-31	2.291E 10	2.291E 10
18- 1	2.344E 10	2.344E 10
18-31	2.455E 10	2.455E 10
19- 1	2.570E 10	2.570E 10
19-31	2.630E 10	2.630E 10
20- 1	2.754E 10	2.754E 10
20-31	2.884E 10	2.818E 10
21- 1	2.951E 10	2.951E 10
21-31	3.020E 10	3.020E 10
22- 1	3.090E 10	3.090E 10
22-31	3.162E 10	3.162E 10
23- 1	3.162E 10	3.162E 10
23-31	3.236E 10	3.236E 10

Table A11

LATITUDE= 30.0 DEG ALTITUDE= 90.0 KM

TIME(HR-MIN)	N(O)	N(O3)
0- 1	4.677E 11	1.104E 08
0-37	4.786E 11	1.114E 08
1- 1	4.786E 11	1.117E 08
1-37	4.786E 11	1.127E 08
2- 1	4.786E 11	1.130E 08
2-37	4.898E 11	1.138E 08
3- 1	4.898E 11	1.138E 08
3-37	4.898E 11	1.148E 08
4- 1	4.898E 11	1.146E 08
4-37	4.898E 11	1.153E 08
5- 1	4.898E 11	1.151E 08
5-37	4.898E 11	1.156E 08
6- 1	4.898E 11	1.153E 08
6-37	4.898E 11	1.159E 08
7- 0	4.898E 11	3.083E 08
7-44	4.898E 11	2.911E 09
8-29	4.786E 11	4.842E 09
8-59	4.786E 11	5.834E 09
9-29	4.786E 11	6.637E 09
9-59	4.677E 11	7.295E 09
10-30	4.677E 11	7.816E 09
11- 0	4.571E 11	8.260E 09
11-30	4.571E 11	8.610E 09
12- 0	4.571E 11	8.892E 09
12-30	4.467E 11	9.141E 09
13- 0	4.467E 11	9.333E 09
13-30	4.365E 11	9.484E 09
14- 0	4.365E 11	9.616E 09
14-30	4.266E 11	9.727E 09
15- 0	4.266E 11	9.817E 09
15-30	4.266E 11	9.886E 09
16- 0	4.169E 11	9.954E 09
16-30	4.169E 11	1.000E 10
17- 0	4.074E 11	1.000E 10
17- 0	4.074E 11	1.000E 10
17-33	4.169E 11	9.852E 07
18- 3	4.169E 11	9.860E 07
18-37	4.169E 11	9.884E 07
19- 1	4.169E 11	9.877E 07
19-37	4.266E 11	9.935E 07
20- 1	4.266E 11	9.936E 07
20-37	4.266E 11	1.000E 08
21- 1	4.266E 11	1.002E 08
21-37	4.266E 11	1.012E 08
22- 1	4.365E 11	1.014E 08
22-37	4.365E 11	1.023E 08
23- 1	4.365E 11	1.026E 08
23-37	4.467E 11	1.038E 08

Table A12

LATITUDE= 30.0 DEG ALTITUDE= 80.0 KM

DECLINATION=23.5 DEG

TIME(HR-MIN)	N(O)	N(O3)
0- 7	2.089E 11	1.858E 09
0-31	2.188E 11	1.910E 09
1- 7	2.239E 11	1.963E 09
1-31	2.291E 11	2.018E 09
2- 7	2.344E 11	2.065E 09
2-33	2.399E 11	2.109E 09
3- 7	2.455E 11	2.153E 09
3-33	2.512E 11	2.188E 09
4- 7	2.512E 11	2.234E 09
4-33	2.570E 11	2.254E 09
5- 7	2.570E 11	2.280E 09
5-33	2.630E 11	2.291E 09
6- 7	2.630E 11	2.301E 09
6-33	2.630E 11	2.296E 09
7- 0	2.570E 11	6.067E 09
7-45	1.950E 11	5.248E 10
8-30	1.413E 11	8.318E 10
9- 0	1.148E 11	9.550E 10
9-30	9.120E 10	1.072E 11
10- 0	7.244E 10	1.148E 11
10-30	5.754E 10	1.202E 11
11- 0	4.571E 10	1.230E 11
11-30	3.548E 10	1.288E 11
12- 0	2.818E 10	1.288E 11
12-30	2.188E 10	1.318E 11
13- 0	1.738E 10	1.349E 11
13-30	1.349E 10	1.349E 11
14- 0	1.047E 10	1.349E 11
14-30	8.241E 09	1.349E 11
15- 0	6.442E 09	1.380E 11
15-30	5.047E 09	1.380E 11
16- 0	3.945E 09	1.380E 11
16-30	3.083E 09	1.380E 11
17- 0	2.404E 09	1.380E 11
17- 0	2.399E 09	1.380E 11
17-33	1.380E 11	1.230E 09
18- 3	1.413E 11	1.242E 09
18-37	1.445E 11	1.268E 09
19- 1	1.479E 11	1.279E 09
19-37	1.514E 11	1.334E 09
20- 3	1.549E 11	1.371E 09
20-37	1.622E 11	1.422E 09
21- 3	1.660E 11	1.466E 09
21-37	1.738E 11	1.528E 09
22- 3	1.778E 11	1.570E 09
22-37	1.862E 11	1.637E 09
23- 3	1.905E 11	1.683E 09
23-37	1.995E 11	1.746E 09

Table A13

LATITUDE= 30.0 DEG ALTITUDE= 70.0 KM

TIME(HR-MIN)	N(O)	N(O3)
0- 3	1.148E 11	1.202E 10
0-31	1.175E 11	1.230E 10
1- 1	1.175E 11	1.259E 10
1-31	1.202E 11	1.259E 10
2- 1	1.202E 11	1.288E 10
2-31	1.202E 11	1.288E 10
3- 1	1.202E 11	1.288E 10
3-33	1.202E 11	1.288E 10
4- 3	1.202E 11	1.259E 10
4-37	1.175E 11	1.259E 10
5- 3	1.175E 11	1.230E 10
5-37	1.148E 11	1.202E 10
6- 7	1.096E 11	1.175E 10
6-33	1.072E 11	1.148E 10
7- 0	8.710E 10	2.818E 10
7-33	8.260E 09	9.550E 10
8- 7	6.887E 08	1.000E 11
8-45	1.000E 08	1.023E 11
9-15	1.000E 08	1.023E 11
9-45	1.000E 08	1.023E 11
10-30	1.000E 08	1.023E 11
11- 0	1.000E 08	1.023E 11
11-30	1.000E 08	1.023E 11
12- 0	1.000E 08	1.023E 11
12-30	1.000E 08	1.023E 11
13- 0	1.000E 08	1.023E 11
13-30	1.000E 08	1.023E 11
14- 0	1.000E 08	1.023E 11
14-30	1.000E 08	1.023E 11
15- 0	1.000E 08	1.023E 11
15-30	1.000E 08	1.023E 11
16- 0	1.000E 08	1.023E 11
16-30	1.000E 08	1.023E 11
17- 0	1.000E 08	1.023E 11
17- 0	1.000E 08	1.023E 11
17-37	8.913E 10	9.462E 09
18- 3	8.710E 10	9.376E 09
18-33	8.710E 10	9.376E 09
19- 3	8.913E 10	9.462E 09
19-33	8.913E 10	9.616E 09
20- 3	9.120E 10	9.795E 09
20-31	9.333E 10	1.000E 10
21- 1	9.772E 10	1.023E 10
21-31	1.000E 11	1.072E 10
22- 1	1.023E 11	1.096E 10
22-31	1.047E 11	1.122E 10
23- 1	1.096E 11	1.148E 10
23-33	1.122E 11	1.175E 10

Table A14

LATITUDE= 30.0 DEG ALTITUDE= 60.0 KM

DECLINATION=23.5 DEG

TIME(HR-MIN)	N(O)	N(O3)
0- 0	3.548E 10	3.162E 10
0-31	3.631E 10	3.162E 10
1- 1	3.548E 10	3.162E 10
1-30	3.548E 10	3.162E 10
2- 1	3.548E 10	3.090E 10
2-31	3.548E 10	3.090E 10
3- 1	3.467E 10	3.090E 10
3-31	3.388E 10	3.020E 10
4- 0	3.388E 10	2.951E 10
4-31	3.236E 10	2.884E 10
5- 1	3.162E 10	2.818E 10
5-31	3.090E 10	2.692E 10
6- 0	2.951E 10	2.630E 10
6-31	2.818E 10	2.455E 10
7- 0	6.123E 09	4.266E 10
7-37	1.000E 08	4.898E 10
8- 3	1.000E 08	4.898E 10
8-37	1.000E 08	4.898E 10
9- 3	1.000E 08	4.898E 10
9-37	1.000E 08	4.898E 10
10- 7	1.000E 08	4.898E 10
10-33	1.000E 08	4.898E 10
11- 7	1.000E 08	4.898E 10
11-37	1.000E 08	4.898E 10
12- 1	1.000E 08	4.898E 10
12-33	1.000E 08	4.898E 10
13- 7	1.000E 08	4.898E 10
13-33	1.000E 08	4.898E 10
14- 7	1.000E 08	4.898E 10
14-31	1.000E 08	4.898E 10
15- 7	1.000E 08	4.898E 10
15-33	1.000E 08	4.898E 10
16- 7	1.000E 08	4.898E 10
16-33	1.000E 08	4.898E 10
17- 0	1.000E 08	4.898E 10
17-33	2.512E 10	2.188E 10
18- 1	2.512E 10	2.188E 10
18-31	2.570E 10	2.239E 10
19- 3	2.692E 10	2.344E 10
19-31	2.754E 10	2.455E 10
20- 1	2.884E 10	2.570E 10
20-31	3.020E 10	2.630E 10
21- 1	3.162E 10	2.754E 10
21-33	3.236E 10	2.818E 10
22- 3	3.311E 10	2.951E 10
22-33	3.388E 10	3.020E 10
23- 3	3.467E 10	3.020E 10
23-33	3.467E 10	3.090E 10

Table A15

LATITUDE= 15.0 DEG ALTITUDE= 90.0 KM

DECLINATION=23.5 DEG

TIME(HR-MIN)	N(O)	N(O3)
0- 7	4.467E 11	9.822E 07
0-31	4.467E 11	9.846E 07
1- 7	4.571E 11	9.945E 07
1-31	4.571E 11	9.962E 07
2- 7	4.571E 11	1.005E 08
2-31	4.571E 11	1.007E 08
3- 7	4.677E 11	1.014E 08
3-31	4.677E 11	1.014E 08
4- 7	4.677E 11	1.021E 08
4-31	4.677E 11	1.019E 08
5- 7	4.677E 11	1.026E 08
5-31	4.677E 11	1.023E 08
6- 7	4.677E 11	1.028E 08
6-30	4.677E 11	3.581E 08
7-14	4.677E 11	2.564E 09
7-44	4.571E 11	3.664E 09
8-29	4.571E 11	4.875E 09
8-59	4.571E 11	5.470E 09
9-29	4.467E 11	5.929E 09
9-59	4.467E 11	6.281E 09
10-30	4.365E 11	6.561E 09
11- 0	4.365E 11	6.792E 09
11-30	4.365E 11	6.966E 09
12- 0	4.266E 11	7.096E 09
12-30	4.266E 11	7.211E 09
13- 0	4.169E 11	7.295E 09
13-30	4.169E 11	7.362E 09
14- 0	4.169E 11	7.430E 09
14-30	4.074E 11	7.464E 09
15- 0	4.074E 11	7.499E 09
15-30	3.981E 11	7.534E 09
16- 0	3.981E 11	7.551E 09
16-30	3.981E 11	7.568E 09
17- 0	3.890E 11	7.586E 09
17-15	3.890E 11	7.586E 09
17-30	3.890E 11	7.603E 09
18- 3	3.981E 11	8.631E 07
18-33	3.981E 11	8.641E 07
19- 7	3.981E 11	8.667E 07
19-31	3.981E 11	8.652E 07
20- 7	3.981E 11	8.723E 07
20-31	3.981E 11	8.712E 07
21- 7	3.981E 11	8.800E 07
21-31	4.074E 11	8.796E 07
22- 7	4.074E 11	8.902E 07
22-31	4.074E 11	8.902E 07
23- 7	4.169E 11	9.022E 07
23-31	4.169E 11	9.022E 07

Table A16

LATITUDE= 15.0 DEG ALTITUDE= 80.0 KM DECLINATION=23.5 DEG

TIME(HR-MIN)	N(O)	N(O3)
0- 3	1.778E 11	1.343E 09
0-37	1.862E 11	1.396E 09
1- 3	1.905E 11	1.439E 09
1-37	1.995E 11	1.486E 09
2- 3	2.042E 11	1.528E 09
2-37	2.089E 11	1.570E 09
3- 3	2.138E 11	1.607E 09
3-37	2.188E 11	1.644E 09
4- 3	2.239E 11	1.671E 09
4-37	2.291E 11	1.702E 09
5- 7	2.291E 11	1.718E 09
5-33	2.291E 11	1.726E 09
6- 3	2.291E 11	1.730E 09
6-30	2.239E 11	5.998E 09
7-15	1.778E 11	4.169E 10
7-45	1.479E 11	5.754E 10
8-30	1.122E 11	7.413E 10
9- 0	9.120E 10	8.318E 10
9-30	7.413E 10	8.913E 10
10- 0	6.026E 10	9.333E 10
10-30	4.898E 10	9.772E 10
11- 0	3.981E 10	1.000E 11
11-30	3.236E 10	1.023E 11
12- 0	2.570E 10	1.047E 11
12-30	2.089E 10	1.047E 11
13- 0	1.698E 10	1.072E 11
13-30	1.349E 10	1.072E 11
14- 0	1.096E 10	1.072E 11
14-30	8.710E 09	1.072E 11
15- 0	6.998E 09	1.096E 11
15-30	5.623E 09	1.096E 11
16- 0	4.508E 09	1.096E 11
16-30	3.622E 09	1.096E 11
17- 0	2.904E 09	1.096E 11
17-15	2.600E 09	1.096E 11
17-31	2.312E 09	1.096E 11
18- 3	1.122E 11	8.433E 08
18-33	1.148E 11	8.551E 08
19- 7	1.175E 11	8.810E 08
19-31	1.202E 11	8.892E 08
20- 7	1.259E 11	9.441E 08
20-33	1.288E 11	9.795E 08
21- 7	1.349E 11	1.026E 09
21-33	1.413E 11	1.064E 09
22- 7	1.479E 11	1.119E 09
22-33	1.549E 11	1.159E 09
23- 7	1.622E 11	1.216E 09
23-33	1.660E 11	1.256E 09

Table A17

LATITUDE= 15.0 DEG ALTITUDE= 70.0 KM

TIME(HR-MIN)	N(O)	N(O3)
0- 3	1.175E 11	1.096E 10
0-31	1.175E 11	1.096E 10
1- 1	1.202E 11	1.122E 10
1-33	1.230E 11	1.148E 10
2- 3	1.230E 11	1.148E 10
2-31	1.230E 11	1.148E 10
3- 1	1.230E 11	1.148E 10
3-33	1.230E 11	1.148E 10
4- 3	1.230E 11	1.148E 10
4-31	1.202E 11	1.122E 10
5- 3	1.175E 11	1.096E 10
5-33	1.148E 11	1.072E 10
6- 3	1.122E 11	1.047E 10
6-30	8.511E 10	3.311E 10
7- 7	8.110E 09	9.550E 10
7-37	1.112E 09	1.000E 11
8-15	1.000E 08	1.023E 11
8-45	1.000E 08	1.023E 11
9-15	1.000E 08	1.023E 11
9-45	1.000E 08	1.023E 11
10-30	1.000E 08	1.023E 11
11- 0	1.000E 08	1.023E 11
11-30	1.000E 08	1.023E 11
12- 0	1.000E 08	1.023E 11
12-30	1.000E 08	1.023E 11
13- 0	1.000E 08	1.023E 11
13-30	1.000E 08	1.023E 11
14- 0	1.000E 08	1.023E 11
14-30	1.000E 08	1.023E 11
15- 0	1.000E 08	1.023E 11
15-30	1.000E 08	1.023E 11
16- 0	1.000E 08	1.023E 11
16-30	1.000E 08	1.023E 11
17- 0	1.000E 08	1.023E 11
17-15	1.000E 08	1.023E 11
17-31	1.000E 08	1.023E 11
18- 7	8.913E 10	8.453E 09
18-33	8.913E 10	8.414E 09
19- 3	8.913E 10	8.433E 09
19-33	9.120E 10	8.531E 09
20- 1	9.333E 10	8.670E 09
20-33	9.55CE 10	8.892E 09
21- 3	9.772E 10	9.120E 09
21-33	1.000E 11	9.397E 09
22- 3	1.023E 11	9.660E 09
22-31	1.072E 11	9.954E 09
23- 1	1.096E 11	1.023E 10
23-33	1.122E 11	1.047E 10

Table A18

LATITUDE= 15.0 DEG ALTITUDE= 60.0 KM

DECLINATION=23.5 DEG

TIME(HR-MIN)	N(O)	N(O3)
0- 0	3.715E 10	3.090E 10
0-31	3.715E 10	3.090E 10
1- 1	3.715E 10	3.090E 10
1-33	3.715E 10	3.090E 10
2- 3	3.715E 10	3.020E 10
2-33	3.631E 10	3.020E 10
3- 3	3.631E 10	2.951E 10
3-33	3.548E 10	2.884E 10
4- 3	3.467E 10	2.818E 10
4-33	3.388E 10	2.754E 10
5- 3	3.236E 10	2.692E 10
5-33	3.090E 10	2.570E 10
6- 1	2.951E 10	2.455E 10
6-30	3.296E 09	4.677E 10
7- 7	1.000E 08	5.012E 10
7-33	1.000E 08	5.012E 10
8- 7	1.000E 08	5.012E 10
8-37	1.000E 08	5.012E 10
9- 3	1.000E 08	5.012E 10
9-37	1.000E 08	5.012E 10
10- 7	1.000E 08	5.012E 10
10-33	1.000E 08	5.012E 10
11-15	1.000E 08	5.012E 10
11-31	1.656E 08	5.012E 10
12- 7	1.000E 08	5.012E 10
12-37	1.000E 08	5.012E 10
13- 7	1.000E 08	5.012E 10
13-33	1.000E 08	5.012E 10
14- 7	1.000E 08	5.012E 10
14-37	1.000E 08	5.012E 10
15- 7	1.000E 08	5.012E 10
15-33	1.000E 08	5.012E 10
16- 7	1.000E 08	5.012E 10
16-37	1.000E 08	5.012E 10
17- 7	1.000E 08	5.012E 10
17-31	1.000E 08	5.012E 10
18- 1	2.630E 10	2.188E 10
18-33	2.630E 10	2.188E 10
19- 3	2.692E 10	2.239E 10
19-33	2.818E 10	2.291E 10
20- 3	2.951E 10	2.399E 10
20-33	3.090E 10	2.512E 10
21- 3	3.236E 10	2.630E 10
21-31	3.311E 10	2.692E 10
22- 1	3.388E 10	2.818E 10
22-31	3.548E 10	2.884E 10
23- 3	3.548E 10	2.951E 10
23-31	3.631E 10	3.020E 10

Table A19

LATITUDE= 0.0 DEG ALTITUDE= 90.0 KM

TIME(HR-MIN)	N(O)	N(O3)
0- 7	4.074E 11	8.935E 07
0-33	4.074E 11	8.973E 07
1- 7	4.169E 11	9.054E 07
1-33	4.169E 11	9.084E 07
2- 7	4.169E 11	9.142E 07
2-33	4.169E 11	9.180E 07
3- 3	4.169E 11	9.220E 07
3-37	4.266E 11	9.256E 07
4- 1	4.266E 11	9.311E 07
4-37	4.266E 11	9.307E 07
5- 1	4.266E 11	9.371E 07
5-37	4.266E 11	9.345E 07
6- 0	4.266E 11	1.045E 08
6-44	4.266E 11	2.244E 09
7-29	4.169E 11	3.767E 09
7-59	4.169E 11	4.529E 09
8-29	4.074E 11	5.140E 09
8-59	4.074E 11	5.623E 09
9-29	4.074E 11	6.012E 09
9-59	3.981E 11	6.324E 09
10-30	3.981E 11	6.577E 09
11- 0	3.981E 11	6.776E 09
11-30	3.890E 11	6.934E 09
12- 0	3.890E 11	7.079E 09
12-30	3.802E 11	7.178E 09
13- 0	3.802E 11	7.261E 09
13-30	3.802E 11	7.328E 09
14- 0	3.715E 11	7.396E 09
14-30	3.715E 11	7.430E 09
15- 0	3.631E 11	7.464E 09
15-30	3.631E 11	7.499E 09
16- 0	3.631E 11	7.534E 09
16-30	3.548E 11	7.551E 09
17- 0	3.548E 11	7.568E 09
17-30	3.467E 11	7.586E 09
18- 0	3.467E 11	7.586E 09
18- 0	3.467E 11	7.586E 09
18-33	3.548E 11	7.775E 07
19- 7	3.548E 11	7.771E 07
19-33	3.548E 11	7.815E 07
20- 7	3.548E 11	7.847E 07
20-33	3.631E 11	7.876E 07
21- 7	3.631E 11	7.926E 07
21-33	3.631E 11	7.958E 07
22- 7	3.631E 11	8.022E 07
22-33	3.715E 11	8.061E 07
23- 7	3.715E 11	8.136E 07
23-33	3.715E 11	8.178E 07

Table A20

LATITUDE= 0.0 DEG ALTITUDE= 80.0 KM

DECLINATION=23.5 DEG

TIME(HR-MIN)	N(O)	N(O3)
0- 1	1.698E 11	1.265E 09
0-37	1.778E 11	1.327E 09
1- 1	1.820E 11	1.355E 09
1-37	1.905E 11	1.416E 09
2- 7	1.950E 11	1.462E 09
2-33	1.995E 11	1.493E 09
3- 7	2.042E 11	1.535E 09
3-37	2.089E 11	1.567E 09
4- 3	2.138E 11	1.589E 09
4-33	2.138E 11	1.611E 09
5- 7	2.138E 11	1.626E 09
5-31	2.188E 11	1.637E 09
6- 0	2.138E 11	1.820E 09
6-45	1.698E 11	3.715E 10
7-30	1.318E 11	6.026E 10
8- 0	1.096E 11	7.079E 10
8-30	8.913E 10	7.943E 10
9- 0	7.244E 10	8.511E 10
9-30	5.888E 10	8.913E 10
10- 0	4.786E 10	9.333E 10
10-30	3.890E 10	9.550E 10
11- 0	3.162E 10	9.772E 10
11-30	2.570E 10	1.000E 11
12- 0	2.089E 10	1.023E 11
12-30	1.660E 10	1.023E 11
13- 0	1.349E 10	1.047E 11
13-30	1.096E 10	1.047E 11
14- 0	8.750E 09	1.047E 11
14-30	7.031E 09	1.047E 11
15- 0	5.662E 09	1.047E 11
15-30	4.560E 09	1.072E 11
16- 0	3.664E 09	1.072E 11
16-30	2.951E 09	1.072E 11
17- 0	2.371E 09	1.072E 11
17-30	1.910E 09	1.072E 11
18- 0	1.535E 09	1.072E 11
18- 0	1.730E 09	1.072E 11
18-33	1.072E 11	8.166E 08
19- 3	1.096E 11	8.299E 08
19-37	1.148E 11	8.551E 08
20- 1	1.175E 11	8.730E 08
20-37	1.230E 11	9.204E 08
21- 1	1.259E 11	9.462E 08
21-37	1.318E 11	1.002E 09
22- 1	1.380E 11	1.033E 09
22-37	1.445E 11	1.094E 09
23- 1	1.514E 11	1.127E 09
23-37	1.585E 11	1.189E 09

Table A21

LATITUDE= 0.0 DEG ALTITUDE= 70.0 KM

TIME(HR-MIN)	N(O)	N(O3)
0- 3	1.122E 11	1.047E 10
0-31	1.148E 11	1.072E 10
1- 1	1.175E 11	1.096E 10
1-33	1.175E 11	1.096E 10
2- 3	1.202E 11	1.122E 10
2-31	1.202E 11	1.122E 10
3- 1	1.202E 11	1.122E 10
3-33	1.202E 11	1.122E 10
4- 3	1.175E 11	1.096E 10
4-31	1.148E 11	1.096E 10
5- 1	1.148E 11	1.072E 10
5-31	1.096E 11	1.047E 10
6- 0	1.072E 11	1.072E 10
6-37	9.931E 09	9.333E 10
7- 7	1.371E 09	1.000E 11
7-37	1.875E 08	1.000E 11
8-15	1.000E 08	1.000E 11
8-45	1.000E 08	1.000E 11
9-30	1.000E 08	1.000E 11
10- 0	1.000E 08	1.000E 11
10-30	1.000E 08	1.000E 11
11- 0	1.000E 08	1.000E 11
11-30	1.000E 08	1.000E 11
12- 0	1.000E 08	1.000E 11
12-30	1.000E 08	1.000E 11
13- 0	1.000E 08	1.000E 11
13-30	1.000E 08	1.000E 11
14- 0	1.000E 08	1.000E 11
14-30	1.000E 08	1.000E 11
15- 0	1.000E 08	1.000E 11
15-30	1.000E 08	1.000E 11
16- 0	1.000E 08	1.000E 11
16-30	1.000E 08	1.000E 11
17- 0	1.000E 08	1.000E 11
17-30	1.000E 08	1.000E 11
18- 0	1.000E 08	1.000E 11
18- 0	1.000E 08	1.000E 11
18-37	8.913E 10	8.356E 09
19- 3	8.913E 10	8.318E 09
19-33	8.913E 10	8.375E 09
20- 3	9.120E 10	8.472E 09
20-33	9.120E 10	8.650E 09
21- 3	9.550E 10	8.851E 09
21-31	9.772E 10	9.078E 09
22- 3	1.000E 11	9.354E 09
22-33	1.023E 11	9.638E 09
23- 1	1.047E 11	9.886E 09
23-33	1.096E 11	1.023E 10

Table A22

LATITUDE= 0.0 DEG ALTITUDE= 60.0 KM

DECLINATION=23.5 DEG

TIME(HR-MIN)	N(O)	N(O3)
0- 0	3.631E 10	3.020E 10
0-31	3.715E 10	3.020E 10
1- 1	3.715E 10	3.020E 10
1-31	3.631E 10	3.020E 10
2- 3	3.631E 10	2.951E 10
2-33	3.631E 10	2.951E 10
3- 3	3.548E 10	2.884E 10
3-33	3.467E 10	2.818E 10
4- 3	3.388E 10	2.754E 10
4-33	3.236E 10	2.692E 10
5- 3	3.162E 10	2.570E 10
5-31	3.020E 10	2.455E 10
6- 0	2.512E 10	2.570E 10
6-37	1.000E 08	5.012E 10
7- 3	1.000E 08	5.012E 10
7-37	1.000E 08	5.012E 10
8- 3	1.000E 08	5.012E 10
8-45	1.000E 08	5.012E 10
9- 1	1.469E 08	5.012E 10
9-37	1.000E 08	5.012E 10
10- 7	1.000E 08	5.012E 10
10-33	1.000E 08	5.012E 10
11-15	1.000E 08	5.012E 10
11-31	2.259E 08	5.012E 10
12- 7	1.000E 08	5.012E 10
12-37	1.000E 08	5.012E 10
13- 7	1.000E 08	5.012E 10
13-33	1.000E 08	5.012E 10
14- 7	1.000E 08	5.012E 10
14-37	1.000E 08	5.012E 10
15- 7	1.000E 08	5.012E 10
15-33	1.000E 08	5.012E 10
16- 7	1.000E 08	5.012E 10
16-37	1.000E 08	5.012E 10
17- 3	1.000E 08	5.012E 10
17-45	1.000E 08	5.012E 10
18- 0	3.192E 09	4.677E 10
18-31	2.630E 10	2.188E 10
19- 1	2.630E 10	2.188E 10
19-31	2.754E 10	2.239E 10
20- 1	2.818E 10	2.344E 10
20-31	2.951E 10	2.455E 10
21- 1	3.090E 10	2.512E 10
21-31	3.236E 10	2.630E 10
22- 3	3.311E 10	2.754E 10
22-31	3.388E 10	2.818E 10
23- 1	3.467E 10	2.884E 10
23-31	3.548E 10	2.951E 10

Table A23

LATITUDE=-15.0 DEG ALTITUDE= 90.0 KM

TIME(HR-MIN)	N(O)	N(O3)
0- 7	3.548E 11	7.831E 07
0-33	3.548E 11	7.865E 07
1- 7	3.631E 11	7.933E 07
1-33	3.631E 11	7.961E 07
2- 7	3.631E 11	8.024E 07
2-33	3.631E 11	8.043E 07
3- 7	3.715E 11	8.098E 07
3-33	3.715E 11	8.108E 07
4- 7	3.715E 11	8.140E 07
4-33	3.715E 11	8.159E 07
5- 7	3.715E 11	8.187E 07
5-30	3.715E 11	8.187E 07
6- 7	3.715E 11	1.596E 09
6-44	3.715E 11	2.904E 09
7-29	3.631E 11	4.093E 09
7-59	3.631E 11	4.710E 09
8-29	3.548E 11	5.212E 09
8-59	3.548E 11	5.636E 09
9-29	3.548E 11	5.970E 09
9-59	3.467E 11	6.252E 09
10-30	3.467E 11	6.486E 09
11- 0	3.467E 11	6.683E 09
11-30	3.388E 11	6.839E 09
12- 0	3.388E 11	6.966E 09
12-30	3.311E 11	7.079E 09
13- 0	3.311E 11	7.178E 09
13-30	3.311E 11	7.244E 09
14- 0	3.236E 11	7.311E 09
14-30	3.236E 11	7.362E 09
15- 0	3.162E 11	7.413E 09
15-30	3.162E 11	7.447E 09
16- 0	3.162E 11	7.482E 09
16-30	3.090E 11	7.499E 09
17- 0	3.090E 11	7.516E 09
17-30	3.090E 11	7.534E 09
18- 0	3.020E 11	7.551E 09
18- 7	3.020E 11	7.568E 09
18-30	3.090E 11	8.750E 08
19- 3	3.090E 11	6.771E 07
19-33	3.090E 11	6.796E 07
20- 7	3.090E 11	6.821E 07
20-37	3.090E 11	6.852E 07
21- 3	3.162E 11	6.881E 07
21-33	3.162E 11	6.920E 07
22- 3	3.162E 11	6.967E 07
22-37	3.162E 11	7.013E 07
23- 3	3.236E 11	7.057E 07
23-37	3.236E 11	7.122E 07

Table A24

LATITUDE=-15.0 DEG ALTITUDE= 80.0 KM

DECLINATION=23.5 DEG

TIME(HR-MIN)	N(O)	N(O3)
0- 1	1.549E 11	1.164E 09
0-37	1.622E 11	1.227E 09
1- 7	1.698E 11	1.265E 09
1-33	1.738E 11	1.306E 09
2- 7	1.778E 11	1.349E 09
2-33	1.820E 11	1.380E 09
3- 7	1.862E 11	1.419E 09
3-33	1.905E 11	1.439E 09
4- 7	1.950E 11	1.466E 09
4-33	1.950E 11	1.476E 09
5- 3	1.950E 11	1.483E 09
5-30	1.950E 11	1.486E 09
6- 7	1.660E 11	2.754E 10
6-45	1.349E 11	4.786E 10
7-30	1.023E 11	6.457E 10
8- 0	8.511E 10	7.244E 10
8-30	6.918E 10	7.943E 10
9- 0	5.623E 10	8.318E 10
9-30	4.677E 10	8.710E 10
10- 0	3.802E 10	9.120E 10
10-30	3.090E 10	9.333E 10
11- 0	2.512E 10	9.550E 10
11-30	1.995E 10	9.550E 10
12- 0	1.622E 10	9.772E 10
12-30	1.318E 10	9.772E 10
13- 0	1.072E 10	1.000E 11
13-30	8.650E 09	1.000E 11
14- 0	6.982E 09	1.000E 11
14-30	5.649E 09	1.000E 11
15- 0	4.560E 09	1.000E 11
15-30	3.681E 09	1.000E 11
16- 0	2.972E 09	1.023E 11
16-30	2.404E 09	1.023E 11
17- 0	1.941E 09	1.023E 11
17-30	1.567E 09	1.023E 11
18- 0	1.265E 09	1.023E 11
18- 7	1.197E 09	1.023E 11
18-30	9.120E 10	1.148E 10
19- 7	1.023E 11	7.780E 08
19-33	1.047E 11	7.907E 08
20- 3	1.072E 11	8.128E 08
20-37	1.122E 11	8.453E 08
21- 3	1.175E 11	8.730E 08
21-37	1.230E 11	9.162E 08
22- 3	1.259E 11	9.528E 08
22-37	1.318E 11	9.977E 08
23- 3	1.380E 11	1.038E 09
23-45	1.445E 11	1.099E 09

Table A25

LATITUDE=-15.0 DEG ALTITUDE= 70.0 KM

TIME(HR-MIN)	N(O)	N(O3)
0- 3	1.072E 11	9.931E 09
0-33	1.072E 11	1.000E 10
1- 1	1.096E 11	1.023E 10
1-31	1.122E 11	1.047E 10
2- 3	1.122E 11	1.047E 10
2-33	1.122E 11	1.047E 10
3- 1	1.122E 11	1.047E 10
3-33	1.122E 11	1.047E 10
4- 3	1.096E 11	1.023E 10
4-31	1.096E 11	1.023E 10
5- 1	1.072E 11	9.977E 09
5-30	1.023E 11	9.727E 09
6- 3	1.514E 10	8.511E 10
6-37	1.656E 09	9.550E 10
7- 7	2.291E 08	9.550E 10
7-45	1.000E 08	9.772E 10
8-15	1.000E 08	9.772E 10
8-45	1.000E 08	9.772E 10
9-30	1.000E 08	9.772E 10
10- 0	1.000E 08	9.772E 10
10-30	1.000E 08	9.772E 10
11- 0	1.000E 08	9.772E 10
11-30	1.000E 08	9.772E 10
12- 0	1.000E 08	9.772E 10
12-30	1.000E 08	9.772E 10
13- 0	1.000E 08	9.772E 10
13-30	1.000E 08	9.772E 10
14- 0	1.000E 08	9.772E 10
14-30	1.000E 08	9.772E 10
15- 0	1.000E 08	9.772E 10
15-30	1.000E 08	9.772E 10
16- 0	1.000E 08	9.772E 10
16-30	1.000E 08	9.772E 10
17- 0	1.000E 08	9.772E 10
17-30	1.000E 08	9.772E 10
18- 0	1.000E 08	9.772E 10
18- 7	1.000E 08	9.772E 10
18-30	7.943E 10	1.585E 10
19- 3	8.511E 10	8.091E 09
19-33	8.511E 10	8.072E 09
20- 3	8.710E 10	8.147E 09
20-33	8.710E 10	8.260E 09
21- 3	8.913E 10	8.433E 09
21-33	9.120E 10	8.630E 09
22- 3	9.550E 10	8.851E 09
22-33	9.772E 10	9.099E 09
23- 1	1.000E 11	9.333E 09
23-31	1.023E 11	9.572E 09

Table A26

LATITUDE=-15.0 DEG ALTITUDE= 60.0 KM

DECLINATION=23.5 DEG

TIME(HR-MIN)	N(O)	N(O3)
0- 0	3.548E 10	2.951E 10
0-31	3.548E 10	2.884E 10
1- 1	3.548E 10	2.884E 10
1-31	3.548E 10	2.884E 10
2- 3	3.467E 10	2.884E 10
2-33	3.467E 10	2.818E 10
3- 3	3.388E 10	2.754E 10
3-33	3.311E 10	2.754E 10
4- 3	3.236E 10	2.630E 10
4-33	3.090E 10	2.570E 10
5- 1	2.951E 10	2.455E 10
5-30	2.818E 10	2.291E 10
6- 7	1.000E 08	5.012E 10
6-33	1.000E 08	5.012E 10
7- 7	1.000E 08	5.012E 10
7-37	1.000E 08	5.012E 10
8- 3	1.000E 08	5.012E 10
8-45	1.000E 08	5.012E 10
9- 1	1.200E 08	5.012E 10
9-37	1.000E 08	5.012E 10
10- 7	1.000E 08	5.012E 10
10-33	1.000E 08	5.012E 10
11-15	1.000E 08	5.012E 10
11-31	1.820E 08	5.012E 10
12- 7	1.000E 08	5.012E 10
12-37	1.000E 08	5.012E 10
13- 7	1.000E 08	5.012E 10
13-33	1.000E 08	5.012E 10
14- 7	1.000E 08	5.012E 10
14-37	1.000E 08	5.012E 10
15- 7	1.000E 08	5.012E 10
15-33	1.000E 08	5.012E 10
16- 7	1.000E 08	5.012E 10
16-37	1.000E 08	5.012E 10
17- 3	1.000E 08	5.012E 10
17-45	1.000E 08	5.012E 10
18- 1	1.276E 08	5.012E 10
18-30	2.630E 10	2.291E 10
19- 1	2.630E 10	2.138E 10
19-33	2.630E 10	2.188E 10
20- 3	2.692E 10	2.239E 10
20-33	2.818E 10	2.344E 10
21- 3	2.951E 10	2.399E 10
21-33	3.090E 10	2.512E 10
22- 3	3.162E 10	2.570E 10
22-33	3.236E 10	2.692E 10
23- 3	3.311E 10	2.754E 10
23-33	3.388E 10	2.818E 10

Table A27

LATITUDE=-30.0 DEG ALTITUDE= 90.0 KM

TIME(HR-MIN)	N(O)	N(O3)
0- 7	3.467E 11	6.019E 07
0-33	3.467E 11	6.050E 07
1- 7	3.467E 11	6.076E 07
1-33	3.467E 11	6.100E 07
2- 7	3.548E 11	6.144E 07
2-33	3.548E 11	6.150E 07
3- 7	3.548E 11	6.177E 07
3-33	3.548E 11	6.194E 07
4- 3	3.548E 11	6.216E 07
4-37	3.548E 11	6.230E 07
5- 0	3.548E 11	6.234E 07
5-37	3.548E 11	1.138E 09
6-14	3.548E 11	1.845E 09
6-44	3.548E 11	2.213E 09
7-14	3.467E 11	2.460E 09
7-44	3.467E 11	2.636E 09
8-29	3.388E 11	2.793E 09
8-59	3.388E 11	2.864E 09
9-29	3.388E 11	2.911E 09
9-59	3.388E 11	2.938E 09
10-30	3.311E 11	2.965E 09
11- 0	3.311E 11	2.979E 09
11-30	3.311E 11	2.985E 09
12- 0	3.236E 11	2.992E 09
12-30	3.236E 11	2.999E 09
13- 0	3.236E 11	3.006E 09
13-30	3.162E 11	3.006E 09
14- 0	3.162E 11	3.006E 09
14-30	3.162E 11	3.013E 09
15- 0	3.090E 11	3.013E 09
15-30	3.090E 11	3.013E 09
16- 0	3.090E 11	3.013E 09
16-30	3.020E 11	3.013E 09
17- 0	3.020E 11	3.013E 09
17-30	3.020E 11	3.013E 09
18- 0	2.951E 11	3.013E 09
18-15	2.951E 11	3.013E 09
18-37	2.951E 11	3.013E 09
19- 0	2.951E 11	7.907E 08
19-33	2.951E 11	5.196E 07
20- 3	2.951E 11	5.219E 07
20-37	3.020E 11	5.234E 07
21- 3	3.020E 11	5.254E 07
21-37	3.020E 11	5.297E 07
22- 3	3.020E 11	5.304E 07
22-37	3.090E 11	5.337E 07
23- 3	3.090E 11	5.361E 07
23-33	3.090E 11	5.393E 07

Table A28

LATITUDE=-30.0 DEG ALTITUDE= 80.0 KM

DECLINATION=23.5 DEG

TIME(HR-MIN)	N(O)	N(O3)
0- 7	1.096E 11	6.501E 08
0-33	1.148E 11	6.761E 08
1- 3	1.175E 11	7.047E 08
1-37	1.230E 11	7.345E 08
2- 1	1.288E 11	7.621E 08
2-37	1.318E 11	7.834E 08
3- 1	1.349E 11	8.091E 08
3-37	1.380E 11	8.204E 08
4- 1	1.413E 11	8.318E 08
4-37	1.413E 11	8.395E 08
5- 0	1.413E 11	8.414E 08
5-37	1.230E 11	1.660E 10
6-15	1.047E 11	2.884E 10
6-45	9.120E 10	3.631E 10
7-30	7.244E 10	4.467E 10
8- 0	6.166E 10	4.898E 10
8-30	5.248E 10	5.129E 10
9- 0	4.467E 10	5.495E 10
9-30	3.802E 10	5.623E 10
10- 0	3.236E 10	5.888E 10
10-30	2.692E 10	6.026E 10
11- 0	2.291E 10	6.166E 10
11-30	1.950E 10	6.166E 10
12- 0	1.622E 10	6.310E 10
12-30	1.380E 10	6.310E 10
13- 0	1.148E 10	6.457E 10
13-30	9.683E 09	6.457E 10
14- 0	8.147E 09	6.457E 10
14-30	6.839E 09	6.607E 10
15- 0	5.754E 09	6.607E 10
15-30	4.831E 09	6.607E 10
16- 0	4.055E 09	6.607E 10
16-30	3.404E 09	6.607E 10
17- 0	2.858E 09	6.607E 10
17-30	2.404E 09	6.607E 10
18- 0	2.018E 09	6.607E 10
18-15	1.845E 09	6.607E 10
18-37	1.618E 09	6.607E 10
19- 0	5.129E 10	1.698E 10
19-37	6.918E 10	4.102E 08
20- 3	7.079E 10	4.198E 08
20-33	7.244E 10	4.345E 08
21- 3	7.586E 10	4.539E 08
21-37	8.128E 10	4.808E 08
22- 1	8.511E 10	4.920E 08
22-37	8.913E 10	5.333E 08
23- 7	9.550E 10	5.649E 08
23-33	1.000E 11	5.888E 08

Table A29

LATITUDE=-30.0 DEG ALTITUDE= 70.0 KM

TIME(HR-MIN)	N(O)	N(O3)
0- 7	1.000E 11	7.516E 09
0-37	1.000E 11	7.656E 09
1- 3	1.023E 11	7.762E 09
1-37	1.047E 11	7.852E 09
2- 3	1.047E 11	7.925E 09
2-37	1.047E 11	7.962E 09
3- 3	1.047E 11	7.962E 09
3-37	1.047E 11	7.907E 09
4- 3	1.023E 11	7.852E 09
4-33	1.023E 11	7.727E 09
5- 0	1.000E 11	7.568E 09
5-37	1.549E 10	7.762E 10
6- 7	3.020E 09	8.710E 10
6-37	5.781E 08	8.710E 10
7-15	1.000E 08	8.913E 10
7-45	1.000E 08	8.913E 10
8-30	1.000E 08	8.913E 10
9- 0	1.000E 08	8.913E 10
9-30	1.000E 08	8.913E 10
10- 0	1.000E 08	8.913E 10
10-30	1.000E 08	8.913E 10
11- 0	1.000E 08	8.913E 10
11-30	1.000E 08	8.913E 10
12- 0	1.000E 08	8.913E 10
12-30	1.000E 08	8.913E 10
13- 0	1.000E 08	8.913E 10
13-30	1.000E 08	8.913E 10
14- 0	1.000E 08	8.913E 10
14-30	1.000E 08	8.913E 10
15- 0	1.000E 08	8.913E 10
15-30	1.000E 08	8.913E 10
16- 0	1.000E 08	8.913E 10
16-30	1.000E 08	8.913E 10
17- 0	1.000E 08	8.913E 10
17-30	1.000E 08	8.913E 10
18- 0	1.000E 08	8.913E 10
18-15	1.000E 08	8.913E 10
18-37	1.000E 08	8.913E 10
19- 0	6.310E 10	2.455E 10
19-33	8.128E 10	6.138E 09
20- 1	8.128E 10	6.180E 09
20-37	8.128E 10	6.237E 09
21- 3	8.318E 10	6.339E 09
21-33	8.511E 10	6.471E 09
22- 3	8.710E 10	6.637E 09
22-33	8.913E 10	6.808E 09
23- 3	9.120E 10	6.982E 09
23-33	9.333E 10	7.161E 09

Table A30

LATITUDE=-30.0 DEG ALTITUDE= 60.0 KM

DECLINATION=23.5 DEG

TIME(HR-MIN)	N(C)	N(C3)
0- 0	3.548E 10	2.570E 10
0-33	3.548E 10	2.512E 10
1- 3	3.548E 10	2.512E 10
1-31	3.548E 10	2.512E 10
2- 3	3.467E 10	2.512E 10
2-33	3.467E 10	2.455E 10
3- 1	3.388E 10	2.399E 10
3-31	3.311E 10	2.344E 10
4- 1	3.162E 10	2.291E 10
4-31	3.020E 10	2.188E 10
5- 0	2.884E 10	2.089E 10
5-37	1.000E 08	4.898E 10
6- 7	1.000E 08	4.898E 10
6-37	1.000E 08	4.898E 10
7- 7	1.000E 08	4.898E 10
7-37	1.000E 08	4.898E 10
8- 7	1.000E 08	4.898E 10
8-37	1.000E 08	4.898E 10
9- 7	1.000E 08	4.898E 10
9-37	1.000E 08	4.898E 10
10- 7	1.000E 08	4.898E 10
10-37	1.000E 08	4.898E 10
11- 7	1.000E 08	4.898E 10
11-33	1.000E 08	4.898E 10
12- 7	1.000E 08	4.898E 10
12-33	1.000E 08	4.898E 10
13- 7	1.000E 08	4.898E 10
13-33	1.000E 08	4.898E 10
14- 7	1.000E 08	4.898E 10
14-33	1.000E 08	4.898E 10
15- 7	1.000E 08	4.898E 10
15-33	1.000E 08	4.898E 10
16- 7	1.000E 08	4.898E 10
16-33	1.000E 08	4.898E 10
17- 7	1.000E 08	4.898E 10
17-37	1.000E 08	4.898E 10
18- 7	1.000E 08	4.898E 10
18-37	1.000E 08	4.898E 10
19- 0	2.570E 10	2.291E 10
19-31	2.754E 10	1.950E 10
20- 1	2.754E 10	1.950E 10
20-33	2.818E 10	1.995E 10
21- 3	2.884E 10	2.089E 10
21-33	3.020E 10	2.138E 10
22- 3	3.090E 10	2.239E 10
22-33	3.236E 10	2.291E 10
23- 3	3.311E 10	2.344E 10
23-33	3.388E 10	2.399E 10

Table A31

LATITUDE=-45.0 DEG ALTITUDE= 90.0 KM

TIME(HR-MIN)	N(O)	N(O3)
0- 7	2.951E 11	4.889E 07
0-31	2.951E 11	4.872E 07
1- 7	2.951E 11	4.934E 07
1-33	2.951E 11	4.953E 07
2- 7	3.020E 11	4.977E 07
2-31	3.020E 11	4.972E 07
3- 7	3.020E 11	5.015E 07
3-33	3.020E 11	5.028E 07
4- 3	3.020E 11	5.038E 07
4-33	3.020E 11	5.082E 08
5-14	3.020E 11	1.265E 09
5-44	2.951E 11	1.600E 09
6-14	2.951E 11	1.820E 09
6-44	2.951E 11	1.968E 09
7-29	2.884E 11	2.099E 09
7-59	2.884E 11	2.153E 09
8-29	2.884E 11	2.188E 09
8-59	2.884E 11	2.208E 09
9-29	2.818E 11	2.228E 09
9-59	2.818E 11	2.239E 09
10-30	2.818E 11	2.244E 09
11- 0	2.754E 11	2.249E 09
11-30	2.754E 11	2.254E 09
12- 0	2.754E 11	2.254E 09
12-30	2.692E 11	2.254E 09
13- 0	2.692E 11	2.259E 09
13-30	2.692E 11	2.259E 09
14- 0	2.692E 11	2.259E 09
14-30	2.630E 11	2.259E 09
15- 0	2.630E 11	2.259E 09
15-30	2.630E 11	2.259E 09
16- 0	2.570E 11	2.259E 09
16-30	2.570E 11	2.259E 09
17- 0	2.570E 11	2.259E 09
17-30	2.512E 11	2.259E 09
18- 0	2.512E 11	2.259E 09
18-30	2.512E 11	2.259E 09
19- 0	2.512E 11	2.259E 09
19-15	2.455E 11	2.259E 09
19-33	2.455E 11	2.259E 09
20- 1	2.512E 11	4.163E 07
20-33	2.512E 11	4.160E 07
21- 7	2.512E 11	4.188E 07
21-31	2.512E 11	4.241E 07
22- 7	2.512E 11	4.229E 07
22-33	2.570E 11	4.258E 07
23- 7	2.570E 11	4.275E 07
23-33	2.570E 11	4.296E 07

Table A32

LATITUDE=-45.0 DEG ALTITUDE= 85.0 KM

DECLINATION=23.5 DEG

TIME(HR-MIN)	N(O)	N(O3)
0- 7	6.457E 10	5.795E 07
0-33	6.761E 10	5.972E 07
1- 7	7.079E 10	6.265E 07
1-33	7.244E 10	6.431E 07
2- 7	7.586E 10	6.700E 07
2-33	7.762E 10	6.834E 07
3- 7	7.943E 10	7.053E 07
3-33	7.943E 10	7.125E 07
4- 3	8.128E 10	7.170E 07
4-33	8.128E 10	7.762E 08
5-14	7.762E 10	2.312E 09
5-44	7.762E 10	3.273E 09
6-29	7.413E 10	4.498E 09
6-59	7.244E 10	5.200E 09
7-29	7.079E 10	5.808E 09
7-59	6.918E 10	6.353E 09
8-29	6.761E 10	6.839E 09
8-59	6.607E 10	7.278E 09
9-29	6.310E 10	7.656E 09
9-59	6.166E 10	7.998E 09
10-30	6.026E 10	8.299E 09
11- 0	5.888E 10	8.570E 09
11-30	5.754E 10	8.810E 09
12- 0	5.495E 10	9.037E 09
12-30	5.370E 10	9.226E 09
13- 0	5.248E 10	9.397E 09
13-30	5.129E 10	9.550E 09
14- 0	4.898E 10	9.705E 09
14-30	4.786E 10	9.840E 09
15- 0	4.677E 10	9.954E 09
15-30	4.467E 10	1.000E 10
16- 0	4.365E 10	1.023E 10
16-30	4.266E 10	1.023E 10
17- 0	4.074E 10	1.023E 10
17-30	3.981E 10	1.047E 10
18- 0	3.890E 10	1.047E 10
18-30	3.715E 10	1.047E 10
19- 0	3.631E 10	1.072E 10
19-15	3.548E 10	1.072E 10
19-33	3.467E 10	1.072E 10
20- 1	4.571E 10	4.076E 07
20-33	4.677E 10	4.138E 07
21- 7	4.786E 10	4.308E 07
21-33	5.012E 10	4.456E 07
22- 7	5.248E 10	4.713E 07
22-33	5.495E 10	4.869E 07
23- 7	5.754E 10	5.059E 07
23-33	6.026E 10	5.333E 07

Table A33

LATITUDE=-45.0 DEG ALTITUDE= 80.0 KM

TIME(HR-MIN)	N(O)	N(O3)
0- 7	5.012E 10	1.786E 08
0-33	5.248E 10	1.879E 08
1- 7	5.623E 10	2.009E 08
1-33	5.888E 10	2.104E 08
2- 3	6.166E 10	2.203E 08
2-37	6.457E 10	2.301E 08
3- 1	6.607E 10	2.382E 08
3-37	6.761E 10	2.421E 08
4- 3	6.918E 10	2.455E 08
4-33	6.607E 10	2.612E 09
5-15	6.026E 10	7.396E 09
5-45	5.495E 10	1.023E 10
6-30	4.786E 10	1.349E 10
7- 0	4.365E 10	1.514E 10
7-30	3.981E 10	1.660E 10
8- 0	3.548E 10	1.778E 10
8-30	3.236E 10	1.862E 10
9- 0	2.884E 10	1.950E 10
9-30	2.630E 10	1.995E 10
10- 0	2.344E 10	2.089E 10
10-30	2.138E 10	2.138E 10
11- 0	1.905E 10	2.188E 10
11-30	1.698E 10	2.239E 10
12- 0	1.514E 10	2.239E 10
12-30	1.349E 10	2.291E 10
13- 0	1.230E 10	2.291E 10
13-30	1.096E 10	2.344E 10
14- 0	9.750E 09	2.344E 10
14-30	8.710E 09	2.344E 10
15- 0	7.780E 09	2.399E 10
15-30	6.950E 09	2.399E 10
16- 0	6.209E 09	2.399E 10
16-30	5.546E 09	2.399E 10
17- 0	4.943E 09	2.399E 10
17-30	4.416E 09	2.399E 10
18- 0	3.936E 09	2.455E 10
18-30	3.508E 09	2.455E 10
19- 0	3.133E 09	2.455E 10
19-15	2.958E 09	2.455E 10
19-33	2.754E 09	2.455E 10
20- 1	2.754E 10	1.000E 08
20-33	2.884E 10	1.026E 08
21- 7	3.090E 10	1.102E 08
21-33	3.236E 10	1.169E 08
22- 7	3.548E 10	1.282E 08
22-33	3.802E 10	1.361E 08
23- 7	4.169E 10	1.500E 08
23-33	4.467E 10	1.592E 08

Table A34

LATITUDE=-45.0 DEG ALTITUDE= 75.0 KM

DECLINATION=23.5 DEG

TIME(HR-MIN)	N(O)	N(O3)
0- 3	7.244E 10	9.705E 08
0-37	7.586E 10	1.021E 09
1- 3	7.762E 10	1.054E 09
1-37	8.128E 10	1.099E 09
2- 7	8.511E 10	1.132E 09
2-33	8.511E 10	1.156E 09
3- 3	8.710E 10	1.180E 09
3-37	8.913E 10	1.200E 09
4- 3	8.913E 10	1.211E 09
4-33	7.762E 10	1.202E 10
5-15	5.129E 10	2.884E 10
5-45	3.631E 10	3.548E 10
6-30	2.138E 10	4.169E 10
7- 0	1.479E 10	4.365E 10
7-30	1.023E 10	4.467E 10
8- 0	6.982E 09	4.571E 10
8-30	4.786E 09	4.677E 10
9- 0	3.281E 09	4.677E 10
9-30	2.244E 09	4.786E 10
10- 0	1.535E 09	4.786E 10
10-30	1.047E 09	4.786E 10
11- 0	7.161E 08	4.786E 10
11-30	4.887E 08	4.786E 10
12- 0	3.334E 08	4.786E 10
12-30	2.280E 08	4.786E 10
13- 0	1.556E 08	4.786E 10
13-30	1.062E 08	4.786E 10
14- 0	1.000E 08	4.786E 10
14-30	1.000E 08	4.786E 10
15- 0	1.000E 08	4.786E 10
15-30	1.000E 08	4.786E 10
16- 0	1.000E 08	4.786E 10
16-30	1.000E 08	4.786E 10
17- 0	1.000E 08	4.786E 10
17-30	1.000E 08	4.786E 10
18- 0	1.000E 08	4.786E 10
18-30	1.000E 08	4.786E 10
19- 0	1.000E 08	4.786E 10
19-15	1.000E 08	4.786E 10
19-33	1.000E 08	4.786E 10
20- 1	4.786E 10	6.486E 08
20-31	4.898E 10	6.637E 08
21- 7	5.129E 10	6.966E 08
21-33	5.370E 10	7.244E 08
22- 3	5.623E 10	7.603E 08
22-37	6.026E 10	8.035E 08
23- 1	6.166E 10	8.492E 08
23-37	6.607E 10	8.892E 08

Table A35

LATITUDE=-45.0 DEG ALTITUDE= 70.0 KM

TIME(HR-MIN)	N(O)	N(O3)
0- 3	7.762E 10	3.750E 09
0-37	8.128E 10	3.855E 09
1- 3	8.318E 10	3.936E 09
1-33	8.318E 10	4.009E 09
2- 7	8.511E 10	4.074E 09
2-33	8.710E 10	4.112E 09
3- 7	8.710E 10	4.130E 09
3-33	8.710E 10	4.130E 09
4- 3	8.511E 10	4.112E 09
4-33	5.012E 10	3.388E 10
5- 7	1.514E 10	5.754E 10
5-37	4.932E 09	6.310E 10
6-15	1.208E 09	6.607E 10
6-45	3.908E 08	6.607E 10
7-15	1.262E 08	6.607E 10
7-45	1.000E 08	6.607E 10
8-30	1.000E 08	6.607E 10
9- 0	1.000E 08	6.607E 10
9-30	1.000E 08	6.607E 10
10- 0	1.000E 08	6.607E 10
10-30	1.000E 08	6.607E 10
11- 0	1.000E 08	6.607E 10
11-30	1.000E 08	6.607E 10
12- 0	1.000E 08	6.607E 10
12-30	1.000E 08	6.607E 10
13- 0	1.000E 08	6.607E 10
13-30	1.000E 08	6.607E 10
14- 0	1.000E 08	6.607E 10
14-30	1.000E 08	6.607E 10
15- 0	1.000E 08	6.607E 10
15-30	1.000E 08	6.607E 10
16- 0	1.000E 08	6.607E 10
16-30	1.000E 08	6.607E 10
17- 0	1.000E 08	6.607E 10
17-30	1.000E 08	6.607E 10
18- 0	1.000E 08	6.607E 10
18-30	1.000E 08	6.607E 10
19- 0	1.000E 08	6.607E 10
19-15	1.000E 08	6.607E 10
19-33	1.000E 08	6.607E 10
20- 1	6.310E 10	3.006E 09
20-31	6.310E 10	3.041E 09
21- 3	6.457E 10	3.105E 09
21-33	6.607E 10	3.192E 09
22- 7	6.918E 10	3.296E 09
22-33	7.079E 10	3.388E 09
23- 3	7.244E 10	3.499E 09
23-33	7.586E 10	3.606E 09

Table A36

LATITUDE=-45.0 DEG ALTITUDE= 65.0 KM

DECLINATION=23.5 DEG

TIME(HR-MIN)	N(O)	N(O3)
0- 7	5.623E 10	8.995E 09
0-37	5.623E 10	9.141E 09
1- 3	5.754E 10	9.247E 09
1-31	5.754E 10	9.311E 09
2- 1	5.754E 10	9.333E 09
2-37	5.754E 10	9.311E 09
3- 7	5.623E 10	9.204E 09
3-33	5.623E 10	9.078E 09
4- 3	5.495E 10	8.851E 09
4-33	9.099E 09	4.898E 10
5- 7	2.350E 08	5.623E 10
5-37	1.000E 08	5.623E 10
6-15	1.000E 08	5.623E 10
6-45	1.000E 08	5.623E 10
7-30	1.000E 08	5.623E 10
8- 0	1.000E 08	5.623E 10
8-30	1.000E 08	5.623E 10
9- 0	1.000E 08	5.623E 10
9-30	1.000E 08	5.623E 10
10- 0	1.000E 08	5.623E 10
10-30	1.000E 08	5.623E 10
11- 0	1.000E 08	5.623E 10
11-30	1.000E 08	5.623E 10
12- 0	1.000E 08	5.623E 10
12-15	1.000E 08	5.623E 10
12-45	1.000E 08	5.623E 10
13-30	1.000E 08	5.623E 10
14- 0	1.000E 08	5.623E 10
14-30	1.000E 08	5.623E 10
15- 0	1.000E 08	5.623E 10
15-30	1.000E 08	5.623E 10
16- 0	1.000E 08	5.623E 10
16-30	1.000E 08	5.623E 10
17- 0	1.000E 08	5.623E 10
17-15	1.000E 08	5.623E 10
17-45	1.000E 08	5.623E 10
18-30	1.000E 08	5.623E 10
19- 0	1.000E 08	5.623E 10
19-15	1.000E 08	5.623E 10
19-33	1.000E 08	5.623E 10
20- 1	4.786E 10	7.780E 09
20-33	4.786E 10	7.745E 09
21- 3	4.786E 10	7.798E 09
21-37	4.898E 10	7.962E 09
22- 7	5.012E 10	8.147E 09
22-33	5.129E 10	8.318E 09
23- 1	5.248E 10	8.511E 09
23-31	5.370E 10	8.730E 09

Table A37

LATITUDE=-45.0 DEG ALTITUDE= 60.0 KM

TIME(HR-MIN)	N(O)	N(O3)
0- 0	3.388E 10	1.820E 10
0-33	3.467E 10	1.820E 10
1- 3	3.467E 10	1.862E 10
1-33	3.467E 10	1.862E 10
2- 1	3.467E 10	1.862E 10
2-31	3.467E 10	1.820E 10
3- 3	3.388E 10	1.778E 10
3-33	3.311E 10	1.738E 10
4- 1	3.162E 10	1.698E 10
4-31	2.173E 08	4.571E 10
5- 7	1.000E 08	4.571E 10
5-45	1.000E 08	4.571E 10
6-15	1.000E 08	4.571E 10
6-33	1.000E 08	4.571E 10
7- 7	1.000E 08	4.571E 10
7-45	1.000E 08	4.571E 10
8-15	1.000E 08	4.571E 10
8-33	1.000E 08	4.571E 10
9- 7	1.000E 08	4.571E 10
9-45	1.000E 08	4.571E 10
10- 7	1.000E 08	4.571E 10
10-37	1.000E 08	4.571E 10
11- 7	1.000E 08	4.571E 10
11-45	1.000E 08	4.571E 10
12- 7	1.000E 08	4.571E 10
12-37	1.000E 08	4.571E 10
13- 7	1.000E 08	4.571E 10
13-45	1.000E 08	4.571E 10
14- 7	1.000E 08	4.571E 10
14-37	1.000E 08	4.571E 10
15- 7	1.000E 08	4.571E 10
15-45	1.000E 08	4.571E 10
16- 7	1.000E 08	4.571E 10
16-37	1.000E 08	4.571E 10
17- 7	1.000E 08	4.571E 10
17-45	1.000E 08	4.571E 10
18- 7	1.000E 08	4.571E 10
18-37	1.000E 08	4.571E 10
19- 7	1.000E 08	4.571E 10
19-33	1.000E 08	4.571E 10
20- 1	2.951E 10	1.549E 10
20-33	2.951E 10	1.549E 10
21- 1	2.951E 10	1.549E 10
21-31	3.020E 10	1.585E 10
22- 1	3.090E 10	1.660E 10
22-33	3.236E 10	1.698E 10
23- 3	3.311E 10	1.738E 10
23-31	3.388E 10	1.778E 10

2. COMPUTATIONAL CONSIDERATIONS

The entire computer program used in numerical integration of the O and O_3 differential equations is given in Tables A38 through A42. Many important notes are contained on the comment cards within each subprogram. All computations directly involved in the numerical integration of the differential equations were done in double precision to decrease round-off errors. The program is written in Fortran IV for the IBM System/360. The actual numerical integration is done by the DRKGS Subroutine which is provided for the IBM System/360 by IBM. The integration was done by means of the fourth order Runge-Kutta formulae in the modification due to Gill. The comment cards in Table A42 contain more information on this method. The maximum absolute error in concentration per integration was limited to a factor of roughly .0005 times the initial value of the concentration for each constituent O and O_3. It is unlikely that such errors would accumulate significantly as the integration proceeds because an excess or dearth of a species results in a corresponding increase or decrease of its rate of destruction. During most of the calculations this error limit was satisfied while integrating in 15-minute jumps, but at sunrise and sunset, the integration interval dropped to 1 second or less. The typical IBM System/360 computer running time for a 6-day profile of O and O_3 was about 3 minutes.

Following is a list of notes pertaining to the programs. Additional information is contained on comment cards within each program.

Main Program Table A38

ZØ2 = integral of Ø2 from 300 km to altitude of interest, LAT = latitude, DEC = declination TXPLOT, TYX, TYPLOT, SIZEX, SIZES are control vectors for the "calcomp" plotter. All statements of the form CALL CCP . . . are plotting

Table A38

```
                C     MAIN PROGRAM - OXYGEN ATMOSPHERE
 ISN 0002             EXTERNAL FCT,OUTP
 ISN 0003             DIMENSION Y(2),DERY(2),PRMT(5),AUX(8,2),X1(7,8),X3(7,8)
 ISN 0004             DIMENSION     T(7,8),ZO2(7,8),R(87),S2(87),S3(87),VA(13),VB(13)
 ISN 0005             DIMENSION TXPLOT(2),TYPLOT(2)
 ISN 0006             DIMENSION WAVE(87)
 ISN 0007             DIMENSION TYX(2)
 ISN 0008             DOUBLE PRECISION Y,DERY,PRMT,AUX,X,X2,ZO2,B1,B2,B3,X1,X3,T,W,S,
                     1RATE,VA,VB,A,F2,F3,LAT,DEC,S2,S3,R,H
 ISN 0009             COMMON K,M
 ISN 0010             COMMON/BFCT/ B1(7,8),B2(7,8),B3(7,8),X2(7,8),A
 ISN 0011             COMMON/BOUTP/W,S,NIN
 ISN 0012             COMMON /BFCCU/ RATE(5)
 ISN 0013             COMMON /BFCFL/ F2(7,8),F3(7,8)
 ISN 0014             COMMON /BOUFL/ LAT(8),DEC(8)
 ISN 0015             COMMON/BFLUX/ R,S2,S3,ZO2,VA,VB,T
 ISN 0016             COMMON/BCHI/COSCHI,YW(300),YW3(300),XW(300),YS(49),YS3(49),XHR(49)
 ISN 0017             DOUBLE PRECISION COSCHI
 ISN 0018             READ(5,1)X2
 ISN 0019             READ(5,1)ZO2
 ISN 0020             READ(5,1)T
 ISN 0021             READ(5,1)X1
 ISN 0022             READ(5,1)X3
 ISN 0023             READ(5,1)B1
 ISN 0024             READ(5,1)B2
 ISN 0025             READ(5,1)B3
 ISN 0026             READ(5,1 )LAT
 ISN 0027             READ(5,1 )DEC
 ISN 0028       1     FORMAT(1P8D10.3)
                C     X1=(O1) X2=(O2) X3=(O3) T=TEMP B1,B2,B3=K1,K2,K3 RATE COEFFICIENTS (DASA)
                C     A=(FRACTIONAL COMPOSITION OF O2 TO (M))**-1
                C     YS,YS3,XHR ARE VALUES OF O1,O3,&TIME FOR THE LAST 24 HRS (PUNCHED ON CARDS)
                C     YW,YW3,XW ARE PRINTED VALUES OF O1,O3,&TIME USED BY PLOTTER
                C     SEE SUBROUTINE DRKGS FOR VALUES OF PRMT,Y,AND DERY
                C     ALL CALCULATIONS INVOLVING DIFF. EQNS. USE DOUBLE PRECISION
 ISN 0029             READ (5,22) WAVE
 ISN 0030       22    FORMAT(1P8E10.3)
 ISN 0031             NDIM=2
 ISN 0032             A=4.7824
 ISN 0033             PRMT(1)=0.0
 ISN 0034             PRMT(2)=518400.
 ISN 0035             PRMT(3)=1799.99
 ISN 0036             TXPLOT(1)=0.0
 ISN 0037             TXPLOT(2)=6.0
 ISN 0038             TYX(1)=7.0
 ISN 0039             TYX(2)=1.0
 ISN 0040             TYPLOT(1)=8.0
 ISN 0041             TYPLOT(2)=1.0
 ISN 0042             CALL CCP1PL(1.5,0.5,-3)
 ISN 0043             WRITE(6,5)
 ISN 0044       5     FORMAT (1H1,6X,8HINTERVAL,11X,1HR,14X,2HS2,14X,2HS3,10X,
                     1  10HWAVELENGTH,/)
 ISN 0045             DO 6 I=1,87
 ISN 0046       6     WRITE(6,7)I,R(I),S2(I),S3(I),WAVE(I)
 ISN 0047       7     FORMAT(10X,I2,10X,1PD9.2,2(7X,1PD9.2),8X,0PF5.0)
 ISN 0048             DO 2 M=3,7
 ISN 0049             FLAT=LAT(M)*57.295
 ISN 0050             FDEC=DEC(M)*57.295

 ISN 0051             DO 3 K=1,2
 ISN 0052             IF (M-1) 31,30,31
 ISN 0053       31    IF (M-7) 32,30,32
 ISN 0054       32    IF (K-2) 30,40,33
 ISN 0055       33    IF (K-4) 30,40,34
 ISN 0056       34    IF (K-6) 30,40,30
 ISN 0057       30    CONTINUE
 ISN 0058             NIN=0
 ISN 0059             Y(1)=X1(K,M)
 ISN 0060             Y(2)=X3(K,M)
 ISN 0061             PRMT(4)=.001*Y(2)
 ISN 0062             DERY(1)=Y(2)/(Y(1)+Y(2))
 ISN 0063             DERY(2)=1.0-DERY(1)
 ISN 0064             W=0.0
 ISN 0065             S=0.0
 ISN 0066             WRITE(6,8)
 ISN 0067       8     FORMAT(1H1,7X,1HO,11X,2HO2,11X,2HO3,8X,9HO2 INTEG.,6X,4HTEMP,10X,
                     12HB1,11X,2HB2,11X,2HB3,8X,3HALT ,/)
```

Table A38 (Continued)

```
ISN 0068            DO 9 I=1,7
ISN 0069            JALT=95-5*I
ISN 0070        9   WRITE(6,10)X1(I,M),X2(I,M),X3(I,M),ZO2(I,M),T(I,M),B1(I,M),B2(I,M)
                   1,B3(I,M),JALT,M
ISN 0071       10   FORMAT(1P8D13.3,5X,I2,3X,I1)
               C    CHAPMAN FUNCTION COEFFICIENTS
               C    CHAPMAN VALUES ARE LINEAR EXTRAPOLATION OF DATA BETWEEN X=900 TO 1000
               C      AND THIS DATA IS EXTENDED FOR ALL OTHER X'S
               C    DATA IS FROM M.V. WILKES TABULATIONS.
ISN 0072            VB(1)=.00018
ISN 0073            VB(2)=.00023
ISN 0074            VB(3)=.00031
ISN 0075            VB(4)=.00043
ISN 0076            VB(5)=.00063
ISN 0077            VB(6)=.00095
ISN 0078            VB(7)=.00150
ISN 0079            VB(8)=.00253
ISN 0080            VB(9)=.00461
ISN 0081            VB(10)=.00916
ISN 0082            VB(11)=.02033
ISN 0083            VB(12)=.05143
ISN 0084            VB(13)=.132
ISN 0085            VA(1)=  5.590 -1000.*VB(1)
ISN 0086            VA(2)=  6.164 -1000.*VB(2)
ISN 0087            VA(3)=  6.867 -1000.*VB(3)
ISN 0088            VA(4)=  7.745 -1000.*VB(4)
ISN 0089            VA(5)=  8.870 -1000.*VB(5)
ISN 0090            VA(6)= 10.352 -1000.*VB(6)
ISN 0091            VA(7)= 12.378 -1000.*VB(7)
ISN 0092            VA(8)= 15.277 -1000.*VB(8)
ISN 0093            VA(9)= 19.670 -1000.*VB(9)
ISN 0094            VA(10)=26.830 -1000.*VB(10)
ISN 0095            VA(11)=39.648 -1000.*VB(11)
ISN 0096            VA(12)=65.505 -1000.*VB(12)
ISN 0097            VA(13)=120.00 -1000.*VB(13)
ISN 0098            CALL DRKGS(PRMT,Y,DERY,NDIM,IHLF,FCT,OUTP,AUX)
ISN 0099            FALT=95-5*K
ISN 0100            N=W
ISN 0101            SIZEX=N/12+1
ISN 0102            SIZES=SIZEX+1.

               C    PLOT RESULTS ON CALCOMP
ISN 0103            CALL CCP1PL(0.0,4.4,-3)
ISN 0104            CALL CCP5AX(0.0,0.0,11HTIME(HOURS),-11,SIZEX,0.0,TXPLOT)
ISN 0105            CALL CCP5AX(0.0,0.0,26HLOG(10) OF O CONCENTRATION,26,4.7,90.0,
                   1TYPLOT)
ISN 0106            CALL CCP2SY(1.00,4.6,.15,4HLAT=,0.0,4)
ISN 0107            CALL CCP3NR(0.0,0.0,-.15,FLAT,0.0,2)
ISN 0108            CALL CCP2SY(2.75,4.6,.15,4HDEC=,0.0,4)
ISN 0109            CALL CCP3NR(0.0,0.0,-.15,FDEC,0.0,2)
ISN 0110            CALL CCP2SY(4.50,4.6,.15,4HALT=,0.0,4)
ISN 0111            CALL CCP3NR(0.0,0.0,-.15,FALT,0.0,2)
ISN 0112            CALL CCP6LN(XW,YW,N,1,TXPLCT,TYPLOT)
ISN 0113            CALL CCP1PL(0.0,-4.4,-3)
ISN 0114            CALL CCP5AX(0.0,0.0,33H      LOG(10) OF O3 CONCENTRATION, 33,3.9,
                   1 90.0,TYX)
ISN 0115            CALL CCP5AX(0.0,0.0,11HTIME(HOURS),-11,SIZEX,0.0,TXPLOT)
ISN 0116            CALL CCP6LN(XW,YW3,N,1,TXPLCT,TYX)
ISN 0117            CALL CCP1PL(SIZES,0.0,-3)
ISN 0118       40   CONTINUE
ISN 0119        3   CONTINUE
ISN 0120        2   CONTINUE
ISN 0121            STOP
ISN 0122            END
```

commands, W and S are used in controlling print-out. R = photon flux; S2 = O_2 absorb. cross-x: $S_3 = O_3$ absorp. cross-x, the 13 VA values are the y intercept values for the Chapman function approximations for 1° intervals from 80° to 93°. The 13VB values are the slopes of the Chapman function linear approximations for the 1° interval from 80° to 93°. PRMT, DERY, NDIM, AUX, Y, X are described in Table A42.

The values of R, S2, and Se were incorporated into the program in a Bloch DATA subprogram which was in common with the labelled common /BFLUX/.

Subroutine FCT TABLE A39

This subroutine is called by the integration routine DRKGS. It calculates the time rate of charge of O3 (DERY(2)) from the values of O(Y(2)) which have been calculated in subroutine DRKGS. Subroutine FCT calls Subroutine Flux to calculate the dissociation rate $Jo_2(F2)$ and $Jo_3(F_3)$.

Subroutine Flux TABLE A40

This subroutine calculates the photodissociation rates Jo_2 and Jo_3 (F_2 and F_3) as the solar zenith angle χ changes. COSCHI = cos χ where χ is the solar zenith angle. COSCHI is calculated from the latitude, declination, and hour angle in subroutine flux. For $\chi > 90°$, COSCHI is less than zero in ISN 13 so all dissociation rates are set to zero in ISN 14 and 15. For $\chi > 90°$, the values are checked in ISN 17 to determine whether the Chapman function approximation is required. From ISN 22 to ISN 29 new values of the dissociation rates F2 and F3 are summed over contributions from all 87 wavelength intervals in which solar flux and cross section data were tabulated. ISN 26 checks for large negative arguments and sets contributions from such terms to zero to avoid an exponential underflow.

Table A39

```
ISN 0002            SUBROUTINE FCT(X,Y,DERY)
ISN 0003            DIMENSION Y(2),DERY(2),PRMT(5),AUX(8,2)
ISN 0004            DOUBLE PRECISION Y,DERY,PRMT,AUX,X,X2,ZO2,B1,B2,B3,X1,X3,T,W,S,
                   1RATE,VA,VB,A,F2,F3,LAT,DEC,S2,S3,R,H
ISN 0005            DOUBLE PRECISION DABS
ISN 0006            COMMON K,M
ISN 0007            COMMON/BFCT/ B1(7,8),B2(7,8),B3(7,8),X2(7,8),A
ISN 0008            COMMON /BFCCU/ RATE(5)
ISN 0009            COMMON /BFCFL/ F2(7,8),F3(7,8)
ISN 0010            COMMON /BOUFL/ LAT(8),DEC(8)
ISN 0011            COMMON/ BFLUX/ R(87),S2(87),S3(87),ZO2(7,8),VA(13),VB(13),T(7,8)
                C   RATE(1)=K1*O1*O2*M
                C   RATE(2)=K3*O1*O3
                C   RATE(3)=2.*K2*O1**2*M
                C   RATE(4)=2.*J2*O2
                C   RATE(5)=J3*O3
                C   Y(1)=(O1)
                C   Y(3)=(O3)
                C   DERY(1)=RATE OF CHANGE OF (O1)
                C   DERY(2)=RATE OF CHANGE OF (O3)
ISN 0012            CALL FLUX(R,S2,S3,ZO2,F2,F3,X,DEC,LAT,K,M,VA,VB,T)
ISN 0013            RATE(1)=B1(K,M)*Y(1)*A*X2(K,M)**2
ISN 0014            RATE(2)=B3(K,M)*Y(1)*Y(2)
ISN 0015            RATE(3)=2.*B2(K,M)*Y(1)**2*A*X2(K,M)
ISN 0016            RATE(4)=2.*F2(K,M)*X2(K,M)
ISN 0017            RATE(5)=F3(K,M)*Y(2)
ISN 0018            DERY(1)=-RATE(1)-RATE(2)-RATE(3)+RATE(4)+RATE(5)
ISN 0019            DERY(2)=RATE(1)-RATE(2)-RATE(5)
ISN 0020            RETURN
ISN 0021            END
```

Table A40

```
ISN 0002            SUBROUTINE FLUX(R,S2,S3,ZO2,F2,F3,X,DEC,LAT,K,M,VA,VB,T)
ISN 0003            COMMON/BCHI/COSCHI,YW(300),YW3(300),XW(300),YS(49),YS3(49),XHR(49)
                C   SUBROUTINE FOR COMPUTING PHOTODISSOCIATION RATES J2=F2 J3=F3
                C   R(J)=INCIDENT PHOTON FLUX IN THE JTH INTERVAL AT INFINITY
                C   S2=O2 ABSORB. COEFF.  S3=O3 ABSORB. COEFF.
                C   ZO2=INTEGRAL OF O2 FROM 300 KM TO ALTITUDE UNDER STUDY-US STAND ATM. SUPP.
ISN 0004            DIMENSION Y(2),DERY(2),PRMT(5),AUX(8,2)
ISN 0005            DOUBLE PRECISION Y,DERY,PRMT,AUX,X,X2,ZO2,B1,B2,B3,X1,X3,T,W,S,
                   1RATE,VA,VB,A,F2,F3,LAT,DEC,S2,S3,R,H
ISN 0006            DOUBLE PRECISION SED,VX,CCSCHI,ARG,HANG
ISN 0007            DOUBLE PRECISION DSIN,DCOS,DATAN,DEXP
ISN 0008            DIMENSION     T(7,8),ZO2(7,8),R(87),S2(87),S3(87),VA(13),VB(13)
ISN 0009            DIMENSION      F2(7,8),F3(7,8)
ISN 0010            DIMENSION      LAT(8),DEC(8)
                C   DEC= SOLAR DECLINATION IN RADIANS  LAT=LATITUDE IN RADIANS
                C   HANG= LOCAL HOUR ANGLE OF SUN MEASURED FROM NOON  CHI= SOLAR ZENITH ANGLE
ISN 0011            HANG=7.272205*10.**(-5)*X
ISN 0012            COSCHI=DSIN(LAT(M))*DSIN(DEC(M))+DCOS(LAT(M))*DCOS(DEC(M))*
                   1DCOS(HANG)
ISN 0013            IF(COSCHI)1,2,2
                C   ALL FLUX IS SET = 0.0 FOR CHI GREATER THAN 90.0 DEGREES
ISN 0014        1   F2(K,M)=0.0
ISN 0015            F3(K,M)=0.0
ISN 0016            GO TO 7
ISN 0017        2   IF (COSCHI-.17)3,3,4
                C   COSCHI LESS THAN .17 MEANS CHAPMAN FUNCTION REQUIRED
ISN 0018        3   COMPCH=DATAN(COSCHI)
ISN 0019            I =11.5-COMPCH *57.29578
ISN 0020            VX =220310./T(K,M)
                C   LINEAR APPROX. TO CHAP. FXN. AS FXN. OF X IS MADE
                C   DIFFERENT APPROX. IS USED FOR EACH ANGLE FROM 80 TO 92 DEGREES
ISN 0021            COSCHI = 1./(VA(I)+VB(I)*VX)
ISN 0022        4   F2(K,M)=0.0
ISN 0023            F3(K,M)=0.0
                C   COMPUTATION OF J2=F2  J3=F3
ISN 0024            DO 5 J=1,87
ISN 0025            ARG=S2(J)*ZO2(K,M)/CCSCHI
ISN 0026            IF (ARG-90.16,5,5
ISN 0027        6   SED =R(J)*DEXP(-ARG)
ISN 0028            F2(K,M) = F2(K,M)+S2(J)*SED
ISN 0029            F3(K,M) = F3(K,M)+S3(J)*SED
ISN 0030        5   CONTINUE
ISN 0031        7   CONTINUE
ISN 0032            RETURN
ISN 0033            END
```

Subroutine ØOTP TABLE A41

This subroutine controls the printing of the relevant data.

NIN = number °/ time that output has been called by the equation solving Subroutine DRKGS. Hence, it represents the number of integrations that have been required to that point.

X = TIME in seconds

CHI = Solar zenith angle in degrees calculated from the cosine of chi calculated in Subroutine Flux. The differential equation routine integrate for 6 days under the values of O_3 concentration are with 5% at successive noons in which case the program terminates by setting PRMI(5) = 5.0. This check and resultant termination results in ISN 29 through ISN 33.

ALAT, ADEC are the latitude and declination in degrees. A typical sheet of output is shown in Table A43.

H and SH = integration increment.

Subroutine DRKGS TABLE A42

This is a library subroutine furnished by IBM. It is the subroutine which actually integrates the differential equation. The subroutine has been modified slightly by including the variable H in the arguments of all Subroutine Output statements to transmit the integration interval. Also the card DRKG 0216 has been replaced by the card, 25 CONTINUE, to permit unlimited bisections of the initial integration interval.

Table A41

```
ISN 0002            SUBROUTINE OUTP(X,Y,DERY,IHLF,NDIM,PRMT,H)
ISN 0003            DIMENSION Y(2),DERY(2),PRMT(5),AUX(8,2)
ISN 0004            DIMENSION YA(8)
ISN 0005            DOUBLE PRECISION Y,DERY,PRMT,AUX,X,X2,Z02,B1,B2,B3,X1,X3,T,W,S,
                   1RATE,VA,VB,A,F2,F3,LAT,DEC,S2,S3,R,H
ISN 0006            COMMON K,M
ISN 0007            COMMON/BOUTP/W,S,NIN
ISN 0008            COMMON /BFCOU/ RATE(5)
ISN 0009            COMMON /BOUFL/ LAT(8),DEC(8)
ISN 0010            COMMON/BCHI/COSCHI,YW(300),YW3(300),XW(300),YS(49),YS3(49),XHR(49)
ISN 0011            DOUBLE PRECISION COSCHI
ISN 0012            NIN=NIN+1
                C   RESULTS ARE PRINTED EVERY 1800 SECONDS (HALF HOUR)
ISN 0013            IF (X-1800.*W) 1,2,2
ISN 0014        2   W=W+1.
ISN 0015            K=W
ISN 0016            CHI=57.3*DARCOS(COSCHI)
                C   STORAGE OF RESULTS FOR CALCOMP
ISN 0017        35  YW(N)= DLOG10(Y(1))
ISN 0018            YW3(N)= DLOG10(Y(2))
ISN 0019            XW(N)=X/3600.
ISN 0020            IF (YW(N)-8.0) 33,34,34
ISN 0021        33  YW(N)=8.0
ISN 0022        34  IF (YW3(N)-7.0) 42,43,43
ISN 0023        42  YW3(N)=7.0
ISN 0024        43  CONTINUE
                C   NEW PAGE EVERY 86400 SECS (24 HOURS)
ISN 0025            IF (X-86400.*S)3,4,4
ISN 0026        4   S=S+1.
ISN 0027            IF (X-PRMT(2)) 41,23,23
ISN 0028        41  CONTINUE
                C   IF X IS WITHIN 15 MINUTES OF TWELVE NOON, THE RESULTS OF SUCCESSIVE
                C         NOON VALUES ARE COMPARED
ISN 0029            MP=S
ISN 0030            YA(MP)=Y(2)
ISN 0031            IF (MP-1) 21,21,22
ISN 0032        22  IF(ABS(YA(MP)-YA(MP-1))-.05*YA(MP)) 23,23,21
ISN 0033        23  PRMT(5)=5.0
ISN 0034            MSAC=XW(N-48)/24.
ISN 0035            TAC=MSAC
                C   STORAGE OF LAST 24 HOUR RESULTS FOR PUNCHING
ISN 0036            DO 30 I=1,49
ISN 0037            YS(I)=YW(N-49+I)
ISN 0038            YS3(I)=YW3(N-49+I)
ISN 0039            XHR(I)=XW(N-49+I)-24.*TAC
ISN 0040            IF (XHR(I)-24.) 31,31,32
ISN 0041        32  XHR(I)=XHR(I)-24.
ISN 0042        31  CONTINUE
ISN 0043        30  CONTINUE
ISN 0044        21  CONTINUE
ISN 0045            J=95-5*K
ISN 0046            ALAT=LAT(M)*57.3
ISN 0047            ADEC=DEC(M)*57.3
ISN 0048            WRITE(6,7) J,ALAT,ADEC
ISN 0049        7   FORMAT(1H1,5X,4HALT=,I2,2HKM,5X,4HLAT=,0PF5.1,3HDEG,5X,4HDEC=,F4.1
                   1,3HDEG,///)
ISN 0050            WRITE(6,5)
ISN 0051        5   FORMAT(4X,4HTIME,9X,
                   1         1HD,9X,2HD3,7X,7HDERY(D),4X,8HDERY(D3),3X,7HRATE(1),3X,7
                   2HRATE(2),3X,7HRATE(3),3X,7HRATE(4),3X,7HRATE(5), 3X,3HCHI,3X,
                   35HDEL T,2X,5H# INT,2X,4HIHLF,/)
ISN 0052        3     CONTINUE
                C   TIME IS GIVEN AS DAYS-HOURS-MINUTES
                C   CONVERSION OF TIME TO HOURS-MIN-SEC
ISN 0053            LX=X
ISN 0054            LDAY=LX/86400
ISN 0055            LHR=LX/3600-24*LDAY
ISN 0056            LMIN=LX/60-1440*LDAY-60*LHR
ISN 0057            SH=H
ISN 0058            WRITE(6,6)LDAY,LHR,LMIN,Y,DERY,RATE,CHI,SH,NIN,IHLF
ISN 0059        6   FORMAT(2X,I3,1H-,I2,1H-,I2, 2(2X,1PD9.3),
                   11P2D11.2,1P5D10.2,2X,0PF5.1,2X,0PF5.0,2X,I5,2X,I3)
ISN 0060        1   CONTINUE
ISN 0061            RETURN
ISN 0062            END
```

Table A42

```
      SUBROUTINE DRKGS(PRMT,Y,DERY,NDIM,IHLF,FCT,OUTP,AUX)                DRKG1070
C                                                                         DRKG  10
C     ******************************************************************DRKG  20
C                                                                         DRKG  30
C        SUBROUTINE DRKGS                                                 DRKG  40
C                                                                         DRKG  50
C     CARD DRKG 0216 WAS REPLACED BY  A CARD (#25  CONTINUE) TO ALLOW UNLIMITED
C     BISECTIONS OF THE INITIAL INTEGRATION INTERVAL IN ORDER TO REACH THE
C     DESIRED ACCURACY
C        PURPOSE                                                          DRKG  60
C           TO SOLVE A SYSTEM OF FIRST ORDER ORDINARY DIFFERENTIAL        DRKG  70
C           EQUATIONS WITH GIVEN INITIAL VALUES.                          DRKG  80
C                                                                         DRKG  90
C        USAGE                                                            DRKG 100
C           CALL DRKGS (PRMT,Y,DERY,NDIM,IHLF,FCT,OUTP,AUX)               DRKG 110
C           PARAMETERS FCT AND OUTP REQUIRE AN EXTERNAL STATEMENT.        DRKG 120
C                                                                         DRKG 130
C        DESCRIPTION OF PARAMETERS                                        DRKG 140
C           PRMT   - DOUBLE PRECISION INPUT AND OUTPUT VECTOR WITH        DRKG 150
C                    DIMENSION GREATER THAN OR EQUAL TO 5, WHICH          DRKG 160
C                    SPECIFIES THE PARAMETERS OF THE INTERVAL AND OF      DRKG 170
C                    ACCURACY AND WHICH SERVES FOR COMMUNICATION BETWEENDRKG 180
C                    OUTPUT SUBROUTINE (FURNISHED BY THE USER) AND        DRKG 190
C                    SUBROUTINE DRKGS. EXCEPT PRMT(5) THE COMPONENTS      DRKG 200
C                    ARE NOT DESTROYED BY SUBROUTINE DRKGS AND THEY ARE   DRKG 210
C           PRMT(1)- LOWER BOUND OF THE INTERVAL (INPUT),                 DRKG 220
C           PRMT(2)- UPPER BOUND OF THE INTERVAL (INPUT),                 DRKG 230
C           PRMT(3)- INITIAL INCREMENT OF THE INDEPENDENT VARIABLE        DRKG 240
C                    (INPUT),                                             DRKG 250
C           PRMT(4)- UPPER ERROR BOUND (INPUT). IF ABSOLUTE ERROR IS      DRKG 260
C                    GREATER THAN PRMT(4), INCREMENT GETS HALVED.         DRKG 270
C                    IF INCREMENT IS LESS THAN PRMT(3) AND ABSOLUTE       DRKG 280
C                    ERROR LESS THAN PRMT(4)/50, INCREMENT GETS DOUBLED.DRKG 290
C                    THE USER MAY CHANGE PRMT(4) BY MEANS OF HIS          DRKG 300
C                    OUTPUT SUBROUTINE.                                   DRKG 310
C           PRMT(5)- NO INPUT PARAMETER. SUBROUTINE DRKGS INITIALIZES     DRKG 320
C                    PRMT(5)=0. IF THE USER WANTS TO TERMINATE            DRKG 330
C                    SUBROUTINE DRKGS AT ANY OUTPUT POINT, HE HAS TO      DRKG 340
C                    CHANGE PRMT(5) TO NON-ZERO BY MEANS OF SUBROUTINE    DRKG 350
C                    OUTP. FURTHER COMPONENTS OF VECTOR PRMT ARE          DRKG 360
C                    FEASIBLE IF ITS DIMENSION IS DEFINED GREATER         DRKG 370
C                    THAN 5. HOWEVER SUBROUTINE DRKGS DOES NOT REQUIRE    DRKG 380
C                    AND CHANGE THEM. NEVERTHELESS THEY MAY BE USEFUL     DRKG 390
C                    FOR HANDING RESULT VALUES TO THE MAIN PROGRAM         DRKG 400
C                    (CALLING DRKGS) WHICH ARE OBTAINED BY SPECIAL         DRKG 410
C                    MANIPULATIONS WITH OUTPUT DATA IN SUBROUTINE OUTP.    DRKG 420
C           Y      - DOUBLE PRECISION INPUT VECTOR OF INITIAL VALUES      DRKG 430
C                    (DESTROYED). LATER ON Y IS THE RESULTING VECTOR OF    DRKG 440
C                    DEPENDENT VARIABLES COMPUTED AT INTERMEDIATE          DRKG 450
C                    POINTS X.                                            DRKG 460
C           DERY   - DOUBLE PRECISION INPUT VECTOR OF ERROR WEIGHTS       DRKG 470
C                    (DESTROYED). THE SUM OF ITS COMPONENTS MUST BE       DRKG 480
C                    EQUAL TO 1. LATER ON DERY IS THE VECTOR OF           DRKG 490
C                    DERIVATIVES, WHICH BELONG TO FUNCTION VALUES Y AT    DRKG 500
C                    INTERMEDIATE POINTS X.                               DRKG 510
C           NDIM   - AN INPUT VALUE, WHICH SPECIFIES THE NUMBER OF        DRKG 520
C                    EQUATIONS IN THE SYSTEM.                             DRKG 530
C           IHLF   - AN OUTPUT VALUE, WHICH SPECIFIES THE NUMBER OF       DRKG 540
C                    BISECTIONS OF THE INITIAL INCREMENT. IF IHLF GETS     DRKG 550
C                    GREATER THAN 10, SUBROUTINE DRKGS RETURNS WITH       DRKG 560
C                    ERROR MESSAGE IHLF=11 INTO MAIN PROGRAM. ERROR       DRKG 570
C                    MESSAGE IHLF=12 OR IHLF=13 APPEARS IN CASE           DRKG 580
C                    PRMT(3)=0 OR IN CASE SIGN(PRMT(3)).NE.SIGN(PRMT(2)-DRKG 590
C                    PRMT(1)) RESPECTIVELY.                               DRKG 600
C           FCT    - THE NAME OF AN EXTERNAL SUBROUTINE USED. THIS        DRKG 610
C                    SUBROUTINE COMPUTES THE RIGHT HAND SIDES DERY OF     DRKG 620
C                    THE SYSTEM TO GIVEN VALUES X AND Y. ITS PARAMETER    DRKG 630
C                    LIST MUST BE X,Y,DERY. SUBROUTINE FCT SHOULD         DRKG 640
C                    NOT DESTROY X AND Y.                                 DRKG 650
C           OUTP   - THE NAME OF AN EXTERNAL OUTPUT SUBROUTINE USED.      DRKG 660
C                    ITS PARAMETER LIST MUST BE X,Y,DERY,IHLF,NDIM,PRMT.DRKG 670
C                    NONE OF THESE PARAMETERS (EXCEPT, IF NECESSARY,      DRKG 680
C                    PRMT(4),PRMT(5),...) SHOULD BE CHANGED BY            DRKG 690
C                    SUBROUTINE OUTP. IF PRMT(5) IS CHANGED TO NON-ZERO,DRKG 700
C                    SUBROUTINE DRKGS IS TERMINATED.                      DRKG 710
C           AUX    - DOUBLE PRECISION AUXILIARY STORAGE ARRAY WITH 8      DRKG 720
C                    ROWS AND NDIM COLUMNS.                               DRKG 730
C                                                                         DRKG 740
```

Table A42 (Continued)

```
C
C       REMARKS                                                          DRKG 750
C          THE PROCEDURE TERMINATES AND RETURNS TO CALLING PROGRAM, IF   DRKG 760
C          (1) MORE THAN 10 BISECTIONS OF THE INITIAL INCREMENT ARE      DRKG 770
C              NECESSARY TO GET SATISFACTORY ACCURACY (ERROR MESSAGE     DRKG 780
C              IHLF=11),                                                 DRKG 790
C          (2) INITIAL INCREMENT IS EQUAL TO 0 OR HAS WRONG SIGN         DRKG 800
C              (ERROR MESSAGES IHLF=12 OR IHLF=13),                      DRKG 810
C          (3) THE WHOLE INTEGRATION INTERVAL IS WORKED THROUGH,         DRKG 820
C          (4) SUBROUTINE OUTP HAS CHANGED PRMT(5) TO NON-ZERO.          DRKG 830
C                                                                        DRKG 840
C       SUBROUTINES AND FUNCTION SUBPROGRAMS REQUIRED                    DRKG 850
C          THE EXTERNAL SUBROUTINES FCT(X,Y,DERY) AND                    DRKG 860
C          OUTP(X,Y,DERY,IHLF,NDIM,PRMT) MUST BE FURNISHED BY THE USER.  DRKG 870
C                                                                        DRKG 880
C       METHOD                                                           DRKG 890
C          EVALUATION IS DONE BY MEANS OF FOURTH ORDER RUNGE-KUTTA       DRKG 900
C          FORMULAE IN THE MODIFICATION DUE TO GILL. ACCURACY IS         DRKG 910
C          TESTED COMPARING THE RESULTS OF THE PROCEDURE WITH SINGLE     DRKG 920
C          AND DOUBLE INCREMENT.                                         DRKG 930
C          SUBROUTINE DRKGS AUTOMATICALLY ADJUSTS THE INCREMENT DURING   DRKG 940
C          THE WHOLE COMPUTATION BY HALVING OR DOUBLING. IF MORE THAN    DRKG 950
C          10 BISECTIONS OF THE INCREMENT ARE NECESSARY TO GET           DRKG 960
C          SATISFACTORY ACCURACY, THE SUBROUTINE RETURNS WITH            DRKG 970
C          ERROR MESSAGE IHLF=11 INTO MAIN PROGRAM.                      DRKG 980
C          TO GET FULL FLEXIBILITY IN OUTPUT, AN OUTPUT SUBROUTINE       DRKG 990
C          MUST BE FURNISHED BY THE USER.                                DRKG1000
C          FOR REFERENCE, SEE                                            DRKG1010
C          RALSTON/WILF, MATHEMATICAL METHODS FOR DIGITAL COMPUTERS,     DRKG1020
C          WILEY, NEW YORK/LONDON, 1960, PP.110-120.                     DRKG1030
C                                                                        DRKG1040
C     ..................................................................DRKG1050
C                                                                        DRKG1060
C                                                                        DRKG1080
C                                                                        DRKG1090
ISN 0003        DIMENSION Y(1),DERY(1),AUX(8,1),A(4),B(4),C(4),PRMT(1)   DRKG1100
ISN 0004        DOUBLE PRECISION PRMT,Y,DERY,AUX,A,B,C,X,XEND,H,AJ,BJ,CJ,R1,R2,  DRKG1110
               1DELT                                                     DRKG1120
ISN 0005        DOUBLE PRECISION DABS
ISN 0006        DO 1 I=1,NDIM                                            DRKG1130
ISN 0007      1 AUX(8,I)=.06666666666666667D0*DERY(I)                    DRKG1140
ISN 0008        X=PRMT(1)                                                DRKG1150
ISN 0009        XEND=PRMT(2)                                             DRKG1160
ISN 0010        H=PRMT(3)                                                DRKG1170
ISN 0011        PRMT(5)=0.D0                                             DRKG1180
ISN 0012        CALL FCT(X,Y,DERY)                                       DRKG1190
              C                                                          DRKG1200
              C     ERROR TEST                                           DRKG1210
ISN 0013        IF(H*(XEND-X))38,37,2                                    DRKG1220
              C                                                          DRKG1230
              C     PREPARATIONS FOR RUNGE-KUTTA METHOD                  DRKG1240
ISN 0014      2 A(1)=.5D0                                                DRKG1250
ISN 0015        A(2)=.29289321881345248D0                                DRKG1260
ISN 0016        A(3)=1.70710678118654750D0                               DRKG1270
ISN 0017        A(4)=.16666666666666667D0                                DRKG1280
ISN 0018        B(1)=2.D0                                                DRKG1290
ISN 0019        B(2)=1.D0                                                DRKG1300
ISN 0020        B(3)=1.D0                                                DRKG1310
ISN 0021        B(4)=2.D0                                                DRKG1320
ISN 0022        C(1)=.5D0                                                DRKG1330
ISN 0023        C(2)=.29289321881345248D0                                DRKG1340
ISN 0024        C(3)=1.70710678118654750D0                               DRKG1350
ISN 0025        C(4)=.5D0                                                DRKG1360
              C                                                          DRKG1370
              C     PREPARATIONS OF FIRST RUNGE-KUTTA STEP               DRKG1380
ISN 0026        DO 3 I=1,NDIM                                            DRKG1390
ISN 0027        AUX(1,I)=Y(I)                                            DRKG1400
ISN 0028        AUX(2,I)=DERY(I)                                         DRKG1410
ISN 0029        AUX(3,I)=0.D0                                            DRKG1420
ISN 0030      3 AUX(6,I)=0.D0                                            DRKG1430
ISN 0031        IREC=0                                                   DRKG1440
ISN 0032        F=H+H                                                    DRKG1450
ISN 0033        IHLF=-1                                                  DRKG1460
ISN 0034        ISTEP=0                                                  DRKG1470
ISN 0035        IEND=0                                                   DRKG1480
              C                                                          DRKG1490
              C                                                          DRKG1500
              C     START OF A RUNGE-KUTTA STEP                          DRKG1510
ISN 0036      4 IF((X+H-XEND)*H)7,6,5                                    DRKG1520
ISN 0037      5 H=XEND-X                                                 DRKG1530
ISN 0038      6 IEND=1                                                   DRKG1540
```

Table A42 (Continued)

```
                C                                                               DRKG1550
                C     RECORDING OF INITIAL VALUES OF THIS STEP                  DRKG1560
ISN 0039          7 CALL OUTP(X,Y,DERY,IREC,NDIM,PRMT,H)                        DRKG1570
ISN 0040            IF(PRMT(5))40,8,40                                          DRKG1580
ISN 0041          8 ITEST=0                                                     DRKG1590
ISN 0042          9 ISTEP=ISTEP+1                                               DRKG1600
                C                                                               DRKG1610
                C                                                               DRKG1620
                C     START OF INNERMOST RUNGE-KUTTA LOOP                       DRKG1630
ISN 0043            J=1                                                         DRKG1640
ISN 0044         10 AJ=A(J)                                                     DRKG1650
ISN 0045            BJ=B(J)                                                     DRKG1660
ISN 0046            CJ=C(J)                                                     DRKG1670
ISN 0047            DO 11 I=1,NDIM                                              DRKG1680
ISN 0048            R1=H*DERY(I)                                                DRKG1690
ISN 0049            R2=AJ*(R1-BJ*AUX(6,I))                                      DRKG1700
ISN 0050            Y(I)=Y(I)+R2                                                DRKG1710
ISN 0051            R2=R2+R2+R2                                                 DRKG1720
ISN 0052         11 AUX(6,I)=AUX(6,I)+R2-CJ*R1                                  DRKG1730
ISN 0053            IF(J-4)12,15,15                                             DRKG1740
ISN 0054         12 J=J+1                                                       DRKG1750
ISN 0055            IF(J-3)13,14,13                                             DRKG1760
ISN 0056         13 X=X+.5D0*H                                                  DRKG1770
ISN 0057         14 CALL FCT(X,Y,DERY)                                          DRKG1780
ISN 0058            GOTO 10                                                     DRKG1790
                C     END OF INNERMOST RUNGE-KUTTA LOOP                         DRKG1800
                C                                                               DRKG1810
                C                                                               DRKG1820
                C     TEST OF ACCURACY                                          DRKG1830
ISN 0059         15 IF(ITEST)16,16,20                                           DRKG1840
                C                                                               DRKG1850
                C     IN CASE ITEST=0 THERE IS NO POSSIBILITY FOR TESTING OF ACCURACY  DRKG1860
ISN 0060         16 DO 17 I=1,NDIM                                              DRKG1870
ISN 0061         17 AUX(4,I)=Y(I)                                               DRKG1880
ISN 0062            ITEST=1                                                     DRKG1890
ISN 0063            ISTEP=ISTEP+ISTEP-2                                         DRKG1900
ISN 0064         18 IHLF=IHLF+1                                                 DRKG1910
ISN 0065            X=X-H                                                       DRKG1920
ISN 0066            H=.5D0*H                                                    DRKG1930
ISN 0067            DO 19 I=1,NDIM                                              DRKG1940
ISN 0068            Y(I)=AUX(1,I)                                               DRKG1950
ISN 0069            DERY(I)=AUX(2,I)                                            DRKG1960
ISN 0070         19 AUX(6,I)=AUX(3,I)                                           DRKG1970
ISN 0071            GOTO 9                                                      DRKG1980
                C                                                               DRKG1990
                C     IN CASE ITEST=1 TESTING OF ACCURACY IS POSSIBLE           DRKG2000
ISN 0072         20 IMOD=ISTEP/2                                                DRKG2010
ISN 0073            IF(ISTEP-IMOD-IMOD)21,23,21                                 DRKG2020
ISN 0074         21 CALL FCT(X,Y,DERY)                                          DRKG2030
ISN 0075            DO 22 I=1,NDIM                                              DRKG2040
ISN 0076            AUX(5,I)=Y(I)                                               DRKG2050
ISN 0077         22 AUX(7,I)=DERY(I)                                            DRKG2060
ISN 0078            GOTO 9                                                      DRKG2070
                C                                                               DRKG2080
                C     COMPUTATION OF TEST VALUE DELT                            DRKG2090
ISN 0079         23 DELT=0.D0                                                   DRKG2100
ISN 0080            DO 24 I=1,NDIM                                              DRKG2110
ISN 0081         24 DELT=DELT+AUX(8,I)*DABS(AUX(4,I)-Y(I))                      DRKG2120
ISN 0082            IF(DELT-PRMT(4))28,28,25                                    DRKG2130
                C                                                               DRKG2140
ISN 0083         25 CONTINUE
                C     ERROR IS TOO GREAT                                        DRKG2150
ISN 0084         26 DO 27 I=1,NDIM                                              DRKG2170
ISN 0085         27 AUX(4,I)=AUX(5,I)                                           DRKG2180
ISN 0086            ISTEP=ISTEP+ISTEP-4                                         DRKG2190
ISN 0087            X=X-H                                                       DRKG2200
ISN 0088            IEND=0                                                      DRKG2210
ISN 0089            GOTO 18                                                     DRKG2220
                C                                                               DRKG2230
                C     RESULT VALUES ARE GOOD                                    DRKG2240
ISN 0090         28 CALL FCT(X,Y,DERY)                                          DRKG2250
ISN 0091            DO 29 I=1,NDIM                                              DRKG2260
ISN 0092            AUX(1,I)=Y(I)                                               DRKG2270
ISN 0093            AUX(2,I)=DERY(I)                                            DRKG2280
ISN 0094            AUX(3,I)=AUX(6,I)                                           DRKG2290
ISN 0095            Y(I)=AUX(5,I)                                               DRKG2300
ISN 0096         29 DERY(I)=AUX(7,I)                                            DRKG2310
ISN 0097            CALL OUTP(X-H,Y,DERY,IHLF,NDIM,PRMT,H)                      DRKG2320
```

Table A42 (Continued)

```
ISN 0098            IF(PRMT(5))40,30,40                                  DRKG2330
ISN 0099         30 DO 31 I=1,NDIM                                       DRKG2340
ISN 0100            Y(I)=AUX(1,I)                                        DRKG2350
ISN 0101         31 DERY(I)=AUX(2,I)                                     DRKG2360
ISN 0102            IREC=IHLF                                            DRKG2370
ISN 0103            IF(IEND)32,32,39                                     DRKG2380
                 C                                                       DRKG2390
                 C     INCREMENT GETS DOUBLED                            DRKG2400
ISN 0104         32 IHLF=IHLF-1                                          DRKG2410
ISN 0105            ISTEP=ISTEP/2                                        DRKG2420
ISN 0106            H=H+H                                                DRKG2430
ISN 0107            IF(IHLF)4,33,33                                      DRKG2440
ISN 0108         33 IMOD=ISTEP/2                                         DRKG2450
ISN 0109            IF(ISTEP-IMOD-IMOD)4,34,4                            DRKG2460
ISN 0110         34 IF(DELT-.0200*PRMT(4))35,35,4                        DRKG2470
ISN 0111         35 IHLF=IHLF-1                                          DRKG2480
ISN 0112            ISTEP=ISTEP/2                                        DRKG2490
ISN 0113            H=H+H                                                DRKG2500
ISN 0114            GOTO 4                                               DRKG2510
                 C                                                       DRKG2520
                 C                                                       DRKG2530
                 C     RETURNS TO CALLING PROGRAM                        DRKG2540
ISN 0115         36 IHLF=11                                              DRKG2550
ISN 0116            CALL FCT(X,Y,DERY)                                   DRKG2560
ISN 0117            GOTO 39                                              DRKG2570
ISN 0118         37 IHLF=12                                              DRKG2580
ISN 0119            GOTO 39                                              DRKG2590
ISN 0120         38 IHLF=13                                              DRKG2600
ISN 0121         39 CALL OUTP(X,Y,DERY,IHLF,NDIM,PRMT,H)                 DRKG2610
ISN 0122         40 RETURN                                               DRKG2620
ISN 0123            END                                                  DRKG2630
```

Table A43

ALT=85KM LAT=-45.0DEG DEC=23.5DEG

TIME	O	O3	DERY(O)	DERY(O3)	RATE(1)	RATE(2)	RATE(3)	RATE(4)	RATE(5)	CHI	DEL T	# INT	IHLF
5- 0- 7	6.489D 10	5.795D 07	1.50D 06	-1.87D 03	5.91D 05	3.08D 03	1.38D 04	1.52D 06	6.16D 05	68.6	450.	1156	2
5- 0-33	6.724D 10	5.972D 07	1.48D 06	1.28D 03	6.10D 05	3.12D 03	1.47D 04	1.50D 06	6.05D 05	69.0	225.	1164	3
5- 1- 7	7.022D 10	6.265D 07	1.44D 06	-1.88D 03	6.39D 05	3.58D 03	1.62D 04	1.44D 06	6.63D 05	70.6	450.	1170	2
5- 1-33	7.241D 10	6.431D 07	1.37D 06	1.18D 03	6.56D 05	3.61D 03	1.70D 04	1.39D 06	6.51D 05	72.0	225.	1178	3
5- 2- 7	7.507D 10	6.700D 07	1.25D 06	-2.20D 03	6.82D 05	4.08D 03	1.84D 04	1.24D 06	7.07D 05	75.1	450.	1184	2
5- 2-33	7.694D 10	6.834D 07	1.11D 06	9.56D 02	6.96D 05	4.07D 03	1.92D 04	1.12D 06	6.91D 05	77.3	225.	1192	3
5- 3- 7	7.856D 10	7.053D 07	8.66D 05	-2.95D 03	7.16D 05	4.51D 03	2.03D 04	8.19D 05	7.44D 05	81.7	450.	1198	2
5- 3-33	8.015D 10	7.125D 07	6.35D 05	5.53D 02	7.24D 05	4.41D 03	2.07D 04	5.85D 05	7.19D 05	84.5	225.	1206	3
5- 4- 3	8.100D 10	7.170D 07	3.26D 05	3.76D 03	7.31D 05	4.49D 03	2.12D 04	2.96D 05	7.25D 05	87.9	225.	1212	3
5- 4-33	8.043D 10	7.769D 08	-7.94D 05	6.77D 05	7.24D 05	5.73D 04	2.07D 04	0.0	0.0	93.1	225.	1228	3
5- 5-14	7.837D 10	2.313D 09	-8.66D 05	5.67D 05	7.00D 05	1.68D 05	1.94D 04	0.0	0.0	101.4	900.	1234	1
5- 5-44	7.678D 10	3.272D 09	-9.05D 05	4.99D 05	6.85D 05	2.17D 05	1.86D 04	0.0	0.0	106.4	900.	1236	1
5- 6-29	7.427D 10	4.499D 09	-9.45D 05	4.13D 05	6.55D 05	2.90D 05	1.69D 04	0.0	0.0	116.7	1800.	1238	0
5- 6-59	7.256D 10	5.198D 09	-9.62D 05	3.64D 05	6.55D 05	2.90D 05	1.69D 04	0.0	0.0	116.7	3600.	1239	0
5- 7-29	7.082D 10	5.814D 09	-9.72D 05	3.22D 05	6.23D 05	3.38D 05	1.54D 04	0.0	0.0	127.3	1800.	1240	0
5- 7-59	6.906D 10	6.360D 09	-9.76D 05	2.85D 05	6.23D 05	3.38D 05	1.54D 04	0.0	0.0	127.3	3600.	1241	0
5- 8-29	6.730D 10	6.843D 09	-9.76D 05	2.53D 05	5.91D 05	3.67D 05	1.38D 04	0.0	0.0	137.8	1800.	1242	0
5- 8-59	6.555D 10	7.272D 09	-9.72D 05	2.24D 05	5.91D 05	3.67D 05	1.38D 04	0.0	0.0	137.8	3600.	1243	0
5- 9-29	6.381D 10	7.653D 09	-9.65D 05	2.00D 05	5.60D 05	3.82D 05	1.24D 04	0.0	0.0	147.5	1800.	1244	0
5- 9-59	6.208D 10	7.992D 09	-9.54D 05	1.78D 05	5.60D 05	3.82D 05	1.24D 04	0.0	0.0	147.5	3600.	1245	0
5-10-29	6.037D 10	8.296D 09	-9.42D 05	1.59D 05	5.29D 05	3.87D 05	1.11D 04	0.0	0.0	155.3	1800.	1246	0
5-10-59	5.869D 10	8.567D 09	-9.28D 05	1.42D 05	5.29D 05	3.87D 05	1.11D 04	0.0	0.0	155.3	3600.	1247	0
5-11-29	5.703D 10	8.810D 09	-9.12D 05	1.28D 05	5.00D 05	3.85D 05	9.88D 03	0.0	0.0	158.5	1800.	1248	0
5-11-59	5.541D 10	9.028D 09	-8.95D 05	1.15D 05	5.00D 05	3.85D 05	9.88D 03	0.0	0.0	158.5	3600.	1249	0
5-12-29	5.381D 10	9.224D 09	-8.77D 05	1.03D 05	4.71D 05	3.78D 05	8.79D 03	0.0	0.0	155.3	1800.	1250	0
5-12-59	5.225D 10	9.401D 09	-8.58D 05	9.33D 04	4.71D 05	3.78D 05	8.79D 03	0.0	0.0	155.3	3600.	1251	0
5-13-29	5.072D 10	9.560D 09	-8.39D 05	8.43D 04	4.44D 05	3.68D 05	7.80D 03	0.0	0.0	147.5	1800.	1252	0
5-13-59	4.923D 10	9.705D 09	-8.20D 05	7.64D 04	4.44D 05	3.68D 05	7.80D 03	0.0	0.0	147.5	3600.	1253	0
5-14-29	4.777D 10	9.836D 09	-8.00D 05	6.93D 04	4.18D 05	3.55D 05	6.91D 03	0.0	0.0	137.8	1800.	1254	0
5-14-59	4.635D 10	9.955D 09	-7.80D 05	6.30D 04	4.18D 05	3.55D 05	6.91D 03	0.0	0.0	137.8	3600.	1255	0
5-15-29	4.496D 10	1.006D 10	-7.60D 05	5.73D 04	3.93D 05	3.41D 05	6.12D 03	0.0	0.0	127.3	1800.	1256	0
5-15-59	4.361D 10	1.016D 10	-7.41D 05	5.23D 04	3.93D 05	3.41D 05	6.12D 03	0.0	0.0	127.3	3600.	1257	0
5-16-29	4.230D 10	1.025D 10	-7.21D 05	4.78D 04	3.70D 05	3.26D 05	5.42D 03	0.0	0.0	116.7	1800.	1258	0
5-16-59	4.102D 10	1.033D 10	-7.02D 05	4.38D 04	3.70D 05	3.26D 05	5.42D 03	0.0	0.0	116.7	3600.	1259	0
5-17-29	3.977D 10	1.041D 10	-6.83D 05	4.01D 04	3.48D 05	3.11D 05	4.79D 03	0.0	0.0	106.4	1800.	1260	0
5-17-59	3.856D 10	1.048D 10	-6.64D 05	3.68D 04	3.48D 05	3.11D 05	4.79D 03	0.0	0.0	106.4	3600.	1261	0
5-18-29	3.738D 10	1.054D 10	-6.45D 05	3.39D 04	3.27D 05	2.96D 05	4.23D 03	0.0	0.0	96.6	1800.	1262	0
5-18-59	3.624D 10	1.060D 10	-6.27D 05	3.12D 04	3.27D 05	2.96D 05	4.23D 03	0.0	0.0	96.6	3600.	1263	0
5-19-14	3.568D 10	1.063D 10	-6.18D 05	3.00D 04	3.17D 05	2.88D 05	3.97D 03	0.0	0.0	92.0	900.	1264	1
5-19-33	3.499D 10	1.066D 10	-6.07D 05	2.85D 04	3.14D 05	2.86D 05	3.91D 03	0.0	0.0	90.8	225.	1266	3
5-20- 1	4.557D 10	4.076D 07	4.22D 05	-1.08D 03	4.12D 05	1.43D 03	6.70D 03	4.31D 05	4.10D 05	86.3	112.	1322	4
5-20-33	4.664D 10	4.138D 07	7.31D 05	2.15D 03	4.22D 05	1.50D 03	7.05D 03	7.43D 05	4.19D 05	82.6	225.	1330	3
5-21- 7	4.839D 10	4.308D 07	1.00D 06	6.84D 02	4.41D 05	1.64D 03	7.68D 03	1.07D 06	4.40D 05	78.2	450.	1338	2
5-21-33	5.011D 10	4.456D 07	1.17D 06	9.88D 02	4.54D 05	1.74D 03	8.17D 03	1.20D 06	4.52D 05	75.8	225.	1344	3
5-22- 7	5.264D 10	4.713D 07	1.32D 06	-2.27D 03	4.80D 05	2.06D 03	9.12D 03	1.36D 06	5.08D 05	72.6	450.	1350	2
5-22-33	5.479D 10	4.869D 07	1.40D 06	1.20D 03	4.97D 05	2.08D 03	9.77D 03	1.43D 06	4.94D 05	71.0	225.	1358	3
5-23- 7	5.771D 10	5.159D 07	1.47D 06	-1.99D 03	5.26D 05	2.46D 03	1.10D 04	1.49D 06	5.52D 05	69.3	450.	1364	2
5-23-33	6.003D 10	5.333D 07	1.49D 06	1.28D 03	5.45D 05	2.49D 03	1.17D 04	1.51D 06	5.41D 05	68.7	225.	1372	3

REFERENCES

Arnold, H. R. and E. T. Pierce (1963), The ionosphere below 100 km, Stanford Research Institute, Research Memorandum II.

Barth, C. A. (1964), Rocket measurement of the nitric oxide dayglow, J. Geophys. Res. 69, 3301-3303.

Barth, C. A. (1966), Rocket measurement of nitric oxide in the upper atmosphere, Planet. Space Sci. 14, 623-630.

Bates, D. R. and A. E. Witherspoon (1952), The photo-chemistry of some minor constituents of the earth's atmosphere (CO_2, CO, CH_4, N_2O), Monthly Notices Roy. Astrom. Soc. 112, 101-124.

Baulknight, C. W. and M. H. Bortner (1964), AFCRL-64-142.

Benson, S. W. and A. E. Axworthy, Jr. (1965), Reconsideration of the rate constants from the thermal decomposition of ozone, J. Chem. Phys. 42, 2614-2615.

Biondi, M. A. (1967), Recombination processes (charged particles), DASA Reaction Rate Handbook, Chapter 11.

Campbell, I. M. and B. A. Thrush (1968), cited in DASA Reaction Rate Handbook, 1967, Chapter 14.

Carver, J. H., B. H. Horton and F. G. Burger (1966), Nocturnal ozone distribution in the upper atmosphere, J. Geophys. Res. 71, 4189-4191.

Clyne, M. A. A. and B. A. Thrush (1961), Kinetics of the reactions of active nitric oxide, Proc. Roy. Soc. (London), A261, 259-273.

Clyne, M. A. A. and B. A. Thrush (1962), Mechanism of chemiluminescent reactions involving nitric oxide--the H + NO reaction, Disc. Faraday Soc. 33, 139-148.

Clyne, M. A. A., B. A. Thrush and R. P. Wayne (1964), Kinetics of the chemiluminescent reaction between nitric oxide and ozone, Trans. Faraday Soc. 60, 359-370.

Clyne, M. A. A., D. J. McKenney and B. A. Thrush (1965), Rate of combination of oxygen atoms with oxygen molecules, Trans. Faraday Soc. 61, 2701-2709.

COSPAR International Reference Atmosphere (1965), North-Holland Publishing Company, Amsterdam.

Craig, R. A. (1950), The observations and photochemistry of atmospheric ozone and their meteorological significance, Meteorological Monographs I, No. 2, American Meteorological Society.

Craig, R. A. (1965), Ed. The Upper Atmosphere, Academic Press, 279-316.

deJager, C. (1967), Theoretical aspects of solar X-radiation, Electromagnetic Radiation in Space, Ed. J. G. Emming, Springer-Verlag, New York, 101-124.

Evans, W. F. J., D. M. Hunten, J. Llewellyn and A. Vallance-Jones (1968), Attitude profile of the infrared atmospheric system of oxygen in the dayglow, J. Geophys. Res. 73, 2885-2896.

Fedynskii, A. V., S. P. Perov and A. F. Chizhov (1967), An attempt to measure directly the concentration of water vapor and atomic oxygen in the mesosphere, Atmosph. and Oceanic Phys. 3, 557-561.

Fehsenfeld, F. C. and E. E. Ferguson (1968), Further laboratory measurements of negative reactions of atmospheric interest, Planet. Space Sci. 16, 701-702.

Fehsenfeld, F. C., A. L. Schmeltekopf, H. I. Schiff and E. E. Ferguson (1967), Laboratory measurements of negative ion reactions of atmospheric interest, Planet. Space Sci. 15, 373-379.

Ferguson, E. E. (1967), Ionospheric ion-molecule reaction rates, Revs. Geophys. 5, 305-327.

Friedman, H. (1963), Ultraviolet and X rays from the sun, Ann. Rev. Astron. Astrophys. 1, 59-96.

Geisler, J. E. and R. E. Dickinson (1968), Vertical motions and nitric oxide in the upper mesosphere, J. Atmosph. Terr. Phys. 30, 1505-1521.

Ghielmetti, H. S., N. Becerra, A. M. Godel, N. Heredia and J. C. Roederer (1965), X-ray intensity measurements at balloon altitudes in the South American anomaly, Space Research V, North-Holland Publ. Co. Eds. D. G. King-Hele, P. Muller and G. Righini, Amsterdam, 271-272.

Gowan, E. H. (1947a), Ozonosphere temperatures under radiation equilibrium, Proc. Roy. Soc. A190, 219-226.

Gowan, E. H. (1947b), Night cooling of the ozonosphere, Proc. Roy. Soc. A190, 227-231.

Hampson, J. (1965), Chemiluminescent emissions observed in the stratosphere and mesosphere, Conference on Meteorology of the Stratosphere and Mesosphere, Paris.

Hesstvedt, E. (1964), On the water vapor content in the high atmosphere, Geofysiske Publikasjoner Geophysica Norvegica XXV, No. 3, 1-18.

Hesstvedt, E. (1965), Some characteristics of the oxygen-hydrogen atmosphere, Geofysiske Publikasjoner Geophysica Norvegica XXVI, No. 1, 1-30.

Hesstvedt, E. (1968), On the effect of vertical eddy transport on atmospheric composition in the mesosphere and lower thermosphere, Geofysiske Publikasjoner Geophysica Norvegica, XXVII, No. 4, 1-35.

Hinteregger, H. E., L. A. Hall and S. Schmidtke (1965), Solar XUV radiation and neutral particle distribution in July 1963 thermosphere, Space Research V Eds. D. G. King-Hele, P. Muller and G. Righini, North-Holland Publ. Co. Amsterdam, 1175-1190.

Hirsch, M. N., C. M. Malpern, N. S. Wolf and J. A. Slevin (1967), Paper presented at the DASA Symposium on Physics and Chemistry of the Lower Atmosphere, Boulder, Colorado.

Hulburt, E. O. (1930), Atmospheric ionization by cosmic radiation, Phys. Rev. 37, 1-8.

Hultqvist, B. (1965), Aurora and the lower ionosphere in relation to satellite observations of electron precipitation, Space Research V, Eds. D. G. King-Hele, P. Muller and G. Righini, North-Holland Publ. Co. Amsterdam, 91-117.

Hunt, B. G. (1963), A discussion of the reactions and data relevant to photochemical ozone calculations, Weapons Research Establishment Report, Technical Note SAD 123, Australian Defense Scientific Service.

Hunt, B. G. (1966a), The need for a modified photochemical theory of the ozonosphere, J. Atmosph. Sci. 23, 88-95.

Hunt, B. G. (1966b), Photochemistry of ozone in a moist atmosphere, J. Geophys. Res. 71, 1385-1398.

Hunten, D. M. and M. B. McElroy (1968), Metastable $O_2(^1\Delta)$ as a major source of ions in the D region, J. Geophys. Res. 73, 2421-2428.

Ivanov-Kholodny, G. S. (1965), Maintenance of the night ionosphere and corpuscular fluxes in the upper atmosphere, Space Research V, Eds. D. G. King-Hele, P. Muller and G. Righini, North-Holland Publ. Co., Amsterdam, 19-42.

Jones, W. M. and N. Davidson (1962), The thermal decomposition of ozone in a shock tube, J. Am. Chem. Soc. 84, 2868-2878.

Johnson, F. S., J. D. Purcell and R. Tousey (1954), Rocket Exploration of the Upper Atmosphere, Pergamon Press, 189-199.

Kaufman, F. (1964), Aeronomic reactions involving hydrogen: a view of recent laboratory studies, Ann. de Geophys. 20, 106-114.

Kaufman, F. (1967), Neutral reactions, DASA Reaction Rate Handbook, Chapter 14.

Kaufman, F. (1968), Neutral reactions involving hydrogen and other minor constituents, Proceedings of Symposium on Laboratory Measurements of Aeronomic Interest, Toronto, Canada, 235-248.

Kaufman, F. and J. Kelso (1964), Rate constant of the reaction $O + 2O_2 \rightarrow O_3 + O_2$, Disc. Faraday Soc. 37, 26-37.

Konashenok, V. N. (1967), A model of an oxygen-hydrogen mesosphere, Atmosph. and Oceanic Phys. 3, 129-133.

Lazarev, V. I. (1967), Absorption of the energy of an electron beam in the upper atmosphere, Geomag. Aeron. 7, 219-223.

London, J. (1967), The average distribution and time variation of ozone in the stratosphere and mesosphere, Space Research VII, Ed. R. L. Smith-Rose, North-Holland Publ. Co. Amsterdam, 172-185.

Maeda, K. and A. C. Aikin (1968), Variations of polar mesospheric oxygen and ozone during auroral events, Planet. Space Sci. 16, 371-384.

Mathais, A. and H. I. Schiff (1964), Mass spectrometric studies of atom reactions Part 4.-Kinetics of O_3 formation in a stream of electrically discharged O_2, Disc. Faraday Soc. 37, 38-45.

McGrath, W. D. and J. J. McGarvey (1967), The production, deactivation and chemical reactions of $O(^1D)$ atoms, Planet. Space Sci. 15, 427-455.

Mechtly, E. A. and J. S. Shirke (1968), Rocket electron density measurements on winter days of anomalous and normal absorption, J. Geophys. Res. 73, 6243-6247.

Mechtly, E. A. and L. G. Smith (1968a), The growth of the D region at sunrise, J. Atmosph. Terr. Phys. 30, 363-369.

Mechtly, E. A. and L. G. Smith (1968b), Seasonal variation of the lower ionosphere at Wallops Island during the IQSY, J. Atmosph. Terr. Phys. 30, 1555-1562.

Mikirov, A. Ye. (1965), Estimate of ozone concentration at heights of 44-102 km during night launchings of geophysical rockets, Geomag. and Aeron. 5, 882-884.

Mitra, A. P. (1966), An ionospheric estimate of nitric oxide concentration in the D-region, J. Atmosph. Terr. Phys. 28, 945-955.

Mitra, A. P. (1968), A review of D-region processes in non-polar latitudes, J. Atmosph. Terr. Phys. 30, 1065-1114.

Morgan, J. E. and H. I. Schiff (1963), Recombination of oxygen atoms in the presence of inert gases, J. Chem. Phys. 38, 1495-1500.

Narcisi, R. (1968), Mass spectrographic measurements, Presented at the 49th AGU Meeting, Washington, D. C.

Nicolet, M. (1964), Introduction to chemical aeronomy. 1. Reactions and photochemistry of atoms and molecules, Disc. Faraday Soc. 37, 7-20.

Nicolet, M. (1965a), Nitrogen oxides in the chemosphere, J. Geophys. Res. 70, 679-689.

Nicolet, M. (1965b), Ionospheric processes and nitric oxide, J. Geophys. Res. 70, 691-701.

Nicolet, M. and A. C. Aikin (1960), The formation of the D region of the ionosphere, J. Geophys. Res. 65, 1469-1483.

O'Brien, B. J., F. R. Allum and H. C. Goldwire (1965), Rocket measurement of midlatitude airglow and particle precipitation, J. Geophys. Res. 70, 161-175.

Ohshio, M., R. Maeda and H. Sakagami (1966), Height distribution of local photoionization efficiency, J. Radio Res. Lab. (Japan) 13, 245-269.

Paulikas, G. A., J. B. Blake and S. C. Freden (1966), Precipitation of energetic electrons at middle latitudes, J. Geophys. Res. 71, 3165-3172.

Pearce, J. B. (1968), Dayglow measurements of nitric oxide concentrations, Meteorological and Chemical Factors in D-region Aeronomy--Record of the Third Aeronomy Conference, Aeronomy Report No. 32, Aeronomy Laboratory, University of Illinois, Urbana, 182-186.

Phillips, L. F. and H. I. Schiff (1962), Mass spectrometric studies of atom reactions. 1. Reactions in the atomic nitrogen-ozone system, J. Chem. Phys. 36, 1509-1517.

Radicella, S. M. (1968), Theoretical models of electron and ion density in the nighttime D region, J. Atmosph. Terr. Phys. 30, 1745-1760.

Rawcliffe, R. D., G. E. Meloy, R. M. Friedman and E. H. Rogers (1963), Measurement of vertical distribution of ozone from a polar orbiting satellite, J. Geophys. Res. 68, 6425-6429.

Reed, E. I. (1968), A night measurement of mesospheric ozone by observations of ultraviolet airglow, J. Geophys. Res. 73, 2951-2957.

Rees, M. H. (1963), Auroral ionization and excitation by incident energetic electrons, Planet. Space Sci. 11, 1209-1218.

Rutherford, J. A. and B. R. Turner (1967), The production of NO_2^- by electron transfer from O^-, O_2^-, O_3^-, and OH^- to NO_2, J. Geophys. Res. 72, 3795-3800.

Ryan, K. R. (1968), The production of nitric oxide around 100 km, J. Atmosph. Terr. Phys. 30, 1331-1340.

Schofield, K. (1967), An evaluation of kinetic rate data for reactions of neutrals of atmospheric interest, Planet. Space Sci. 15, 643-670.

Tulinov, V. F. (1967), On the role of corpuscular radiation in the formation of the lower ionosphere (below 100 km), Space Research VII, Vol. 1, Ed. R. L. Smith-Rose, North-Holland Publ. Co. Amsterdam, 386-390.

Tulinov, V. F., L. V. Shiboeva and S. G. Jakovlev (1969), The ionization of the lower ionosphere under the influence of corpuscular radiation, Space Research IX, Eds. K. S. W. Champion, P. A. Smith and R. L. Smith-Rose, North-Holland Publ. Co. Amsterdam, 231-236.

U. S. Standard Atmosphere Supplement (1966).

Wagner, C. U. (1966), The distribution of nitric oxide in the lower ionosphere, J. Atmosph. Terr. Phys. 28, 607-615.

Watanabe, K. (1954), Photoionization and total absorption cross section of gases. 1. Ionization potentials of several molecules. Cross sections of NH_3 and NO, J. Chem. Phys. 22, 1564-1570.

Watanabe, K. (1958), Ultraviolet absorption processes in the upper atmosphere, Advances in Geophysics 5, Academic Press, 153-221.

Watanabe, K., M. Zelikoff and C. Y. Inn (1953), Absorption coefficients of several atmospheric gases, (Geophys. Res. Directorate) AF CRC No. 21.

Whitten, R. C. and I. G. Poppoff (1964), Ion kinetics in the lower ionosphere, J. Atmosph. Sci. 21, 117-133.

Young, R. A. and G. Black (1966), Excited-state formation and destruction in mixtures of atomic oxygen and nitrogen, J. Phys. Chem. 42, 3741-3751.

Zmuda, A. J. (1966), Ionization enhancement from Van Allen electrons in the South Atlantic magnetic anomaly, J. Geophys. Res. 71, 1911-1917.